THE ROLE OF EXOGENOUS INTERLEUKIN-4 IN MODULATING THE MONONUCLEAR PHAGOCYTE RESPONSE TO ACUTE LIVER INJURY

Dr. Ruairi Lynch

Doctor of Philosophy

University of Edinburgh | 2019

Acknowledgements

I would like to start by thanking Steve Jenkins, my supervisor, who has provided guidance throughout my PhD and who was always available to talk over experiments. I would also like to thank Stuart Forbes who stepped in as my second supervisor and has been a great sounding board for ideas.

I'd also like to thank everyone in W2.29, who made the three plus years in the lab a great experience. I would especially like to thank Cathy who showed me the ropes of liver preps from day 1 and Anna for her help on big experiment days.

I would also like to thank all the ECAT directors for their guidance and Jo Ness for her help in coordinating everything from the ECAT side of things.

I would like to extend a special thanks to Calum Bain who has dedicated a lot of time and effort to my project whilst a post-doc in the Jenkins lab but also after he became an independent PI with his own lab. His contribution to my project has been invaluable not only from a scientific perspective but also as a mentor.

I would also like to thank my parents who have always supported me through all my studies.

Finally and most importantly I want to thank my wife Sarah and children Emily and Hugo. I appreciate that it has a been a busy time for all of us but as a family you have all helped get me through this PhD with your endless support.

Contents

Figures and tables

Declaration

I declare that the thesis has been composed by myself and that the work has not be submitted for any other degree or professional qualification. I confirm that the work submitted is my own, except where work has been included that was performed by Eleni Papachristoforou and Andrew Muir, two BSc Honours project students that I helped supervise who stained and quantified tissue sections for BrdU. Work has also been included which formed part of a jointly-authored publication, my contribution and those of the other authors to this publications has been explicitly indicated below. I confirm that appropriate credit has been given within this thesis where reference has been made to the work of others.

The work presented in Chapter 4 was previously published in the Journal of Leukocyte Biology as: “An efficient method to isolate Kupffer cells eliminating endothelial cell contamination and selective bias” by Ruairi W. Lynch*, Catherine A. Hawley*, Antonella Pellicoro, Calum C. Bain, John P. Iredale, and Stephen J. Jenkins (Supervisor). I designed, performed, and analysed the experiments and wrote the manuscript with Catherine A. Hawley as a co-author.

Ruairi Lynch

Abstract

Background

Acute liver failure has significant mortality for which the only reliable treatment is transplantation. Murine models of acute liver injury are characterised by dramatic changes in the hepatic macrophage compartment, with an initial accumulation of pro-inflammatory Ly6C^{hi} monocytes and loss of Kupffer cells, followed by the dominance of Ly6C^{lo} macrophages that promote liver repair. The canonical type 2 immune cytokine Interleukin 4 (IL-4) prevents damaging inflammation and accelerates tissue repair following helminth infection and physical wounding, partly through effects on myeloid cells including macrophages. Furthermore, exogenous IL-4 administered prior to injury with the hepatotoxin carbon tetrachloride (CCl_4) has been shown to be hepatoprotective by directly promoting hepatocyte proliferation. For this reason, in my thesis I aimed to assess the effects of therapeutic IL-4 administered following acute liver injury and examine the underlying pathways with an emphasis on the effects of IL-4 on hepatic myeloid cells.

Methods

Male C57Bl/6 mice were given CCl_4 intraperitoneally to induce an acute liver injury. IL-4 in the form of IL-4 complex (IL-4c) was administered subcutaneously to manipulate the repair and regeneration process. To investigate the role of IL-4Rα signalling in bone marrow derived cells, whole-body and tissue-protected chimeras were generated with wild type or IL-4Ra$^{-/-}$ donor bone marrow. An in vitro culture system was developed to validate the observed effect of IL-4 on Ly6C^{hi} monocytes. Models of acetaminophen (APAP) induced acute liver injury as well as dextran sulfate sodium (DSS) colitis were used to investigate the translational potential of IL-4c therapy. The effect of IL-4c in experiments was assessed through immunohistochemical analysis of tissue sections, analysis of serum biochemistry and flow cytometric analysis of leukocyte populations.

Results

Therapeutic administration of IL-4c following CCl_4 induced liver injury reduced markers of hepatic injury (ALT and necrotic area) and enhanced hepatic regeneration as measured by hepatocyte proliferation. This was paralleled by profound alterations to the monocyte/macrophage pool, with increases in the number of hepatic Ly6C^{lo} macrophages but also a large reduction in the number of hepatic Ly6C^{hi} monocytes. Using chimeras, I have shown that cell-intrinsic, IL-4Rα-dependent proliferation contributes to the observed accumulation of Ly6C^{lo} macrophages. Importantly, the loss of hepatic Ly6C^{hi} monocytes following administration of IL-4c was associated with a systemic IL-4Rα dependent loss of Ly6C^{hi} monocytes. Analysis of tissues and blood revealed an increased detection of dead and apoptotic monocytes and culture of monocytes with IL-4 in vitro directly induced the monocyte death, a feature that could be overcome by high levels of the macrophage colony-stimulating factor (CSF-1). Hence, the systemic reduction in Ly6C^{hi} monocytes in response to therapeutic delivery of IL-4c is due to IL-4Rα-dependent death of circulating monocytes rather than decreased output from the bone marrow. Experiments using APAP and DSS suggested that the beneficial effect of IL-4c may be dependent on the timing of delivery following injury.

Conclusion

I have demonstrated a therapeutic effect for IL-4c following CCl_4 mediated acute liver injury and I have also identified a novel role for IL-4 in promoting the death of Ly6C^{hi} monocytes. This effect of IL-4 may offer insights and potential therapeutic targets in other inflammatory pathologies characterised by monocytosis. However, preliminary assessments in the APAP and DSS models would suggest that this may need careful optimisation.

Lay summary

In humans, toxins to the liver, for example an overdose of paracetamol, are a significant cause of severe liver injury. Liver failure can follow severe liver injury and kills 1 in 3 of those affected.

The liver has an outstanding capacity to repair itself but when this process is overwhelmed due to a very severe injury the only available treatment is to have a liver transplant. Undergoing liver transplant involves major surgery with lifelong consequences and there is a limited supply of donor livers available. It is therefore important to try and find other treatments that don’t rely on transplantation.

One potential target for treatment is enhancing the in-built repair capacity of the liver. Parasitic worm infections represent a different type of injury to the liver and in this setting the body’s defence mechanisms work through specific chemical messengers to activate repair and regeneration pathways.

I aimed to give this chemical messenger as a treatment to animals following severe liver injury with a toxin. When I did this, it resulted in improved repair and regeneration of injured livers. At the same time, this chemical messenger directly killed a cell type associated with injury and increased a cell type associated with the repair process. Careful assessment of the timing of administration of the chemical messenger treatment may in the future enable the manipulation of these cells to improve survival in human severe liver injury and reduce our reliance on liver transplantation.

List of abbreviations

ALF	Acute liver failure
ALT	Alanine aminotransferase
APAP	Acetaminophen
AST	Aspartate aminotransferase
BM	Bone marrow
BMDM	Bone marrow derived macrophages
CCl_4	Carbon tetrachloride
CIA	Collagen induced arthritis
CLPs	Chitinase like proteins
cMoP	Common monocyte progenitor
CMP	Common myeloid progenitor
CSF-1	Macrophage colony stimulating factor
CVC	Cenicriviroc
CX3CL1	Fractalkine
DAI	Disease activity index
DAMPs	Damage-associated molecular patterns
DILI	Drug induced liver injury
DSS	Dextran sodium sulfate
FACS	Fluorescence-activated cell sorting
FMO	Fluorescence minus one
FSC	Forward scatter
FVD	Fixable viability dye
G-CSF	Granulocyte colony stimulating factor
GFP	Green fluorescent protein
GM-CSF	Granulocyte macrophage colony-stimulating factor
GMP	Granulocyte-macrophage progenitor
HMGB-1	High mobility group box 1
HSC	Haematopoietic stem cells
IBD	Inflammatory bowel disease

IFN-γ	Interferon gamma
IL	Interleukin
IL-4c	Interleukin-4 complex
IL-4R	Interleukin-4 receptor
JAK	Janus kinase
KC	Kupffer cell
KO	Knock-out
LPS	Lipopolysaccharides
LSEC	Liver sinusoidal endothelial cell
M1	Classically activated
M2	Alternatively activated
MCP-1	Monocyte chemotactic protein-1
MDP	Macrophage and DC precursor
MERTK	Mer tyrosine kinase
MFI	Mean fluorescence intensity
MHC	Major histocompatibility complex
MI	Myocardial infarction
MMP	Matrix metalloproteinase
MPS	Mononuclear phagocyte system
NK	Natural killer
PAP	Pulmonary alveolar proteinosis
PAS	Periodic acid schiff
RA	Rheumatoid arthritis
RELMα	Resistin-like molecule
ROS	Reactive Oxygen species
SD	Standard deviation
SP-A	Surfactant protein a
SSC	Side scatter
STAT	Signal transducer and activator of transcription
TGF-β	Transforming growth factor beta
TNF-α	Tumour necrosis factor alpha
TpMo	Transitional premonocyte

TREML4	Triggering Receptor Expressed On Myeloid Cells Like 4
VEGF-A	Vascular endothelial growth factor A
WT	Wild-type

Chapter 1 General introduction

1.1 Introduction

Acute liver failure (ALF) is a rare but life-threatening condition first defined in the 1970s as: “an illness characterised by a severe liver injury which is potentially reversible in nature and with onset of hepatic encephalopathy within 8 weeks of first symptoms in the absence of pre-existing liver disease”[1,2]. This definition was further refined in the early 1990’s to encompass hyperacute liver failure (within 7 days of onset of jaundice); acute liver failure (within 8-28 days of onset of jaundice) and subacute liver failure (within 5-12 weeks of onset of jaundice)[3]. Globally acute viral infection with hepatitis A, B and E are the commonest causes of ALF[4–6], however in the United Kingdom (UK) and United States (US) drug induced liver injury (DILI) is the commonest cause of ALF and accounts for 68% and 52% of cases respectively[1]. Of these, 57% in the UK and 39% in the US are attributable to acetaminophen (APAP) overdose, be it unintentional through therapeutic misadventure or deliberate overdose with suicidal intent. Liver failure secondary to APAP overdose is hyperacute and although N-acetylcysteine is used to treat APAP toxicity, it has been shown that in the setting of established ALF there is no benefit to N-acetylcysteine treatment[7–10]¹¹¹¹¹¹. Indeed, although multiple treatments for ALF using liver assist devices have been trialled, none have shown benefit in randomised control trials and therefore liver transplantation is the only definitive treatment currently available for ALF[8]. As many as 55% of patients with ALF require a transplant to survive[12,13]. Transplantation, however, is not a panacea as there is a finite supply of organs available for transplantation and although 1 year survival is good at 80% in ALF patients, it is slightly worse than in patients who have received a routine transplantation for chronic liver disease which likely reflects how unwell these patients are at the time of transplant[12]. Interestingly however, at 4 years post-transplant outcomes are better in those transplanted for ALF when compared to those transplanted for chronic liver disease[13]. Furthermore, transplantation requires lifelong immunosuppression with the associated complications of increased risk of opportunistic infections and malignancy in a population that are often young, with an average age 38 years[13,14]. Furthermore, in survivors of APAP induced ALF it has been demonstrated that there is no increased mortality compared to those who had an APAP induced liver injury but didn't develop ALF[11]. There is currently work ongoing looking at the long-term outcomes in patients that developed ALF and survived with/without transplant but this is yet to be published. For all of the above reasons there is a need to develop therapies that can improve transplant free survival.

The immune response plays an important role in the response to APAP induced ALF. Recent human data would suggest that monocyte and macrophages specifically play an important role in this immune response. For instance, Moore et al. have shown that blood monocytopenia is associated with worse outcome in patients with ALF following APAP overdose[15]. Moreover, Stutchfield et al. have proposed an important role for macrophages as lower plasma levels of the CSF-1 are associated with poorer outcomes[16]. Human data is plagued by the rapid onset of injury in DILI and also the availability of liver tissue samples. Murine models have therefore provided further insight into DILI be it secondary to APAP overdose or high dose carbon tetrachloride (CCl_4), both of which cause a centrilobular hepatocyte necrosis[17–20]. Following injury with CCl_4 or APAP there is an initial influx of pro-inflammatory Ly6C^{hi} monocytes with subsequent conversion into Ly6C^{lo} macrophages that are important to the repair process following injury[21–23]. It has been proposed that altering the dynamics of Ly6C^{hi} monocyte recruitment and/or Ly6C^{lo} macrophage accumulation could be a potential target to ameliorate outcomes[21,23,24].

Interleukin-4 (IL-4) in conjunction with Interleukin-13 (IL-13) are canonical type 2 immune (Th2) cytokines which have been classically associated with preventing damaging inflammation and promoting repair during helminth infection[25,26]. In helminth infection endogenous IL-4 polarises macrophages to a pro-reparative phenotype to promote wound repair and potentially restrict helminth migration[26–28]. Relevant to DILI, there is recent evidence to suggest that IL-4 receptor (IL-4R) signalling contributes to a pro-wound repair and anti-inflammatory state in macrophages in pathologies not previously associated with “classical” Th2 immunity, such as physical colonic injury, skin injury and hepatic listeriosis[29–31]. IL-4 can be administered exogenously complexed to an anti-IL-4 antibody (IL-4c) to prolong its half-life[32] and Goh et al. have demonstrated that combined administration of IL-4c pre and post injury with an acute dose of CCl_4 resulted in reduced liver injury as measured by a reduction in serum alanine aminotransferase (ALT) and a reduction in necrotic cell area[33]. They also demonstrated increased hepatic regeneration which was demonstrated by an increase in hepatocyte proliferation in IL-4c treated mice. Goh et al. demonstrated that the enhanced recovery is secondary to IL-4c directly promoting hepatocyte proliferation. It would, however, be surprising if there was no role for the myeloid compartment in the observed regeneration given the role of IL-4 signalling to myeloid cells in non-hepatic wound repair and the role for myeloid cells in the liver’s innate regenerative capacity. In my project I therefore sought to establish if IL-4c could be administered therapeutically following acute CCl_4 injury and whether any observed phenotype might be mediated by signalling to myeloid cells.

I initially compared a pre-treatment and therapeutic regimen for IL-4c following acute CCl_4 injury as previous work had only shown a beneficial effect with pre-treatment with IL-4c. Having established that IL-4c could be administered therapeutically, I then wanted to establish whether signalling to myeloid cells was integral to the observed response using the LysMCreIL-4R$\alpha^{-/flox}$ mouse line[28]. However, as Vannella et al. had shown at a gene expression level[34], I established that this mouse line was inefficient at removing the IL-4Rα from myeloid cells during injury. Instead, using a combination of both whole body and tissue protected bone marrow chimeras I was able to identify novel cell intrinsic effects of IL-4 on monocytes. While I was unable to demonstrate definitively if IL-4R signalling to monocytes/macrophages contributed to accelerated liver repair, I chose to further characterised the effect of IL-4 on monocytes using a combination of ex vivo and in vitro assays given the novelty and potential implications of the findings. Towards the end of my project I sought to establish whether this novel phenotype could be translated into two other models of acute inflammation APAP and dextran sodium sulphate (DSS) colitis. Hence in my introduction I will focus on the processes underlying liver injury and the role of monocytes both in this process and in homeostasis. In order to understand potential effects of exogenous administration of IL-4 I will then summarise the role of endogenous IL-4 in both classical and non-classical type 2 immunity with a final focus on the IL-4Rα as a potential therapeutic target.

1.2 Hepatic physiology and pathophysiology

The liver is the largest solid organ in the body and plays an important role in metabolism, synthesis of digestive enzymes and production of a variety of proteins. It also possesses a remarkable regenerative capacity when injured.

During homeostasis all the blood from the gut and pancreas passes through the liver via the portal venous circulation and because of this the liver plays an important role in the metabolism of not only nutrients that are absorbed from the gut but also drugs. The liver is a highly vascularized organ and the portal vein provides blood from the digestive tract and pancreas containing nutrients, bile acids, and hormones including insulin and glucagon, which flow along sinusoids leading to the hepatic vein (Fig. 1.1)[35]. These sinusoids are lined by highly specialised fenestrated liver sinusoidal endothelial cells (LSECs) which maintain blood cells in the sinusoid but allow passage of metabolites, plasma proteins, pharmaceutical drugs, lipoproteins, small chylomicron remnants, viruses (<200 nm) and exosomes into the space of Disse[35]. This process ensures exposure of these particles to hepatocytes and stellate cells within the space of Disse, allowing hepatocytes to perform their crucial role within the liver of maintaining metabolic homeostasis, storing nutrients, secreting bile and detoxifying drugs[19]. During homeostasis, LSECs

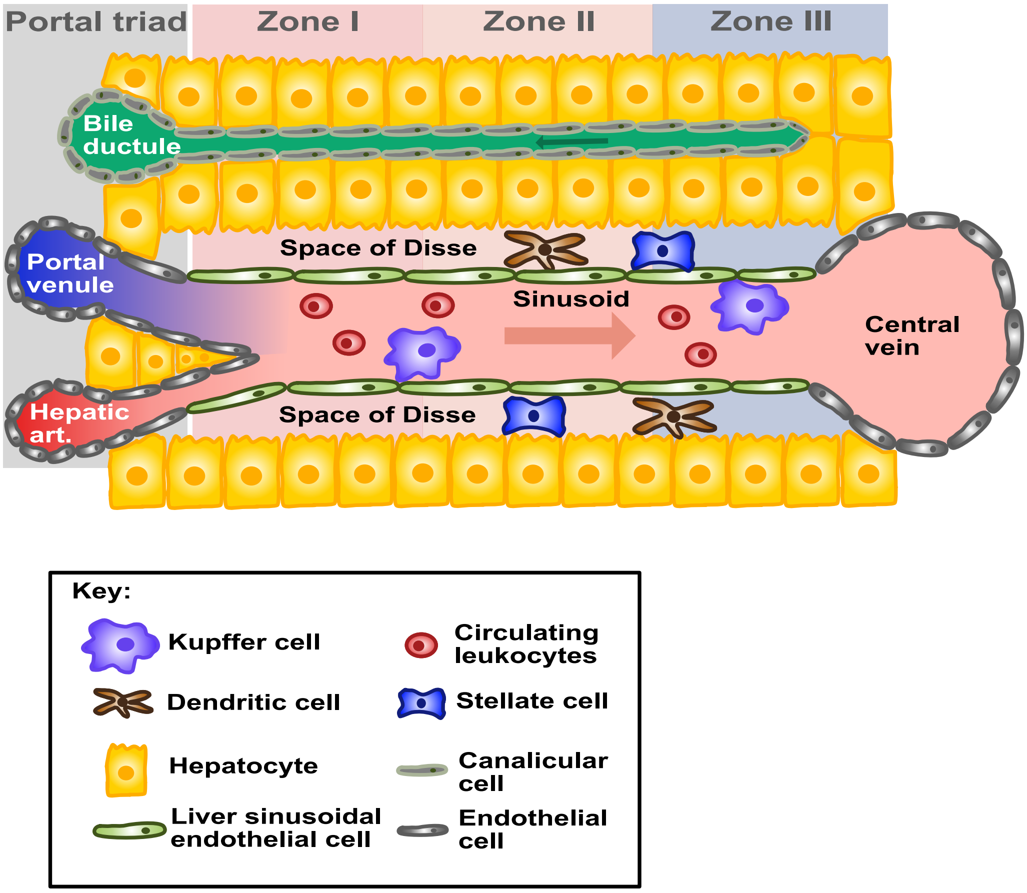

Figure 1-1 Hepatic sinusoid.

The portal triad is made up of the bile ductule, portal venule and the hepatic arteriole (art.). The portal venule supplies blood from the GI tract (portal circulation) to the liver and the hepatic arteriole (art.) supplies oxygenated arterial blood from the systemic circulation. Blood then travels along hepatic sinusoid in the direction of the arrow from the portal triad towards the central vein. The liver sinusoidal endothelial cells allow the diffusion of metabolites, plasma proteins, pharmaceutical drugs, lipoproteins, small chylomicron remnants, viruses (<200 nm) and exosomes into the space of Disse. There is an oxygen gradient along the sinusoid reflected by the zones from high oxygen concentration in zone I to lower concentration in zone III. The oxygen gradient affects what metabolic processes performed by hepatocytes in each zone. Bile made by hepatocytes drains along the bile canaliculi lined with canicular cells in the direction of the arrow towards the bile ductule.

can also clear small molecules and particles from the bloodstream using pinocytic receptors[36]. Within the sinusoids there are also resident leukocyte populations of liver dendritic cells and hepatic macrophages, Kupffer cells (KC), which are in close interaction with the LSECs. KC are the most abundant tissue macrophage in the body and during homeostasis they perform multiple roles including: scavenging apoptotic cells and antigenic particles[37]; maintenance of immunological tolerance[38]; recycling iron from erythrocytes[39] and acting as a firewall against any bloodborne gut-derived commensal bacteria[40].

There are a multitude of insults that can affect the liver throughout our lifetimes: acute and chronic ingestion of toxins, obesity, viruses and autoimmune diseases. Toxins like APAP (in overdose) and CCl_4 cause hepatocyte necrosis and in APAP overdose this necrosis occurs in a dose dependent manner due to accumulation of the reactive metabolite, N-acetyl-p-benzo-quinoneimine (NAPQI) [7,41]. This accumulation, leads to profound mitochondrial dysfunction which results in disruption of ion homeostasis and consequently oncotic necrosis of hepatocytes[42]. This necrosis occurs in zone 3 of the liver lobule which is an area of relatively low oxygen tension surrounding the central vein[43]. Similar to APAP, CCl_4 is a hepatotoxin that causes zone 3 necrosis due to generation of reactive oxygen species in this region of relative hypoxia in the acute setting and it also results in fibrosis when administered long term[17,18]. Although now used purely to model acute and chronic liver injury, CCl_4-mediated injury was more commonplace in the early 20th century when it was used as a solvent for dry cleaning. ALT and aspartate transaminase (AST) are enzymes that are found in hepatocytes that are released in the event of hepatocyte damage and are therefore markers of liver injury that can be measured in serum[44]. However it is important to note that AST is also found in other tissues and can therefore be elevated following injury of heart, skeletal muscle, kidneys, brain, pancreas and lungs[44]. Measurement of these enzymes does not provide information on hepatic function and this is better assessed by markers of synthetic function such as albumin level and platelet count in chronic disease and coagulation in both chronic disease and acute injury. However, coagulation is difficult to measure from the small volumes of blood obtained from mice, therefore necrotic cell area is used as another marker of degree of liver damage[20,21,23].

Hepatocytes are normally quiescent but following injury or signals from non-parenchymal cells (LSECs, stellate cells and leukocytes) they can proliferate and this proliferative capacity contributes to the liver's remarkable regenerative capacity which allows restoration of function, architecture and hepatic size following injury[19,45]. The capacity of the liver to regenerate following injury has been recognised for millennia but it was first demonstrated experimentally in the partial hepatectomy model presented by Higgins et al. in 1931 where they removed two thirds of a rat liver and demonstrated that the residual lobes hypertrophy to compensate for the removed liver mass within 5-7 days[46,47]. This regenerative capacity is employed in liver transplantation when a whole donor liver is split into a left and right segment with the smaller left segment being used in a child and the larger right in an adult[48]. The engrafted livers then enlarge through regeneration to provide the required hepatic function for the recipient[47]. Following toxic liver injury causing hepatocyte necrosis there is also hepatocyte regeneration which occurs through proportionate proliferation of hepatocytes[45]. Interestingly, the liver regeneration observed in this setting is dose dependent and Bhushan et al. have demonstrated that high doses of APAP resulted in poorer regeneration[41]. This failure of regeneration is associated with macrophage-derived transforming growth factor–β1 (TGF–β 1) ligand dependent induction of senescence in hepatocytes impairing their ability to proliferate[49]. It has also been suggested that resident and recruited macrophage phagocytic ability has an effect on regeneration with higher hepatocyte proliferation being seen in mice treated with CSF-1 which increases both macrophage number and phagocytic capacity[16]. The inflammatory response to injury and subsequent hepatocyte regeneration are therefore intricately linked.

The proliferative capacity of hepatocytes provides for a simple read-out of regeneration in that the proportion of proliferating cells can be used as a marker of regeneration as it is known that in the resting state ~2% of hepatocytes are proliferating[19,33]. We can therefore quantify the proportion of proliferating hepatocytes and quantify regeneration in murine models using antibodies to detect markers of proliferation. Two markers that I have used in my project are the cell cycle protein Ki67 which can be identified using an antibody or the thymidine analogue Bromodeoxyuridine (BrdU) which can be injected into mice and is incorporated into cells during S phase of mitosis labelling cells that are proliferating[33].

As outlined above toxins such as APAP and CCl_4 can cause damage to the parenchymal cells of the liver but they also have effects on the resident leukocytes to cause a reduction in the number of KC termed the "macrophage disappearance reaction"[16,21,22,50]. This loss of KC obviously has a negative effect on the homeostatic functions performed by these cells and can negatively impact the liver's ability to act as a firewall against blood-borne infection[16,40]. The mechanisms behind the macrophage disappearance are not fully understood but the inflammatory response to acute toxic insults such as APAP and CCl_4 involves recruitment of neutrophils and subsequently monocytes that develop into recruited macrophages[21–23]. In APAP, the hepatocyte damage results in the release of danger associated molecular patterns (DAMPs) such as high mobility group protein B1 (HMGB-1) which activates the remaining KC[51] causing them to release chemokines and cytokines that attract neutrophils and subsequently monocytes[21,51,52]. Monocytes and macrophages play a critical role in the response to acute liver injury and this will be explored below following a review of the biology of monocytes and macrophages in physiology.

1.3 Monocytes in physiology

We saw above that monocytes and their macrophage descendants play an important role in acute liver injury. I will later examine in more depth the roles of monocytes and macrophages in acute liver injury and my rationale for trying to manipulate these cells. However, in order to attempt to manipulate monocyte/macrophage responses it is important to have an understanding of the mononuclear phagocyte system (MPS) in both physiology and pathology.

The MPS was first described by van Furth et al. in 1972 to include all highly phagocytic mononuclear cells and their precursors[53]. In this system, they proposed that monocyte precursors in the bone marrow gave rise to peripheral blood monocytes and tissue macrophages. However, the history and study of these populations goes back a lot further to 1880 when Paul Ehrlich first described cells that would later go on to be named monocytes and Elie Metchnikoff first established the idea of the phagocyte in 1882[54,55]. Over recent years our definition of the MPS has grown to include DCs but there have also been significant developments in our understanding of the function and ontogeny of cells of the MPS with the application of elegant lineage-tracing techniques and the advent of novel technologies, such as single cell transcriptomic analysis[56]. Along with their role in physiology, monocytes and macrophages play both beneficial and detrimental roles in pathology and are therefore seen as potential targets for immunotherapy to dampen inflammation as well as promoting healing and regeneration.

1.3.1 Monocyte subsets

Monocytes are a heterogeneous population of cells in the blood that in humans are identified depending on their expression of the cell surface markers CD14 and CD16[57]. Using these surface markers it is possible to subdivide monocytes into classical ($CD14^{hi}$ $CD16^{-}$), intermediate ($CD14^{hi}$ $CD16^{lo}$) and non-classical monocytes ($CD14^{lo}$ $CD16^{hi}$)[58]. In humans, classical monocytes make up ~85% of all circulating monocytes [57,59] whereas in mice classical monocytes only make up ~50% of all monocytes[60]. In mice, classical and non-classical monocyte subsets were originally identified using what was at the time a novel reporter mouse for the receptor for Fractalkine (CX_3CL1), CX_3CR1. Fractalkine is a chemokine that is a chemoattractant but is also responsible for leukocyte adhesion and trafficking into tissues[61]. Using the CX_3CR1 reporter mouse, in whom green fluorescent protein (GFP) is 'knocked in' to the *Cx3cr1* locus, Geissmann et al. were able to identify two populations of mouse monocytes termed classical or $Ly6C^{hi}$ (CX_3CR1^{lo} $CCR2^{+}$ $Ly6C^{+}$) and non-classical or $Ly6C^{lo}$ (CX_3CR1^{hi} $CCR2^{-}$ $Ly6C^{lo}$)[62]. Subsequently Ingersoll et al. have demonstrated that there is relative conservation in the transcriptome in both classical and non-classical monocytes between humans and mice[60]. Owing to it not always being possible to use CX_3CR1 reporter mice, Ingersoll et al. also proposed that all monocytes should be identified by their surface expression of the CSF1R (also known as CD115) and then subdivided using Ly6C expression[60]. Briseno et al. recently demonstrated that once $Ly6C^{hi}$ monocytes start to express the TREM-like transcript 4 protein (TREML4) they are committed to becoming $Ly6C^{lo}$ monocytes in the circulation[63]. Therefore, in addition to being a positive marker of $Ly6C^{lo}$ monocytes, TREML4 is also a positive marker of transitioning $Ly6C^{hi}$ monocytes, homologous to the human $CD16^{lo}$ $CD14^{hi}$ population[58,63]. This is supported by single cell transcriptomic and epigenetic analyses showing that $Ly6C^{hi}$ monocytes represent an unstable cell population with a default differentiation potential toward $Ly6C^{lo}$ monocytes[64]. This transition process has been shown to rely on the transcription factor C/EBPβ which activates *Nr4a1* expression[64], a transcription factor previously demonstrated to be a master regulator of survival of $Ly6C^{lo}$ monocytes[65–67].

1.3.2 Monocyte development

Given the short half-life of monocytes it is important to understand their development prior to entering the circulation.

Haematopoiesis

Haematopoiesis is the dynamic process by which self-renewing haematopoietic stem cells (HSCs) generate progeny that differentiate into progressively restricted cells of the erythroid, myeloid, or lymphoid lineages

(Fig. 1.2)[68]. Leukocyte development relies on multipotent progenitors (MPPs) in the bone marrow which arise from haematopoietic stem cells and develop

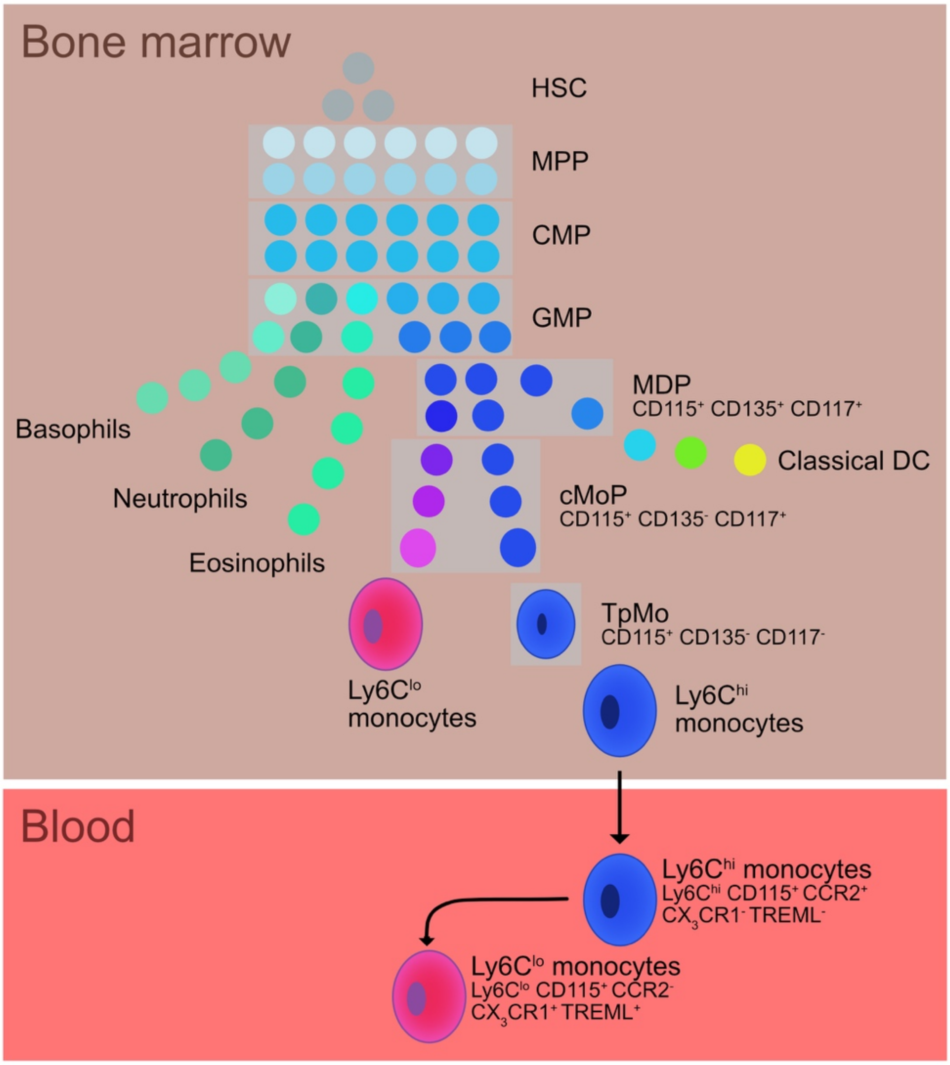

Figure 1-2 Myeloid cell development.

Current understanding of myeloid cell development. Haematopoietic stem cells (HSC); multipotent progenitors (MPP); common myeloid progenitor (CMP); granulocyte-macrophage progenitors (GMP); macrophage and DC precursor (MDP); common monocyte progenitor (cMoP); transitional premonocytes (TpMo). Light coloured boxes identify all cells that belong to the population name on the right. Downstream of MDP surface markers used to identify each population are outlined including $Ly6C^{hi}$ and $Ly6C^{lo}$ monocytes in blood. Adapted from Guilliams et al.[339]

into the common myeloid progenitor (CMP)[69,70]. CMPs give rise to the granulocyte-macrophage progenitors (GMP) and subsequent macrophage and DC precursor (MDP), which in turn gives rise to monocytes and DC in lymphoid and non-lymphoid tissues[71,72]. MDPs can be identified by their expression of CD117 (cKit), CD135 (Flt3) and CSF1R[73]. It has recently been demonstrated that there is a monocyte- and macrophage-committed progenitor cell derived from the MDP[74], termed the common monocyte progenitor (cMoP). cMoP can be identified by its lack of CD135 expression when compared to MDPs.

The use of novel transcriptomic and genetic approaches is challenging our understanding of early haematopoiesis and suggest that there is a lot more cellular plasticity during haematopoiesis than previously thought. Velten et al. have proposed that early HSCs emerge from a cloud of cells and gradually acquire lineage biases without passing through distinct early progenitor populations[75]. In keeping with this hypothesis, Giladi et al. have used single cell transcriptomic and CRISP-seq gene expression perturbation to demonstrate that specific transcriptional programs for neutrophils and monocytes can be identified in early progenitors[76]. These results, in conjunction with others that have used single cell transcriptomic approaches, suggest that although haematopoiesis is still the result of progressive restriction of developmental potential, there is a continuous flow of differentiation and lineage commitment may occur earlier than previously thought[68,75–77].

It had been thought that cMoPs gave rise to CD135$^{–}$ Ly6C^{hi} monocytes that are ready to enter the blood stream. However, it has now been demonstrated that this Ly6C^{hi} population is heterogeneous and actually represents two distinct populations: CXCR4^{hi} transitional pre-monocytes and CXCR4^{lo} mature monocytes[78]. Chong et al. have shown that these CXCR4^{hi} transitional pre-monocytes are immobilised in the bone marrow through a CXCL12-CXCR4 axis and proliferate prior to becoming mature CXCR4^{lo}

Ly6C^{hi} monocytes. Importantly these cells are no longer progenitor cells because they have lost the ability to self-renew likely due to the loss of CD117 (cKit)[78,79].

Regulators of monocyte development

Monocytes rely on CSF1R for their development as evidenced by the accumulation of monocyte precursors and deficiency in monocyte production in CSF-1R$^{-/-}$ mice[73,80]. Furthermore, it has also been shown that exogenous CSF-1 can instruct HSC fate at a single cell level, but it is not clear whether this occurs in homeostasis[81]. More recently it has been proposed that CSF-1 is most important in late steady state MPS development[82]. In this work, Louis et al. demonstrated that antibody mediated CSF-1 neutralisation resulted in a reduction in both BM and circulating Ly6C^{lo} monocytes but had little effect on precursor number or proliferation. Interestingly, Ly6C^{hi} monocytes are less affected in the absence of CSF-1 or CSF-1R.

Although the role of CSF-1 in monocyte development has not been fully elucidated, the transcription factor PU.1 has been identified as a master regulator of monocyte development. PU.1 has been shown to regulate differentiation pathways and proliferation of granulocytes and monocyte/macrophage precursors during haematopoeisis[83,84]. It has specifically been shown by DeKoter et al. using PU.1$^{-/-}$ mice that monocyte specification of haematopoietic precursors is dependent of PU.1[83] and it has been suggested that monocyte/macrophages gain sufficient and stable PU.1 levels by lengthening cell cycle [85].

Monocyte migration

CCR2 is expressed by Ly6C^{hi} monocytes in the bone marrow and circulation[62,78,86]. Although studies using CCR2$^{-/-}$ mice had implicated a role for this receptor in the recruitment of monocytes to inflamed sites and monocyte migration[87,88], it was subsequently shown in 2006 by Serbina et al. that CCR2 expression by bone marrow Ly6C^{hi} monocytes was a critical requirement for their egress from the bone marrow both during homeostasis and in a model of *Listeria monocytogenes* infection[89]. Notably, CXCR4 expression by transitional pre-monocytes is thought to reduce levels of CCR2, thereby leading to retention of these precursors in the bone marrow, while CXCR4-negative mature monocytes remain able to egress via CCR2[78]. The role of CCR2 in recruitment of monocytes from blood to tissues is less clear and the experiments required to demonstrate this are difficult to perform given that CCR2 is involved in monocyte egress from the BM. Nevertheless, mixed BM chimeric have been utilised to show that monocytes use CCR2 to enter the gut mucosa and peritoneal cavity under steady state conditions[90,91].

1.3.3 Monocyte function in steady state

Classically it is thought that Ly6C^{hi} monocytes represent a short-lived population that is predominately involved in inflammatory responses, whereas Ly6C^{lo} monocytes are longer lived and patrol blood vessels for signs of injury[62,92]. However, we will see below that Ly6C^{hi} monocytes also have a role during homeostasis.

Ly6C^{hi} monocytes and tissue macrophages in steady state

Resident tissue macrophages are one of the most abundant populations of leukocytes in the body that are involved in innate immunity, inflammation, tissue development and repair of damaged tissue[93]. These functions are tissue specific and as such there is dramatic variation in the identity of resident macrophages between tissues which is independent of the ontogeny of the cells[94]. Traditionally macrophages have been referred to as being classically activated (M1) when associated with bacterial infection or exposure to type 1 cytokines (e.g. IFNγ) or alternatively activated (M2) when associated with type 2 inflammation or tissue repair and regeneration. In recent years it has become more evident that there is a spectrum of macrophage activation and that they have specialized properties that are precisely adapted to individual tissues and circumstances[93].

In van Furth's original model of the MPS all tissue macrophages were considered to be derived from circulating monocytes. However this model has been challenged by studies using parabiosis and genetic fate mapping techniques to show that in most adult tissues macrophages are derived from progenitors derived from the yolk sac or foetal liver[86,95,96]. However, soon after these revelations, two tissues were described wherein circulating adult monocytes contribute to the resident tissue macrophage population during homeostasis: the adult colon[72,90,97] and dermis[98]. It was proposed that the colon and dermis behave differently because of their constant exposure to microorganisms with resultant low grade inflammation referred to as "primed homeostasis" [73,99]. The suggestion is that this low grade inflammation results in a constant recruitment of monocytes that replace the resident macrophages[100]. However, this paradigm has recently been challenged by the observation of low-level engraftment of monocytes into tissue resident macrophage populations in several additional tissues[86,101].

Using tissue protected irradiation BM chimeras to fatemap the origin of macrophages, Bain et al. demonstrated that in addition to dermal and colonic macrophages there was a reliance on blood monocytes for the maintenance of cardiac, kidney, lung interstitial, pleural and peritoneal macrophages[91]. In the lamina propria of the colon the concept of continual replacement of resident macrophages by Ly6C^{hi} monocytes has also been challenged with the finding that, in addition to the rapidly turning over population of macrophages, there is also a population of locally maintained resident macrophages[102]. This work by Shaw et al. also challenged the idea of the "primed homeostasis" in the gut because analysis in germ free mice revealed that absolute numbers were decreased in all populations of gut macrophages irrespective of their ontogeny[102]. Despite this, some tissue macrophage populations do exist independently of circulating monocytes during adulthood, including Langerhans cells in the epidermis, microglia and alveolar macrophages[96,103,104]. The current thinking is therefore that there is a spectrum of contribution of adult monocytes to tissue macrophage populations and the differences between tissues is likely reflective of the local environment.

Upon entering the tissue, blood Ly6C^{hi} monocytes gradually acquire the surface characteristics of tissue macrophages: gaining expression of the macrophage markers CD64, Mer tyrosine kinase (MerTK) and major histocompatibility complex class II (MHCII) whilst downregulating the monocyte surface markers Ly6C and CCR2[98]. It has been demonstrated that in addition to acquiring the surface phenotype of a resident macrophage, recruited Ly6C^{hi} monocytes that have engrafted into tissue macrophage pools have the ability to adopt functions of the resident population[50,105,106]. Furthermore, it has been demonstrated in the liver that 30 days after experimental engraftment of adult monocytes in the resident cell niche they have the same functional response to infective and drug induced liver injury as embryonically derived resident KC[107]. In the lung, it has also been demonstrated that engrafted adult monocytes can acquire the function of resident alveolar macrophages. Mice lacking alveolar macrophages develop pulmonary alveolar proteinosis (PAP) but a year after engraftment of adult monocytes there is no increase in PAP when compared to mice with embryonically derived alveolar macrophages [108,109]. Both these models are artificial and do not necessarily reflect what happens in pathophysiology, but they do provide insight on the ability of adult monocytes to engraft into tissue resident populations. The signals that regulate the differentiation of a Ly6C^{hi} monocyte into a tissue resident macrophage during homeostasis are not fully understood but it is thought that both cytokines and cell-cell interactions play tissue specific roles in the so-called “niche” to dictate resident macrophage genotype, phenotype and function[101].

In addition to becoming Ly6C^{lo} macrophages it has been demonstrated that monocytes can differentiate into DC[56]. Similar to classical DC they express CD11c and can present antigen to T cells in response to a variety of stimuli such as allergens and bacteria[110,111]. In contrast to classical DC they are efficient at phagocytosis have a poor migratory capability[98] and express macrophage markers such as F4/80, MERTK and CD64[98,110,112].

Ly6C^{lo} monocytes in steady state

During homeostasis Ly6C^{lo} monocytes patrol the vasculature looking for any signs of damage or inflammation and have therefore been referred to as the "housekeepers of the vasculature" [67]. This housekeeping function is mediated by monocyte expression of lymphocyte function associated antigen 1 (LFA1) and endothelial expression of intercellular adhesion molecule 1 (ICAM1)[62,67,92]. The human homologue of Ly6C^{lo} monocytes, CD14^{dim} circulating monocytes, have been demonstrated to have similar behaviour and are involved in the innate local surveillance of tissues[113]. In addition to their immune surveillance role Ly6C^{lo} monocytes have been demonstrated to scavenge peptides and microparticles from the lumen of blood vessels[67,114]. In so doing, it has been suggested that they can play a role in maintaining homeostasis and inhibiting pathology by removing amyloid beta, which is a peptide associated with cerebral amyloid angiopathy and the development of Alzheimer's disease[114].

1.3.4 Monocytes during inflammation

In addition to providing a source of tissue macrophages during homeostasis, Ly6C^{hi} monocytes are a dynamic, rapidly recruitable pool of cells primed to respond to inflammatory stimuli and extravasate into tissues[62,100].

Ly6C^{hi} monocytes during pathology

Recruitment of Ly6C^{hi} monocyte to the site of acute and chronic sterile inflammation/injury has been demonstrated in many settings and many tissues, including the liver[21,22,115], colon [116,117], heart[118–120] and peritoneum[86,121]. During infection with bacteria or helminths Ly6C^{hi} monocyte recruitment to the site of infection has also been demonstrated[31,89,122,123]. In fact, Ly6C^{hi} monocytes are recruited to most areas of inflammation and are therefore involved in a multitude of pathologies that also include cancer[124] and autoimmune disease[125]. It had initially been proposed that all monocyte recruitment to sites of injury was dependent on CCR2 and this has been demonstrated in sterile inflammation [21,98,117,118] and certain infections such as *Toxoplasma gondii* in the central nervous system[126,127]. However, it has been demonstrated that during thioglycolate elicited inflammation in the peritoneal cavity the dependence on CCR2 for Ly6C^{hi} monocyte recruitment seemed to be time sensitive[89,128]. Furthermore, it has been shown that in atherosclerosis CCR5 and CX_3CR1 deficiency negatively impacted Ly6C^{hi} monocyte recruitment implying that they are required in addition to CCR2 for Ly6C^{hi} monocyte recruitment[129].

Following recruitment of Ly6C^{hi} monocytes to sites of inflammation by chemokines such as, adhesion molecules on their surface interact with their binding partners expressed on endothelial cells. This results in monocyte trafficking into tissues which involves rolling, adhesion and transmigration via the endothelial cells that make up the blood vessel wall[130]. During tethering and rolling monocytes express L-selectin which binds glycoproteins on endothelial cells. The subsequent adhesion is in part due to lymphocyte function-associated antigen 1 (LFA1) and macrophage receptor 1 on monocytes binding to intercellular adhesion molecule 1 (ICAM1) on endothelial cells during steady state patrolling and inflammation respectively[130,131]. Ly6C itself could also be involved in the adhesion of monocytes because although its function in monocytes is not fully understood it has been shown that it is important for the homing of T cells to lymph nodes[132]. In fact in vitro experiments performed by Hanninen et al. suggested that it promotes the firm adhesion of T cells to ICAM1 enhancing their compartmentalization into lymph nodes. Finally transendothelial migration relies on the platelet/endothelial-cell-adhesion molecule (PECAM1/CD31)[133]. During homeostasis in the liver it has been suggested that downregulation of ICAM1 limits leukocyte influx[134]. However, it has been shown that ICAM1 expression is important for regeneration following partial hepatectomy and inflammation results in the upregulation of ICAM1[134,135]. During hepatic infection with *Listeria monocytogenes* it has been shown that although egress from bone marrow is CCR2 dependent this was not required locally for recruitment within the liver and it was the local induction of ICAM1 adjacent to areas of infection that was important for the targeting of Ly6C^{hi} monocytes[131]. Therefore, in addition to chemokines monocyte adhesion molecules and their binding partners expressed on endothelial cells play an important role in regulating monocyte trafficking.

It is evident that mechanisms underlying the recruitment and differentiation of Ly6C^{hi} monocytes during inflammation vary depending on the stimulus, the tissue and the duration of the insult. However, one common feature of Ly6C^{hi} monocyte recruitment in both sterile inflammation and infection is the ability of these cells to become Ly6C^{lo} macrophages once recruited to the site of injury[31,89,97]. The murine model of myocardial infarction (MI) is an eloquent model of how our understanding of monocyte conversion into macrophages has evolved. In this model, it was previously thought that pro-reparative Ly6C^{lo} monocytes were mobilised into the injured tissue as a second wave following an initial influx of pro-inflammatory Ly6C^{hi} monocytes[118]. However, using *Nr4a1* deficient mice that lack Ly6C^{lo} monocytes it has been subsequently shown that Ly6C^{hi} monocytes are recruited to the injured heart and then convert into Ly6C^{lo} macrophages in situ[136]. This result epitomises the current prevailing theory of monocyte macrophage dynamics during inflammation, whereby recruited Ly6C^{lo} macrophages arise from Ly6C^{hi} monocytes, while Ly6C^{lo} monocytes do not generally enter tissues. In the liver it has been demonstrated using adoptive transfer experiments that during both acute injury APAP overdose and chronic injury with CCl_4 there is conversion of Ly6C^{hi} monocytes into Ly6C^{lo} macrophages that are required to orchestrate the resolution of inflammation[21,115].

In addition to $Ly6C^{hi}$ monocytes being precursors to $Ly6C^{lo}$ macrophages during inflammation they also play pro-inflammatory roles and modulate the immune response. For example, in the dextran sodium sulphate (DSS) model of colitis inhibition of $Ly6C^{hi}$ monocyte recruitment results in a less severe disease phenotype in this model. Zigmond et al. have shown that $Ly6C^{hi}$ monocytes isolated from DSS treated colons had a proinflammatory signature with high expression of TREM-1, iNOS, IL-6, and IL-23[116]. While this fits with their initial classification as ‘inflammatory’ monocytes, it is now clear that $Ly6C^{hi}$ monocytes have wider roles. For instance, they appear to regulate the innate immune response in APAP overdose by regulating the neutrophil response to injury[52]. Graubardt et al. showed that in monocyte deficient livers there was a reduction in apoptotic neutrophils which was associated with a reduction in proapoptotic genes. This monocyte orchestrated control of neutrophils is important to prevent excessive tissue damage. A similar regulatory role for monocytes has been shown in *Toxoplasma gondii*-induced ileitis where they produce IL-10 and regulate neutrophil reactive oxygen species (ROS) production[137].

$Ly6C^{lo}$ monocytes during pathology

As outlined above, although it was previously thought that during pathology $Ly6C^{lo}$ monocytes were recruited to tissues[118], recent work using intravital imaging in *Nr4a1* deficient mice suggests that $Ly6C^{lo}$ monocytes are restricted to the vasculature[65,67]. Even though $Ly6C^{lo}$ monocytes are restricted to the vasculature, it has been demonstrated that they have a role in pathology involving the vascular wall. In the kidney they can sense danger signals which causes CX_3CR1 dependent adhesion to the endothelium. The adherent $Ly6C^{lo}$ monocytes then coordinate neutrophil recruitment to mediate the focal necrosis of the endothelial cells[67]. Furthermore, they have been demonstrated to interact with metastasising tumour cells in the tumour microvasculature promoting NK cell recruitment and activation to prevent metasatases[138]. The inhibition of tumour metastases and their role in clearing circulating amyloid outlined earlier demonstrate that although $Ly6C^{lo}$

monocytes are limited to the vasculature they can have important systemic effects and roles in pathology[114,138].

Summary

The concept of recruitment of $Ly6C^{hi}$ monocytes to inflamed tissues is common to a multitude of pathologies in various tissues but there are nuances in the factors that mediate these responses that are tissue and aetiology dependent[95,139]. Below I will therefore focus on monocytes and macrophages in acute liver injury as this was the focus of my project.

1.3.5 Resident and recruited macrophages in liver injury

As alluded to above, the regeneration following acute liver injury is reliant on the innate immune system which is critical for maintaining immunity and coordinating regeneration. The roles of these cell types is outlined below and in Table 1.1.

KC during liver injury and repair

During homeostasis KC have been shown to play a primarily tolerogenic role acting as a firewall to intestinal microbes and regulating the local immune environment in the liver however following injury they play divergent roles[40,93]. Following acute injury there is a macrophage disappearance reaction which results in a significant reduction in KC and is followed by a recovery of KC during the regenerative phase of injury[21–23,115]. It has not yet been established whether the KC population is restored by local proliferation or incorporation of monocyte derived macrophages into the resident KC population. Mossanen et al. proposed that restoration of the KC population occurs unhindered following APAP-driven acute liver injury in $CCR2^{-/-}$ mice, suggesting the recovery of KC does not require a contribution from the monocyte pool[23].

Concurrent with the macrophage disappearance following injury, KC are activated by the release of danger-associated molecular patterns (DAMPs) from damaged hepatocytes[51,140]. In conjunction with hepatic stellate cells and

Table 1-1 Monocyte, macrophage and neutrophil functions in acute DILI

Cell type	Function
Kupffer cells	•Recruit monocytes through release of CCL2[22,141,142] •Secrete pro-inflammatory cytokines: TNF-α, IL-1β, IL-6[140] •Attract neutrophils through release of CXCL1, CXCL2, and CXCL8[143]
Neutrophils	• Phagocytose necrotic debris[52] • Amplify the inflammatory response and damage hepatocytes with increased ROS production[19,52]
Ly6C^{hi} monocyte	• Aggravate early injury and upregulate pro-inflammatory genes and chemokines: *Trem1*, *Nos2*, COX2, CCl2 and CCl7[21] • Concurrently express pro-reparative genes: *Arg1*, *Chil3, Vegfa,* semaphorin 4A and D, *Hif1a* and *Plaur*[21] • Promote neutrophil mediated phagocytosis and activation[52]. • Suppress neutrophil pro-apoptotic genes and cell survival molecules (BCL21A) to control neutrophil activation[52]. • Convert into Ly6C^{lo} macrophages required for resolution & repair[23,99]
Recruited Ly6C^{lo} macrophage	• Downregulate expression of pro-inflammatory genes found in Ly6C^{hi} monocytes[21] • Upregulate genes associated with type 2 immune responses: *Mrc1*, *Retnla*, *Trem2* and *Igf1*[21] • Clear necrotic cell area[144] • Restore the liver firewall by phagocytosing bacteria[16,40]

hepatocytes, activated KC release monocyte chemotactic protein-1 (MCP-1 also termed CCL2) which is elevated in blood and liver early following acute liver injury and serves to attract Ly6C^{hi} monocytes to the injured liver in both humans and mice[22,141,142]. Activated KC also serve to amplify the pro-inflammatory phenotype by secreting pro-inflammatory cytokines (TNF-α, IL-1β, IL-6) and are important for the generation of CXC chemokines that attract neutrophils (CXCL1, CXCL2, and CXCL8)[140,143]. Nevertheless, it has been reported that the transcriptional signature of KC later during injury (72hrs following APAP) is indistinguishable from steady state KC[21]. Whether KC and recruited macrophages play distinct roles remains to be determined with certainty. Transcriptional analysis has shown that when compared with recruited macrophages, KC exclusively express genes to mediate the engulfment of phosphatidylserine expressing apoptotic cells (*Timd4, Stab2*) and have higher levels of scavenger receptors (*Marco, CD163 and Mrc1*)[21]. Furthermore, KC and recruited Ly6C^{lo} macrophages upregulate different repertoires of extracellular matrix remodelling enzymes.

Given the differing kinetics and transcriptome of resident and recruited macrophages it is likely they play different functions in the repair process post injury. However, experimentally it remains difficult to target only one population as most genetic tools (e.g. LysM-Cre, CSF1R-Cre) will affect both KC and recruited cells. The recent identification of Clec4F as a unique feature of KC and the generation of Clec4F-Cre and Clec4F-DTR mice should allow targeting of the hepatic resident population and not recruited monocytes[50].

Monocytes/monocyte-derived macrophages during injury and repair

Recent work has charted monocyte and macrophage dynamics following APAP overdose, showing that the number of Ly6C^{hi} monocytes peaks at 24 hours and the number of resultant Ly6C^{lo} macrophage peaks at 72hrs post injury[52]. However, if and how monocytes and macrophages change following acute CCl_4 induced injury has not yet been elucidated.

We saw above that there is an increase in hepatic concentrations of the CCR2 ligand, MCP-1 (CCL2) following injury, as such it was hypothesised that the recruitment of monocytes was dependent on CCR2 in liver injury[21–23,128,145]. Indeed in both acute CCl_4 and APAP overdose monocyte recruitment has been demonstrated to be primarily CCR2 dependent[23]. Given the importance of CCR2 in monocyte recruitment attempts have been made to manipulate the CCL2/CCR2 axis which have in turn shone light on the role of monocytes during acute injury and regeneration. Zigmond et al. demonstrated that inhibition of Ly6C^{hi} monocyte recruitment using an anti-CCR2 mAb (MC21) resulted in a reduction in newly recruited Ly6C^{lo} macrophages and evidence of prolonged histopathological damage, with worse necrosis in livers of MC21-treated mice at both 24 and 48 h following APAP administration[21]. Upon early administration of a CCR2/CCR5 inhibitor (Cenicriviroc; CVC), Mossanen et al. demonstrated a CCR2 dependent inhibition of monocyte recruitment and an early improvement in ALT and necrotic cell area, however this this benefit was lost if CVC was administered 12 hours after APAP[23]. These divergent results could be explained by the apparent accumulation of monocyte-derived "pro-reparative" Ly6C^{lo} macrophages in the CVC model at 48hrs that also suggests recruitment of these cells in the later phase of injury is independent of CCR2. The accumulation of Ly6C^{lo} macrophages was completely inhibited through the course of APAP when MC21 was used to deplete monocytes from 12hr prior to injury[21,23]. Furthermore, in humans it has been demonstrated that monocytopenia is associated with worse outcomes following APAP overdose[15]. Hence, together these data suggest that while monocytes may initially aggravate liver injury caused by APAP, these cells, or their descendants subsequently play a beneficial role in the repair/regeneration process. This pro-reparative function of monocyte-derived macrophages would seemingly mirror the repair response during ischaemic cardiac injury, wherein the rapid recruitment of pro-inflammatory monocytes to a different sterile injury site is required to generate sufficient numbers of macrophages to initiate the repair process[146].

Consistent with their role in many other pathologies, Ly6C^{hi} monocytes recruited during APAP injury express a pro-inflammatory transcriptional profile. When compared to recruited Ly6C^{lo} macrophages (at 72hrs post APAP), Ly6C^{hi} monocytes (at 24hrs post APAP) expressed high levels of pro-inflammatory genes: triggering receptor expressed on myeloid cells-1 (*Trem1*), NO synthase 2 (*Nos2*), COX2 (*Ptgs2*), and the chemokines *Ccl*2 and *Ccl7*. Interestingly both Zigmond (at 24hrs post APAP) and Mossanen (at 12hrs post APAP) demonstrated that Ly6C^{hi} monocytes expressed pro-reparative genes concurrent with their pro-inflammatory gene profile, suggesting that the relationship between pro-inflammatory and pro-restorative monocyte derived cells is not dichotomous and could represent a continuum. In Ly6C^{hi} monocytes the pro-reparative phenotype was exemplified by the upregulation of genes associated with a type 2 immune response: arginase 1 (*Arg1*) and chitinase-3-like protein 3 (*Chil3*) (reviewed below). The pro-reparative potential of the Ly6C^{hi} monocytes was further emphasised by the expression of genes associated with angiogenesis including: vascular endothelial growth factor-A (VEGF-A; *Vegfa*), semaphorin 4A and D (*Sema4a* and *Sema4d*), hypoxia-inducible factor-1a (*Hif1a*) and the plasminogen activator urokinase receptor gene (*Plaur*)[21]. Concurrent with their maturation into Ly6C^{lo} macrophages, Ly6C^{hi} monocytes downregulate expression of Ly6C and the pro-inflammatory genes. To realise their reparative potential they also upregulate other genes associated with type 2 immune responses like: mannose receptor 1 (*Mrc1*), the resistin- like molecule a (*Retnla*), *Trem2* and insulin- like growth factor 1 (*Igf1*)[21].

Macrophages in human liver injury

Encouragingly data from murine studies reflects the limited data available from human studies, where an expansion of circulating monocytes and hepatic macrophages expressing MerTK occurs following acute APAP induced liver injury[144]. MerTK activation in macrophages mediates suppression of pro-inflammatory cytokines and promotes efferocytosis of apoptotic cells[147]. Consistently, Triantafyllou et al. demonstrated that MerTK^{+} monocytes secreted pro-reparative mediators and down regulate pro-inflammatory mediators. Furthermore, they demonstrated that APAP injured MerTK$^{-/-}$ mice had impaired recovery with increased necrotic cell area and persistence of neutrophils[144]. This demonstrates a functional mechanism for MerTK in monocytes and macrophages following DILI. The importance of macrophages in human APAP overdose is also inferred by the negative correlation of serum CSF-1 levels with survival demonstrated by Stutchfield et al.[16]. Using murine models, these authors showed that exogenous CSF-1 reduced ALT and increased proliferation in recruited and resident macrophages. Concurrent with this increase in macrophages, they also demonstrated increased phagocytosis of pHrodo *E. coli* bioparticles by infiltrating macrophages in mice treated with exogenous CSF-1. It was therefore proposed that CSF-1 may be important in APAP induced liver injury through restoring the liver firewall by enhancing the capacity of macrophages to phagocytose bacteria[16,40]. Further studies in humans are required but are hindered by access to samples in this acutely unwell group. However, there is promising work on the use of FNA biopsies of liver that although not validated in patients with ALF may provide the opportunity for flow-cytometric analysis of hepatic leukocytes during DILI[148].

In chronic injury the therapeutic benefits of delivery of autologous alternatively activated macrophages are currently being evaluated in humans in the MAcrophage Therapy for liver CirrHosis (MATCH) trial[21,149]. The MATCH trial is a dose-escalation phase I and randomised controlled phase II study assessing the effect of infusion of autologous alternatively activated monocyte derived macrophages[150]. The trial follows on from work demonstrating that peripheral blood monocytes (PBMCs) can be isolated from cirrhotic patients and then matured into CD206 (mannose receptor) expressing alternatively activated macrophages[151]. Moore et al. went on to demonstrate that these alternatively activated macrophages could be adoptively transferred into fibrotic CCl_4 treated mice resulting in a reduction in fibrosis and injury as assessed by picosirius red staining, ALT and AST.

Although all the data would suggest that Ly6C^{lo} recruited macrophages have a role in promoting repair as demonstrated by their transcriptome and phagocytic functions, no definitive functional evidence has been provided that they do indeed have a beneficial effect on repair[16,21,144,145]. The difficulty in establishing a functional role in this setting is in developing a tool to target only recruited macrophages and not their precursors (the monocytes) or the resident macrophage populations.

Summary

Initially monocytes play an important role in the inflammatory response in acute liver injury but they are also necessary for the repair process. However it remains unclear whether it is possible to manipulate the monocyte/macrophage response to lessen the inflammatory insult and at the same time enhance repair and regeneration. It is hoped that single cell genomic approaches and the use of novel KC specific Cre lines will enable further dissection of this process including establishing the contribution of the various cells to the initiation of injury and regeneration following injury.

1.4 Type 2 immunity

Type 2 immunity is a major effector response against helminth infection and atopy that has many host protective effects during helminth infection but can also be pathogenic. It is considered a counterbalance to, and inhibitory of, the inflammatory type 1 immune response generated in response to bacterial, viral, fungal and protozoal infections. Many novel therapies for chronic inflammatory conditions and cancers rely on directly manipulating our immune responses. The host protective response seen in type 2 immunity would therefore seem a potential target to enhance repair in not only helminth infection but other inflammatory diseases. However, prior to manipulating type 2 immune responses it is very important to understand the cytokines and pathways involved in order to avoid promoting the potentially pathogenic effects of type 2 immune activation.

1.4.1 Interleukin-4 and interleukin-13

IL-4 and IL-13 are the canonical T helper type 2 (Th2) cytokines that largely co-ordinate type 2 immunity. Accordingly, these cytokines have a large variety of functions in type 2 immunity that depend on target cell type and context. IL-4 and IL-13 have many overlapping but also distinct functions, with IL-13 specifically being demonstrated to have a pro-fibrotic role and be associated with increased mucus production[152–154]. This is intriguing because both IL-4 and IL-13 signal to cells through a common receptor, the IL-4Ra. The actions of these cytokines and how differences in function arise are considered next.

IL-4 and IL-13 signalling

The IL-4 receptor (IL-4R) is the central mediator of type 2 immune responses and has two subtypes that share a common IL-4Rα chain (Fig. 1.3). The type I receptor comprises an IL-4Rα chain which is a heterodimer with an IL-2Rγ_2 chain, to which only IL-4 can bind[155]. The type II receptor is a heterodimer of IL-4Rα and the IL-13Rα1 and both IL-4 and IL-13 can bind to this receptor[156]. The effector functions of both type I and type II IL-4R are mediated by a transcription factor that is selectively coupled to the IL-4R: signal transducer and activator of transcription 6 (STAT6)[157]. There is also a 3rd receptor in the family; the monomer IL-13Rα2 which lacks canonical Janus kinase (JAK)–STAT signalling and has a high affinity specifically for IL-13 (Fig. 1.3)[158,159]. It is therefore known as a decoy receptor because its binding results in internalisation of the ligand preventing IL-13 from engaging with IL-13Rα1. Through this action of clearing IL-13 without inducing STAT-6 activation, the decoy receptor functions to dampen the effect of IL-13 [155,160,161]. This difference in the ability of IL-4 and IL-13 to bind to the type I and II receptors means there are potentially different downstream effects of both IL-4 and IL-13 which can in part be mediated by differential expression of the receptors by various cell types[162,163]. One recent example of this is the IL-13 dependent activation of the ductular reaction, steatosis and fibrosis seen in the liver[152].

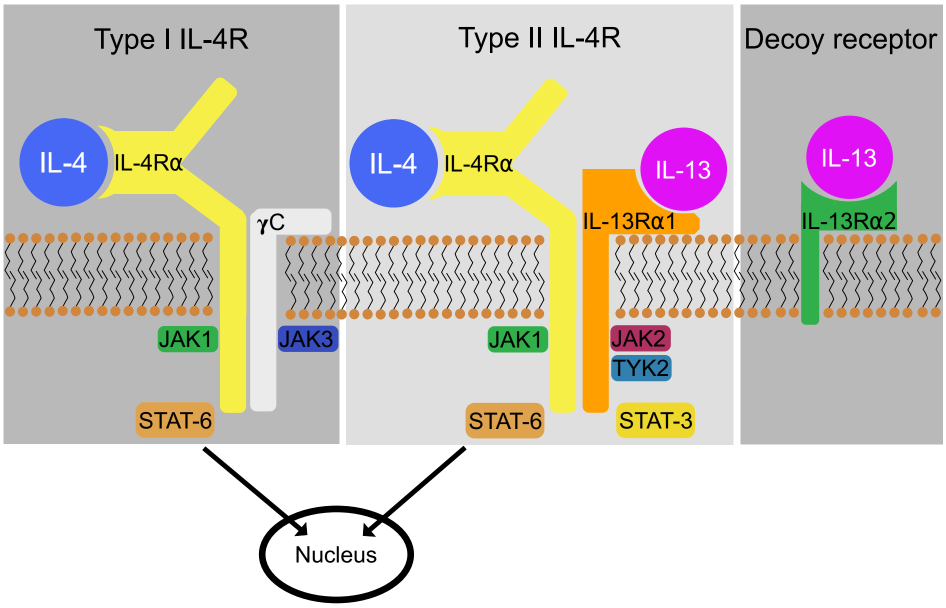

Figure 1-3 Il-4 receptors and downstream signals.

Type I and II IL-4 receptors (IL-4R) and decoy receptor. Binding of IL-4 (blue circle) or IL-13 (magenta circles) results in dimerisation of the receptors and activation of the associated tyrosine kinases: janus kinases (JAKs) and Tyk2. This results in phosphorylation of signal transducer and activator of transcription 6 (STAT-6) which dimerises and is transported to the nucleus where it binds to the promoters of IL-4 and IL-13 sensitive genes. In non-haematopoeitic cells binding of IL-13 to the IL-13Ra1 can result in STAT-3 activation. Adapted from Wills-Karp et al.[156]

The differential effects of IL-4 and IL-13 have been well studied in the helminth infection model of *Schistosoma mansoni* which causes schistosomiasis. Schistosomiasis is a disease characterised by an initial acute phase during the first 3-5 weeks following infection where there is migration of worms to the liver and maturation in the portal vein[164]. This acute phase is dominated by a pro-inflammatory T_H1 response with production of pro-inflammatory cytokines like tumour necrosis factor (TNF), interleukin 1

(IL-1) and interleukin 6 (IL-6)[164]. Concurrent with the onset of egg production by mature schistosome, the acute phase is followed by a chronic phase starting in week 6 which is characterised by granuloma formation around newly deposited eggs in the liver and hepatic fibrosis. This chronic phase is dominated by a strong Th2 response, and has been used as a model to study the regulation of Th2 responses and in particular sheds some light on the differences between IL-13 and IL-4 signalling. Using a soluble IL-13 receptor α2-Fc fusion protein (sIL-13Rα2-Fc) that blocks IL-13 activity and IL-$4^{-/-}$ mice Chiaramonte et al. demonstrated that IL-4 and IL-13 are both independently sufficient for granuloma formation but that reduction in fibrosis observed in IL-4–deficient mice was much less pronounced than that in sIL-13Rα2-Fc–treated animals[153]. They therefore concluded that IL-4 was integral for mast cell differentiation, eosinophil differentiation and recruitment and IL-13 was required for the development of hepatic fibrosis. Further insight into the divergent functions of the IL-4 and IL-13 was revealed by using IL-13Rα$1^{-/-}$ mice which have a deficiency in the type II receptor but still have an intact type I receptor [163]. In this setting Ramalingam et al. demonstrated that the type II receptor could supress T_H2 responses and was involved in the activation of important mesenchymal cells such as fibroblasts and epithelial cells, which contribute to the development of chronic morbidity and mortality in schistosomiasis and in allergic asthma. Furthermore and importantly for the work in my project the type I receptor was proposed as the dominant receptor in inducing alternative activation of macrophages[163]. In vitro Heller et al. have dissected the differing transcriptomic effects of IL-4 and IL-13. In so doing they demonstrated that IL-4 induced stronger macrophage expression of mRNA that encoding proteins associated with type 2 immunity (Ym1, Fizz1 and Arginase 1) when compared to IL-13[165].

1.4.2 IL-4 driving tissue repair

The importance of IL-4 in tissue repair has been elucidated by indepth study of helminth infections and more recently in non-helminth settings.

During S. mansoni infection IL-4 is important for survival because in IL-4$^{-/-}$ mice that develop haemorrhagic lesions in the small intestine die during the acute phase of the infection[166]. In WT mice adult worms develop in the blood stream and then lay eggs that cross the basement membrane of the vein, and traverse the intervening tissue, basement membrane and epithelium of the intestine for excretion[164]. This is normally associated with a TH2 response characterised by granuloma formation and eosinophilia, however in IL-4$^{-/-}$, but not in IL-13$^{-/-}$ mice this type 2 immune response is lost and there is increased production of pro-inflammatory Interferon-γ (IFN-γ) by CD4^{+} lamina propria T cells[166,167]. These experiments point towards a specific role for IL-4 in preventing tissue damage associated with gut translocation of *Schistosoma mansoni eggs*. During the chronic phase of Schistosomiasis hepatic granuloma formation is impaired in STAT6 deficient mice however there is no significant difference in granuloma formation observed in IL-4$^{-/-}$ mice[153,160,168]. This supports the idea that IL-13 is important for the granuloma formation and consistent with this, IL-13$^{-/-}$ mice exhibit impaired granuloma formation[153]. Taken together these results would suggest that in Schistosomiasis IL-4 is important for the repair process following helminth induced damage and IL-13 is important for the fibrotic disease and containment of the infection[26].

The importance of IL-4 in limiting acute damage has also been seen in another helminth infection associated with a profound type 2 immune response. *Nippostrongylus brasiliensis,* is a nematode that migrates to the lung alveoli where it results in destruction of alveoli and long term airway hyperresponsiveness even though they only spend 3-4 days in the alveolar space[169]. The tissue destruction is evident both histologically and by identification of acute haemorrhage in the bronchoalveolar lavage (BAL) obtained from infected mice. Chen et al. have demonstrated that acute haemorrhage was worse in IL-4R$\alpha^{-/-}$ mice and this was also associated with a higher number of neutrophils in the BAL of these mice[25]. In this model they propose that in addition to IL-4 being required to limit the acute injury macrophages are also critical for the repair of the injured lung. More recently it has also been shown that IL-4Rα dependent protein Ym1 (discussed below) is important at directing the initial response to *N. brasiliensis* towards a repair phenotype[170]. During the recovery phase Ym1 limits excessive immune activation further emphasising the importance of IL-4Rα signalling in orchestrating the reparative response to *N. brasiliensis*[170].

As well as playing a role in tissue repair in Th2 dominated infections, IL-4 has recently been demonstrated to play a crucial role during infection with the foodborne bacterial pathogen *Listeria monocytogenes*[31]. Bleriot et al. demonstrate that there is a switch on day 3 post infection from an early type 1 immune response characterised by high levels of *Ifng* expression in mononuclear phagocytes to an increase in *Ym1* and *Arg1* expression characteristic of a type 2 immune response[26,31]. They demonstrate the importance of IL-4 to the repair process as the bacteria are cleared in IL-4$^{-/-}$ mice but the inflammation persists. Furthermore, they demonstrate that administration of IL-4c at the time of infection results in an inability to control the infection whereas hyperpolarisation of the type 2 response on day 3 post infection resulted in a significant reduction in inflammatory infiltrate but a failure to clear the infection and the persistence of bacteria in the liver. Hence this is a key demonstration of the need for IL-4 to switch off inflammation even in ostensibly Th1-dominated infection.

1.4.3 Endogenous IL-4 in acute liver injury

De Angelis were the first to demonstrate that there was a role for endogenous IL-4 in the regenerative process in murine liver following partial hepatectomy[171]. De Angelis et al demonstrated that there was increased mortality in IL-4$^{-/-}$ mice following partial hepatectomy and proposed IL-4 produced by NKT cells was essential to control complement activation that normally negatively regulates the induction of IL-6 by hepatic macrophages. As IL-6 has been proposed to be integral to hepatic regeneration due to its effect of promoting hepatocyte proliferation[172], IL-4 would then appear to indirectly contribute to the regeneration by potentiating IL-6-driven hepatocyte proliferation. Consistent with this, DeAngelis observed near absent hepatocyte proliferation in IL-4$^{-/-}$ mice[171]. Similarly, an important role for IL-4 has also been demonstrated in acute liver injury secondary to APAP (300mg/kg) where IL-4$^{-/-}$ mice and mice administered anti-IL-4 antibodies have increased mortality and higher ALTs[173]. These results led to the work by Goh et al. who showed that IL-4 promoted liver regeneration in both the partial hepatectomy model and the acute CCl_4 model of liver injury[33]. In contrast to the work of De Angelis et al, Goh et al proposed that recruited eosinophils were the key source of endogenous IL-4 rather than NKT cells. Using ΔdblGATA (eosinophil deficient) and using IL4Rα$^{fl/fl}$AlbCre (hepatocyte specific IL-4Rα deletion) mice they demonstrated that IL-4 directly promoted hepatocyte proliferation following CCl_4 injury and partial hepatectomy and that hepatocyte proliferation was reduced in the absence of eosinophils. Furthermore, by analysing both 4-get, IL-4 reporter mice, and 4get ΔdblGATA mice it appeared that eosinophils were the predominant IL-4 producing cells in the liver following CCl_4 injury. In CCl_4 injured mice hepatocyte specific loss of IL-4Rα (IL4Rα$^{fl/fl}$AlbCre) resulted in a reduction of hepatocyte proliferation from ~60% to ~45% but notably this proliferation didn’t return to the baseline hepatocyte proliferation observed in other experiments suggesting unsurprisingly that factors other than IL-4 signalling are involved in driving the elevated hepatocyte proliferation. However, a lack of uninjured control mice in these experiments make it difficult to say for certain what degree of injury-related proliferation occurs via this pathway. Furthermore, Goh et al did not report if IL-4 signalling to hepatocytes effected necrotic cell area or serum ALT levels, so whether the beneficial effect of endogenous IL-4 is restricted to induction of hepatocyte proliferation remained unclear.

These studies certainly demonstrate a role for IL-4 in liver injury and repair but there remain questions to be answered whether there is a role for IL-4Rα dependent leukocytes.

1.5 IL-4 and IL-13 regulation of monocytes and macrophages

We have seen that Chen et al. proposed that macrophages were important in the repair process in the type 2 immune setting characterised by *N brasiliensis* infection. Indeed, the concept of the alternative activation of macrophages upon exposure to type 2 immune cytokines was first proposed by Stein et al. in 1992 when they showed that inflammatory macrophages exposed to IL-4 developed a high capacity for endocytic clearance of mannosylated ligands, enhanced MHC class II antigen expression, and reduced pro-inflammatory cytokine secretion (Fig. 1.4)[174].

1.5.1 Alternatively activated macrophages

Murine alternatively activated macrophages are characterised by the expression of a specific gene profile: *Chil3*, *arginase-1* and *Retnla* leading to the secretion of their intracellular effector molecules: Ym1, arginase-1 and Resistin-like molecule (RELM)α [175,176]. Further understanding the function of these effector molecules will help identify the specific contribution of alternatively activated macrophages to tissue repair and regeneration.

Chitinase like proteins (CLPs):

CLPs are found in type 2 immune activation with evidence for roles in helminth infection[177], allergy[178], cancer [179], and wound healing[180,181]. Mice have 3 different CLPs Ym1 encoded by *Chil3*; Ym2 encoded by *Chil4*; and BRP-39 encoded by *Chil1*[182–184]. Ym1 is the most abundant alternatively activated macrophage protein in many helminth infection models, and all the murine CLPs are induced via IL-4Rα signalling[185]. Ym1 specifically has been identified in acute injury models associated with alternative activation in the

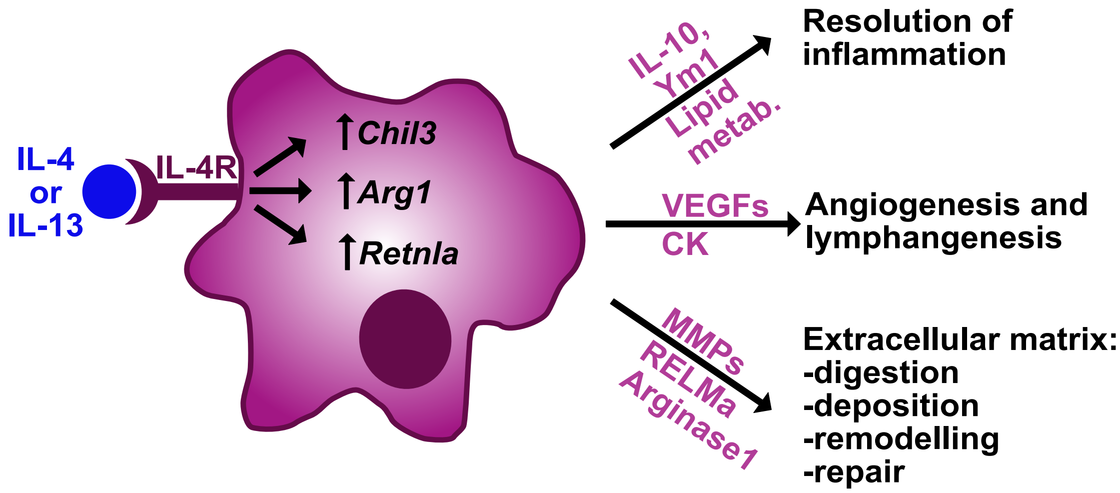

Figure 1-4 IL-4R mediated alternative activation of macrophages.

IL-4 or IL-13 bind the IL-4R resulting in upregulation of the alternative activation gene profile *Chil3*, *Arg1* and *Retnla.* This results in the production of factors that promote repair and regeneration: interleukin 10 (IL-10), Ym1, lipid metabolites, vascular endothelial growth factors (VEGFs), chemokines (CK), matrix metalloproteinases (MMPs), Relma and arginase 1.

mouse peritoneum and peripheral nerves[180,181]. However, a specific tissue repair function for either Ym1 or any of the other CLPs remained elusive until recently. In *N. brasiliensis* in the mouse Sutherland et al. have shown that CLPs promoted IL-17 responses and using an anti-Ym1 antibody they demonstrated that Ym1 specifically enhanced neutrophil and macrophage number during *N. brasiliensis* migration through the lung. They postulated that Ym1 might control parasite worm burden by directing both neutrophils and macrophages to damage larvae in the skin or lungs before they reach the gut[186]. We also saw above that the same group have shown that Ym1 directs the initial immune response to *N. brasiliensis* towards a repair phenotype and during the repair phase it limits excessive immune activation[170].

Arginase-1

Arginase-1 is probably one of the better studied effector molecules of alternatively activated macrophages and has been shown to be involved in tissue repair and regulation of inflammation[187,188]. It was shown as early as 2001 by Hesse et al. that arginase-1 played a critical role in the type 2 immune response to *S. mansoni* induced pathology[189]. Hesse et al. demonstrated that blocking of the enzyme immediately downstream of arginase-1 resulted in increased liver fibrosis and granuloma size in infected mice. It was subsequently demonstrated that alternatively activated macrophages from *Brugia malayi* infected mice also expressed high levels or *arginase-1*[177]*.*

The functional importance of arginase-1 in macrophages however remained unknown. To answer this question Pesce et al. used multiple myeloid specific arginase deficient mouse strains ($Arg^{-/flox}$;LysMcre and $Arg1^{flox/flox}$;$Tie2^{cre}$). Using these mice they showed that myeloid specific Th2-inducible Arginase-1 isoform inhibited CD4+ T cell effector function resulting in suppression of hepatic Th2 driven chronic inflammation and fibrosis[190]. However, the same group demonstrated that in models of acute and chronic Th2 mediated lung inflammation there was neither a pathogenic nor a protective role for myeloid-expressed arginase-1[191].

It is important to note that Arginase 1 expression can also be induced in classically activated macrophages during bacterial infection whereby it supresses the pro-inflammatory response to IFN-γ/LPS by inhibiting inducible Nitric Oxide Synthase (iNOS) production[192–194].

These results outline the context dependent effects of arginase-1 and more importantly that its effector function is not solely related to alternatively activated macrophages; indeed it has been shown to be upregulated in myeloid cells in response to various stimuli including: Granulocyte-macrophage colony-stimulating factor (GM-CSF), prostaglandin and catecholamines[195–197].

Resistin-like molecule α

RELMα is encoded by the *Retnla* gene that is induced in response to type 2 immune cytokines and has previously been demonstrated in alternatively activated macrophages in addition to epithelia and eosinophils[177,198]. It has been suggested by Nair et al. that it may limit the pathogenesis of Th2 cytokine mediated pulmonary inflammation following challenge with *S. mansoni* eggs[199]. They showed that RELMα supressed Th2 cytokines and RELMα knock-out macrophages promoted exaggerated Th2 cell differentiation. We shall also see below that RELMα is important for wound repair in a model of cutaneous injury where it directs collagen crosslinking through *Plod2* expression in myofibrobalsts[30].

1.5.2 Alternatively activated macrophages in helminth infection

The distinct roles for alternatively activated macrophages in tissue repair and regulation of inflammation are not dichotomous as they occur simultaneously[175]. In the following sections I will initially explore these functions of macrophages in helminth infection and then in the more novel settings of type 2 immunity in sterile inflammation. The type 2 immune response is characterised by the alternative activation of macrophages and it has been proposed that during helminth infection the specific functions of alternatively activated macrophages are in parasite killing, tissue repair and regulating inflammation[175].

In *N. brasiliensis* Chen et al. demonstrated that the observed IL-4Rα dependent repair in the lung was the result of a change towards an alternatively activated macrophage phenotype[25]. They suggested that IL-17 driven damage was inhibited by IL-4Rα driven macrophage production of IGF1 and IL-10 which contributed to rapid resolution of the damage. In *S. mansoni* infection an important role for IL-4Rα signalling to macrophages has been demonstrated using a macrophage/neutrophil specific IL-4Rα deficient mouse (LysMCreIL-4Rα$^{-/flox}$) developed by Herbert et al.[28]. Vannella et al.

showed that LysM is expressed at high levels in tissue macrophages and were therefore able to demonstrate that these $LysM^{hi}$ $F4/80^{+}$ $CD11b^{+}$ cells were critical to suppress the helminth mediated inflammation in the liver[34]. They also used this system to demonstrate that recruited $LysM^{lo}$ $F4/80^{+}$ $CD11b^{+}$ cells produced large amounts of arginase-1 and were responsible for the inhibition of fibrosis during chronic infection[34,200].

Both these results point towards a potential role for IL-4Rα signalling to macrophages contributing to repair in helminth infection. There is also growing evidence of the importance of IL-4Rα signalling being involved in the repair process in in pathologies not associated with classical type 2 immunity.

1.5.3 Alternatively activated macrophages outwith helminth infection

The concept of the alternatively activated macrophage was first proposed in the early 90s but it wasn't until the late 00s that their involvement in tissue repair outwith the realm of helminth infection or atopy was proposed[181]. Only recently has Knipper et al. definitively shown a role for alternatively activated macrophages in a sterile injury model[30].

Loke et al. first proposed that acute injury resulted in alternative activation of macrophages independent of infection, fibrosis or atopy[181]. Using $IL\text{-}4R\alpha^{-/-}$ mice they demonstrated that in their acute injury induced by sham surgery the observed innate expression of Ym1, Fizz1 and arginase 1 was dependent on type 2 cytokines. Seno et al. were the first to demonstrate a critical role for IL-4 and IL-13 in non-classical Th2 wound repair when they showed they were required for effective colonic wound repair[29]. They demonstrated that efficient colonic healing required triggering receptor on myeloid cells 2 (TREM2) which delivers signals to regulate myeloid cell function and is expressed on newly differentiated and alternatively activated macrophages[29,201]. They developed a punch biopsy model of colonic injury and demonstrated increased mRNA expression of TNF-α and IFN-γ in the wound beds of *Trem2*$^{-/-}$ mice. This increased expression of pro-inflammatory genes was coupled with a reduction in type 2 gene expression: arginase 1, Ym1 and the mannose receptor. This polarisation of the immune response to a type 1 pro-inflammatory one in *Trem2*$^{-/-}$ mice suggested that Trem2 was inhibiting cytokines that can enhance classical activation of macrophages and promote alternative macrophage activation. Although Seno et al. did demonstrate that IL-4Rα signalling (specifically STAT-6) was required for efficient wound repair they did not definitively demonstrate that this was dependent on IL-4Rα signalling to alternatively activated macrophages. However, Liao et al. have taken the work forward by looking at the role of Krüppel-like factor 4 (KLF4) in macrophage polarisation and wound repair[202]. They initially demonstrated in vitro that IL-4 stimulation of macrophages resulted in KLF4 expression and using myeloid specific KLF4 knock-outs (Mye-KO) they were able to show that KLF4 expression was required for macrophages to become alternatively activated upon stimulation with IL-4[202]. Having demonstrated that KLF4 is important for alternative activation of macrophages they subsequently showed in vivo that there was delayed wound closure in Mye-KO mice following a 6mm incisional wound when compared to Mye-WT mice. This provided further evidence that alternative activation of macrophages may be important for wound repair but it wasn't until Knipper et al. demonstrated defective granulation tissue and a failure of the repair process in LysMCreIL-4R$\alpha^{-/flox}$ mice that evidence for a definitive role of IL-4Rα signalling in macrophages was demonstrated in this sterile injury model[30]. Knipper at al. showed that IL-4Rα signalling is required for the switch from early pro-inflammatory macrophages that express *Nos2* to late pro-reparative macrophages expressing *Cd163, Rentla, Cd206 (mannose receptor)* and *Il10*. They demonstrated that this IL-4Rα mediated switch in macrophages was integral to wound healing as RELMα production directed accurate collagen crosslinking through *Plod2* expression in myofibrobalsts[30]. This seminal paper demonstrated the important role that IL-

4R-signalling to macrophages and RELMα production by alternatively activated macrophages played in sterile wound repair.

In acute CCl_4 induced liver injury Goh et al. attempted to address whether the IL-4Rα dependent repair was mediated by IL-4Rα signalling to macrophages. They ruled out a contribution of IL-4Rα signalling in the myeloid compartment by using LysMCreIL-4Rα$^{-/flox}$ mice to show no change in hepatocyte proliferation or ALT at 36 and 48 hours post CCl_4 administration respectively[33]. However, during sterile inflammation in the peritoneal cavity the LysMCreIL-4Rα$^{-/flox}$ fails to cause deletion of the IL-4Rα in inflammatory macrophages and macrophages in the liver during during S. mansoni infection[34]. It is therefore unclear whether this system can be used to draw conclusions about the lack of contribution of myeloid IL-4Rα signalling to the repair phenotype observed by Goh in this acute injury model[33].

1.5.4 Origin of alternatively activated macrophages

The functional effects of alternatively activated macrophages outlined above rely on accumulation of alternatively activated macrophages at the site of injury or infection. These alternatively activated macrophages can accumulate either through recruitment or local proliferation and it has been demonstrated that the origin of these cells affects their function.

Monocyte recruitment

As with acute inflammation in the liver secondary to APAP overdose or acute CCl_4[21–23] recruitment of monocytes has been demonstrated in multiple models of type 2 immunity: allergic dermatitis (skin); *Litomososides sigmodontis* (pleural cavity) and *S. mansoni* (liver)[123,203–205]. Nascimento et al. demonstrated using a CCR2-DTR mouse that the expansion of macrophages during *S. mansoni* infection was dependent on recruitment of monocytes[21,22,204]. Furthermore they demonstrated that outcomes were dependent on Ly6C^{hi} monocytes because their depletion resulted in severe acute weight loss[122,167].

Local proliferation

A hallmark of Th2 immunity is the accumulation of alternatively activated macrophages due to IL-4Ra dependent local proliferation[121,206]. Jenkins et al. demonstrated that in *L. sigmodontis* there was an expansion of the pleural macrophage populations that was dependent on IL-4Rα signalling to macrophages. Furthermore they demonstrated that IL-4 can drive proliferation in monocyte-derived macrophages recruited during thioglycolate elicited peritoneal inflammation[206]. They proposed during *L. sigmodontis* infection that IL-4 promoted the expansion of resident macrophages but also the establishment of a noninflammatory environment allowing the polarisation of any recruited macrophages to an alternatively activated phenotype[121].

Function according to origin

Vannella et al. were the first to propose that that recruited macrophages ($Lyz2^{lo}$) and resident macrophages ($Lyz2^{hi}$) might have differing function in *Schistosoma mansoni* infection[34]. Recent work by Gundra et al. has built on this work and demonstrated that there is indeed a functional difference in recruited and resident alternatively activated macrophages[203]. Using a thioglycolate model of peritoneal inflammation in combination with IL-4 treatment they demonstrated a fundamentally different molecular signature between monocyte-derived and resident macrophages when alternatively activated. They found that monocyte derived alternatively activated macrophages up-regulate genes important in immune response whereas genes involved in metabolic processes are upregulated in resident alternatively activated macrophages. In monocyte derived alternatively activated macrophages they also demonstrated significantly elevated expression of *Raldh2* which they demonstrated induced FoxP3 Treg differentiation proposing therefore that monocyte-derived alternatively activated macrophages have a more active roles in directing host responses[203]. Gundra et al. also subsequently suggested that monocyte derived macrophages could convert into a resident phenotype in a vitamin A and retinoic acid dependent manner[207]. This work started to introduce the concept of environmental control of alternative activation in macrophages.

1.5.5 The effect of the microenvironment on alternative activation of macrophages

We have seen above that IL-4 and IL-13 can alternatively activate macrophages and promote control of helminth infection and tissue repair but we have also seen that they are involved in fibrosis. Recently published work has started to shed light on other signals that could be involved in influencing the function of alternatively activated macrophages.

Clearance of apoptotic cells is linked to the resolution of inflammation and Bosurgi et al. proposed that the tissue repair, remodelling and anti-inflammatory programmes upregulated as part of alternative activation of macrophages could be promoted by the presence of apoptotic cells[208,209]. They demonstrated in vitro that when bone marrow derived macrophages (BMDMs) were cultured with IL-4 the addition of apoptotic neutrophils resulted in enhanced expression of archetypal markers of alternative activation, *Retnla* and *Chil3*[175,208]*.* Furthermore, when the phagocytic receptors AXL and MERTK were deleted on BMDMs there was lower amounts of *Retnla*, *Chil3* and *Arg1* upon IL-4 stimulation[208]. In vivo infection with *N. brasiliensis* in *Axl*$^{-/-}$ *Mertk*$^{-/-}$ mice resulted in impaired healing in the lung and a substantial reduction in tissue repair and anti-inflammatory genes suggesting that the inability to recognise apoptotic cells had a negative impact on the type 2 immune repair programme normally seen in *N. brasiliensis* infection. In addition to apoptotic cells enhancing responses in inflamed tissues Minutti et al. have recently demonstrated that there are tissue specific signals that promote repair in the lung and liver[210]. During *N. brasiliensis* infection they demonstrated that when surfactant protein A (SP-A), a major constituent of pulmonary surfactant, was knocked-out there was reduced secretion of RELMα and Ym1 in the alveolar fluid. The effect of SP-A was mediated by the receptor myosin 18A (Myo18A) which is also a receptor for C1q (the first component of the complement system) which is produced by myeloid cells in peripheral tissues[211]. They demonstrated that IL-4c treatment resulted in SP-A and C1q upregulation by myeloid cells and specifically they observed C1q upregulation in the liver. As with SP-A in the lung during *N. brasiliensis,* C1q was required for macrophage alternative activation and improvement in indices of liver injury during *L. monocytogenes*[31,210]. Hence, the work by Borsugi et al. and Minutti et al. emphasises the importance of local factors in mediating the type 2 immune response.

1.5.6 Alternative activation of Ly6C^{hi} monocytes

As discussed above, the recent work by Nascimento et al. highlighted the importance of recruitment of Ly6C^{hi} monocytes in host protective accumulation of macrophages during Schistosomiasis[204]. There is however little work on the direct effects of IL-4 on monocytes in vivo which is surprising given that they have been shown to be the precursors of several resident macrophage populations in homeostasis[90,91,98,212] and recruited macrophages in most models of inflammation[21,115,120,207,213].

Jenkins et al. have shown that delivery of exogenous IL-4c alone is not sufficient to recruit monocytes to tissue, contrasting the concurrent proliferation of macrophages and recruitment of monocytes that occurs with injection of exogenous CSF1-Fc [121,206]. In fact, co-injection studies from the Allen lab (L. Jackson Jones, unpublished) demonstrated that IL-4c actually blocks the recruitment monocytes induced by CSF1. However, it remains to be determined whether this inhibitory effect of IL-4 on monocyte recruitment may also occur under conditions of inflammation.

To study monocyte dynamics in vivo during a sterile injury model Dal-Secco et al. employed a burn model of liver injury where a focal necrotic injury is induced on the surface of the mouse liver with a thermal probe[214,215]. In this model, they demonstrate that there is recruitment of classical (Ly6C^{hi})

$CCR2^{hi}$ $CX3CR1^{low}$ monocytes to the wound edge and subsequent IL-4 and IL-10 dependent conversion from a $CCR2^{hi}$ $CX3CR1^{low}$ classical monocyte phenotype to a $CCR2^{lo}$ $CX3CR1^{hi}$ non-classical monocyte phenotype. They demonstrated that this conversion could be inhibited by the use of an anti-IL-4/anti-IL-10 antibody which resulted in an impaired repair process as demonstrated by decreased clearance of cellular debris and decreased collagen deposition[215]. Notably in this model Dal-Secco et al. suggested that the observed conversion was to a non-classical monocyte phenotype not to a macrophage phenotype because of the lack of F4/80 or MERTK expression on the $CCR2^{lo}$ $CX3CR1^{hi}$ cells. This result was interesting because as outlined above, sterile injury and inflammatory responses in the liver, colon, heart and peritoneal cavity are characterised by the recruitment of $Ly6C^{hi}$ monocytes from the circulation to the inflammatory site following which they convert into $Ly6C^{lo}$ macrophages with varying functions[21,115,120,121,207]. The different fate of $Ly6C^{hi}$ monocytes reported by Dal-Secco et al. could relate to the artificial model employed which does not reflect mammalian pathology. Indeed they don't state whether their burn model results in any systemic monocytosis[216] and they propose that the recruited $CCR2^{hi}$ $CX3CR1^{low}$ monocytes represent a unique hepatic population of patrolling monocytes that are recruited locally. It is therefore possible that this population behave differently to other monocyte populations. Notwithstanding the caveats surrounding the model, they did show that IL-4 and IL-10 in combination appeared to play an important role in the downregulation of CCR2 expression in $CCR2^{hi}$ $CX3CR1^{low}$ monocytes.

Further insight into the effect of IL-4 on monocytes has recently been provided by an examination of the transcriptomic effects of differentiating human monocytes in vitro with IL-4 in combination with GM-CSF[217]. Sander et al. identified NCOR2 as a key transcription factor linked to IL-4-dependent differentiation of monocytes[217]. The previously identified functions of NCOR2 could shed some light on its function in monocyte responses to IL-4 because it is known to be involved in controlling cell fate, repression of pro-inflammatory genes and cell cycle regulation, all processes associated with IL-4[121,175,177,218]. Furthermore they demonstrated the importance of timing of IL-4 administration because in conjunction with GM-CSF changes in timing of IL-4 could alter the monocyte differentiation along a continuum from more macrophage like cells to more dendritic like cells[217].

Interestingly, Ikeda et al. have recently identified a subset of Ly6C^{hi} monocytes that express the alternative activation marker Ym1[219]. They developed a novel mouse line that harboured the Venus gene in the Chil3 (Ym1-coding gene) locus which enabled identification of Ym1 expressing cells. Using this Ym1-venus mouse they demonstrated that there was an increase in the proportion of blood Ym^{+} Ly6C^{hi} 48hrs following a single dose of LPS and 1 day following 5 days of 2% DSS colitis. They suggested that these changes correlated with the recovery phases of these pathologies and using a novel Ym1-DTR mouse they conditionally deleted these cells on day 3 and day 5 following cessation of DSS colitis. Conditional deletion of these cells resulted in worse outcomes with observed increased histological evidence of inflammation and impaired recovery of body weight.

There is little data on the direct effect of IL-4 on monocytes but the work by Dal-Secco et al. and Sander et al. would both suggest there is a role for IL-4 in influencing the fate of monocytes and the more recent work by Ikeda et al. would suggest that Ly6C^{hi} monocytes can adopt an alternatively activated phenotype. Interestingly in vitro data from human monocytes from 1992 would suggest that IL-4 can lead to cell death in monocytes stimulated with IL-1 and TNF-α but they found that IL-4 had little effect on monocytes when they were stimulated with GM-CSF or CSF1[220].

1.6 IL-4 signalling as a therapeutic target

The pro-reparative and anti-inflammatory effects of IL-4 that have been observed not only in helminth infection but in a multitude of inflammatory/injury conditions, make this cytokine a potential target to augment pro-reparative responses, particularly those involving a significant inflammatory response. However there are potential pitfalls in attempting to modulate IL-4Rα signalling, we saw earlier that type 2 immune responses can enhance fibrosis in a context and tissue dependent manner[152,210] whilst administration of exogenous IL-4 early during infection with *L. monocytogenes* can be deleterious[31]. Furthermore, pathological overproduction of type 2 cytokines results in atopy which is reviewed elsewhere but includes atopic dermatitis, allergy and anaphylaxis[221]. Type 2 immunity has also been shown to impair antiviral and mycobacterial immunity[222,223] and alternative activation of macrophages can potentiate tumour growth[224,225]. It is therefore important to take these potentially deleterious effects when planning to manipulate IL-4Rα signalling.

1.6.1 IL-4 and IL-13 as targets

As the central receptor in type 2 immunity the IL-4Rα and its ligands IL-4 and IL-13 would appear to be ideal targets for any potential therapy to engage or manipulate this system. In immunotherapies it is possible to enhance the function of cytokines through administration of recombinant forms of the cytokine or block the function of particular cytokines through binding to the cytokine itself or binding of the cytokine's receptor.

Blocking IL-4 and IL-13

In murine models of asthma IL-13 and not IL-4 is thought to be the key mediator of the pathological features associated with lung inflammation and remodelling[226]. However, unlike in helminth infection IL-4 doesn't appear to mediate a beneficial effect and actually promotes the accumulation of inflammatory cells in the airways[227]. Approaches have therefore been developed to block the function of Th2 cytokines in asthma. One phase II trial demonstrated an improvement in lung function with Lebrikizumab (a monoclonal antibody directed against IL-13); and another trial of Dupilumab (a monoclonal antibody against the IL-4Rα) resulted in fewer asthma exacerbations[228,229]. However, neither of these drugs have yet been licensed for the treatment of asthma, although notably Dupilimumab has been licensed for the treatment of atopic dermatitis the pathogenesis of which involves IL-4 and IL-13[230].

Enhancing IL-4Rα signalling in models other than acute liver injury
The simplest way to experimentally enhance the action of IL-4 is to administer it exogenously. This can be done by simply administering the cytokine alone however, exogenous IL-4 administered in the form of a complex (IL-4c) between IL-4 and anti-IL-4 antibody (11B11) significantly increases the half-life of IL-4 from a few minutes to ~24hrs and results in slower dissociation to maintain high levels of IL-4 for 3-5 days[32,231,232].

There are multiple experimental models of sterile inflammation like rheumatoid arthritis (RA) and psoriasis where exogenous IL-4 has been used in attempt to modulate the immune response to improve healing. RA is an autoimmune disease process characterised by persistent sterile inflammation in the synovium, cartilage and bone of joints which is driven by T cells polarised to a Th1 phenotype[233]. The two central mediators of the pathology are TNF-α, which promotes the inflammation and IL-1 that mediates the bone destruction[234]. Anti-TNF-α therapy with Infliximab is well established and effective in the treatment of RA[235]. There is very little evidence of type 2 cytokines within the inflammatory joint during RA, it was therefore postulated that skewing the T cell phenotype from Th1 to Th2 would be beneficial[233]. Indeed in the murine model of collagen induced arthritis (CIA) daily administration of IL-4 to mice with established CIA resulted in prevention of cartilage and bone erosion but no significant anti-inflammatory effect of IL-4 within the inflamed joint[236]. It was felt that this could in part be mediated by the effect of IL-4 on osteoclasts which are the tissue resident macrophages in bone and are responsible for bone resorption. Joosten et al. demonstrated that IL-4 treatment resulted in a reduction in their number[236] and it has also been demonstrated in vitro that IL-4 can not only inhibit osteoclast development but also mature osteoclast function[233,237]. Interestingly IL-4 therapy alone didn't have any effect on the influx of inflammatory cells into inflamed joints but could be combined with low dose dexamethasone or IL-10 to illicit an inhibitory effect on the inflammatory cells[236,238]. There is evidence from a model of pleuritis that IL-4 can have an effect on the inflammatory infiltrate; Fine et al. have demonstrated that exogenous IL-4 inhibits leukocyte trafficking to the pleura during inflammation, specifically limiting recruitment of macrophages and completely inhibiting polymorphonuclear cell recruitment when compared to saline controls[239].

Like RA, psoriasis is an autoimmune disease involving sterile inflammation of the joints but also the skin. Also like RA there are no type 2 immune cytokines detectable in the stereotypical skin lesions that develop[240]. Unlike RA, however, it is thought to be a Th17 driven pathology with increased levels of interleukin (IL-)17A, IL-22 and IL- 23[241]. In a small study in humans it has been demonstrated that daily administration of recombinant human IL-4 resulted in decreased plaque size and decreased epidermal thickness both of which are markers of disease improvement[240]. Furthermore, Ghoreschi et al. demonstrated a concomitant Th2 differentiation in human CD4+ T cells upon IL-4 treatment. In addition to polarising T cells to a Th2 phenotype it has been suggested that IL-4 might inhibit IL-1β and IL-6 secretion by epidermal cells from psoriatic lesions[242]. In a murine model of hypertension in pregnancy it has also been shown that exogenous IL-4 administration normalised blood pressure and also reduced that proportion of CD3+/γδ+ T cells which are thought might exacerbate hypertension during pregnancy[243].

The above results suggest that exogenous IL-4 can promote an anti-inflammatory milieu during models of sterile inflammation and during RA and pleuritis there are concomitant effects on the leukocyte populations.

The concern with cytokine based therapy is the potential for off target systemic effects which can sometimes be detrimental as was seen during a trial of a CD28 agonist (Theralizumab) which resulted in a cytokine storm and death when administered in a phase I human trial[244]. It could be that in humans systemic administration of IL-4 may require a targeted approach. One such approach is the use of diabody fusion proteins, in RA and psoriasis one such diabody has been designed to target inflammation by binding fibronectin that is expressed during neoangiogenesis[245–247]. The diabody is composed of IL-4 and the F8 antibody that binds fibronectin resulting in delivery of IL-4 to the site of inflammation. This fusion protein (F8-IL-4) results in improvement in indices of disease severity and in combination with dexamethasone promotes the number of T regs and alternatively activated macrophages in murine arthritic joints[246,248].

Autoimmunity is driven by the maladaptation of immunological self-tolerance in lymphocytes[249] and in the above examples of RA and psoriasis it was suggested that the common pro-reparative function of IL-4 was to polarise T cells to a Th2 phenotype. However, there were indications that in the setting of sterile inflammation exogenous IL-4 was having effects on non-lymphoid cells like osteoclasts, epidermal cells and infiltrating myeloid cells[237,239,242]. The commonality between these models was that IL-4 could contribute to reduced inflammation as demonstrated by a variety of outcome measures and it may therefore be useful to use in other sterile injury models such as acute liver injury.

1.6.2 IL-4Rα signalling as a target in sterile liver injury

Administration of exogenous IL-4 during liver injury may not be the most obvious therapeutic given that it had previously been suggested that constant IL-4 expression in the liver is deleterious[250]. Guillot et al. induced sustained IL-4 expression in mouse hepatocytes using a murine IL-4 adenovirus (AdmIL-4) that was injected via the hepatic portal vein. Sustained IL-4 expression due to the gene transfer resulted in lethal hepatotoxicity that they suggested was dependent solely on hepatocyte apoptosis and not related to effects on the hepatic leukocytes[250]. Furthermore, they suggested that IL-4 alone was sufficient to kill hepatocytes in vitro, highlighting a potential side effect of long-term IL-4 administration.

In contrast to Guillot et al., Goh et al. enhanced IL-4 signalling during acute liver injury by administering exogenous IL-4 in the form of IL-4c. By not using constant administration of IL-4 they demonstrated that administration of exogenous IL-4c 24 hours prior to acute CCl_4 and 72hrs later resulted in improvement in indices of liver injury: ALT and necrotic cell area. It also enhanced indices of hepatic regeneration as evidenced by an increase in hepatocyte proliferation with IL-4c administration. However, they did not administer IL-4c in either IL4Rα$^{fl/fl}$AlbCre or LysMCreIL-4Rα$^{-/flox}$ mice during injury, it is therefore impossible to attribute the observed improvement to signalling to a particular cell type. In fact they demonstrated that administration of IL-4c to uninjured IL4Rα$^{fl/fl}$AlbCre^{+} mice resulted in increased hepatocyte proliferation when compared to untreated mice suggesting that there was some Cre inefficiency or signalling to other cell types had an effect hepatocyte proliferation.

There are therefore unanswered questions with regards to the role of IL-4c in acute DILI: can it be administered therapeutically following an acute insult and are any of the pro-reparative effects mediated by the monocyte/macrophage compartment.

1.7 Project aims

I have outlined above that monocytes and macrophages are involved in the repair and regeneration process in APAP and acute CCl_4 toxicity[21,23,52,145] and that IL-4 can promote a tissue repair and regeneration phenotype in macrophages[26,175]. Moreover, Goh et al. have shown that exogenous IL-4 administered prior to and following injury with CCl_4 results in improvements in indices of injury and regeneration. While this was attributed entirely to direct effects of IL-4 on hepatocytes[33], in my PhD project I hypothesised that exogenous IL-4c could be used as a therapy for acute liver injury and that administration of IL-4c would promote a pro-reparative phenotype in the monocyte and macrophage populations in the injured liver. My pilot work identified an effect on the leukocyte population in the liver and given the role for endothelial cells in recruitment of monocytes, I therefore also hypothesised that IL-4Rα signalling to endothelial cells could also affect the recruitment of leukocytes to the injured liver. To test my hypothesis, I aimed to do the following:

- Establish if IL-4c could be administered therapeutically by comparing the pre- and post-injury administration of IL-4c with a post-injury (therapeutic) administration.
    - Interrogate the effects of IL-4c on the recruited leukocyte populations using flow cytometry and establish if there is an IL-4c dose relationship to the observed phenotype.
- Abrogate endogenous signalling to endothelial cells by generating a novel mouse line: Cdh5-Cre-ERT2; IL-4R$\alpha^{fl/fl}$ and establish if there was any phenotype following CCl_4 injury +/- IL-4c.
- Establish the effect of IL-4c signalling to specific leukocyte populations using:
    - Whole body irradiation and tissue protected chimeras using IL-4Ra$^{-/-}$ donor BM to establish the effect of IL-4Rα signalling in BM derived cells.
    - Cell specific Cre mediated excision of the IL-4Rα by crossing the specific Cre with the IL-4Ra$^{fl/fl}$ mouse line.
- Develop ex-vivo and in-vitro assays to further characterise the observed changes in leukocyte populations.
- Establish if the therapeutic effect of IL-4c treatment in acute CCl_4 liver injury can be translated to other models, including
    - The clinically relevant model of APAP overdose
    - DSS colitis, a model also characterised by a significant recruitment of monocytes and macrophages.

Chapter 2 Methods

2.1 Mice

Mice were bred and maintained in specific pathogen free (SPF) facilities at the University of Edinburgh, UK. All mice were male and age matched: 7-9 weeks-old for wild-type (WT) studies and 16-18 weeks-old for chimera experiments. Male mice were used across all experiments for consistency as it has been shown that they have a different and more significant injury response to CCl_4 induced injury when compared to female mice[251]. All experimental studies were conducted in either the Ann Walker Unit (AWU) at King's Buildings or Little France 2 (LF2) at the Chancellor's Building, University of Edinburgh. Unless stated otherwise, all strains were on the C57/BL6 background. All experiments were approved by the University of Edinburgh Animal Welfare and Ethical Review Body under license granted by the UK Home Office.

2.1.1 Wild-type mice

WT mice used in studies conducted in the AWU were purchased from an in-house colony of Harlan (C57BL/6OlaHsd) mice. Of note during the project the AWU switched their breeding colony to Charles River (C57BL/6J) mice. There was no difference in strains noted by anyone using the same models as employed in this study following the switch. Mice used in experiments in LF2 were purchased from Charles River at 6 weeks-old and maintained in the animal unit for at least 2 weeks prior to being used in studies.

2.1.2 Transgenic lines

Congenic C57BL/6 $CD45.1^+CD45.2^+$ mice (Ly5.1 heterozygote) used as recipients in chimera experiments were bred in AWU and all other lines were bred in either Ashworth Building 3 level 5 at King's Buildings or Little France 1 (LF1) at the Chancellor's Building (both University of Edinburgh). Transgenic lines are outlined below in Table 2.1.

Table 2-1 Details of mouse strains

Mouse line	Details
C57BL/6 CD45.1$^+$CD45.2$^+$	Generated by crossing C57BL/6 CD45.1$^+$ (Ly5.1$^+$) with C57BL/6 CD45.2$^+$. Maintained by AWU
C57BL/6 IL-4R$\alpha^{-/-}$	Kindly provided by Dr. Cecile Benezech, University of Edinburgh.
LysM Cre; IL-4R$\alpha^{fl/fl}$	Kindly provided by Prof. Judi Allen, University of Manchester.
LysM Cre; IL-4R$\alpha^{fl/-}$	Maintained by crossing LysM Cre; IL-4R$\alpha^{fl/fl}$ with IL-4R$\alpha^{-/-}$ mice.
Cdh5-Cre-ERT2	Kindly provided by Prof. Neil Henderson, University of Edinburgh.
Cdh5-Cre-ERT2:IL-4R$\alpha^{fl/fl}$	Maintained by crossing Cdh5-Cre-ERT2:IL-4R$\alpha^{fl/fl}$ with IL-4R$\alpha^{fl/fl}$ mice.
Csf1r-EGFP (MacGreen)	Kindly provided by Prof. Jeffrey Polalrd, University of Edinburgh.

2.2 Generation of bone marrow chimeric mice

A combination of both whole body and tissue protected chimeras were used.

2.2.1 Whole body irradiation chimeras

Whole body irradiation chimeras were generated as previously described by Jenkins et al[121]. 6-10-week-old, C57BL/6 CD45.1$^+$CD45.2$^+$ mice were maintained on Baytril (Bayer) in their drinking water for 4 days prior to being irradiated. Mice were given a total dose of 980 rads divided over two doses of 10 minutes and 22 seconds. 24 hours after irradiation mice were reconstituted with CD45.2$^+$ bone marrow from C57BL/6 (WT) or C57BL/6 IL-4R$\alpha^{-/-}$ mice. Following irradiation, mice were maintained on Baytril in their drinking water and mash diet for 4 weeks.

2.2.2 Tissue protected bone marrow chimeras

Tissue protected bone marrow chimeras were generated as previously described by Jenkins et al[206]. 6-8-week-old, C57BL/6 CD45.1$^+$CD45.2$^+$ mice were anesthetized with 8μl/g of s.c. anaesthetic: 0.5ml Medetomidine (Domitor, Vetoquinol) + 0.38ml Ketamine (Vetalar, Boehringer Ingelheim) + 4.12ml sterile PBS (Gibco). Mice were given a total dose of 950 rads over 19 minutes and 30 sec with only their hind limbs and lower pelvis exposed to the radiation source. The rest of their body was shielded from irradiation using a 5cm lead block. Following irradiation mice were administered 100μl s.c. of anaesthetic reversal agent: 0.5mg of Atipamezole (Antisedan, Zoetis) in 100μl sterile dPBS (Gibco). Mice were then placed in an incubator at 37ºC to ensure maintenance of adequate body temperature during recovery. 24 hours after irradiation mice were reconstituted with CD45.2$^+$ bone marrow from C57BL/6 (WT) or C57BL/6 IL-4R$\alpha^{-/-}$ mice. Following irradiation mice were maintained on Baytril in their drinking water and mash diet for 4 and 2 weeks respectively.

2.2.3 Preparation of bone marrow for reconstitution of irradiated mice

C57BL/6 CD45.2$^+$ or C57BL/6 IL-4R$\alpha^{-/-}$ mice were culled via cervical dislocation. Skin was removed from their hind legs and both tibias and femurs were dissected out with care being taken to remove muscle. Intact bones were transferred into ice cold dPBS (Gibco) for transport. The extraction of BM was performed in sterile conditions using a class II biosafety cabinet. Bones were sterilised for 2 minutes in ice cold 70% ethanol and then washed twice in dPBS (Gibco). The distal and proximal ends of bones were removed to expose the bone marrow cavity and the bone marrow flushed out using a 26G needle and 10ml RPMI 1640 (Gibco). A single cell suspension was then formed using a syringe, the single cell suspension was then passed through a sterile 40μm filter (Thermo Fisher) into a 50ml Falcon. Samples were centrifuged at 300G and 4ºC for 5 mins and then red blood cells were lysed for 5 minutes using 5ml of red blood cell (RBC) lysis buffer (Sigma). Cells were then washed in RPMI 1640 (Gibco) and were counted using a haemocytometer. Cells were resuspended at $2.5x10^7$ cells/ml in dPBS. Mice received 200μl of cell suspension via i.v. tail vein injection.

All mice were used 8-9 weeks following reconstitution. Chimerism in blood was checked prior to initiation of experimental models: 20μl of blood was obtained via tail vein bleed and analysed by flow cytometry as outlined below.

2.3 Injury models

Acute carbon tetrachloride (CCl_4)

Acute liver injury was induced with a solution of 25% CCl_4 (Sigma) in olive oil (Sigma). This was made without using plasticware as it is degraded by CCl_4. A dose of 4μl/g of the 25% solution of CCl_4 was injected i.p. into mice as this has been previously shown to generate a significant acute injury[252]. Mice were monitored for 1 hour following CCl_4 injection and then checked daily until the end of the experiment. Control mice were given olive oil at a concentration of 4μl/g.

Acetaminophen (APAP) overdose

To induce an acute liver injury, APAP was administered to mice at a dose of 350mg/kg i.p[16]. A 30mg/ml solution of APAP was made by combining APAP powder (Sigma) with dPBS (Gibco). To dissolve the solute, the solution was heated in a waterbath and cooled immediately prior to administration. Mice were closely monitored following administration of APAP and were checked every 12 hours until the end of the experiment. Controls were either given dPBS or were naïve controls (specified in results).

Dextran Sodium Sulphate (DSS)

Colitis was induced using 2% DSS given ad libitum in drinking water[117]. A 2% solution of DSS was made by diluting DSS (MP Biomedicals) with sterile water. Control mice were given water. All mice were assessed on a daily basis using a disease activity index (DAI) (Table. 2.2)[253]. Owing to the deleterious nature of the model, specific humane endpoints were used: mice showing signs of colitis (blood score ≥ 1, stool consistency ≥ 2, general appearance ≥ 1 or weight loss ≥ 1) for ≥ 48hrs were culled. A score of 4 in any category triggered immediate schedule 1.

Table 2-2 Colitis disease activity index

Score	Weight loss	Blood loss	Stool consistency	General appearance
0	Nil	Nil	Well formed	Normal
1	1-5%	Present in/on faeces	Pasty	Piloerection only
2	5-10%	Visible on rectum	Pasty some blood	Lethargy, piloerection
3	10-20%	-	Non-adherent diarrhoea	-
4	>20%	Visible on fur +/- clinical anaemia	Adherent diarrhoea	-

2.4 Other substances administered to mice

2.4.1 Interleukin-4 complex (IL-4c)

To prolong the half-life of IL-4 it was administered as a complex with anti-IL-4 (IL-4c). Recombinant murine IL-4 (Peprotech) was combined with anti-IL-4 antibody, 11b11 (Bio X Cell) in a 1 to 5 ratio and kept at 4ºC until the addition of dPBS prior to injection s.c.[32]. The volume of dPBS altered depending on the dose of IL-4 being administered. All mice were given a dose of 4μl/g IL-4c. Control mice were given dPBS at a dose of 4μl/g, referred to as vehicle (veh) throughout the project.

2.4.2 Tamoxifen induction of Cre expression

To induce Cre expression in Cdh5-Cre-ERT2:IL-4R$\alpha^{fl/fl}$ mice, tamoxifen was administered i.p. at a dose of 100mg/kg for 5 consecutive days[254]. To limit off target effects of tamoxifen administration mice were left for 2 weeks following the last dose. A 20mg/kg solution of tamoxifen was made by dissolving tamoxifen powder (Sigma) in corn oil (Sigma) at 37ºC in the dark in a 50ml Falcon. Once fully dissolved the solution was sterile filtered using a 0.22μm (Millex) filter and stored at 4ºC prior to warming immediately pre-injection.

2.4.3 Bromodeoxyuridine (BrdU)

BrdU is a thymidine analogue that is incorporated into cells during S phase and can therefore be used to identify cells that are in cell cycle following administration. To label cells 100μl of BrdU (10mg/ml, Sigma-Aldrich) was administered i.p. To identify proliferating cells in tissues, BrdU was administered 2 hours prior to harvesting, with administration staggered according to timing of necropsy[91]. In order to identify descendants of proliferative cells that had emerged from blood into bone marrow it was administered 12 hours prior to necropsy[117].

2.5 Leukocyte isolation protocols for flow cytometry analysis

Outlined below are the protocols employed for isolation of leukocytes from various tissues. All mice were culled using a rising concentration of CO_2. Unless otherwise stated, cells were centrifuged at 300g at 4ºC for 5 minutes and buffers were kept at 4ºC. All wash steps during preparation of samples for flow cytometry entailed centrifugation of cells in buffer with subsequent discarding of supernatant and resuspension of the resultant pellet.

2.5.1 Isolation of leukocytes from liver

Following perfusion of PBS through the inferior vena cava, the whole liver was weighed and 0.5g of the left lobe was placed into RPMI (if there was insufficient mass of left lobe it was supplemented with liver from the right lobe, final weight was documented). Liver was removed from RPMI, finely chopped using a razor blade and digested in 5 ml of pre-warmed (37ºC) enzyme mix: RPMI (Gibco) with 0.625 mg/ml collagenase D (Sigma-Aldrich), 30 U/ml DNase (Roche), 0.85 mg/ml collagenase V (Sigma), and 1 mg/ml dispase (Invitrogen) for 23 min at 37ºC, in an orbital shaker with additional manual shaking every 5 min. Digests were poured through a 100μm strainer and cells washed in 50ml, then 30 ml RPMI (Gibco). Following these washes RBC were lysed with 3ml RBC lysis buffer (Sigma) for 3 min at room temperature, followed by addition of 3 ml FACS buffer: PBS supplemented with 0.5% BSA (Sigma) and 2 mM EDTA (Life Technologies). Cells were washed and resuspended in 6ml FACS buffer prior to passing through a 40μm strainer and live cells counted using a Casey TT counter (Roche)[91].

2.5.2 Isolation of leukocytes from whole blood

Blood was obtained either via tail vein bleed during experiments or via cardiac puncture with a 1ml syringe and a 27G at necropsy. In initial experiments leukocytes were isolated from blood as follows: 20μl of blood was collected into 180μl of blood buffer: HBSS (Gibco) + 5% FCS (Gibco) and 2mM EDTA (Life Technologies). Samples were washed once in PBS prior to staining. Following staining, RBC were lysed using 200μl of 1x RBC lysis buffer (BD Bioscience) for 8 minutes at room temperature[121]. Cells were then washed with FACS buffer prior to acquiring on a flow cytometer.

A more efficient method of isolating blood leukocytes was then established in the Jenkins group. Unless stated otherwise 100μl of blood was collected into a 15ml Falcon with 10μl of 0.5M EDTA (Life Technologies). 1x RBC lysis buffer (Biolegend) was made by diluting 10x stock buffer with dH_2O. RBC lysis buffer was added in a 1:10 ratio to the blood and left for 5 minutes at 4ºC and then washed with 9ml of FACS buffer. This lysis step was then repeated and cells kept on ice until staining for flow cytometry.

2.5.3 Isolation of leukocytes from spleen

Spleens were dissected out and placed into RPMI (Gibco). They were removed from the RPMI, finely chopped with scissors and digested in 2 ml of pre-warmed (37ºC) enzyme mix: RPMI (Gibco) with 1 mg/ml collagenase D (Sigma) for 45 min at 37ºC, in an orbital shaker. Digests were mashed through a 100 μm strainer and washed in 10ml of FACS buffer. RBC were lysed with 3ml RBC lysis buffer (Sigma) for 3 min at room temperature, followed by addition of 3 ml FACS buffer and washing. Cells were resuspended in 5ml FACS buffer and passed through a 40μm strainer and live cells counted using a Casey TT counter (Roche)[91].

2.5.4 Isolation of leukocytes from kidney

The right kidney was dissected out and placed into RPMI (Gibco). Kidneys were removed from the RPMI and finely chopped with scissors and digested in 2 ml of pre-warmed (37ºC) enzyme mix RPMI (Gibco) with 0.625 mg/ml collagenase D (Sigma-Aldrich), 30 U/ml DNase (Roche), 0.85 mg/ml collagenase V (Sigma), and 1 mg/ml dispase (Invitrogen) for 45 min at 37ºC, in an orbital shaker. Digests were mashed through a 100 μm strainer and washed in 10ml of FACS buffer. RBC were lysed with 3ml RBC lysis buffer (Sigma) for 3 min at room temperature, followed by addition of 3 ml FACS buffer. Cells were pelleted (300 g, 5 min) and the supernatant discarded. Pellets were resuspended in 18ml FACS buffer and passed through a 40μm strainer and live cells counted using a Casey TT counter (Roche)[91].

2.5.5 Isolation of peritoneal leukocytes

Skin was removed from the abdomen and 5ml syringes were loaded with 1ml air and 3ml wash buffer: RPMI (Gibco) + 2mM EDTA (Life Technologies) +10mM HEPES (Fisher Scientific). Using a 23G needle the contents of the syringe was instilled into the peritoneal cavity via the midline, the needle was then withdrawn and the peritoneal cavity agitated. The fluid was then withdrawn from the flanks using the same needle and placed in a Falcon tube at 4ºC on ice. This was repeated twice with 3ml of wash buffer and no air, cells were then centrifuged and resuspended in 1ml FACS buffer for counting using a CASY TT counter (Roche)[91].

2.5.6 Isolation of leukocytes from colonic lamina propria

The below protocol was a personal communication from Dr. Jones in Professor MacDonald's group in Manchester. Colons were dissected out, soaked in PBS and had fat and faeces removed. Colons were then opened longitudinally, washed in HBSS (Gibco) supplemented with 2% FCS (Gibco) and cut into 0.5cm segments. Tissue was then incubated in a 50ml Falcon tube with 10 ml of pre-warmed (37ºC) HBSS + 2mM EDTA for 15 min at 37ºC, in an orbital shaker. Supernatant was removed by passing through Nitex mesh and tissue was incubated for another 15 min with 10ml pre-warmed (37ºC) HBSS + 2mM EDTA at 37ºC, in an orbital shaker. Supernatant was removed and EDTA removed by washing with 10ml of warmed (37ºC) HBSS. Tissue was digested in 5 ml of pre-warmed (37ºC) enzyme mix: RPMI (Gibco) with 0.2 mg/ml Liberase TL (Roche) 30 μg/ml DNase (Roche) for 23 min at 37ºC, in an orbital shaker with additional vigorous manual shaking every 5 min. Samples were digested until only small fragments of colon remained. Samples were then passed through a 100μm strainer, resuspended with 30ml FACS buffer and washed. Samples were then resuspended in 2ml FACS buffer for counting using a CASY TT counter (Roche).

2.5.7 Isolation of leukocytes from bone marrow

Skin was removed from hind legs and both tibias and femurs were dissected out with care being taken to remove muscle. Intact bones were transferred into ice cold dPBS (Gibco) for transport. In a class II biosafety cabinet bones were sprayed with ethanol then washed in dPBS (Gibco). The distal and proximal ends of bones were removed to expose the bone marrow cavity and the bone marrow flushed out using a 26G needle and 10ml RPMI (Gibco). A single cell suspension was then formed using a syringe, the single cell suspension was then passed through a 40μm filter into a 50ml Falcon tube. The cells were then centrifuged and RBC were lysed with 3ml RBC lysis buffer (Sigma) for 3 min at room temperature, followed by addition of 3 ml FACS buffer for washing. Cells were resuspended in 30ml FACS buffer for counting using a CASY TT counter (Roche)[117].

2.6 Flow cytometry

The number of cells stained and volume of antibody used differed between tissues and is detailed in Table 2.3. All steps were performed at 4°C and samples were kept in the dark following initiation of staining protocol unless otherwise stated. Cells were plated into a 96 well V bottom plate (VWR) for staining.

Table 2-3 Number of cells stained by tissue

Tissue	Cells to stain/volume of blood	Volume stained in
Liver	$2x10^6$ cells	50μl
Blood	100μl	50μl
Blood for sorting	200μl	200μl
Kidney	$5x10^6$ cells	50μl
Spleen	$5x10^6$ cells	50μl
Colon	All cells	100μl
Bone marrow for sorting	All cells	500μl

2.6.1 Surface staining

At the beginning of the project viability staining was initially performed on all samples with Zombie Aqua (Biolegend). However, later in the project Fixable viability dye (FVD) eFluor 780 (eBiosciences) was used in samples that required fixation and 7-AAD (Biolegend) for cells being analysed live. 10μl of Zombie Aqua or FVD was added to cells at a concentration of 1:100 for 10 minutes at room temperature in the dark. Non-specific antibody binding was blocked using 1:200 anti-CD16/CD32 (Biolegend) + 10% mouse serum (Life technologies) for 10 minutes. The volume of blocking solution depended on total volume in which cells were being stained and the viability stain being employed. In samples that were stained with Zombie Aqua/FVD the volume of blocking solution was 20% of the volume cells were stained in and in samples using 7-AAD this was 40%. Cells were then incubated for 30 minutes using a combination of antibodies documented in Table 2.4 in the volume defined in Table 2.3. Cells were then washed and where necessary incubated with fluorescently-labelled streptavidin for 20 minutes and then washed. All samples were run on the day of necropsy unless intracellular staining was performed. If viability staining was performed using 10μl 7-AAD (Biolegend) this was added prior to sample acquisition.

2.6.2 Annexin assay

Following surface staining cells were washed in Annexin V Binding Buffer (Biolegend). Cells were then incubated for 15 minutes at room temperature with 5μl AF647 Annexin V (Biolegend) and 10μl 7-AAD (Biolegend) in a total of 100μl Annexin V Binding Buffer. Samples were then washed with Annexin V binding buffer and analysed by flow cytometry.

2.6.3 Intracellular staining

For intracellular staining, cells were fixed following surface staining using 100μl Foxp3/transcription factor staining fixation reagent, diluted 1:3 with permeabilization reagent (eBioscience). Samples were then stored at 4°C overnight and washed with 1x Foxp3/transcription factor permeabilization buffer in dH_2O (perm/wash) (eBiosicence).

BrdU and Ki67 staining

To retrieve the BrdU antigen, cells were incubated at 37ºC for 30 minutes with 100μl DNAse-solution: 30% DNase (Sigma Aldrich) + 69% dPBS (Gibco) + 1% $MgCl_2$. BrdU controls were incubated with 100μl dPBS (Gibco) instead of DNAse solution. Cells were washed with perm/wash and then incubated for 30 minutes at room temperature with 1.25μl anti-BrdU and 5μl

Table 2-4 Antibodies

Antibody	Clone	Company	Isotype	Dilution
BrDU	BU20A	Biolegend	Mouse IgG1, κ	1:16
CD102	3c4(MIC2/4)	Biolegend	Rat IgG2a, κ	1:200
CD115	Afs98	Biolegend	Rat IgG2a, κ	1:200
CD117	2b8	Biolegend	Rat IgG2a, κ	1:200
CD11b	M1/70	Biolegend	Rat IgG2a, κ	1:200
CD11c	N418	Biolegend	Hamster IgG	1:200
CD16/32	93	Biolegend	Rat IgG2a, λ	1:200
CD19	6D5	Biolegend	Rat IgG2a, κ	1:200
CD3	17A2	Biolegend	Rat IgG2a, κ	1:200
CD31	Mec13.3	Biolegend	Rat IgG2a, κ	1:200
CD31	390	Biolegend	Rat IgG2a, κ	1:800
CD45.1	A20	Biolegend	Mouse IgG2a, κ	1:200
CD45.2	104	Biolegend	Mouse IgG2a, κ	1:200
CD64	x54-5/7.1	Biolegend	Mouse IgG1, κ	1:200
F4/80	BM8	Biolegend	Rat IgG2a, κ	1:250
IL-4Rα	mIL4R-M1	BD	Rat IgG2a, κ	1:50
Ki67	B56	BD	Mouse IgG1, κ	1:4
Ly6C	hk1.4	invitrogen	Rat IgG2c, κ	1:400
Ly6G	1A8	Biolegend	Rat IgG2a, κ	1:200
MHCII	M5/114.15.2	Biolegend	Rat IgG2b, κ	1:400
NK1.1	PK136	Biolegend	Mouse IgG2a, κ	1:400
Siglec F	E50-2440	BD	Rat IgG2a, κ	1:250
Siglec F	ES22-10D8	Miltenyi	Rat IgG1	1:30
Tim4	RMT4-54	Biolegend	Mouse IgG2a, κ	1:400
Treml4	16E5	Biolegend	Rat IgG1, κ	1:250
Strep. BV650	n/a	Biolegend	n/a	1:200
Xenon AF647	n/a	Life	Rabbit IgG	1:300
Annexin V	n/a	Biolegend	n/a	1:20
FVD eFluor 780	n/a	eBioscience	n/a	1:1000
Zombie Aqua FD	n/a	Biolegend	n/a	1:100

Abbreviations: Strep.: streptavidin; FVD: fixable viability dye; FD: fixable dye anti-Ki67 in a total of 20μl perm/wash. Isotype control was used as Ki67 control. Cells were then washed with perm/wash and acquired[121].

2.6.4 Sample acquisition and analysis

Cells were acquired on an LSR Fortessa (BD Biosciences) and cell sorting was performed on a FACSAriaII (BD) or FACSAria Fusion BD all at the QMRI Flow Cytometry and Cell Sorting Facility.

To generate a compensation control matrix in the FACS Diva software (BD Biosciences) compensation beads (eBioscience) were diluted ~1:10 in FACS buffer and incubated with relevant antibodies at 1:200 for 10 minutes and then washed.

Data was analysed in FlowJo software (10.1r3, Tree Star, Ashland, Oregon)

2.7 Adoptive transfer

BM cells were isolated from male *Csf1r*-EGFP mice as outlined in 2.5.7. Cells were then stained and sorted to identify Ly6C^{hi} GFP^{+} monocytes to be adoptively transferred (gating strategy outlined in results). Cells were sorted into 15ml Falcon tubes containing 5ml FACS buffer. Using the cell counts obtained at sorting, cells were resuspended at 3-5x10^{6} cells/ml in dPBS. 200μl of the suspension of cells was injected at the defined timepoints via the tail vein[117].

2.8 In vitro monocyte culture

BM cells were isolated from 8-week-old male C57Bl/6 mice as outlined in 2.5.7. Cells were then stained and Ly6C^{hi} monocytes sorted into 15ml Falcon tubes containing 5ml of culture media: DMEM + L/Glutamax (Gibco) + 2% pen strep + 10% FCS (Gibco). Sorted monocytes were plated at 1x10^{6}/ml in 100μl in culture media over 16 hours in flat bottom 96 well Nunclon Sphera low adherence plates (Nunc). Cells were either cultured in media alone or a combination of rCSF-1 (Miltenyi), rIL-4 (Peprotech) and rIL-13 (Peprotech) doses are outlined in the results. After 16 hours incubation cells were harvested by the addition of 100µl cold (4°C) FACS buffer by pipetting up and down in the well. Cells were then transferred to a 96 well V bottom plate and washed. A further 100µl cold (4°C) FACS buffer was applied to each well of the low adherence plate to harvest any residual cells, and an inverted microscope (Fisher) at 10x was used to ensure there were no residual cells. The 100µl of FACS buffer used to harvest any residual cells was then added to the appropriate wells of the V bottomed 96 well plate. The V bottomed 96 well plate was then centrifuged ready for staining as per section 2.6.1.

2.9 Nanostring analysis

For Nanostring analysis 300µl of whole blood was processed and sorted using the FACS Aria cell sorter to identify Ly6C^{hi} monocytes as outlined in the results. 5,000 cells were sorted into 2µl of RLT buffer (Qiagen) in a 1.5ml Eppendorf tube. Cells were then spun in a microcentrifuge (Thermo) at 17,000g for 15 seconds, this was repeated following vortexing of the resultant pellet of cells. Following microcentrifugation cells were kept on ice until all samples were processed. Samples were then transferred to a PCR strip tube for storage at -80°C.

The rest of the protocol was performed by Alison Munro at the University of Edinburgh core Nanostring facility located at the Institute of Genetics & Molecular Medicine (IGMM). She performed the hybridisation and then ran the samples using the Nanostring Mouse Myeloid V2 panel on the nCounter platform (Nanostring technologies).

Analysis of results was performed using the nSolver Analysis Software (version 4.0) and advanced analysis performed with the nCounter Advanced Analysis (version 2.0.115).

2.10 Staining of tissue sections

At necropsy the median lobe was dissected from the liver and the left segment placed in 10ml methacarn solution and the right lobe placed in 10ml 10% formalin. Methacarn solution comprises: 60% methanol (Fisher), 30% chloroform (Fisher) and 10% Acetic acid. 10% formalin (3.7% formaldehyde) was made by diluting 37% formaldehyde solution (Sigma) 1:10 with PBS. Livers were left in fixative for 12 hours then removed and placed in 70% ethanol. Livers were embedded in paraffin and sectioned (4μm) at the University of Edinburgh Shared University Research Facilities (SURF). Unless otherwise stated, images were acquired using an Axiovert 200 light microscope (Carl Zeiss) running Axiovision software (version 4.6.3) for image capture.

2.10.1 Periodic acid schiff staining

Staining was performed by the staff in the SURF core facility.

2.10.2 Analysis of necrotic tissue

Analysis of necrosis for the priming vs therapeutic IL-4c experiment (Chapter 3) was performed on thumbnails of whole sections of stained liver acquired using an Olympus Dotslide slide scanner at the IGMM. The acquired images were analysed using ImageJ analysis software with the WEKA segmentation application. The software was trained to recognise parenchyma, necrotic tissue, cellular infiltrate, blood vessels and empty space surrounding tissue. It then performed an automated quantification of all these parameters[255].

Analysis of samples from the whole-body irradiation chimeras (Chapter 5) was performed on whole tissue sections acquired at 5x magnification on a Hamamatsu Nanozoomer. Images were then analysed on the Definiens tissue analysis software package. A script was designed to recognise parenchyma; necrotic area; blood vessels and empty space. The software then performed an automated quantification of all these parameters.

2.10.3 BrdU identification

The following protocol was optimised by myself but the quantitative data presented in this thesis were generated by two undergraduate honours students that I supervised: Eleni Papachristoforou and Andrew Muir.

Staining protocol

Unless otherwise stated all buffers are at room temperature. Slides were dewaxed in xylene, washed in PBS and then endogenous peroxidase activity was blocked with 0.3% hydrogen peroxide (Sigma). Antigen retrieval was performed with 1mg/ml of trypsin (Sigma) for 10 minutes. After two PBS washes, slides were incubated in warmed (37°C) acidified water (12N HCl) for ten minutes. Slides were then washed twice with 0.1M Borax solution (Sigma) and then washed twice with PBS before mounting in Sequenza racks. Non-specific binding of antibodies was blocked with Mouse on Mouse (MOM) IgG blocking reagent (Vector) for one hour, washed twice with PBS, then incubated with MOM protein concentrate for five minutes. Mouse anti-BrdU (DAKO) primary antibody was applied at 1:40 dilution in MOM diluent for thirty minutes, then washed twice with PBS. MOM biotinylated anti-mouse IgG was then applied at 1:250 dilution in MOM diluent for ten minutes. Biotinylated molecules were detected with application of Vectastain Elite ABC reagent (Vector) for ten minutes and followed by liquid DAB^+ (DakoCytomation) for five minutes to develop a brown colour to the biotinylated secondary antibody. Slides were then counterstained with haematoxylin and dehydrated prior to xylene fixation and mounting.

Analysis of $BrdU^+$ hepatocytes

Ten adjacent fields of view (FoV) were captured at 20x magnification for each sample. $BrdU^+$ hepatocytes were identified by positive staining and their morphology. Proportion of $BrdU^+$ hepatocytes was established by counting all hepatocytes per FoV using ImageJ. Quantification of sections was performed blind to treatment groups.

2.10.4 F4/80 staining

The following protocol was optimised by myself but the staining presented in this thesis was generated by Andrew Muir and captured by myself.

Unless otherwise stated all buffers are at room temperature. Slides were dewaxed in xylene, washed in PBS and then endogenous peroxidase activity was blocked with 0.3% hydrogen peroxide (Sigma). Slides were washed with PBS prior to mounting in Sequenza racks for staining. Avidin and biotin were blocked sequentially with 3 drops of avidin and biotin block (Vector). Non-specific antibody binding was blocked with normal rabbit serum (Vector) for 30 minutes and then slides were incubated with 1:50 anti-F4/80 antibody [CI:A3-1] (Abcam) made in antibody diluent reagent solution (Life Technologies). Slides were then washed and incubated with 1:200 rabbit ant-rat secondary (Vector) made in antibody diluent reagent solution (Life Technologies). Biotinylated molecules were detected with application of Vectastain Elite ABC reagent (Vector) for 30 minutes and followed by liquid DAB^{+} (DakoCytomation) for five minutes to develop a brown colour to the biotinylated secondary antibody. Slides were then counterstained with haematoxylin and dehydrated prior to xylene fixation and mounting[115].

2.11 Statistical analysis

All data were analysed in Prism 6 (GraphPad), with statistics detailed in relevant figure legends, all ANOVA performed with Tukey’s multiple comparisons test. *$P < 0.05$, **$P < 0.01$, ***$P < 0.001$, ****$P<0.0001$.

Chapter 3 IL-4 as a therapeutic in acute CCl_4 liver injury

3.1 Introduction

As discussed in Chapter 1 interleukin-4 (IL-4) administration in the form of IL-4c has been shown to be beneficial in the setting of acute liver injury with CCl_4[33]. However, in their study Goh et al. used a mixed prophylactic and treatment administration regimen in which mice were administered IL-4c 24 hours prior to and 48hrs after injury with CCl_4 with a resulting reduction in indices of hepatic injury (circulating ALT and necrotic cell area) and increase in indices of regeneration (hepatocyte proliferation). Thus, it remains unclear whether therapeutic delivery of IL-4 alone leads to beneficial effects on liver repair and regeneration or if prophylactic pre-conditioning is necessary. This question of timing is essential when seeking to understand mechanisms and processes that could be clinically beneficial for patients with acute liver injury.

Hence, in this first results chapter I sought to establish whether IL-4c could be administered therapeutically following injury and have the same beneficial effects as administration pre- and post-injury (Fig. 3.1A). Furthermore, because in the work by Goh et al. ALT is normalising at 48 hours following injury, I proposed that to have any therapeutic effect IL-4c needed to be administered earlier at 24 hours following injury[33]. For any potential human therapy this is important because the aim would be to administer a treatment at maximal injury to try to enhance the repair process.

As also detailed in Chapter 1, endogenous IL-4 has been shown to be important in wound repair not only in the setting of helminth infections but also in the setting of physical injury in the skin and colon[29,30,256]. Specifically, IL-4 signalling to macrophages is important for wound healing and effective collagen deposition in these settings. While experiments in myeloid-specific LysM-Cre IL-4R$\alpha^{fl/fl}$ mice have seemingly discounted a beneficial role of IL-4Rα-signalling to macrophages following acute liver injury[33], it is possible that endogenous IL-4 or IL-13 is not produced at sufficient levels or in the required locale to act on hepatic macrophages. Furthermore, we know from work by Vanella et al. that this Cre-lox system is inefficient during acute inflammation[34] and can therefore not be used to rule out any significant effect of IL-4Rα signalling to myeloid cells during inflammation.

For this reason, my initial experiments aimed not only to assess the effects of therapeutic IL-4c on indices of repair and regeneration but also to assess the effect on the macrophage compartment. For this purpose, I used routine immunohistochemistry (IHC) techniques to stain for macrophages in tissue sections and developed a strategy to analyse macrophages and other leukocyte populations by flow cytometry.

3.2 Comparison of pre- and post IL-4c and therapeutic IL-4c

To determine whether therapeutic delivery of IL-4c alone was sufficient to improve indices of liver injury and regeneration or if combination with prophylactic delivery was necessary for the enhanced repair/regeneration process, I compared two separate regimens of IL-4c administration (Fig. 3.1A):

- Combined prophylactic and therapeutic delivery, termed ‘Priming’ regimen: administration of IL-4c 24 hours before and after CCl_4 injury.
- Therapeutic regimen: IL-4c administration 24 hours after CCl4 injury.

In an attempt to replicate the work of Goh et al., a fixed dose of 2µg/mouse (approx. 0.08 mg/kg) of IL-4c was used in this first experiment. Within the laboratory group the protocol for eliciting an acute liver injury with CCl_4 involved administration of 1 µl/g of CCl_4 (100% w/v) which equates to 1mg/g by weight which is higher that the dose of 0.4mg/g used in Goh et al[33]. Mice were culled 72hrs after administration of CCl_4, a timepoint where measures of both tissue injury (serum liver enzymes, necrotic cell area) and regeneration (hepatocyte proliferation) are apparent, thereby allowing assessments of the effects of IL-4 on a number of distinct processes in liver repair[22,33].

3.2.1 Priming and therapeutic IL-4c regimens are equivalent in improving hepatic enzymes and necrotic cell area

Analysis of serum enzymes of hepatic injury revealed that there was a significant reduction in ALT in the priming (143.2 ± 30.83 P<0.01) and therapeutic (133.0 ± 26.8 P<0.001) regimens when compared to the vehicle treated group (242 ± 61.9) (Fig. 3.1B). Furthermore, there was no significant difference in the degree of reduction between the priming and therapeutic regimens. Notably there were only trends to lower AST in the IL-4c treated groups when compared to vehicle alone (Fig. 3.1C).

Analysis of PAS stained sections revealed that the necrotic area observed in vehicle treated mice (Fig. 3.2A) was replaced with a cellular infiltrate in both the priming and therapeutic regimens (Fig. 3.2B-C). Quantification of necrotic cell area using ImageJ as outlined in the methods revealed a significant reduction in the proportion of necrotic tissue in the priming (0.0% ± 0.0, P<0.001) and therapeutic (0.4% ± 0.6%, P<0.001) regimens when compared to the vehicle treated group (11.6% ± 7.0) (Fig. 3.2D). Furthermore, the reduction in necrotic area was equivalent between priming and therapeutic regimens.

3.2.2 Trend towards higher hepatocyte proliferation with IL-4c

Hepatocyte proliferation is a key measure of tissue regeneration in the liver following acute injury. To allow measurement of cell proliferation in the liver in these experiments, mice were pulsed with the thymidine analogue BrdU 2hr prior to necropsy and BrdU incorporation measured by IHC. CCl_4-induced liver injury resulted in heightened hepatocyte proliferation in all groups compared with olive oil controls (staining and quantification for BrdU performed by Eleni Papachristoforou a BSc honours student) (Fig 3.3A-D). However, there was only a trend to higher levels of proliferation in the priming (16.7% ± 6.4) and therapeutic (12.1% ± 4.9) regimens when compared to the vehicle treated group (11.1% ± 1.9) (Fig. 3.3E), despite the increase proliferation reported by Goh that resulted from a similar priming regimen[33].

Notably when the experiments were analysed separately, the second experiment (RL007) revealed a significant increase in proportion of proliferating hepatocytes in IL-4c treated mice compared to vehicle alone (Fig. 3.3F-G). Importantly, in the first experiment (RL002) all mice were administered BrdU at the same time but culled sequentially, meaning the time for BrdU incorporation varied between mice. In the second experiment and all subsequent experiments, BrdU pulsing was staggered to allow exactly 2 hours between administration of BrdU and culling for each animal.

3.2.3 Exclusion of outlier during analysis

By the time of necropsy, one mouse from the priming group had significant weight loss of 18.6% and exhibited clinical signs of distress unlike the other mice that had received CCl_4. However, because this did not meet any of the pre-determined limits or humane end points this mouse was included in the analyses. When the ALT (576 u/l) and necrotic cell area (29.28%) were analysed they were found to represent significant outliers, as determined using the ROUT method in PRISM with a G value of 0.1%. This result also held true when using Grubbs' test for outliers with Alpha of 0.01 for ALT and 0.0001 for necrotic cell area.

3.3 Identification of liver leukocytes by flow cytometry

To determine the effect of IL-4 treatment on the composition of liver leucocytes, I first used multiparameter flow cytometry to examine single cell suspensions from enzymatically-digested livers. Throughout this project, I have endeavoured to use the same gating process (Fig. 3.4A) based on exclusion of debris, doublets and dead cells using FSC-A versus SSC-A characteristics, FSC-A versus FSC-H properties and negativity for 'Aqua' fixable viability dye, respectively. In later experiments 7-AAD was used to exclude dead cells if fixation was not required, because it provided better discrimination between live and dead cell populations (Fig. 3.4B). Leukocytes were identified amongst liver isolates based on their expression of the pan-leukocyte marker, CD45.

Due to a limitation in the number of parameters available, a ‘lineage’ gate comprising CD19, CD3, Ly6G and Siglec-F in the same fluorescence channel was used to identify T cells, B cells, neutrophils and eosinophils respectively. Although primarily used to exclude lymphocytes and granulocytes from analysis, this lineage gate allowed me to broadly identify and distinguish these populations (Fig. 3.4) using the variety of markers included for characterisation of macrophages and monocytes. In this way, granulocytes were distinguished by their expression of CD11b. Neutrophils were subsequently identified by their SSC-A^{int} profile and high levels of Ly6G expression, revealed as a high degree of staining in the lineage (Lin) gate/channel. Eosinophils were identified by their SSC-A^{hi} characteristics and intermediate position in the lineage channel. T and B cells comprised the Lin^{+}CD11b^{-} fraction and could be distinguished based on MHCII expression; Lin^{+}CD11b^{-}MHCII^{+} B cells and Lin^{+}CD11b^{-}MHCII^{-} T cells. In earlier experiments Siglec-F was detected in a separate channel to identify eosinophils because Goh et al. demonstrated that eosinophils were the source of innate IL-4 following liver injury[33] and I therefore wanted to be able positively identify this population. When reference is made to lineage negative (Lin^{-}) throughout the project I have specified the markers used to make it clear what cells have been excluded.

Amongst the Lin^{-} population resident hepatic Kupffer cells were identified by their high expression of F4/80 and low levels of CD11b (F4/80^{hi}CD11b^{lo}) (Fig. 3.4A) a standard approach that has been used by many groups[50,91,115]. In contrast, the Lin^{-}CD11b^{hi} population are considered to comprise a mixture of recruited monocytes, macrophages and cDC2 dendritic cells [22,115,257]. Classical monocytes were first identified by their high expression of Ly6C and largely low levels of MHCII (Fig. 3.4A). However, beyond this, the discrimination of mature macrophages and migratory DC was more challenging. In my initial experiments, I simply used differential expression of Ly6C and MHCII to define these subsets, with Ly6C^{lo} MHCII^{int} cells being defined as macrophages and Ly6C^{lo} MHCII^{lo} cells as cDC2 (Fig. 3.5C). However, this approach lacked a positive identification marker of macrophages. Later in my project I was able to optimise my flow cytometry panel to including CD64, the high affinity FcγR1, which has been used to positively identify macrophages in a variety of tissues [94,97,98,112]. Using this approach, I was able to identify Ly6C^{hi} CD64^{lo} monocytes, Ly6C^{lo} CD64^{hi} macrophages and Ly6C^{lo} CD64^{lo} cells (Fig. 3.5A). The Ly6C^{lo} CD64^{lo} population had bimodal expression of MHCII, with the MHCII^{hi} population likely representing cDC2 cells (Fig. 3.5B). Thus, by combining Fig. 3.5B and C it is possible to show that the populations of Ly6C^{hi} monocytes and Ly6C^{lo} macrophages are essentially the same independent of whether they were identified using MHCII or CD64 (Fig. 3.5D). Furthermore, IL-4R signalling can affect MHCII expression and therefore I felt it was important to have strategy that did not rely on MHCII[207]. Using fluorescence minus one (FMO) controls I have also been able to show that the relatively higher Ly6C and MHCII expression identified within the Ly6C^{lo} CD64^{hi} macrophage population when compared to cDC2 cells largely represents autofluorescence (Fig. 3.5E).

The staining panel employed to identify Kupffer cells also evolved over the course of the project to include the phagocytic receptor Tim-4, an apoptotic cell receptor that has been used to define resident macrophages in multiple tissues, including the liver and peritoneal cavity [50,258] (Fig. 3.5F). Work in the Jenkins group suggested that Tim-4 expression remains an exclusive property of Kupffer cells following injury. Therefore, the addition of Tim-4 provided better discrimination between *bona fide* resident Kupffer cells (F4/80^{hi} CD11b^{lo}Tim-4^{+}) and short-lived CD11b^{hi} mononuclear phagocytes that lack Tim-4 expression (Fig. 3.5G).

It has been made clear in the text which strategy was used to identify the resident macrophages, and CD11b^{hi} recruited populations in each experiment.

3.4 Effect of IL-4c on monocytes and macrophages

Having established a basic strategy for the identification of monocytes and macrophage subsets in the liver, I next examined the effect of IL-4c on these subsets in the context of CCl_4-induced liver injury. Consistent with previous work[22], I found that CCl_4 administration resulted in a dramatic loss of F4/80^{hi}CD11b^{lo} Kupffer cells and an increase in the abundance of CD11b^{hi} cells compared to olive oil controls (Fig. 3.6A). The expansion of this CD11b^{hi} compartment was due to increases in both the Ly6C^{hi} and Ly6C^{lo} populations (Fig. 3.6C). Strikingly, IL-4c treatment, both therapeutic and priming, resulted in accumulation of CD11b^{hi} cells expressing high levels of F4/80 (Fig. 3.6A-B). This reflected a reduction in the proportion of Ly6C^{hi} monocytes (Fig. 3.6C) and a concomitant trend to an increased proportion of recruited Ly6c^{lo} macrophages (Ly6c^{lo} MHCII^{int}) within this compartment in the recipients of IL-4c (Fig. 3.6C).

Given the marked effects of IL-4c on the monocyte/macrophage compartment, I postulated whether the infiltrating cells observed in the necrotic cell area following IL-4c treatment (Fig. 3.2A-C) could represent macrophages. To this end, I assessed tissue sections from the same mice as analysed above for expression of the pan macrophage marker F4/80. In injured mice given vehicle control, F4/80^{+} macrophages were visible throughout the healthy parenchyma in similar density to those in olive oil control, and likely represent resident KC. However, F4/80^{+} cells were largely absent from the necrotic cell area (Fig. 3.7A). In contrast, there was a striking increase in F4/80^{+} cells within the necrotic cell area in the recipients of IL-4c (Fig. 3.7B).

3.5 Dose titration of therapeutic IL-4c

Having established that IL-4c can be administered therapeutically to enhance reduction of hepatic enzymes and necrotic cell area, I next sought to establish whether using a higher dose would influence the indices of injury and regeneration but also alter the phenotype seen in the monocyte/macrophage compartment. Furthermore, I also wanted to know whether a lower dose of IL-4 would have a similar effect. The priming regimen was also dropped from all subsequent experiments.

3.5.1 Establishing IL-4c dosing

In the initial experiment a fixed dose of 2ug/mouse of IL-4 was administered to each mouse in the form of IL-4c in accordance with the method published by Goh et al[33]. However, to ensure equivalent dosing between individual mice and to perform a dose titration, I subsequently calculated the mean weight-adjusted dose that had been administered on day 1 in the priming vs therapeutic IL-4c experiments (0.082μg/g ± 0.006) and compared this with a dose 2.5x higher and 2.5x lower, 0.2μg/g and 0.032μg/g respectively.

3.5.2 Indices of injury and regeneration with titration of IL-4

IL-4c was administered at the doses outlined above 24 hours following CCl_4 induced injury (Fig 3.8A). In this set of experiments, only with the high dose of IL-4 did I observe a significant reduction in ALT compared to vehicle alone (152 u/l ± 75.3 vs 404.1 ± 299.6, $P<0.05$) (Fig.3.8B). There was however a significant reduction in AST across all groups treated with IL-4c when compared to vehicle alone, but this reduction was most significant in the high dose IL-4 group (209.2 u/l ± 87.5 vs 450.4 ± 100.6, $P<0.0001$) (Fig. 3.8C). There was no difference observed in another marker of liver injury, bilirubin, between groups (Fig. 3.8D).

The effect of dose on liver regeneration was also measured. Across all doses of IL-4c there was increased tissue regeneration compared to vehicle control, as measured by an increased proportion of $BrdU^+$ hepatocytes (stained and quantified by Andrew Muir BSc honours student) (Fig. 3.8E). Notably the mean proportion of $BrdU^+$ hepatocytes was highest in the high dose group (23.3% $\pm$ 5.8) and there was lower variability as measured by standard deviation in this group compared to the low dose (21.3% $\pm$ 8.3) and medium dose (21.1% $\pm$ 6.5) groups. As weight was measured as part of the dosing regimen, I decided to assess whether weight loss might provide an additional readout of beneficial effects of IL-4. However, despite a trend to greater weight loss in mice receiving CCl_4, no significant differences were seen between treatment groups (Fig. 3.8F).

3.5.3 Altered monocyte/macrophages dynamics in response to IL-4c

Given the effects of IL-4c on monocyte/macrophage dynamics revealed in my comparison of the priming vs therapeutic IL-4c regimens, I wanted to ascertain if these were also dependent on IL-4c dose. Quantification of the changes in $Ly6C^{hi}$ monocytes revealed a significant reduction both in proportion of $Ly6C^{hi}$ monocytes and in number with all doses of IL-4 (Fig. 3.9A-C). During liver injury it is thought that $Ly6C^{hi}$ monocytes convert locally into $Ly6C^{lo}$ macrophages [21,115] and that these cells are important for limiting prolonged hepatic damage[21]. Indeed, the reduction in $Ly6C^{hi}$ monocytes in recipients of IL-4c was paralleled by increases in the frequency of $Ly6C^{lo}$ $MHCII^{int}$ macrophages (Fig. 3.9D). However, it was noted that only the high dose of IL-4c led to a significant increase in the absolute number of $Ly6C^{lo}$ $MHCII^{int}$ macrophages when compared to vehicle ($1.34 \times 10^7 \pm 6.79 \times 10^6$ vs $6.84 \times 10^6 \pm 3.28 \times 10^6$). In keeping with a significant liver insult, I observed a reduction in proportion and total number of Kupffer cells with CCl_4 injury (Fig. 3.9F). However, while not significant, the reduction in proportion of Kupffer cells that occurred with injury was less apparent in mice given therapeutic IL-4c irrespective of dose (Fig. 3.9F) and there was a trend to higher numbers of Kupffer cells with IL-4c treatment that reached significance in the mice that received the highest dose (0.2μg/g).

3.5.4 Effect of IL-4 on other leukocyte populations

It has been shown that during acute liver injury neutrophils are important regulators of the repair process[21] and Goh et al. also showed that eosinophil production of IL-4 is important for hepatocyte regeneration[33]. For this reason, I have also looked at the effect of exogenous IL-4 on other leukocyte populations. By day 3 post injury there was a significant increase in proportion of eosinophils with all IL-4c treatment doses and when corrected for cell number this bore true for the high dose of IL-4c too (Fig. 3.10A, B). IL-4c had no significant effect on the proportion or number of neutrophils following injury (Fig. 3.10C, D). Within the lymphocyte populations IL-4c had no effect on frequency or number of T cells (Fig. 3.10E, F) but high dose IL-4c did cause a significant reduction in frequency of B cells (Fig. 3.10G). Furthermore both medium and high dose IL-4c showed a significant reduction in the number of B cells (Fig. 3.10H).

Hence, exogenous IL-4 has a varying effect on the inflammatory infiltrate causing a reduction in $Ly6C^{hi}$ monocytes and an increase in the number of $Ly6C^{lo}$ macrophages. Furthermore, it causes a dose independent increase in proportion of eosinophils and the high dose of IL-4 causes a significant reduction in the proportion of B cells.

3.5.5 Exclusion of 2 mice during analysis

One mouse in the CCl_4 + veh group was found to have what was thought to be an iatrogenic perforated colon at the time of necropsy and was therefore excluded from all analyses. During sample preparation of one of the olive oil samples for flow cytometry the Falcon tube containing the cell suspension was cracked and it was therefore not possible to analyse by flow-cytometry.

3.6 IL-4Rα expression on leukocytes

As a first step to establish whether the observed effects of IL-4 on the composition of inflammatory infiltrate could be due to direct IL-4R signalling, I set out to establish expression of the IL-4Rα by leukocyte subsets 24 hrs post injury, the timepoint at which IL-4c is usually administered in my model. As expected, Ly6C^{hi} monocytes were found to express the IL-4Rα (Fig. 3.11A)[34,259]. In this experiment, discrimination of F4/80^{hi} CD11b^{lo} Kupffer cells from recruited CD11b^{hi} cells proved particularly difficult due the high level of CD11b expression observed on the former. This appeared to be caused by the combination of antibodies used (F4/80 conjugated to PE-Cy7 and CD11b conjugated to Pacific Blue) that was necessitated by the need to include an antibody to IL-4Rα on AF647 (Fig. 3.11B). I suspect this is a result of the fluorophore combination because Kupffer cells are known to express low levels of CD11b[50,93] and in later experiments using Tim-4 I have observed this lower expression of CD11b. Thus, IL-4Rα expression was examined on all Ly6C^{lo} MHCII^{int} macrophages, which included both the Ly6C^{lo} MHCII^{int} macrophages and Kupffer cells. Here, like in monocytes, the macrophages were found to uniformly express the IL-4Rα (Fig. 3.11C). In fact, all populations that we examined expressed the IL-4Rα at 24 hours following acute CCl_4, apart from eosinophils on which no expression was detected (Fig. 3.11D-G). Because of the technical difficulties described above, this experiment was repeated with F4/80 conjugated to PE-Cy7 and CD11b conjugated to APC-Cy7) and in so doing we could establish that both Kupffer cells and recruited macrophages expressed the IL-4Rα (Fig. 3.12A). However, it is important to note that at the 24 hour timepoint there is a paucity of recruited Ly6C^{lo} MHCII^{int} macrophages making assessment of MFI not the most reliable in this population. Notably in this repeat experiment we did not have IL4ra$^{-/-}$ controls so MFIs were calculated using FMO controls. This repeat experiment also confirmed that neutrophils and B cells expressed IL-4Rα, while eosinophils lacked IL-4Rα expression. While T cells appeared to lack IL-4Rα in this repeat experiment, it is important to note that only very low levels of expression were observed on these cells in the first experiment.

3.7 Discussion

In previous work Goh et al.[33] demonstrated that IL-4c administered in a priming regimen had a beneficial effect on reducing indices of hepatic injury and enhancing indices of regeneration. Taking this work further I have shown in this chapter that administration of exogenous IL-4 has a beneficial effect on both markers of liver injury, ALT, AST and necrotic cell when administered as a therapy following CCl_4 induced injury. Furthermore, I demonstrated that regeneration as assessed by hepatocyte proliferation was improved following administration of therapeutic IL-4c. Interestingly elevated proliferation of hepatocytes with IL-4c treatment was not apparent in my first experiment RL002 (Fig. 3.3E) in either the priming or therapeutic regimen. This is likely due to a technical problem with the staining protocol because more BrdU$^+$ hepatocytes were found in injured mice compared to olive oil controls. Indeed, enhanced proliferation in IL-4 treated groups was seen in the dose titration experiment at all doses. A potential explanation is that in RL002 all mice were administered BrdU at the same time, whereas in later experiments injections were staggered to account for the delay in culling mice, thereby ensuring that all mice received a 2-hour pulse of BrdU. The lack of effect of IL-4 may therefore reflect a technical issue with the timing of the assay. Notwithstanding the technical issues these results indicated that therapeutic administration of IL-4 resulted in the same beneficial outcome as the priming regimen previously reported.

Using multicolor flow cytometry to study leukocyte populations it was possible to identify different cells through the expression of specific surface markers in the livers of all treatment groups. It was evident from the first experiment that the beneficial effect of IL-4c corresponded with marked changes in the profile of the recruited leukocytes. However, it took several experiments to establish a staining panel that would identify resident from recruited macrophages and it also took a couple of experiments to establish the subtle nuances of the staining protocol to obtain good leukocyte isolates to stain and generate useable data. It was therefore not until the dose titration experiments that I am confident of the data and it is the flow-cytometry results from these experiments that I refer to in the rest of this discussion. The two most striking effects revealed by the flow cytometry data were the reduction in Ly6C^{hi} monocytes and the increase in Ly6C^{lo} macrophages. This reduction in Ly6C^{hi} cells might be predicted to be beneficial as these cells are thought to contribute to injury during early acute drug induced liver injury as they express pro-inflammatory genes[21,23,145]. Similarly an increase in Ly6C^{lo} macrophages may also be beneficial as they are considered to have pro-reparative functions in regulating angiogenesis and extracellular matrix remodelling[21,23,145]. Notably it remains unclear during injury what controls the switch from a pro-inflammatory to a pro-reparative mononuclear phagocyte population. Thus, using IL-4c to manipulate the inflammatory infiltrate may have potential advantages over alternatives, such as blocking monocyte recruitment through the administration of anti-CCR2/CCR5 antibodies (e.g. CVC). For instance, IL-4c appears to result in the reduction of potentially deleterious Ly6C^{hi} monocytes whilst seemingly not inhibiting the accumulation of pro-reparative monocyte derived Ly6C^{lo} macrophages, which is one of the limitations of anti-CCR2 treatment[21]. Although the global effects of exogenous IL-4c on the monocyte-macrophage compartment in this setting remain unclear at this stage, IL-4 is known to promote macrophage proliferation and this could potentially be the mechanism of expansion of Ly6C^{lo} macrophages observed here[206]. Moreover, IL4c could promote the conversion of Ly6C^{hi} monocytes to Ly6C^{lo} macrophages, and these alternatives are the focus of subsequent chapters.

Amongst the other leukocyte populations IL-4c seemed to cause the most marked change in the number of eosinophils even though these cells did not express the IL-4Rα. This change therefore likely represents an indirect effect of IL-4 on another cell type leading to an increase in eosinophils. In fact it has already been demonstrated that alternatively activated macrophages recruit eosinophils to tissues by secreting Ym1[183,260,261]. Goh et al. already demonstrated that eosinophils are important for the innate repair process following acute CCl_4 mediated liver injury[33], and recent work by Toor et al. has suggested that low eosinophil counts are associated with poor outcome following myocardial infarction, and IL-4c administration may ameliorate outcomes by increasing eosinophil numbers[262]. I would therefore suggest that the observed increase in eosinophils is likely beneficial although in asthma it is thought that eosinophils are detrimental as they may contribute to airway hyperresponsiveness[263]. Interestingly, although I demonstrated a significant reduction in Ly6C^{hi} monocytes at this day 3 timepoint there was not a concomitant reduction in neutrophils as was reported by Zigmond et al. in APAP injury when monocytes were depleted[21]. This could be because the neutrophilia may have occurred earlier and is addressed in subsequent result chapters with the timecourse I performed later during my project.

Initial experiments employed a dose of 2ug of IL-4/mouse because this was the dose used by Goh et al. Weight adjusted doses of IL-4c appear to be rarely used in the literature but the high dose of 0.2μg/g would equate to 5μg of IL-4 in a 25g mouse. This dose of 5μg of IL-4/mouse is used in the majority of studies where exogenous IL-4 is studied[206,208,210]. It therefore seemed that this was an appropriate dose to trial to assess whether the effects of IL-4c administration could be enhanced with higher doses. I also wanted to establish whether there was a true dose dependent effect by reducing the dose of IL-4 and so a dose 2.5x lower than initially used was also trialed. There did appear to be a dose dependent effect with increasing doses of IL-4c leading to reduced serological indices of injury and elevated indices of regeneration. Furthermore, there was less variation in ALT and AST results with higher doses of IL-4c and less variation in the proportion of BrdU$^+$ hepatocytes. The analysis of flow cytometry data revealed that all doses of IL-4c resulted in a significant reduction in frequency and number of $Ly6C^{hi}$ monocytes but as with the indices of injury and regeneration there was less variation with the higher dose. Furthermore, when the increase in number of $Ly6C^{lo}$ macrophages was calculated there were only significantly more with the higher dose of IL-4c. Similarly, the increase in number of Kupffer cells compared to injury alone was only significant in the high dose of IL-4c group. There was a marginally significant increase with the number of Kupffer cells in the high dose IL-4c group. All these results suggested that the higher dose was more effective. The increase in resident Kupffer cells with IL-4c treatment is not surprising given that IL-4c has been previously demonstrated to promote resident macrophage proliferation[121,207]. It is notable that the number of Kupffer cells was still far outweighed by the dramatic increase in $Ly6C^{lo}$ macrophages. Going forward I decided to use the higher dose of IL-4c because it appeared to provide more significant and homogenous results.

In homeostasis the resident population of $F4/80^+$ macrophages in the liver are termed Kupffer cells, and are located in the sinusoids throughout the parenchyma[16,264]. In tissue sections there appeared to be a loss of $F4/80^+$ cells in the parenchyma in CCl_4 treated mice when compared to olive oil control mice which would be in keeping with the previously reported "disappearance reaction" in acute liver injury[21,22,145]. However, IL-4c appeared to be having an effect on the $F4/80^+$ cells which was evident by a dramatic increase in F4/80 cells surrounding the central vein only in the IL-4 treated group. In conjunction with Andrew Muir I attempted to quantify this staining but it was not possible to differentiate between the $F4/80^+$ cells in the parenchyma and those surrounding the central vein using a machine learning based approach. The assumption was that the cells in the parenchyma represented Kupffer cells and those in the necrotic area were the recruited macrophages. It remains possible that Kupffer cells may be recruited to the necrotic area, however, to identify whether this was the case would require staining for a Kupffer cell specific marker, for instance Tim4[39]. Cathy Hawley, another member of the group, tried extensively to get the Tim4 staining to work on paraffin embedded sections and found that it only worked on fresh frozen sections. Unfortunately, all my relevant samples were archived in paraffin embedded blocks.

In this chapter I have identified that IL-4c can be used therapeutically following acute liver injury with CCl_4. Furthermore, the main effect of IL-4c on leukocyte populations appears to be the reduction of Ly6C^{hi} monocytes and increase in Ly6C^{lo} macrophages. In the coming chapters I will endeavor to further characterize this phenotype using a timecourse and establish the intrinsic effect of IL-4Rα signaling on the observed phenotype.

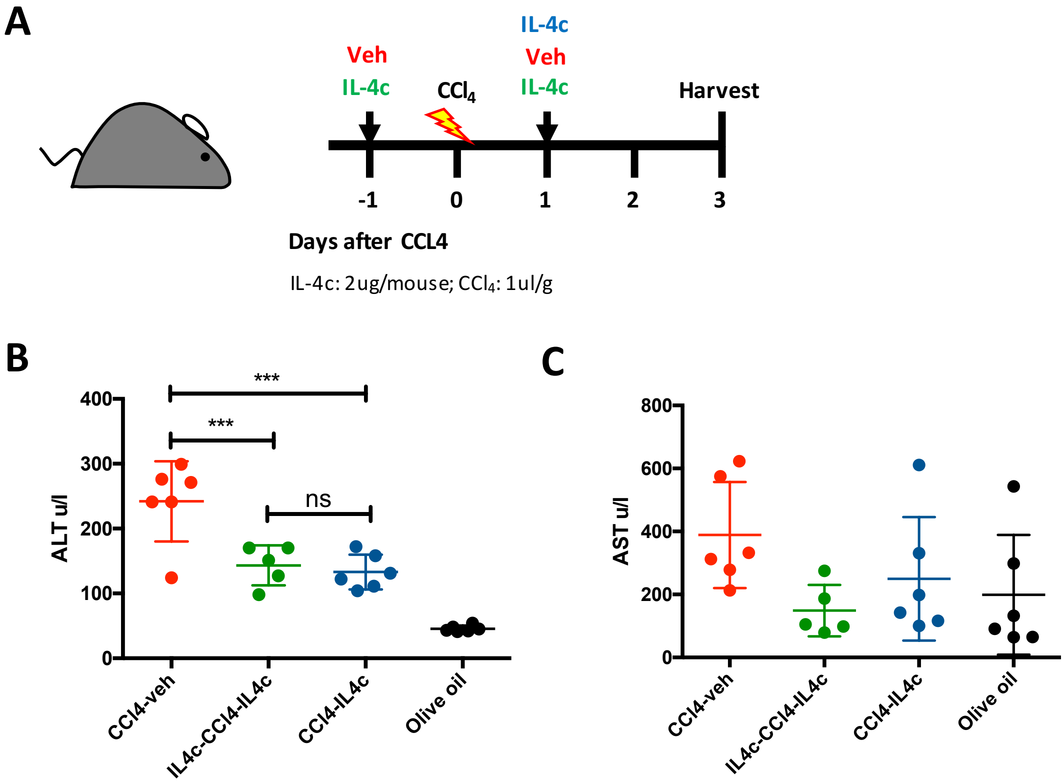

Figure 3-1 Serum markers of hepatocyte injury with IL-4c treatment.

(A) Schematic of experimental model with the green and blue groups representing the priming and therapeutic IL-4 regimens respectively. All mice received 2ug IL-4 s.c. in the form of IL-4c at the specified timepoints. Red, vehicle treated mice received 100ul PBS s.c. at the indicated timepoints. (B-C) Serum ALT and AST by treatment group. N=5-6 pooled from 2 independent experiments (one-way ANOVA).

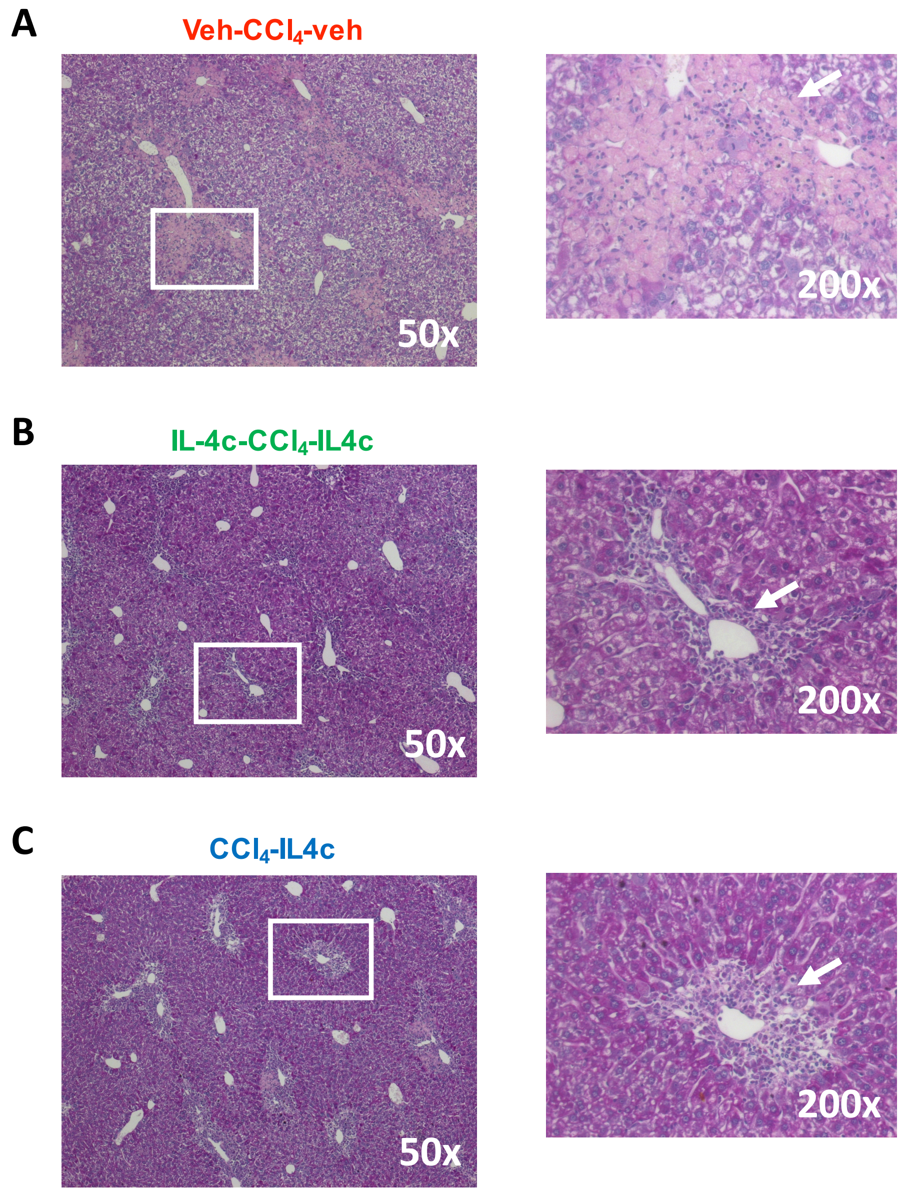

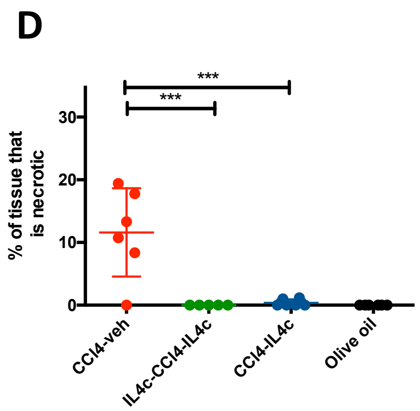

Figure 3-2 Changes to necrotic cell area with IL-4c treatment.

(A-C) Representative 50x images with 200x inserts of PAS stained sections from the outlined groups from the same experiment as Fig. 3.1. Arrows demonstrate necrotic area in A and cellular infiltrate in B-C. (D) Quantification of necrotic cell area in all treatment groups. N=5-6 pooled from 2 experiments (one-way ANOVA).

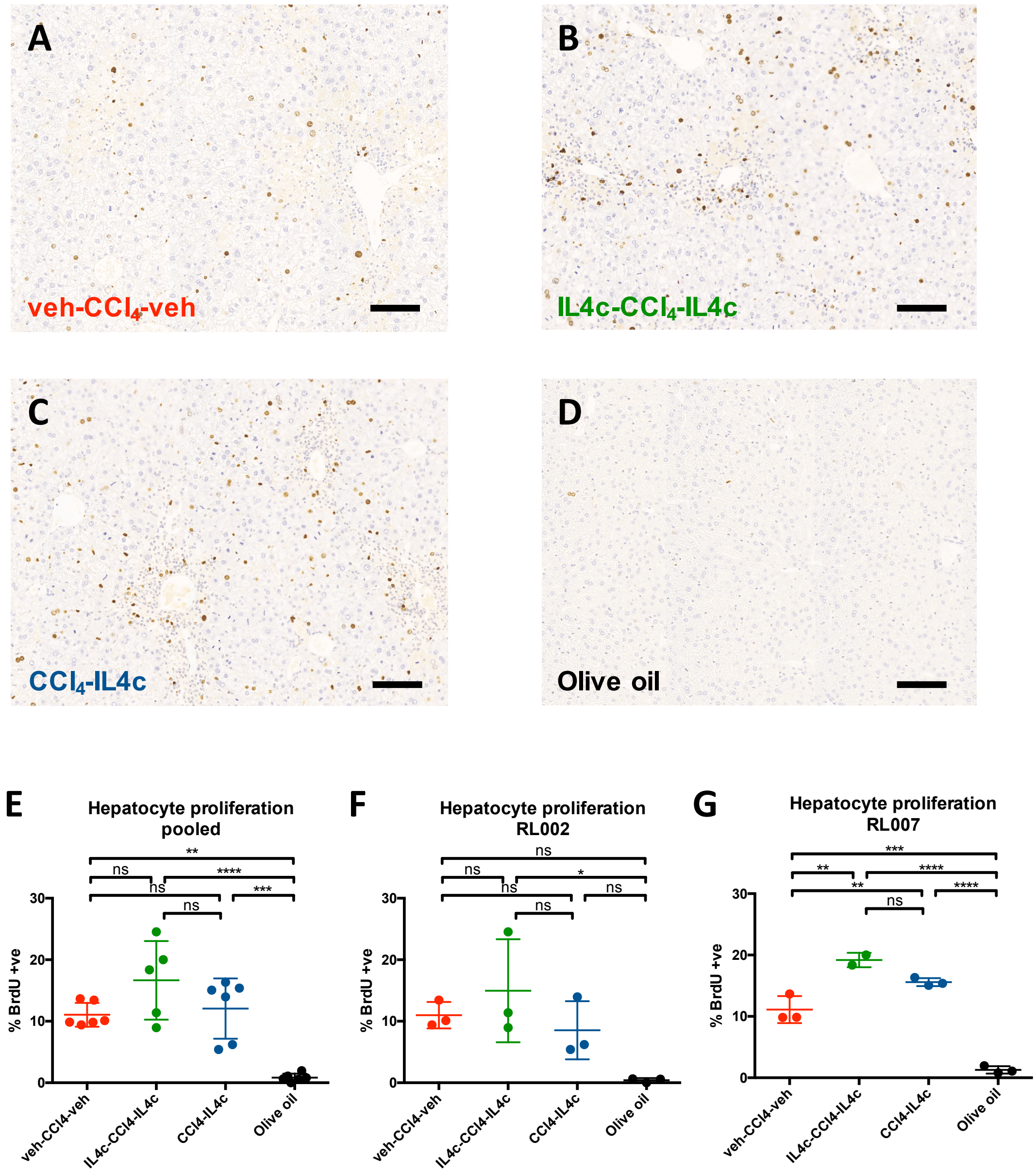

Figure 3-3 Effect of IL-4c on hepatic regeneration.

In the same experiment as Fig. 3.1 all mice were pulsed with 1mg BrdU via intraperitoneal injection 2 hours prior to necropsy. (A-D) Representative immunohistochemistry images from sections stained for BrdU from vehicle, priming IL-4, therapeutic IL-4 and olive oil respectively, scale bar 100μm. (E-G) Quantification of proportion of $BrdU^+$ hepatocytes from 10 non overlapping fields of view per animal. (E) Pooled results from 2 experiments n=5-6. (F-G) Separate graphs of results pooled for E (one-way ANOVA).

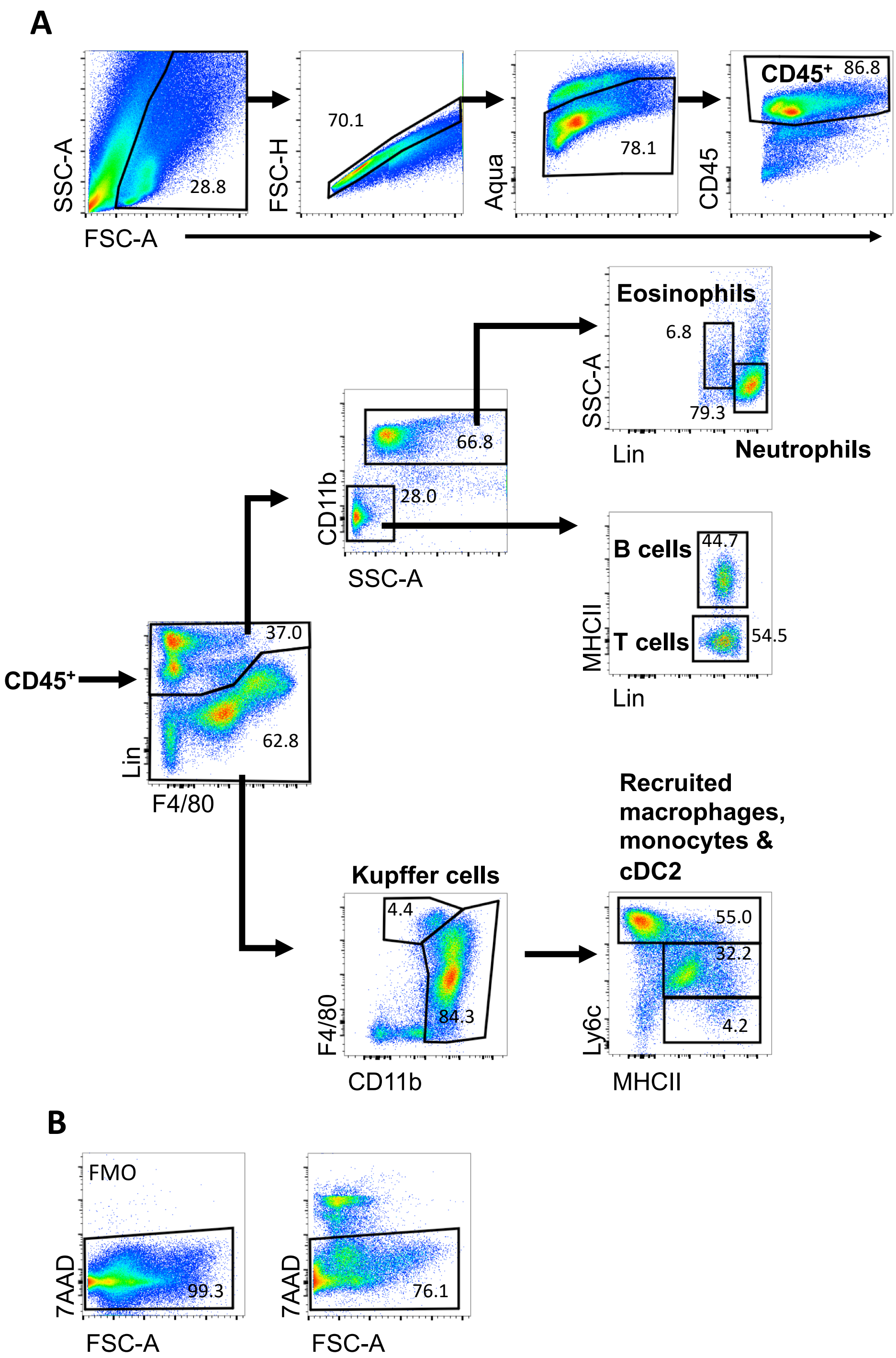

Figure 3-4 Identification of leukocyte populations in liver.

(A) Representative flow cytometry plots of cells isolated from CCl_4-veh treated liver. Lineage gate comprises CD3, CD19, Ly6G and Siglec F. (B) Representative flow plot of 7AAD FMO and fully stained sample (from a different experiment to the above plots)

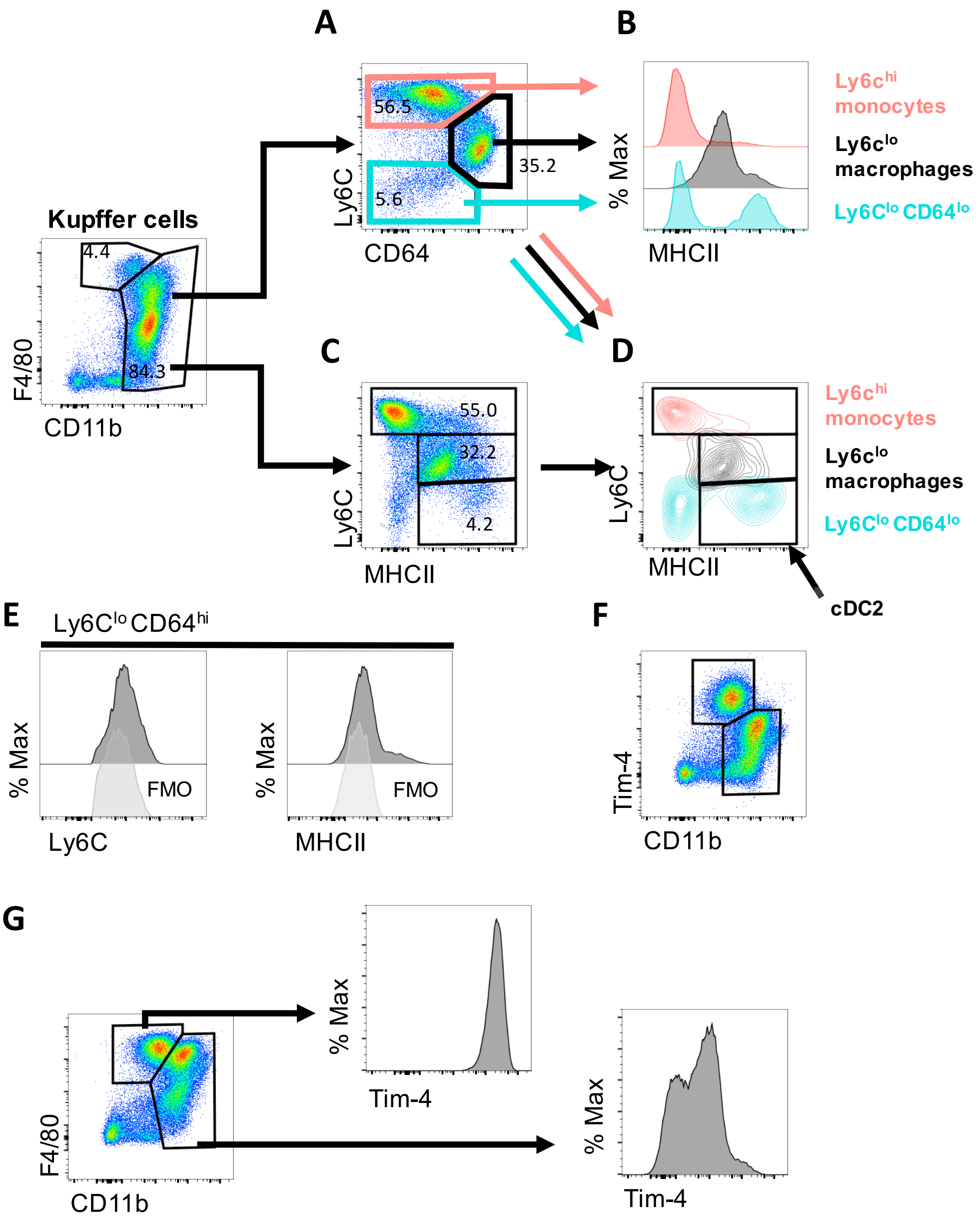

Figure 3-5 Positive identification of macrophages in liver.

(A) Recruited (CD11b^{hi}) Ly6c^{hi} CD64^{lo} monocytes; Ly6c^{lo} CD64^{hi} macrophages and Ly6c^{lo} CD64^{lo} cells identified using CD64. (B) Demonstration of MHCII expression in the populations from A. (C) Ly6c^{hi} monocytes, Ly6c^{lo} macrophages and cDC2 cells as identified using MHCII. (D) Populations identified using CD64 backgated onto Ly6C MHCII gating strategy. (E) Histograms of Ly6C and MHCII expression in Ly6C^{lo} CD64^{hi} cells compared to FMO. (F) Identification of kupffer cells and recruited CD11b^{hi} mononuclear phagocytes using Tim-4 and CD11b n.b. different experiment to rest of figure. (G) Tim-4 expression in Kupffer cells (top) and recruited CD11b^{hi} mononuclear phagocytes (bottom).

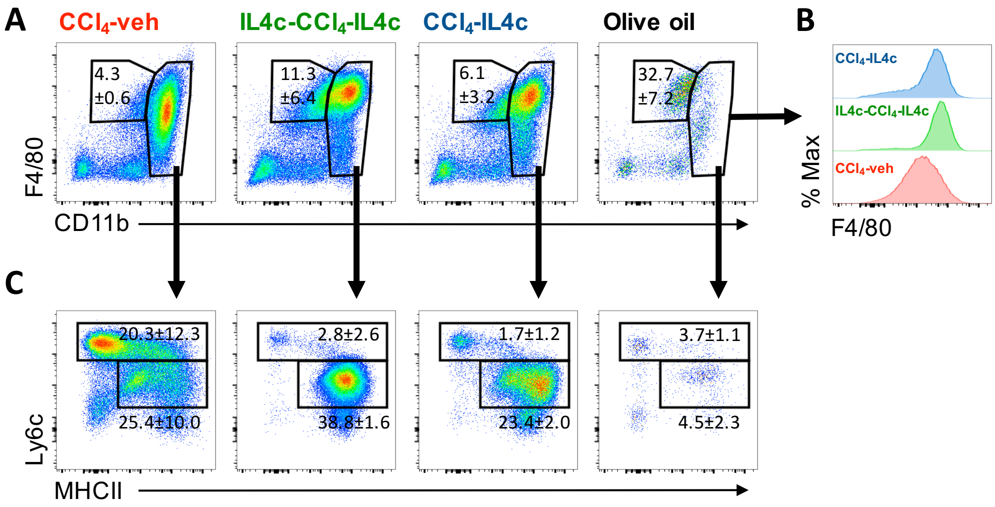

Figure 3-6 Flow cytometric assessment of the effect of IL-4c on monocyte macrophage populations.

Representative plots from experiment in Fig. 3.1. (A) Representative expression of F4/80 and CD11b by Live (aqua$^-$) Lin$^-$ liver leukocytes (CD45$^+$) from CCl4-treated mice that received CCl_4 alone (CCl_4-veh), with IL-4c 24hrs before and after CCl_4 administration (IL4c-CCl_4-IL4c) or IL4c 24hrs after CCl_4 (CCl_4-IL4c), or from mice that received olive oil alone. (B) Representative histograms of F4/80 expression by CD11b^{hi} recruited mononuclear phagocytes from mice treated with CCl_4 alone or in combination with IL-4c. (C) Representative expression of Ly6C and MHCII by CD11b^{hi} cells identified in (A). Means of proportion of CD45 for each population ± SD included on plots N=3/group apart from IL4c-CCl_4-IL4c where N=2.

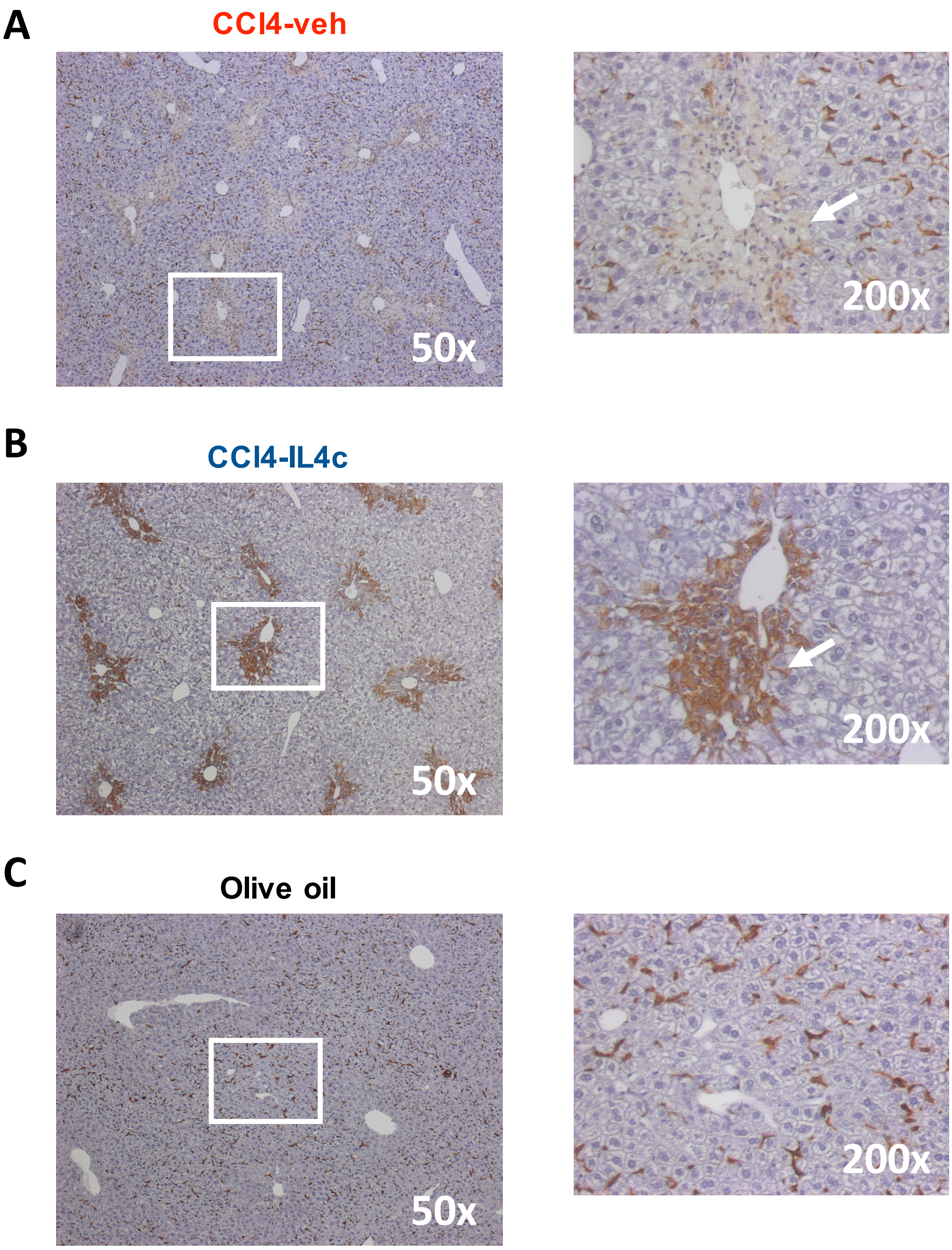

Figure 3-7 F4/80 expression in tissue sections.

Representative 50x immunohistochemistry images with 200x inserts of F4/80 stained sections from (A) CCl_4-vehicle, (B) CCl_4-IL4c and (C) olive oil treated mice. Increased F4/80 staining is noted in the necrotic cell area of the IL-4c treated mice (white arrow).

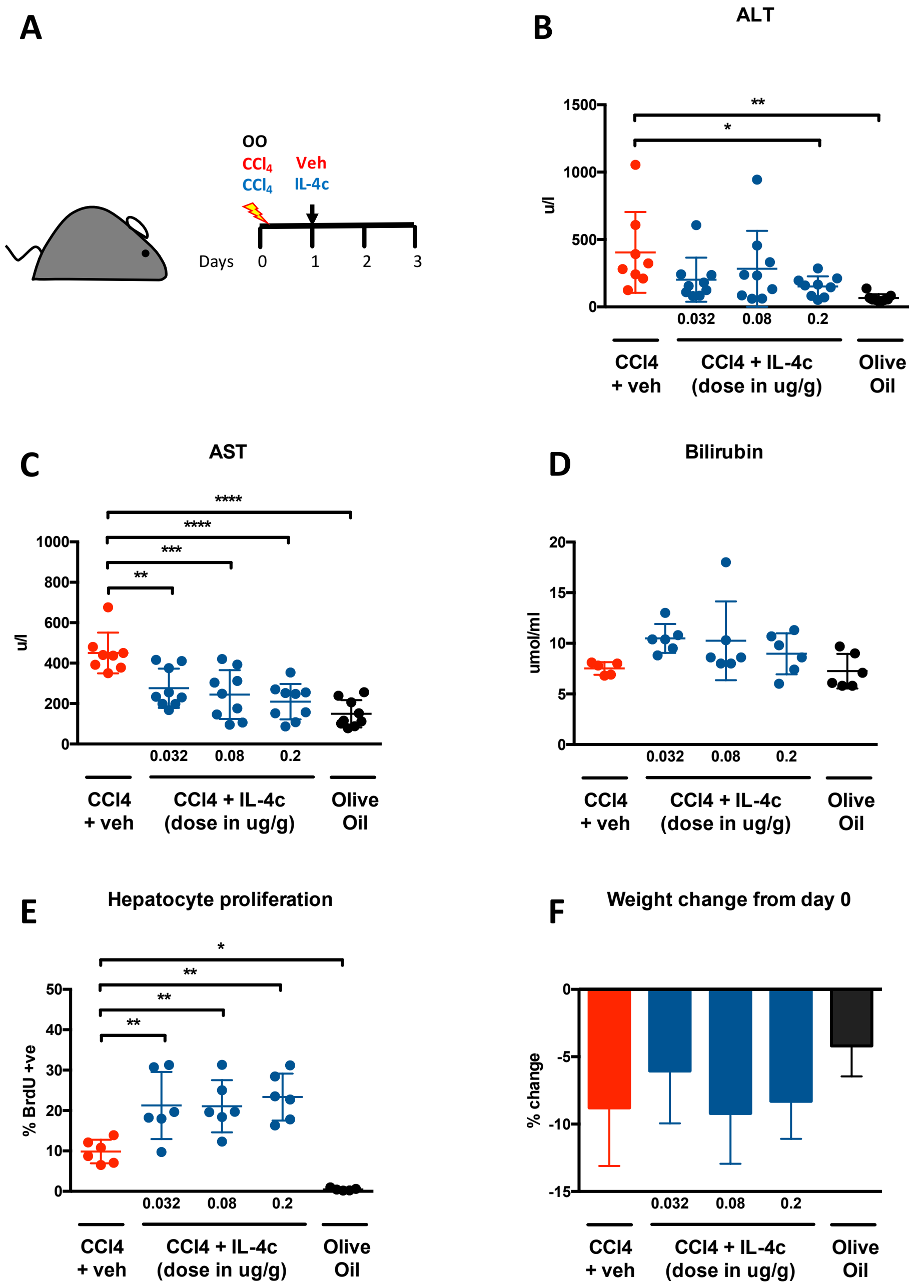

Figure 3-8 Effect of varying doses of therapeutic IL-4 on indices of repair and regeneration.

(A) Schematic of experimental model, CCl_4 injured mice received 0.032µg/g, 0.08µg/g or 0.2µg/g IL-4 s.c. in the form of IL-4c or 4µl/g PBS vehicle. (B-D) ALT, AST and bilirubin levels measured in peripheral blood. N=8-9, pooled data from 3 independent experiments. (E) Quantification of proportion of $BrdU^+$ hepatocytes from 10 non overlapping fields of view per animal. (F) % weight change from day 0. N=6, pooled data from 2 experiments (one-way ANOVA comparing means to CCl_4 + veh group).

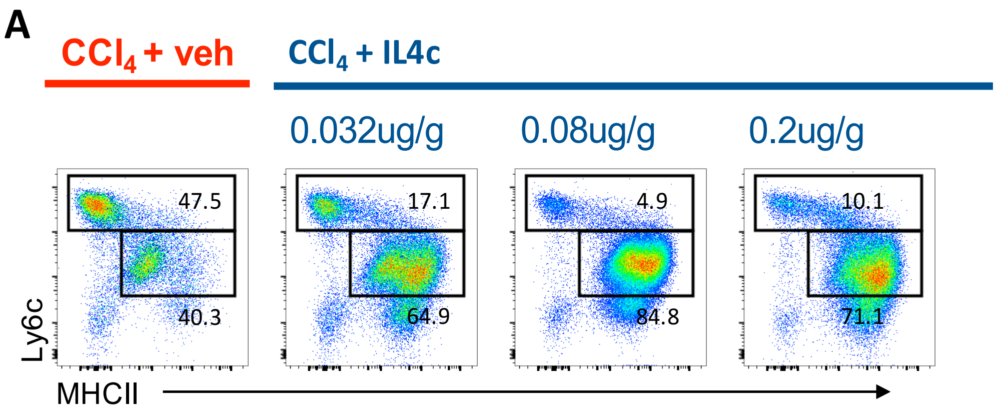

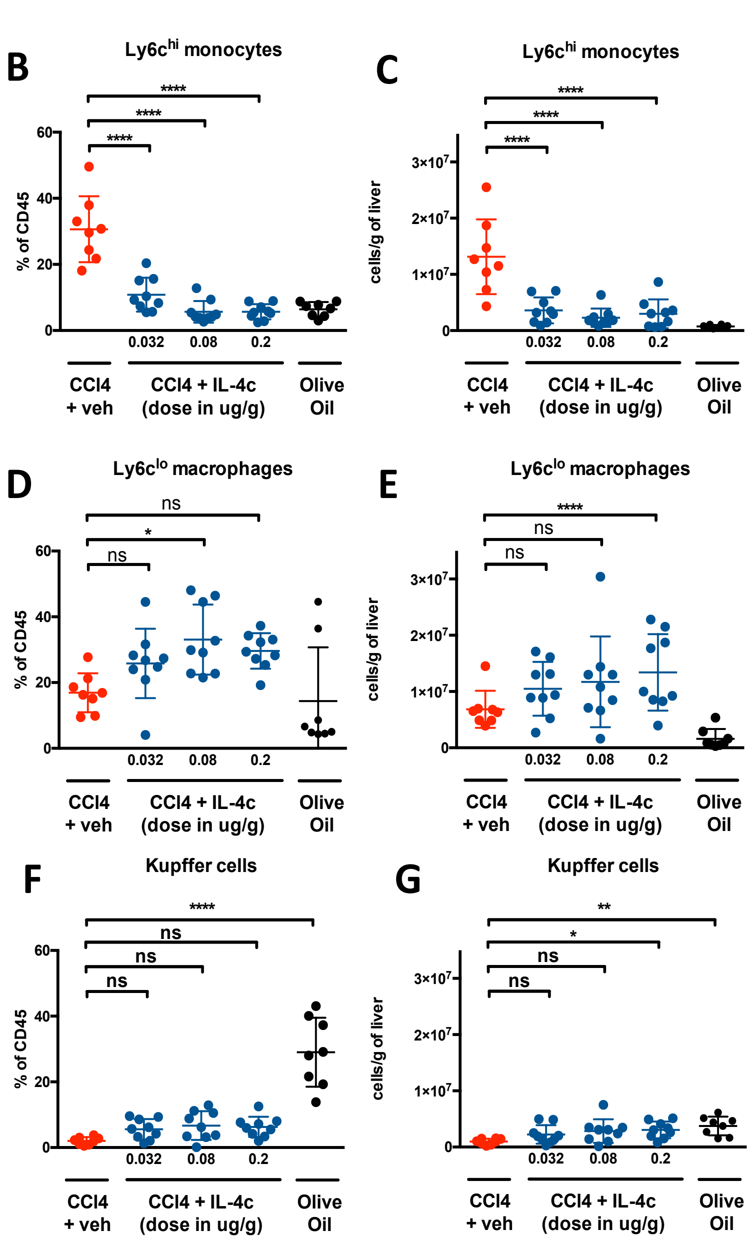

Figure 3-9 Effect of varying doses of IL-4 on recruited monocytes and macrophages.

(A) Representative plots of Live (aqua), CD45$^+$, Lin$^-$, CD11b^{hi} cells demonstrating consistent loss of Ly6c^{hi} monocytes and increase in Ly6c^{lo} MHCII^{int} macrophages. (B,D,F) proportion of CD45$^+$ cells (C,E,G) number of cells per gram of liver tissue. N=8-9, pooled from 3 independent experiments (one-way ANOVA comparing means to CCl_4 + veh group).

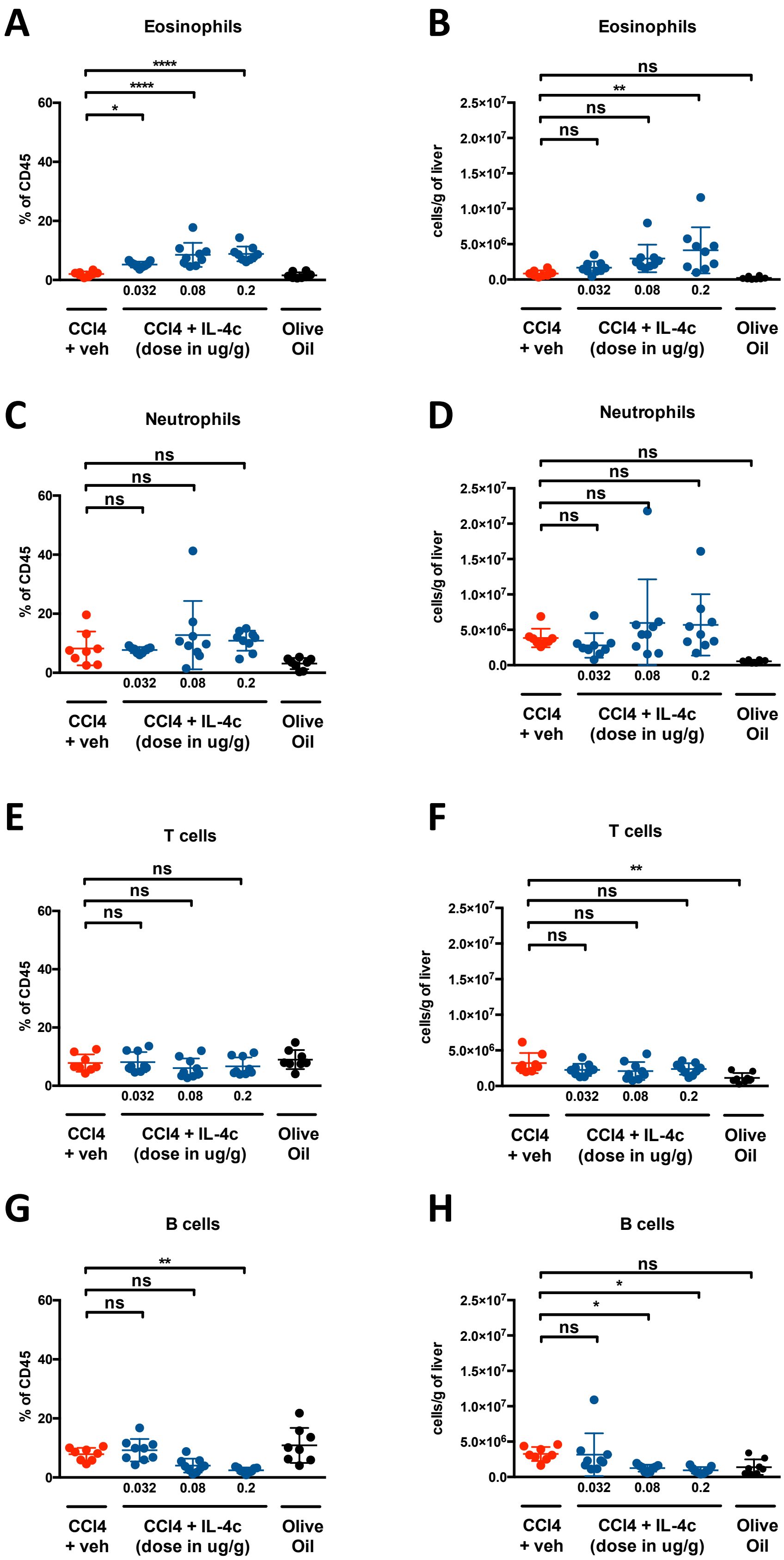

Figure 3-10 Effect of varied doses of IL-4 on other leukocyte populations.

(A-H) Cell populations as labelled as a proportion of $CD45^+$ cells and cells/g of liver. N=8-9, pooled from 3 independent experiments (one-way ANOVA).

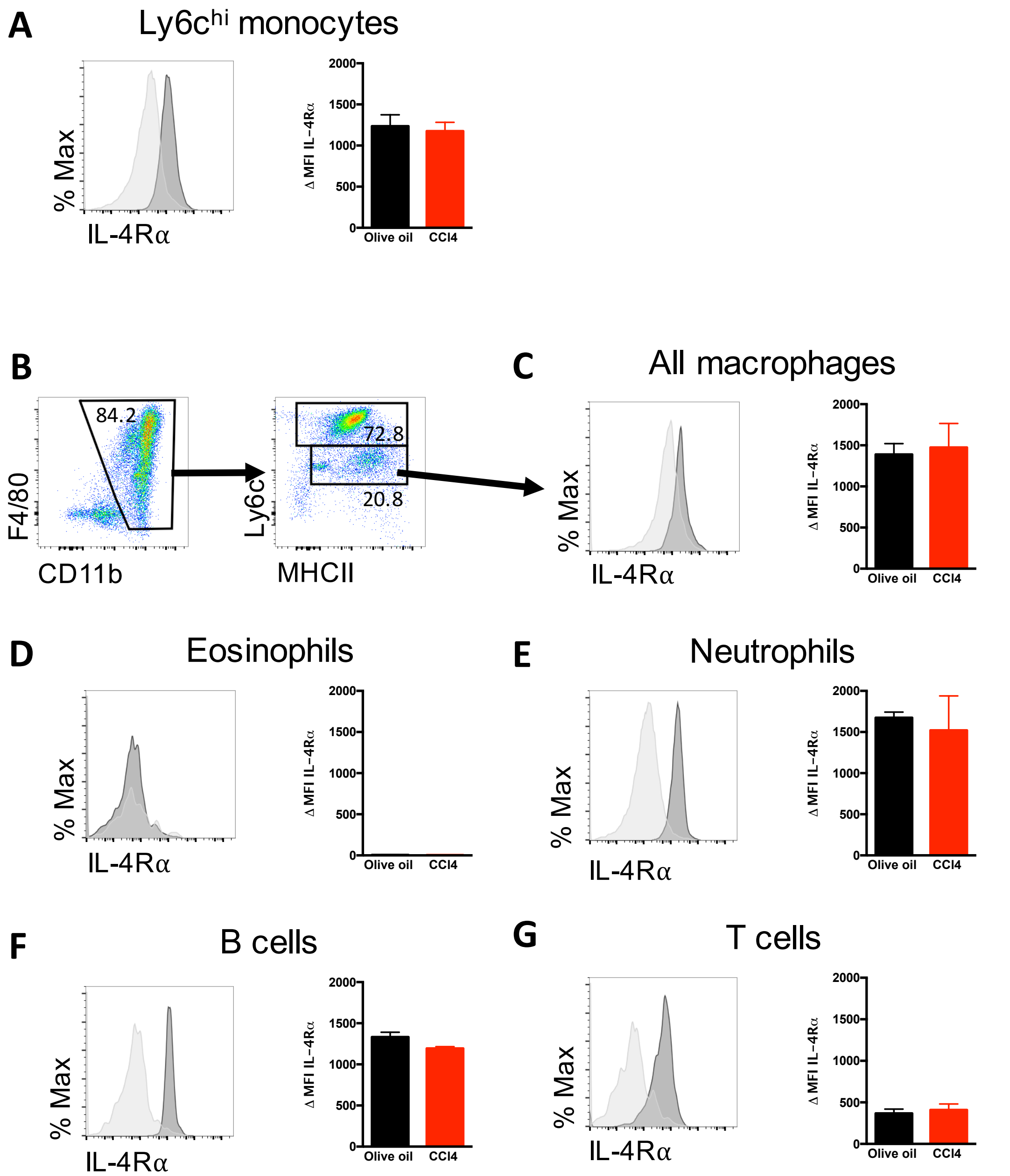

Figure 3-11 IL-4ra expression at 24 hours post CCl_4.

(A,C-G) Histograms show representative IL-4Rα expression in CCl_4 treated mice in dark grey with control IL-4Rα$^{-/-}$ mice also treated with CCl_4 in light grey. Delta mean fluorescence intensity (MFI) was calculated using separate IL-4Rα$^{-/-}$ mice given either CCl_4 or olive oil. (B) Poor separation between KC and recruited necessitated a gating strategy that would encompass both KC and recruited macrophages. N=3 per group from 1 experiment.

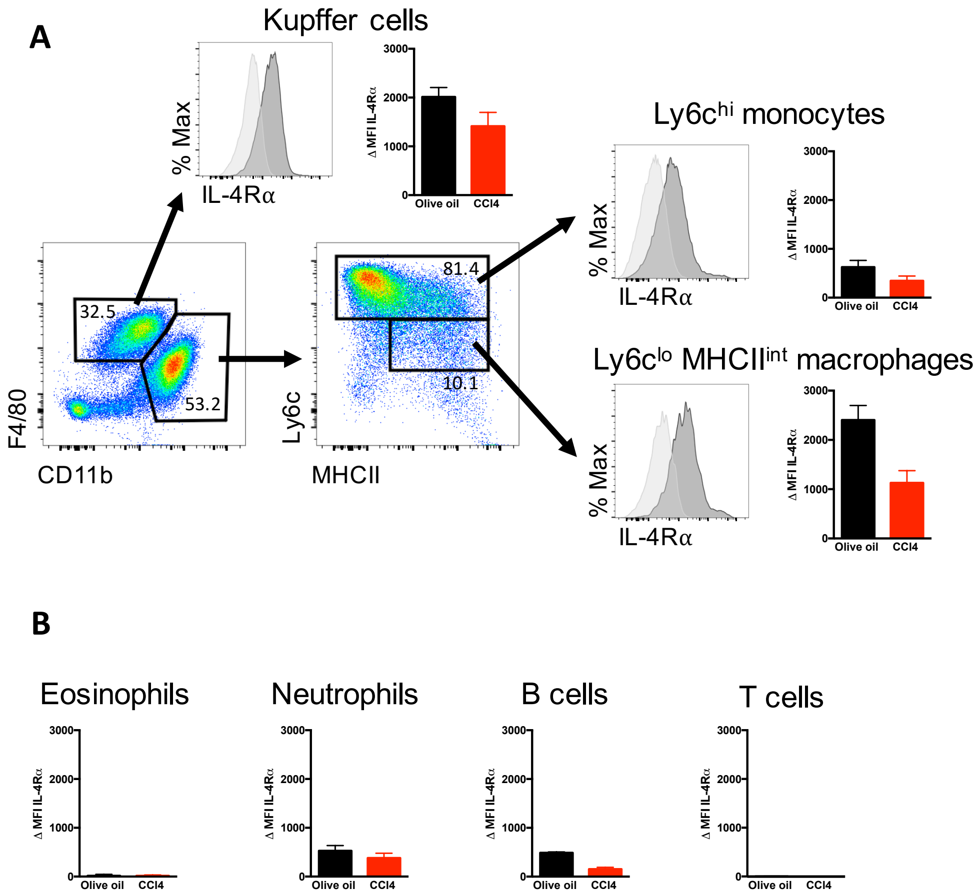

Figure 3-12 IL-4ra expression at 24 hrs post CCl4 with Kupffer cell discrimination.

Histograms show representative IL-4Rα expression in CCl_4 treated mice in dark grey with a pooled FMO in light grey. Delta mean fluorescence intensity (MFI) was calculated using a pooled FMO. (A) Gating strategy used to identify kupffer cells, Ly6c^{hi} monocytes and Ly6c^{lo} MHCII^{int} macrophages from Live (7AAD), CD45^{+}, Lin^{-} cells. Representative histograms for the 3 cell types identified including graphs of delta MFI for IL-4Rα expression. (B) delta MFI for IL-4Rα expression for the outlined cell types. N=3 per group from 1 experiment.

Chapter 4 Endothelial contamination of Kupffer cells

4.1 Introduction

In Chapter 3 I demonstrated that therapeutic delivery of exogenous IL-4 promotes hepatic repair and regeneration following acute injury, and that this corresponds with a significant concomitant effect on the balance between monocyte and macrophage populations. It is known that monocytes and macrophages both play divergent, time-dependent roles during acute hepatic injury and repair [21,23,52] and it was therefore important to understand if IL-4c influenced these roles. However, it was also not clear whether direct IL-4 signalling to monocytes and macrophages was causing this effect or if it was signalling to other cells that could potentially influence monocyte and macrophage numbers indirectly. It was therefore important to consider the possible effects that IL-4 signalling may have on the parenchymal or stromal cells in the liver in promotion of repair and regeneration and orchestration of inflammatory cell recruitment. Indeed, Goh et al. have already shown that direct IL-4Rα signalling in hepatocytes is important, at least in part, for the effects of endogenous IL-4 in promoting liver regeneration[33]. However, no one has yet looked at whether IL-4 of endogenous or exogenous origin influences stromal cells during liver regeneration. One such cell is the liver sinusoidal endothelial cell (LSEC), which is implicated in regeneration following liver injury in a rat model[265,266]. I therefore sought to investigate whether the pro-reparative effect of IL-4 could be related to signalling to the endothelial compartment.

To assess the role of IL-4R signalling in the endothelial compartment, I set out to cross the transgenic mouse strain that expresses the tamoxifen-inducible Cre recombinase under the control of the *Cdh5* promoter (Cdh5-Cre-ERT2[267]) to the IL-4R$\alpha^{fl/fl}$ line[28] to abrogate IL-4Rα signalling in endothelial cells. While *Cdh5*, which encodes cadherin-5, is highly expressed by all endothelial cells, recent publications have revealed that it is also differentially expressed at a gene level by Kupffer cells when compared to other tissue resident macrophages[50,268]. It therefore became important to establish whether *Cdh5* expression by Kupffer cells was sufficient to induce Cre expression, as this would cause deletion of the IL-4Rα in Kupffer cells as well as endothelial cells in the Cdh5-Cre-ERT2; IL-4Rα$^{fl/fl}$ line. Thus, before generating the Cdh5-Cre-ERT2; IL-4Rα$^{fl/fl}$ line, I used the Cdh5-Cre-ERT2; mTmG[269] reporter line available from Professor Neil Henderson's group. In this system all cells express tdTomato but following tamoxifen administration cells that express *Cdh5* undergo Cre-mediated switching from tdTomato to eGFP expression. I used a combination of flow cytometry and confocal microscopy to determine whether Kupffer cell *Cdh5* expression was sufficient to cause Cre activation. In addition to establishing the efficiency of the Cdh5-Cre-ERT2 system in targeting LSECs and other liver endothelial cells, this approach also enabled me to establish whether the observed *Cdh5* expression in Kupffer cells represented genuine expression or an artefact generated by endothelial cell contamination due to the intimate relationship of Kupffer cells and LSECs[101]. This body of work formed a major part of a manuscript that was published in the Journal of Leukocyte Biology and is inserted below.

Unfortunately, due to an outbreak of pinworm in the breeding facility there was significant disruption to the breeding of the Cdh5-Cre-ERT2; IL-4Rα$^{fl/fl}$ line. I was therefore unable to complete a full characterisation of the line in my injury model.

4.2 Contribution to manuscript

The manuscript was co-authored by myself and Cathy Hawley, a fellow PhD student in the Jenkins group. The experiments in the first two figures that identify endothelial cell contamination within Kupffer cells isolated by FACS-sorting were all designed, performed and analysed by myself, except for Fig. 2A, F, G and H which were performed and analysed by Cathy Hawley. The data in the subsequent two figures examining differences in leukocyte isolation methods were performed and analysed by Cathy Hawley, except for one repeat in Fig. 4H which was performed and analysed by Dr Calum Bain.

4.3 Manuscript

DOI: 10.1002/JLB.1TA0517-169R

JOURNAL OF LEUKOCYTE BIOLOGY

TECHNICAL ADVANCE

An efficient method to isolate Kupffer cells eliminating endothelial cell contamination and selective bias

Ruairi W. Lynch | Catherine A. Hawley | Antonella Pellicoro | Calum C. Bain | John P. Iredale* | Stephen J. Jenkins

MRC Centre for Inflammation Research, University of Edinburgh, Edinburgh, United Kingdom

Correspondence
Stephen J. Jenkins, MRC Centre for Inflammation Research, University of Edinburgh, Edinburgh, United Kingdom.
Email: stephen.jenkins@ed.ac.uk

*Current address: Senate House, University of Bristol, Bristol, United Kingdom

Abstract

Multicolor flow cytometry and cell sorting are powerful immunologic tools for the study of hepatic mϕ, yet there is no consensus on the optimal method to prepare liver homogenates for these analyses. Using a combination of mϕ and endothelial cell reporter mice, flow cytometry, and confocal imaging, we have shown that conventional flow-cytometric strategies for identification of Kupffer cells (KCs) leads to inclusion of a significant proportion of CD31^{hi} endothelial cells. These cells were present regardless of the method used to prepare cells for flow cytometry and represented endothelium tightly adhered to remnants of KC membrane. Antibodies to endothelial markers, such as CD31, were vital for their exclusion. This result brings into focus recently published microarray datasets that identify high expression of endothelial cell-associated genes by KCs compared with other tissue-resident mϕ. Our studies also revealed significant and specific loss of KCs among leukocytes with commonly used isolation methods that led to enrichment of proliferating and monocyte-derived mϕ. Hence, we present an optimal method to generate high yields of liver myeloid cells without bias for cell type or contamination with endothelial cells.

KEYWORDS

endothelial cell, flow cytometry, Kupffer cell

1 | INTRODUCTION

Liver Kupffer cells (KCs) are one of the largest populations of resident mϕ in the body. KCs are located in the sinusoids of the liver where they scavenge and phagocytose apoptotic cells and damaged erythrocytes,[1] contribute to maintenance of immunologic tolerance by priming Foxp3$^+$ T-regulatory cells,[2] and capture gut commensal bacteria that enter the circulation.[3] Under homeostatic conditions, KCs proliferate in situ and persist with relatively little input from conventional hematopoiesis in adult mice.[4–6] However, during liver inflammation, stress, or injury, Ly6C^{hi} monocytes are recruited to the liver and subsequently mature into monocyte-derived hepatic mϕ. Both KCs and monocyte-derived mϕ have been attributed prorestorative or proinflammatory roles in models of acute and chronic liver damage.[7–9] To better understand the function of KCs and monocyte derived mϕ, it is important not only to accurately identify these cells but also to ensure a comprehensive portrait of the in vivo population is generated.

Multiparameter flow cytometry is a powerful tool for evaluating changes in number, frequency, and phenotype of diverse monocyte and mϕ populations and is the basis by which these cells are purified for subsequent functional and genomic analyses. Many protocols have been used to isolate leukocytes from the liver, but there is no consensus on which method is most valid, particularly for KCs. Furthermore, although the definition of KCs by flow cytometry is widely accepted as F4/80^{hi}CD11b^{lo} cells, the reliability of this approach has not been fully investigated. For example, several microarray and RNA-seq datasets identified *Cdh5*, a gene typically associated with endothelial cells,[10] as differentially expressed by KCs compared with other tissue-resident mϕ.[11–13]

Abbreviations: *Cdh5*, Cadherin 5; CLEC4F, C-type lectin domain family 4 member F; KCs, Kupffer cells; LSEC, liver sinusoidal endothelial cells

Received: 3 May 2017 | Revised: 14 February 2018 | Accepted: 27 February 2018

Here, we demonstrate that the population of KCs conventionally defined by their F4/80^{hi}CD11b^{lo} phenotype contains a significant proportion of contaminating CD45^{+}CD31^{hi} endothelial cells, and that this contamination was present regardless of the method used for isolating leukocytes from the liver. Inclusion of endothelial markers rather than additional surface markers of mϕ was critical for excluding these cells from analysis. Furthermore, quantity and quality of isolated KCs varied significantly dependent on the purification method used. We therefore present a comprehensive protocol for faithfully isolating leukocytes from the liver and a modified gating strategy to effectively eliminate contaminating endothelial cells.

2 | METHODS

2.1 | Mice

Wild-type (WT) C57BL/6OlaHsd CD45.2^{+}, congenic C57BL/6 CD45.1^{+}CD45.2^{+}, C57BL/6OlaHsd *Csf1r*-mApple^{+} mice,[14] and *Cdh5*-Cre-ERT2 mice[15] crossed with the mTmG (*Rosa26*Sor$^{tm4(ACTB-tdTomato, EGFP)Lou}$/J) line,[16] were bred and maintained in specific pathogen-free facilities at the University of Edinburgh, UK. Mice were sex and age matched, 6–12 weeks for WT studies and 11–12 weeks for *Cdh5* mice. Bone marrow chimeric mice were generated as previously described.[17] Briefly, C57BL/6 CD45.1^{+}CD45.2^{+} mice were anesthetized and hind legs irradiated with 950 rad while remaining tissues were protected by lead. Mice were reconstituted the next day with 2–5 × 10^{6} donor bone marrow cells from congenic CD45.2^{+} animals and rested for 8 weeks prior to analysis. All experiments were approved by the University of Edinburgh Animal Welfare and Ethical Review Body under license granted by the UK Home Office.

2.2 | Tamoxifen administration

To induce Cre expression in *Cdh5*-Cre-ERT2:mTmG mice, sterile filtered tamoxifen (Sigma, Irvine, UK; 100 mg/kg) dissolved in corn oil (Sigma; 20 mg/ml) was administered i.p. for 5 consecutive days and mice left for 2 weeks.

2.3 | CSF1-Fc and BrdU administration

An Fc conjugate of porcine CSF1 (CSF1-Fc) was prepared as described.[18] Analysis of KC and endothelial cell proliferation in response to administration of CSF1-Fc was performed on cells from a larger unpublished study aimed at assessing the effect of chronic CSF1 delivery on KCs origin in tissue-protected bone marrow chimeric mice made as described previously.[17] Tissue protected chimeric mice were given 1 μg/g CSF1-Fc delivered in PBS s.c. or PBS control on day 1, 3, 17, 19, 33, and 35 before analysis on day 37. Mice were pulsed with 1 mg BrdU s.c. 2 h before necropsy.

2.4 | Isolation of leukocytes from liver

Following perfusion of PBS through the inferior vena cava, livers were placed into RPMI, finely chopped using a razor blade and digested in 5 ml of enzyme mix (RPMI with 0.625 mg/ml collagenase D, 30 U/ml DNase [Roche, Burgess Hill, UK], 0.85 mg/ml collagenase V [Sigma], and 1 mg/ml dispase [Invitrogen, Paisley, UK] for 25 min at 37°C, in an orbital shaker with additional manual shaking every 5 min. Digests were poured through a 100 μm strainer and then prepared according to the protocols below. Unless otherwise stated, all wash buffers were kept at 4°C. At the end of all protocols, cell pellets were resuspended, passed through a 40 μm strainer, and live cells counted using a Casey TT counter (Roche).

2.5 | 300 *g* centrifugation

Cells were washed in 50 ml, then 30 ml RPMI, and centrifuged at 300 *g* for 5 min, maximum break and accelerator. RBC lysis buffer (Sigma; 2 ml) was added for 2 min, followed by 2 ml FACS buffer (PBS supplemented with 0.5% BSA and 2 mM EDTA). Cells were pelleted (300 *g*, 5 min) and the supernatant discarded.

2.6 | 33% Percoll^{TM} gradient

Cells were washed twice in 50 ml liver wash buffer (PBS/2% FCS) by centrifugation at 443 *g* for 6 min, maximum break and accelerator. The pellet was resuspended in a room-temperature 33% Percoll gradient (25 ml per sample) and spun at 693 *g* for 12 min, with minimum break and accelerator. The cell pellet was washed in 30 ml liver wash buffer at 300 *g* for 5 min. RBC lysis buffer (5 ml) was added for 5 min, then 30 ml liver wash buffer and cells spun at 300 *g* for 5 min.

2.7 | 50 *g* centrifugation

Cells were washed in 15 ml RPMI containing 10% FCS and centrifuged at 50 *g* for 10 min with minimum break. The supernatant was collected and spun at 340 *g* for 10 min, minimum break. The pellet was lysed for 5 min in 2 ml RBC lysis buffer on ice, topped up with RPMI + 10% FCS and spun at 340 *g* for 10 min, minimum break.

2.8 | Collection of discarded fractions

For the 300 *g* spin and Percoll gradient methods, the supernatant or both the hepatocyte layer, and the supernatant between the hepatocyte layer and the leukocyte pellet, respectively, was collected into a fresh tube and centrifuged at 400 *g* for 5 min. The resultant pellets were counted and stained. For the 50 *g* slow-spin method, the pellet generated following the 50 g spin was counted and stained.

2.9 | Isolation of leukocytes from lung

Perfused lungs were collected into RPMI, homogenized using scissors and digested in 2 ml of the enzyme mix detailed above, for 45 min at 37°C. Digests were filtered through a 100 μm strainer, washed with FACS buffer and RBC lysed in 3 ml RBC lysis buffer (Sigma) for 3 min. After washing, cells were passed through a 40 μm strainer and counted.

2.10 | Flow cytometry

2 × 10^{6} liver cells, or 20 μl of whole blood was incubated with Zombie Aqua fixable viability dye (Biolegend, London, UK) for 10 min at RT and

then with 0.025 μg anti-CD16/32 (2.4G2; Biolegend) in 10% normal mouse serum (Life Technologies, Paisley, UK). Cells were then incubated with antibodies (Supplemental Table 1). Cells were washed, spun at 300 g for 5 min and, where necessary, incubated with fluorescently labeled streptavidin. 7-AAD solution (Biolegend) was added to samples 10 min before acquisition when comparing isolation protocols. DAPI was used as a viability marker for FACS. Liver cells were gated as shown, whereas alveolar and interstitial mϕ were identified as $CD45^+CD11c^+SiglecF^+$ and $CD45^+CD11c^+SiglecF^-MHCII^+CD64^+$ cells, respectively.

For BrdU and Ki67 staining, cells were fixed and permeabilized overnight in FoxP3/Transcription Factor Staining Buffer (eBioscience). Cells were washed in PermWash (eBioscience) and stained with anti-Ki67 and anti-BrdU antibodies.

Cells were acquired on a LSRFortessa (BD Biosciences, Wokingham, UK) or FACSAriaII (BD) at the QMRI Flow Cytometry and Cell Sorting Facility, University of Edinburgh, and data analyzed in FlowJo software (Tree Star, Ashland, Oregon). Fluorescence-minus-one controls were used to set gates.

2.11 | Immunofluorescence

The median lobe from perfused liver of *Cdh5*-Cre-ERT2:mTmG mice was fixed in 4% methanol-free PFA (Thermo Scientific, Paisley, UK) at 4°C for 2–3 h then washed in PBS and resuspended in 15% sucrose gradient for 1 h at room temperature followed by 30% sucrose at 4°C overnight. Tissue was then flash frozen in optimal cutting temperature (OCT) embedding matrix (Fisher Scientific, Loughborough, UK) and stored at −80°C. Seven-micrometer sections were cut using a cryostat.

Following blocking with 20% normal goat serum, sections were stained with rat anti-mouse F4/80 (Abcam, Cambridge, UK; CI:A3-1) then AlexaFluor-594 goat anti-Rat IgG secondary (Abcam). Total number of $F4/80^+$ KCs were enumerated per liver slice and GFP and F4/80 coexpression assessed. Immunofluorescent analysis of single cells was performed on FACS-purified cells. Ten microliters of sorted cells was plated on a perfusion open and closed chamber for analysis at 20× magnification and images acquired using a Leica confocal SP5 microscope.

2.12 | Statistical analysis

Data were analyzed in Prism 6 or 7 (GraphPad), with statistics detailed in relevant figure legends. *$P < 0.05$, **$P < 0.01$, ***$P < 0.001$, ****$P < 0.0001$.

3 | RESULTS

3.1 | $F4/80^{hi}CD11b^{lo}$ KCs identified by flow cytometry contain a subset of $Cdh5^{hi}CD31^{hi}$ cells

KCs have been traditionally defined by their $F4/80^{hi}CD11b^{lo}$ phenotype, which distinguishes them from $F4/80^{lo}CD11b^+$ bone-marrow-derived myeloid cells.[19] Global transcriptomic analyses have demonstrated that, like all tissue mϕ, KCs have a unique transcriptional signature,[11–13] with CLEC4F and Tim4 emerging as markers that aid their discrimination from other hepatic monocytes and mϕ.[12,20] However, these same analyses also identified *Cdh5* (which encodes cadherin-5), a gene strongly associated with endothelial cells,[10] as part of the KC-specific signature.[11–13] Interrogation of the publically available ImmGen resource (www.immgen.org) revealed a similarly high enrichment of *Cdh5* transcripts in KCs compared with other tissue mϕ (data not shown). To establish whether KCs expressed *Cdh5*, we used a transgenic mouse strain that expresses tamoxifen-inducible Cre recombinase under the control of the *Cdh5* promoter (*Cdh5*-Cre-ERT2)[15] crossed to mTmG reporter mice.[16] While all cells in *Cdh5*-Cre-ERT2:mTmG mice express tdTomato, tamoxifen administration results in Cre recombinase activity, excision of the tdTomato cassette, and an irreversible switch to EGFP expression in *Cdh5* expressing cells and their progeny. Flow cytometric analysis of whole liver isolates gated on live, $CD45^+$ $lineage^-$ leukocytes (Fig. 1A) revealed a clear bimodal expression of GFP in $F4/80^{hi}CD11b^{lo}$ KCs, suggesting higher expression of *Cdh5* by a fraction of these cells (Fig. 1B). Bimodal expression of the endothelial marker CD31 was also evident (Fig. 1B), and simultaneous analysis of GFP and CD31 revealed a bright double positive population (Fig. 1C) that accounted for ∼10% of the $F4/80^{hi}CD11b^{lo}$ population (Fig. 1D). In comparison, less than 0.52% of lung interstitial mϕ and 0.53% of alveolar mϕ were $CD31^{hi}GFP^{hi}$ suggesting this phenomenon was not common to all mϕ populations (Fig. 1D). Back-gating of the $CD31^{hi}GFP^{hi}$ and $CD31^{lo}GFP^{lo}$ populations revealed they could not be discriminated based on size, granularity, and expression of other leukocyte markers such as CD45, Ly6C, and MHCII (data not shown). However, whereas tdTomato expression was significantly diminished in the $CD31^{hi}GFP^{hi}$ fraction of KCs (Fig. 1E), the $CD31^{lo}$ GFP^{lo} cells retained identical levels to untreated control mice, indicating that Cre-mediated excision of the tdTomato cassette had not occurred (Fig. 1F). A similar minor increase in GFP fluorescence without loss of tdTomato expression was also observed in B cells, T cells, neutrophils, and monocytes following tamoxifen treatment (data not shown). Hence, although $F4/80^{hi}CD11b^{lo}$-defined KCs contain a subset of $CD31^{hi}$ Cre-expressing cells, it seems likely that the low GFP fluorescence of $CD31^{lo}$ KC from tamoxifen-treated mice does not represent meaningful expression of *Cdh5*-driven Cre.

3.2 | Endothelial cells contaminate the traditional $F4/80^{hi}$ $CD11b^{lo}$ KC gate

We further investigated the identity of the $CD31^{hi}GFP^+$ fraction of $F4/80^{hi}CD11b^{lo}$ cells. Analysis of all $CD31^{hi}$ cells within the liver preparations revealed binding of CD45 and F4/80 antibodies to be specific when compared with their respective isotype controls (Fig. 2A). Unlike $CD31^{lo}$ KCs, the $CD31^{hi}$ $F4/80^{hi}CD11b^{lo}$ cells also expressed high levels of ICAM-2 and Lyve-1 (Fig. 2B), consistent with a lymphatic or liver sinusoidal endothelial phenotype. However, tissue sections from *Cdh5*-Cre-ERT2:mTmG mice suggested little true colocalization of F4/80 with GFP (Figs. 2C and 2D). Indeed, FACS sorting followed by confocal microscopy revealed some $CD45^+F4/80^{hi}CD31^{hi}$ cells to be doublets of $F4/80^{hi}$ KC and $CD31^{hi}$ endothelium (Fig. 2E),

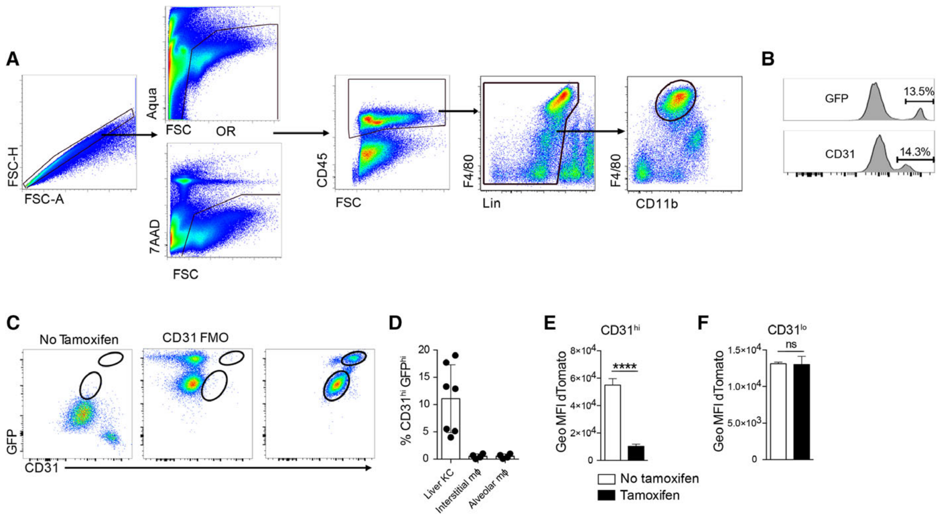

FIGURE 1 **(A) Identification of F4/80^{hi}CD11b^{lo} KCs in murine liver**. Lineage = CD3, CD19, Ly6G, and Siglec F. (B) Representative GFP and CD31 expression by F4/80^{hi}CD11b^{lo} liver cells from *Cdh5*-Cre-ERT2;mTmG mice. Proportion of GFP$^+$ and CD31^{hi} cells shown (mean, n = 7, 3 experiments). (C) Representative GFP and CD31 expression by F4/80^{hi}CD11b^{lo} liver cells from *Cdh5*-Cre-ERT2;mTmG mice ± tamoxifen. (D) The frequency of CD31^{hi}GFP$^+$ cells amongst KCs, lung interstitial and alveolar mϕ. Liver (n = 7, 3 experiments) and lung (n = 4, 2 experiments). (E and F) Geometric mean fluorescence intensity (GeoMFI) of dTomato expression by CD31^{lo}GFP$^-$ KCs (E) and CD31^{hi}GFP$^+$ cells (F) (n = 3/group, representative of 3 experiments)

whereas the majority of CD31^{hi} cells exhibited punctate colocalized surface staining of CD45 and F4/80 indicative of endothelial cells to which surface membrane from KC was tightly adhered (Fig. 2E). Consistent with this, staining for other KC-specific surface markers, such as Tim4 or CLEC4f,[12] could not differentiate the CD31^{hi} and CD31^{lo} populations despite a very marginal difference in expression intensity (Fig. 2F). In contrast, expression of a *Csf1r*-driven mApple transgene, a cytoplasmic marker of myeloid cells,[14] distinguished mApple^{hi}CD31^{lo} KCs from mApple$^-$CD31^{hi} contaminants (Fig. 2G). Furthermore, CD31^{hi}F4/80^{hi}CD11b^{lo} cells did not proliferate in response to the mϕ mitogen CSF1 (Fig. 2H).[18,21] Thus, it would seem most likely that CD45$^+$F4/80^{hi}CD31^{hi} cells identified by flow cytometry represent endothelial cells with remnants of KC membranes that are largely devoid of the intracellular components of these cells. Hence, although transgenic or intranuclear markers of KCs can aid their discrimination, surface staining for CD31 would seem the most technically simple method for excluding these cells during flow cytometry or FACS.

Of note, unbiased analysis of all CD31^{hi} cells expressing the hematopoietic marker CD45 revealed them to comprise both F4/80^{hi}CD11b^{lo} cells as described above but also other hematopoietic cells (Fig. 2I). Rather than bona fide CD45$^+$ endothelial cells, FACS and imaging of CD45$^+$F4/80$^-$CD31^{hi} cells revealed a population of endothelial cells that appeared to envelop small CD45$^+$ cells (Fig. 2J). Although these could be simple doublets, they may also represent transmigrating hematopoietic cells described in human liver sinusoidal endothelial cells (LSECs) in vitro.[22] Either way, we find no evidence that CD45$^+$CD31^{hi} cells represent single cells with both hematopoietic and endothelial characteristics akin to those described in rat liver.[23]

3.3 | Endothelial cell contamination is present irrespective of liver digestion protocol

Multiple methods for generating single cell preparations of murine liver leukocytes have been published and while most protocols involve enzymatic digestion, the separation of leukocytes from hepatocyte debris is more inconsistent. Hence, to exclude the possibility that the observed endothelial cell contamination was an artifact specific to our protocol for isolation of leukocytes from the liver, we compared the frequency of CD31^{hi} cells in the KCs population retrieved using 3 methods representative of commonly published protocols. In brief, all methods used the same enzymatic digestion step but employed either two 300 *g* centrifugation steps (as used for Figs. 1 and 2),[17] an initial 50 *g* prespin to first pellet and discard hepatocytes,[24,25] or a 33% Percoll gradient to remove the majority of hepatic debris.[26,27] The relative frequency of all CD31^{hi} endothelial cells recovered as a proportion of all live cells was equivalent between the 300 *g* and the Percoll gradient methods, though reduced with the 50 *g* prespin method, suggesting a proportion of endothelial cells are removed by this step (Fig 3A). However, there was a clear population of CD31^{hi}

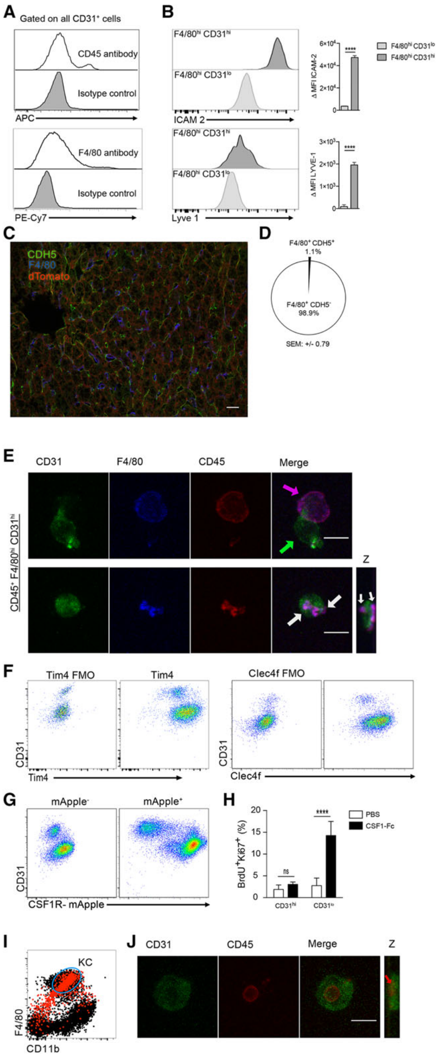

FIGURE 2 **(A) Representative expression of CD45 and F4/80 by total CD31^{hi} liver cells (n = 6, 2 experiments)**. (B) Representative histograms (n = 6, 2 experiments) and delta MFI (n = 3/group, representative of 3 experiments) of ICAM-2 and LYVE-1 expression by F4/80^{hi}CD31^{hi} cells and F4/80^{hi}CD31^{lo} KCs. Significance determined by t-test. (C) Confocal image of liver from *Cdh5*-Cre-ERT2;mTmG mice (dTomato = nonrecombined cells; GFP = recombined cells) stained with F4/80 (blue). Scale bar, 20 μm. (D) Proportion of F4/80^{+}*Cdh5*$^{+}$ cells from (C) (10 FoV at 40× magnification of 4 livers). (E) Representative maximal projections of confocal z-stacks of FACS-purified *(continued on the next column)* F4/80^{hi}CD31^{hi}. CD31 (green), F4/80 (blue), CD45 (red), and merge (purple). White arrows indicate areas of punctate surface F4/80 and CD45 staining by CD31^{+} cells (n = 5 from 2 separate experiments). Scale bar, 10 μm. (F) Representative Tim4, Clec4f, and CD31 expression by F4/80^{hi}CD11b^{lo} cells. (G) Representative mApple and CD31 expression by F4/80^{hi}CD11b^{lo} cells from *Csf1r*-mApple transgenic mice or their negative littermate controls (n = 9, 3 experiments). (H) Proportion of BrdU^{+}Ki67^{+} cells amongst CD31^{hi} and CD31^{lo} F4/80^{hi}CD11b^{lo} cells after administration of CSF1-Fc or PBS (n = 4, 1 experiment). Significance determined by 1-way ANOVA. (I) Overlay of all CD45^{+}CD31^{hi} cells (red) onto CD45^{+}CD31^{lo} cells. (J) Representative maximal projections of confocal z-stacks of FACS sorted CD45^{+}F4/80^{-}CD31^{hi} cells, demonstrating a CD45^{+} cell (red) enveloped in an endothelial cell (green)

cells within the F4/80^{hi}CD11b^{lo} KC gate using all 3 protocols (Figs. 3B and 3C), and most pronounced with the 50 g method. Notably, KC-specific *Cdh5* expression was observed in microarray datasets generated with[11,13] or without[12] Percoll gradient purification and low-speed centrifugation. Hence, although it remains possible that KC express *Cdh5* at higher levels than other resident tissue mϕ, it is highly likely that contaminating endothelial cells contributed significantly to the high expression of this gene by KCs. The exclusion of CD31^{hi} cells (Fig. 3D) is therefore a critical step for the faithful identification of KCs in mouse liver irrespective of isolation protocol.

3.4 | Isolation method can lead to selective loss of KCs

After removal of CD31^{hi} endothelial cells, we observed clear differences in the relative abundance of KCs amongst live CD45^{+} cells between isolation methods, with much lower frequencies using both the Percoll and 50 g prespin methods, whereas the frequency of F4/80^{lo}CD11b^{hi} cells was more consistent (Fig. 4A). To determine whether the difference in relative abundance in KCs between methods was due to selective loss of these cells with the Percoll gradient and 50 g prespin methods or enrichment with the 300 g method, we analyzed the hepatocyte pellet from the 50 g prespin, the supernatant from the first 300 g spin, and the hepatocyte layer from the Percoll gradient alongside the normal isolates. KCs were clearly identifiable in the discards from all protocols but at an elevated frequency in the Percoll and 50 g spin methods (Fig. 4B). Comparison of the frequency of KCs of total CD45^{+}CD31^{-} cells within the isolate compared directly with the frequency of KCs in the discard for each sample showed that KCs were significantly enriched in the discard of both the Percoll and 50 g spin methods, but not in the 300 g spin method (Figs. 4C–4E). Thus, KCs were selectively lost using both the Percoll and the 50 g spin methods, whereas the ratio of all leukocytes including KCs was not altered in the discard versus the isolate with the 300 g spin method. The Percoll method also yielded far fewer CD45^{+} cells compared with the 300 g method (Fig. 4F), that together with the lower abundance of KCs, corresponded to over a 7-fold reduction in yield of KCs using this method (Fig. 4G). It was not possible to obtain accurate cell counts from the 50 g method due to large amount of debris seemingly retained with this method, nor were many KCs present in the pellet extracted from the discarded Percoll (Fig. 4G), suggesting most remained within the

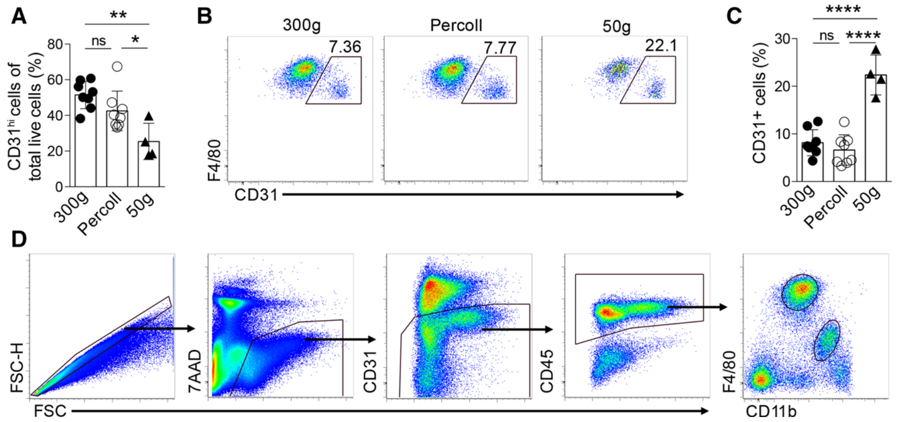

FIGURE 3 **(A) The frequency of CD31^{hi} cells of all live, single cells**. (B and C) Representative flow plots (B) and replicate data (C) of the proportion of CD31^{hi} cells amongst F4/80^{hi}CD11b^{lo} cells obtained with different protocols (300 g, Percoll, 50 g) ($n = 4–8$/group, 2 experiments). (D) Improved gating strategy incorporating CD31 to identify endothelial contaminants from the F4/80^{hi}CD11b^{lo} KCs population. Significance determined by 1-way ANOVA

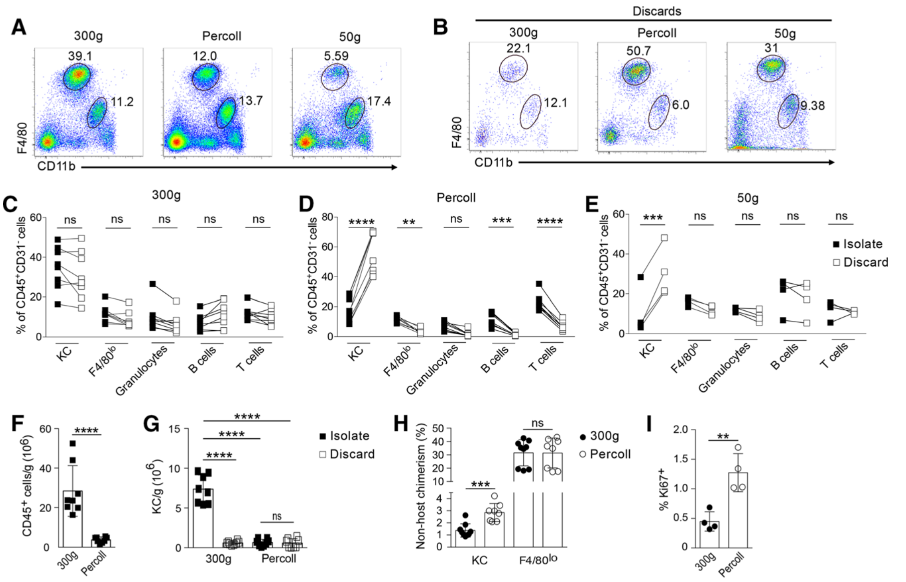

FIGURE 4 **(A and B) Representative flow plots of all isolated (A) and discarded (B) live CD45^{+}CD31^{lo} cells showing proportions of F4/80^{hi}CD11b^{lo} and F4/80^{lo}CD11b^{hi} populations from livers prepared for flow cytometry by 1 of 3 different protocols**. (C–E) The relative frequency of F4/80^{hi}CD11b^{lo} KCs, F4/80^{lo} cells granulocytes, B cells and T cells as a proportion of all CD45^{+}CD31^{lo} leukocytes in the cell isolate linked to the frequency in the discard for the various protocols ($n = 4–8$/group, 2 experiments). Significance determined by multiple *t*-test (Holm-Sidak correction). (F and G) Number of CD45^{+} cells or CD45^{+}F4/80^{hi}CD31^{lo} KCs isolated by either 300 g or Percoll method ($n = 8$/group, 2 experiments). Significance determined by t-test and 1-way ANOVA respectively. (H) Nonhost chimerism amongst KCs and F4/80^{lo} cells from liver of WT > WT tissue-protected BM chimeric mice isolated by 300 g or Percoll protocol ($n = 8$/group, 2 experiments). (I) Proportion of Ki67^{+} KCs isolated from liver by 300 g or Percoll protocol ($n = 4$/group, representative of 2 experiments). Significance determined by *t*-test

Percoll. Importantly, the loss of a large fraction of KCs using the Percoll method also led to different interpretation of important aspects of KCs biology. Specifically, KCs turnover in CD45.1/CD45.2 congenic BM chimeras was exaggerated in Percoll preparations compared with the 300 *g* method, as was the frequency of KCs positive for the cell cycle marker, Ki67 (Figs. 4H–4I). Hence, the choice of isolation method also significantly affected readouts of KCs origin and function. Two 300 *g* centrifugation steps would appear to give the most accurate, unbiased assessment of the frequency of KCs within liver leukocytes, the greatest yield of leukocytes, and hence the most representative portrayal of the characteristics of KCs in vivo.

For simplicity, only 1 slow prespin (50 *g*) and 1 density gradient (33% Percoll) method were compared in our study. However, we acknowledge that there is considerable variation reported in number and speed of centrifugations, as well as gradient concentrations used in protocols to isolate liver leukocytes.[11,13,28,29] Nevertheless, our data suggest that careful optimization of these methods will be required for studies where KCs are the major cell of interest.

4 | SUMMARY

It is imperative that populations isolated for flow cytometric, gene comparison, and functional analyses are representative of those in vivo. We have demonstrated that the established $CD45^{+}F4/80^{hi}CD11b^{lo}$ gating strategy used to identify KCs in liver preparations also contains a population of endothelial cells. These cells could not be excluded using antibodies to KCs surface antigens and because endothelial cells were also found to form aggregates with other $CD45^{+}$ cell types, we propose the simplest method to exclude them from analysis is by inclusion of antibodies to CD31 or other endothelial markers. We suggest that this strategy be adopted universally (Fig. 3D), particularly as endothelial contamination was apparent using all commonly used methods for the preparation of hepatic leukocytes for flow cytometric analysis. Cell conjugates identified by flow cytometry can reveal functionally important in vivo cell interactions[30] and hence, endothelial cells to which KC membrane is tightly bound may well represent those LSECs intimately interacting with KCs at the point of necropsy. Since KCs remain largely static in the steady state[31] further investigation of this subset of LSECs may identify factors controlling the turnover and function of KCs.[32]

AUTHORSHIP

R.W.L. and C.A.H. designed, performed, and analyzed the experiments and wrote the manuscript. A.P. performed the experiments. C.C.B. performed the experiments and edited the manuscript. J.P.I. obtained funding and reviewed the manuscript. S.J.J. conceived the experiments, wrote the manuscript, and obtained funding. R.W.L. and C.A.H. contributed equally to this work.

ACKNOWLEDGMENTS

This work was supported by a MRC grant (MR/L008076/1), a University of Edinburgh PhD studentship to C.A.H., and a Wellcome Trust Clinical PhD studentship (109889/Z/15/Z) to R.L. We thank Prof. N. Henderson for provision of *Cdh5*-Cre-ERT2:mTmG mice, Prof. R. Adams for permission to use the *Cdh5*-Cre-ERT2 mice, and Prof. D. Hume (Roslin Institute, Edinburgh, UK) for providing CSF1-Fc. We thank Trudi Gillespie for help with confocal microscopy.

DISCLOSURE

The authors declare no conflicts of interest.

REFERENCES

1. Terpstra V, van Berkel TJC. Scavenger receptors on liver Kupffer cells mediate the in vivo uptake of oxidatively damaged red blood cells. *Blood*. 2000;95:2157–2163.
2. Heymann F, Peusquens J, Ludwig-Portugall I, et al. Liver inflammation abrogates immunological tolerance induced by Kupffer cells. *Hepatology*. 2015;62:279–291.
3. Balmer ML, Slack E, de Gottardi A, et al. The liver may act as a firewall mediating mutualism between the host and its gut commensal microbiota. *Science Transl Med*. 2014;6:237ra66.
4. Crofton RW, Diesselhoff-Den Dulk MMC, Furth RV. The origin, kinetics, and characteristics of the Kupffer cells in the normal steady state. *J Exp Med*. 1978;148:1–17.
5. Perdiguero EG, Klapproth K, Schulz C, et al. Tissue-resident macrophages originate from yolk-sac-derived erythro-myeloid progenitors. *Nature*. 2014;518:547–551.
6. Yona S, Kim K-W, Wolf Y, et al. Fate mapping reveals origins and dynamics of monocytes and tissue macrophages under homeostasis. *Immunity*. 2013;38:79–91.
7. Dixon LJ, Barnes M, Tang H, Pritchard MT, Nagy LE. Kupffer Cells in the liver. *Compr Physiol*. 2013;3:785–797.
8. Ju C, Tacke F. Hepatic macrophages in homeostasis and liver diseases: from pathogenesis to novel therapeutic strategies. *Cell Mol Immunol*. 2016;13:316–327.
9. Zigmond E, Samia-Grinberg S, Pasmanik-Chor M, et al. Infiltrating monocyte-derived macrophages and resident kupffer cells display different ontogeny and functions in acute liver injury. *J Immunol*. 2014. https://doi.org/10.4049/jimmunol.1400574.
10. Zhang H, Pu W, Tian X, et al. Genetic lineage tracing identifies endocardial origin of liver vasculature. *Nat Genet*. 2016;48:537–543.
11. Okabe Y, Medzhitov R. Tissue-specific signals control reversible program of localization and functional polarization of macrophages. *Cell*. 2014;157:832–844.
12. Scott CL, Zheng F, De Baetselier P, et al. Bone marrow-derived monocytes give rise to self-renewing and fully differentiated Kupffer cells. *Nat Commun*. 2016;7:10321.
13. Lavin Y, Winter D, Belcher-Gonen R, et al. Tissue-resident macrophage enhancer landscapes are shaped by the local microenvironment. *Cell*. 2014;159:1312–1326.
14. Hawley HA, Rojo R, Raper A et al. Csf1r-mApple transgene expression and ligand binding in vivo reveal dynamics of CSF1R expression within the mononuclear phagocyte system. *J Immunol*. 2018;200: 2209–2223.
15. Wang Y, Nakayama M, Pitulescu ME, et al. Ephrin-B2 controls VEGF-induced angiogenesis and lymphangiogenesis. *Nature*. 2010;465: 483–486.
16. Muzudmar MD, Tasic B, Miyamichi K, Li L, Luo L. A global double-fluorescent Cre reporter mouse. *Genesis*. 2007;45:593–605.
17. Bain CC, Hawley CA, Garner H, et al. Long-lived self-renewing bone marrow-derived macrophages displace embryo-derived cells

to inhabit adult serous cavities. *Nat Commun*. 2016. https://doi.org/10.1038/ncomms11852.

18. Gow DJ, Sauter KA, Pridans C, et al. Characterisation of a novel Fc conjugate of macrophage colony-stimulating factor. *Mol Therapy*. 2014;22:1580–1592.
19. Schulz C, Perdiguero EG, Chorro L, et al. A lineage of myeloid cells independent of Myb and hematopoietic stem cells. *Science*. 2012;336:86–90.
20. Yang CY, Chen JB, Tsai TF, et al. CLEC4F is an inducible C-type lectin in F4/80-positive cells and is involved in alpha-galactosylceramide presentation in liver. *PLoS One*. 2013;8:e65070.
21. Jenkins SJ, Ruckerl D, Thomas GD, et al. IL-4 directly signals to tissue-resident macrophages to proliferate beyond homeostatic levels controlled by CSF-1. *J Exp Med*. 2013;210:2477–2491.
22. Patten Daniel A, Wilson Garrick K, Bailey Dala, et al. The Human liver sinusoidal endothelial cells promote intracellular crawling of lymphocytes during recruitment- a new step in migration. *Hepatology*. 2017;65:294–309.
23. Wang Li, Wang Xiangdon, Xie Guanhu, et al. Liver sinusoidal endothelial cell progenitor cells promote liver regeneration in rats. *J Clin Invest*. 2012;122:1567–1573.
24. Ramachandran P, Pellicoro A, Vernon MA, et al. Differential Ly-6C expression identifies the recruited macrophage phenotype, which orchestrates the regression of murine liver fibrosis. *Proc Natl Acad Sci USA*. 2012;109:E3186–3195.
25. Blom KG, Qazi MR, Noronha Matos JB, Nelson BD, DePierres JW, Abedi-Valugerdi M. Isolation of murine intrahepatic immune cells employing a modified prodecure for mechanical disruption and function characterization of the B, T and natural killer T cells obtained. *Clin Exp Immunol*. 2009;155:320–329.
26. Ikarashi M, Nakashma H, Kinoshita M, et al. Distinct development and functions of resident and recruited liver Kupffer cells/macrophages. *J Leuk Biol*. 2013;94:1325–1336.
27. Pythian-Adams AT, Cook PC, Lundie RJ, et al. CD11c depletion severely disrupts Th2 induction and development in vivo. *J Exp Med*. 2010;207:2089–2096.
28. Girgis NM, Gundra UM, Ward LN, Cabrera M, Frevert U, Loke P. Ly6C(high) monocytes become alternatively activated macrophages in schistosome granulomas with help from CD4+ cells. *PLoS Pathog*. 2014;10.
29. Yepes E, Varela-M RE, López-Abán J, Rojas-Caraballo J, Muro A, Mollinedo F. Inhibition of granulomatous inflammation and prophylactic treatment of schistosomiasis with a combination of edelfosine and praziquantel. *PLoS Negl Trop Dis*. 2015;9.
30. Reinhardt RL, Liang HE, Locksley RM. Cytokine-secreting follicular T cells shape the antibody repertoire. *Nat Immunol*. 2009;10:385–393.
31. Wang J, Kubes P. A reservoir of mature cavity macrophages that can rapidly invade visceral organs to affect tissue repair. *Cell*. 2016;165:668–678.
32. Guilliams M, Scott CL. Does niche competition determine the origin of tissue-resident macrophages? *Nat Rev Immunol*. 2017;17:451–460.

SUPPORTING INFORMATION

Additional information may be found online in the supporting information tab for this article.

How to cite this article: Lynch RW, Hawley CA, Pellicoro A, Bain CC, Iredale JP, Jenkins SJ. An efficient method to isolate Kupffer cells eliminating endothelial cell contamination and selective bias. *J Leukoc Biol*. 2018;104:579–586. https://doi.org/10.1002/JLB.1TA0517-169R

4.4 Conclusion

In the above manuscript we showed that LSEC are significant contaminants found within CD45$^+$ liver leukocyte populations when analysed by flow cytometry and they were particularly prevalent within the KC gate. While our data cannot discount that *Cdh5* may be expressed by KC, the level of expression in this population was seemingly insufficient to cause significant Cre-mediated excision of the tdTomato cassette in Cdh5-Cre-ERT2; mTmG mice. Together these results validated the use of the Cdh5-Cre-ERT2 line as a useful tool to specifically interrogate the effect of IL-4R signalling on the endothelial population.

Indeed, in the Cdh5-Cre-ERT2; IL-4R$\alpha^{fl/fl}$ line, I observed that all Cre$^-$ CD31$^+$ CD45$^-$ endothelial cells uniformly expressed the IL-4Rα and induction of Cre resulted in loss of IL-4Rα expression (Fig. 4.1A-D). Importantly, there was no loss of IL-4Rα expression in Kupffer cells (Fig. 4.1E) or other leukocyte populations (Fig. 4.1F), confirming the faithful nature of this Cre driver to the endothelial lineage. Although pinworm infection in the animal unit housing the Cdh5-Cre-ERT2; IL-4R$\alpha^{fl/fl}$ line prevented full investigation of the effect of IL-4c signalling to endothelial cells during CCl_4 injury, I was able to perform some preliminary experiments. These experiments suggested that in acute CCl_4 injury endogenous IL-4 signalling to the endothelia influenced neither the composition of the inflammatory infiltrate, including monocyte, neutrophil, eosinophil recruitment or macrophage content, nor serological indices of liver injury (data not shown). Owing to the issues with the pinworm infection, I instead focused on dissecting the effect of direct signalling by exogenous IL-4 on the function and make-up of the mononuclear phagocyte compartment since this could be performed in wild-type mice and other strains housed in a separate pin-worm free animal facility at the UoE.

As mentioned, the main finding in the above manuscript was the presence of significant endothelial cell contamination of Kupffer cell populations and also other leukocyte populations. It therefore became important to include an endothelial marker in subsequent experiments to ensure that all endothelial contaminants were removed from subsequent analysis. Thus, CD31 (also known as PECAM-1), was included in all flow cytometric analyses to ensure exclusion of endothelial cells, as set out in Fig. 4.1A.

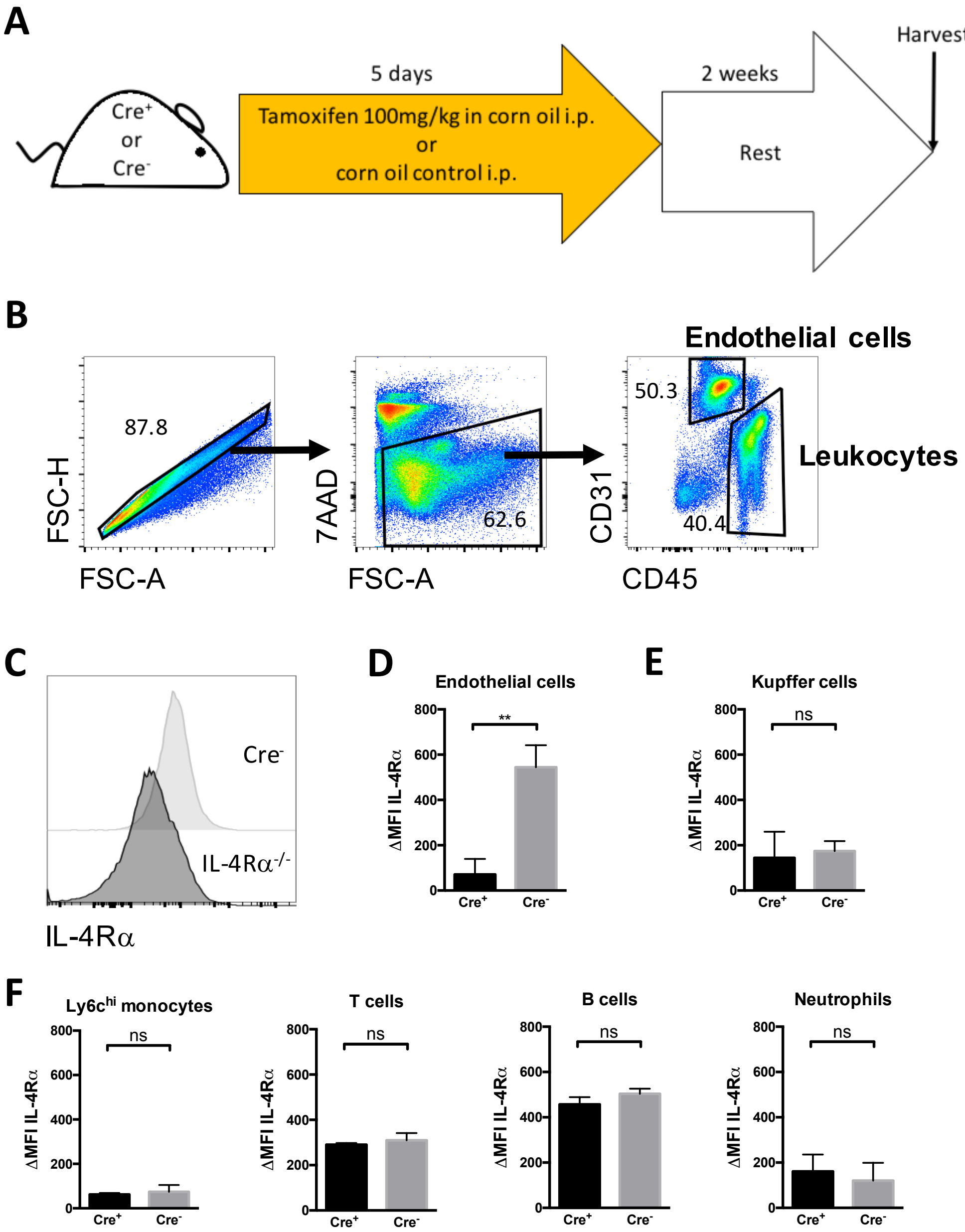

Figure 4-1Characterisation of IL-4Rα expression in Cdh5-Cre-ERT2; IL-4rα$^{fl/fl}$ mice.

(A) Schematic representation of the model: Cre^{+} mice were given tamoxifen daily for 5 days whilst Cre^{-} mice were given corn oil. (B) Flow plots demonstrating gating strategy to identify CD31^{hi} CD45^{-} endothelial cells and CD31^{lo} CD45^{+} leukocytes. (C) Representative histogram of IL-4Ra expression in Cre^{-} CD31^{+} CD45^{-} endothelial cells. (D-F) Delta MFI for IL-4Rα in outlined populations. Kupffer cells (F4/80^{hi} CD11b^{lo}) and Ly6c^{hi} monocytes (Ly6c^{hi} MHCII^{lo}). Delta MFI calculated using IL-4Rα$^{-/-}$ control. N=3 per group (unpaired *t* test).

Chapter 5 Intrinsic effects of IL-4c on leukocyte populations

5.1 Introduction

In Chapter 3 I demonstrated that therapeutic administration of exogenous IL-4 led to a significant improvement in indices of hepatic regeneration and repair in the setting of acute liver injury, and that this was paralleled by significant changes in the monocyte/macrophage compartment. The observed reduction in Ly6C^{hi} monocytes and increase in differentiated macrophages may potentially enhance repair. For example, during acetaminophen (APAP)-induced acute liver injury Ly6C^{hi} monocytes have been shown to express proinflammatory genes, including *Trem1*, *Nos2, Cox2*, *Ccl2* and *Ccl7*[21]. The pro-inflammatory function of Ly6C^{hi} monocytes has been shown to promote pathology in other disease models. For instance, Ly6C^{hi} monocytes and their descendants are responsible for driving tissue destruction in response to harmless microbiota during chemically-induced colitis where they have a similar pro-inflammatory profile to those in APAP liver[21,116,117], and the inhibition of Ly6C^{hi} monocyte recruitment results in a less severe phenotype[116]. Following myocardial infarction (MI) Ly6C^{hi} monocytes dominate the pro-inflammatory phase of injury, whereas Ly6C^{lo} macrophages predominate during the recovery phase[118,270]. A similar pattern has been shown in both acute liver injury with APAP and chronic CCl_4 mediated injury whereby Ly6C^{hi} monocytes convert into Ly6C^{lo} macrophages[21,115]. In APAP this conversion process involves downregulation of the aforementioned proinflammatory genes and upregulation of genes including *Trem2*, *Gpnmb* and *Retnla*[21], which are typically associated with tissue repair[29,185].

The inference from these studies has been that this switch from predominance of Ly6C^{hi} monocytes to Ly6C^{lo} macrophages is an important part of the transition from the inflammatory to repair phases of tissue repair, however, what drives this switch is unclear. More specifically relating to IL-4, it has been long known that IL-4 induces a pro-reparative phenotype in macrophages [28,202,271] and recent work in physical injury models has outlined its importance in promoting repair. In the skin it has been shown that IL-4Rα signalling to macrophages is required to control the restoration of tissue architecture[30]. Moreover, IL-4/IL-13 activated macrophages are integral to rapid mucosal healing following puncture wounds in the colon[29].

As I had observed a loss in Ly6C^{hi} monocytes and an increase in Ly6C^{lo} macrophages in response to IL-4 in the context of injury at a single timepoint, I sought to determine whether the dynamics of the observed monocyte/macrophage phenotype could reveal potential underlying mechanisms by performing a timecourse experiment. Furthermore, I wanted to establish if direct signalling to mononuclear phagocytes was responsible for the observed phenotypic changes and the enhanced repair and regeneration upon IL-4c treatment. To this end, I used a variety of approaches including LysM Cre; IL-4R$\alpha^{fl/-}$ mice, as well as whole body and tissue-protected irradiation chimeras to limit IL4R deficiency to particular cell types.

5.2 Kinetics of therapeutic effect of IL-4

It is known that acute liver injury with CCl_4 causes recruitment of leukocytes, the composition of which changes over time[22]. I therefore performed a timecourse experiment to establish the temporal changes in the composition of the leukocyte compartment in liver and blood following injury with CCl_4, and assess the effects of therapeutic administration of IL-4c (Fig. 5.1A).

5.2.1 The effect of IL-4 on kinetics of disease phenotype

Although the main aim of this experiment was to examine the leukocyte dynamics in blood and liver over time, I also performed phenotypic analyses of the mice using weight and serum enzymes. Two identical experiments were performed and in both experiments I observed initial weight loss in all groups (Fig. 5.1B-C), which was more pronounced in the CCl_4 treated groups compared with the olive oil treated groups. However, it was evident that the dynamics of weight loss and recovery were different between experiments, with weights in the CCl_4 treated groups returning to baseline on day 3 in RL048 but not until day 4 in RL071 (Fig. 5.1B-C). There were also obvious differences in the dynamics of serum ALT and AST between experiments. Overall I observed a lower ALT on day 1 in RL071 (3320 u/l ± 530.3) compared to RL048 (7450 ± 2707.0)(Fig. 5.1D-E). The day 1 ALT levels from RL048 was also more in keeping with a previous experiment where ALTs were examined 24hrs after CCl_4 administration (8393 u/l ± 998). Although data from RL071 more closely matched that of previous experiments with a trend towards lower levels of AST and ALT in IL-4c treated groups at day 3, the levels of ALT at day 1 in this experiment (when peak levels would usually be expected) were unusually low. In RL048 it appears that there may have been an acceleration in the kinetics as there was a reduction in the ALT in IL-4c treated mice by day 2. It remains unclear what could account for the differences given that the animals used for these experiments were sourced from the same supplier and were of similar ages. Furthermore, both experiments were performed in the same animal unit using the same batch of CCl_4.

Like ALT, cell number data obtained during the timecourse also varied considerably between repeat experiments especially in the first 2 days (Fig. 5.1H-I). This seemed largely due to a different kinetic in cell number in the CCl4 + veh alone group, as the kinetic following IL-4c treatment was seemingly the same in both experiments. In IL-4c treated mice there were increased numbers of cells on day 2 which subsequently dropped on day 3 in both experiments.

5.2.2 Early monocytopenia in tissue with IL-4c treatment

Unlike other parameters flow cytometric analysis was consistent between experiments. Flow cytometric analysis of the CD11b^{hi} population revealed marked changes in the Ly6C-defined populations over time (Fig. 5.2A). In both groups Ly6C^{hi} monocytes accumulated within the first 24hrs following CCl_4 treatment and their abundance decreased progressively with time, reaching baseline levels (equivalent to recipients of olive oil) by day 4 (Fig. 5.2B). Importantly, IL-4c treatment led to a rapid reduction in Ly6C^{hi} monocytes as a proportion of total CD45^{+} leukocytes, returning to baseline by day 3; 24hrs earlier than their vehicle control counterparts. The frequency of Ly6C^{lo} CD64^{hi} macrophages increased progressively from day 1 in both groups, peaking at d3-4 before declining again, although not returning to baseline by d5 (Fig. 5.2D). Interestingly in these experiments, IL4c treatment did not alter the abundance of Ly6C^{lo} macrophages cells in terms of proportion of CD45^{+} leukocytes.

5.2.3 Increased cDC2 dendritic cells and neutrophils in IL-4c treated mice

Analysis of the other leukocyte populations revealed that concomitant with the early reduction in Ly6C^{hi} monocytes on day 2, there was a significant increase in the proportion of neutrophils in the IL-4c treated group compared to the vehicle control group at this timepoint (29.2% ± 4.2 vs 18.0% ± 2.6)(Fig. 5.3A). There was a reduction in proportion of KC (Tim4^{hi}) in both CCl_4 groups but there was no difference with IL-4c treatment (Fig. 5.3B). Analysis of eosinophils revealed that the previously observed increase on day 3 in the IL-4c treated group was also reflected by an early increase in their proportion on day 2 (Fig. 5.3C). There were also subtle changes in the lymphocyte populations on day 4 and 5 (Fig. 5.3D-E). As CD64 was used in the timecourse to positively identify macrophages it became evident when analysing the CD11b^{hi} recruited population that there was expansion of a Ly6C^{lo}CD64^{-}CD11b^{hi} population at day 2 and 3 that was only observed in the IL-4c treated groups (Fig. 5.2A). As outlined in Chapter 3 (Fig. 3.3), MHCII^{+} cells amongst this Ly6C^{lo}CD64^{-}CD11b^{hi} population are most probably cDC2 cells (Fig. 5.2A and 5.3A)[56]. Thus, consistent with my earlier findings at the day 3 timepoint, administration of exogenous IL-4 in the context of CCl_4-induced injury results in changes to the abundance of many leukocyte populations. Given the significant contribution of neutrophils, eosinophils, monocytes and macrophages to the injury and repair process in acute liver injury, I have decided to focus on these populations going forward[21,22,33].

5.2.4 Increased proliferation observed in all Ly6c^{lo} MHCII^{int} macrophages in IL-4c treated mice

Given the known effects of IL-4c on recruited as well as resident macrophage proliferation in, for example, the serous cavities[31,121], and also the apparent increase in Ly6C^{lo} macrophages in earlier experiments, I also measured the effect of IL-4c on proliferation of monocyte/macrophage subsets and how this changed over time. Unfortunately, due to limitations in the number of parameters available for these analyses because of inclusion of both Ki67 and BrdU, F4/80 antibody conjugated to PE-Cy7 was used in the first timecourse experiment, meaning it was difficult to faithfully differentiate between Ly6C^{lo} CD64^{+} macrophages and Kupffer cells at each timepoint. In the repeat experiment, I modified the staining panel to mitigate against these issues and was able to incorporate CD64 into the modified staining panel. Hence, I initially performed an analysis across both experiments where the Ly6C^{lo} MHCII^{int} population encompasses both recruited macrophages and Kupffer cells (Fig. 5.4A). Using this approach, I found a significant increase in the proportion of Ki67^{+}BrdU^{+} macrophages in IL-4c treated mice on day 2 and 3 when compared to vehicle treated mice (Fig. 5.4B). Inclusion of Tim4 and CD64 allowed more accurate identification of macrophage subsets in the repeat experiment (RL071). Analysis of CD11b^{hi} Tim4^{lo} CD64^{hi} Ly6C^{lo} recruited macrophages revealed a trend towards higher proliferation on day 2 and 3 (Fig. 5.4C) mirroring the result obtained in the pooled all Ly6C^{lo} MHCII^{int} hepatic macrophages population (Fig. 5.4B). The same effect of IL-4c was found in the Tim4^{+} KC population in experiment RL071 (Fig. 5.4D). Interestingly, IL-4c treatment also induced significant proliferation in the Ly6C^{hi} monocytes on day 2 and day 3 (Fig. 5.4E). In fact, the levels of proliferation in the Ly6C^{hi} monocytes were greater than those observed amongst the more mature Ly6C^{lo} CD64^{hi} macrophages. To establish if this was a property of a small subset of Ly6C^{hi} monocytes, for instance those expressing higher levels of MHCII, all day 2 Lin^{-} $CD11b^{hi}$ $Ki67^{+}BrdU^{+}$ cells were backgated onto the $CD11b^{+}$ population and their MHCII profile assessed. This revealed that proliferating myeloid cells were evenly distributed throughout the $Ly6C^{hi}$ monocyte population and didn't simply represent a maturing monocyte subset (Fig. 5.4F).

5.2.5 Reduction in monocytes reflected in blood

The marked effects of IL-4c on the loss but also proliferative activity of hepatic monocytes, prompted me to assess if IL-4c had wider effects on the mononuclear phagocytes in the context of acute liver injury. For this reason, blood was collected by cardiac puncture post mortem at all timepoints and analysed by flow cytometry. Using the same single, live ($7AAD^{-}$), $CD45^{+}$ cells and lineage gating strategy as in the liver, monocytes were identified as $CD115^{+}$ $CD11b^{+}$ and then subclassified on their levels of Ly6C expression (Fig. 5.5A). In this and subsequent experiments, where accurate identification of transition between $Ly6C^{hi}$ and $Ly6C^{lo}$ monocytes was necessary, TREML4, a member of the triggering receptor expressed on myeloid cells, was used to positively identify $Ly6C^{lo}$ monocytes (Fig 5.5A)[63]. CCl_4 treatment led to a monocytosis, although this was somewhat more striking in RL048 than RL071 and similar to the hepatic leukocyte populations, it was evident that IL-4c treatment appeared to be having an early effect on reducing monocyte populations (Fig 5.5B). Indeed, administration of IL-4c led to fewer $Ly6C^{hi}$ monocytes as a proportion of all $CD45^{+}$ cells compared to veh treated groups in both experiments at all timepoints (Fig. 5.6A-B). As there was considerable heterogeneity in the overall frequency of monocytes in these experiments, I normalised the proportion of monocytes in the CCl_4 + IL-4c mice to the CCl_4 + veh mice at each timepoint to enable pooling of data from the 2 experiments. In so doing it became evident that there was a reduction in proportion of $Ly6C^{hi}$ monocytes 24 hours after IL-4c treatment (day 2), mirroring that seen in the liver which was sustained until day 3 (Fig 5.6C). Although $Ly6C^{lo}$ $TREML4^{hi}$ and transitioning monocytes make up a smaller proportion of total monocytes in the blood, IL-4c administration also caused a rapid significant reduction in their proportion that was sustained until day 3 in transitioning cells and longer in $Ly6C^{lo}$ monocytes (Fig. 5.6D-E). There was also an apparent early neutrophilia in all groups on day 1, including olive oil treated, which subsequently waned but did not differ significantly between treatments (Fig. 5.6F-G).

5.2.6 Technical issues in timecourse

One mouse was removed from the analysis because at the time of injection it was noted that most of the IL-4c was not injected due to movement of the mouse. Subsequent analysis confirmed that this mouse had not been exposed to significant levels of IL-4 because the monocyte/macrophage phenotype was not replicated and macrophages from this mouse failed to show elevated expression of the alternative activation marker RELMα, which is a characteristic feature of macrophages in IL-4c treated mice (data not shown). There was also one mouse from RL048 day 2 CCl_4 + veh population that was excluded from the analysis of proliferation because the BrdU staining didn't work because of an incomplete BrdU injection.

5.3 Assessing gene deletion efficiency in LysM Cre; IL-4R$\alpha^{fl/-}$ mice

Given the significant phenotype observed within the monocyte and macrophage compartment, I sought to establish whether we could successfully abrogate signaling to these cells using the Cre-Lox system. Lysozyme M is a gene expressed highly by myeloid cells and can be used to drive Cre recombinase to cause deletion of loxP-flanked target genes[272]. Generation of IL-4Rα deficiency in macrophages and neutrophils has previously been achieved using the LysM Cre; IL-4R$\alpha^{fl/-}$ line[28]. However, while this system has been shown to be highly efficient during normal physiological conditions, in the context of inflammation the LysM driven Cre activity can be variable. For instance, excision of IL-4Rα has been shown to be poor in recruited macrophages elicited in the peritoneal cavity during thioglycolate induced sterile inflammation and schistosome infection in the liver[34]. To understand the direct effect of IL-4 on monocytes and macrophages, including any therapeutic effects, I wanted to establish if I could abrogate IL-4Rα protein expression in hepatic monocytes and macrophages in the context of CCl_4-induced acute liver injury using the LysM Cre; IL-4Rα$^{fl/–}$.

5.3.1 Generation of mouse line

LysM Cre; IL-4Rα$^{fl/–}$ mice were generated by crossing LysM Cre; IL-4Rα$^{fl/fl}$ with IL-4Rα$^{–/–}$ mice. The experimental mice generated were IL-4Rα hemizygous mice, bearing one floxed IL-4Rα allele and one null allele (LysM Cre^{+}; IL-4Rα$^{fl/–}$). This has been shown to be the most efficient way to achieve IL4Rα deletion since it relies on excision of only one floxed allele[273]. Cre$^{–}$ littermate controls were used as controls.

5.3.2 Efficiency of IL-4Rα deletion during CCl_4 injury

To assess deletion, male Cre^{+} and Cre$^{–}$ mice, as well as IL-4Rα$^{–/–}$ mice, were administered vehicle or CCl_4 and culled 24hrs later. Consistent with my previous results, IL4Rα was expressed by all myeloid cells examined in Cre$^{–}$ mice. Staining for IL-4Rα on the surface of blood neutrophils revealed bimodal expression, with >80% of neutrophils from Cre^{+} mice lacking the IL-4Rα and this did not change between steady state and CCl_4-induced injury (Fig 5.7 A-B). Similar to neutrophils, Ly6C^{hi} monocytes in blood of Cre^{+} mice also demonstrated bimodal expression of IL-4Rα. However, only ~50-60% of Ly6C^{hi} monocytes had deleted IL-4Rα surface expression (Fig 5.7 C-D) and the efficiency of Cre excision was reduced in CCl_4 injured mice (Fig 5.7D).

Given that I was also interested in the effects of IL-4 in tissues, I also examined the efficiency of Cre mediated excision of the IL-4Rα amongst liver leukocytes. Unlike in the blood there was no evidence of bimodal expression of the IL-4Rα on hepatic Ly6C^{hi} monocytes in either olive oil or CCl_4 treated mice (Fig 5.7E). This suggests that there is no significant excision of the IL-

4Rα in this population and this is reflected by no difference in ΔMFI of IL-4Rα between Cre^{+} and Cre^{-} mice (Fig 5.7F). Owing to the paucity of Ly6C^{lo} macrophages in both injured and uninjured liver 24 hours after CCl_4, it was not possible to assess IL-4Rα expression in this population. It was however possible to assess the surface IL-4Rα expression on resident KC. Interestingly, in the olive oil treated population there was bimodal expression of the IL-4Rα but this was abrogated following CCl_4 injury (Fig 5.7G). As expected the ΔMFI of IL-4Rα in the olive oil group was significantly lower in Cre^{+} mice but in the CCl_4 treated group it was also trending to a lower level in Cre^{+} mice (Fig 5.7H).

Owing to the restricted availability of mice, this experiment was repeated without the olive oil control group. Similar levels of Cre efficiency were detected amongst blood neutrophils (87.4%) and blood Ly6C^{hi} monocytes (52.7%) as in the previous experiment (Fig. 5.8A-F). Importantly this means that ~50% of circulating Ly6C^{hi} monocytes will still express the IL-4Rα on their surface. Given this poor efficiency, I decided not to use the LysM Cre; IL-4R$\alpha^{fl/-}$ strain to probe IL-4R signaling in myeloid cells.

5.4 Whole body irradiation chimeras

As an alternative approach to determine the contribution of IL-4Rα signaling to myeloid cells and therapeutic phenotype observed with IL-4c treatment, I decided to generate whole body tissue irradiation chimeras. Using WT recipient mice and IL-4R$\alpha^{-/-}$ BM I was able to limit IL-4Rα deficiency to the haematopoietic compartment. For this purpose 8 week-old CD45.1^{+}/.2^{+} recipient males were reconstituted with wild-type (WT) or IL-4R$\alpha^{-/-}$ (KO) donor BM (CD45.2^{+}) 24 hours after whole body irradiation (Fig. 5.9A). The use of congenic CD45.1^{-}CD45.2^{+} recipients enabled me to confirm the successful engraftment of donor BM, by assessing chimerism by flow cytometry of circulating monocytes 8 weeks post-reconstitution. This confirmed 99.2% ± 1.1 and 99.5% ± 0.4 chimerism in the mice given WT BM

(WT>WT) and in the WT mice given KO BM (KO>WT) mice respectively (Fig. 5.9B). As expected Ly6C^{hi} monocytes and Ly6C^{lo} macrophages were exclusively of donor origin (CD45.1^{-}CD45.2^{+}) by 8 weeks (Fig. 5.9C-D). This model therefore enabled me to establish the effect of IL-4Ra signalling to BM-derived cells in the observed monocyte/macrophage phenotype, as well as the therapeutic effect of IL-4c on liver repair and regeneration.

5.4.1 Phenotypic analysis of weight and serum in whole body chimeras

As expected, administration of CCl_4 resulted in weight loss in all groups, although this appeared to be greater in KO>WT mice irrespective of whether they had received IL-4c treatment (Fig. 5.9E), suggesting even signalling by endogenous IL-4 to BM may limit weight loss in response to liver injury. Analysis of ALT and AST revealed that loss of IL4Rα in the haematopoietic compartment did not affect the elevated levels seen in response to CCl_4 either in mice receiving vehice of IL-4c (Fig. 5.9F-G). Similarly, the reduction in ALT and AST levels in response to exogenous IL-4c was not affected by the loss of IL-4Rα. In the KO>WT recipients IL-4c resulted in a significant reduction in ALT and AST that wasn’t evident in the WT>WT recipients (Fig. 5.9F-G). As in the non-chimeric experiments IL-4c treatment had no effect on bilirubin levels (Fig. 5.10H).

5.4.2 Necrotic cell area and hepatocyte proliferation in whole body irradiation chimeras

A large degree of heterogeneity was apparent within the necrotic cell areas in the chimeric mice making it difficult to establish true necrotic areas (Fig 10A-D). This occurred irrespective of whether recipients were given WT or KO BM or vehicle or IL-4c. It was not possible to perform an accurate analysis of necrotic tissue vs cellular infiltrate as was previously performed (Fig. 5.10A-D). I therefore developed a script in Difiniens to quantify total healthy parenchyma which excluded both cellular infiltrate and necrosis. This surprisingly revealed that there was a trend to lower proportions of viable tissue area in the IL-4c treated mice but that there also seemed to be a trend to lower viable tissue areas in all KO>WT mice (Fig5.10E). Furthermore, visual inspection of samples revealed that in the IL-4c treated mice there did not appear to be a difference in cellular infiltrate between mice receiving WT or KO BM.

In contrast, there did appear to be a trend towards lower hepatocyte proliferation in KO>WT than WT>WT mice following treatment with IL-4c (16.7% ± 6.5 vs 22.4% ± 5.6) (Fig. 5.11F), which was not apparent in the vehicle treated group (14.82 ± 10.6 vs 14.26% ± 6.0) (staining and quantification performed by Andrew Muir). Hence, indices of liver injury and repair were unaffected by loss of IL-4Rα on BM cells. Further experiments using WT>KO mice would be able to confirm if the beneficial effect of exogenous IL-4 on hepatocyte proliferation act at least in part through signalling in haematopoietic cells.

5.4.3 IL-4Rα signalling is key to observed hepatic monocyte/macrophage phenotype

Analysis of recruited monocytes and macrophages by flow cytometry suggested that only when the donor BM cells were IL-4Rα replete (WT donor) was the reduction in $Ly6C^{hi}$ monocytes and increase in $Ly6c^{lo}$ $CD64^{hi}$ observed (Fig. 5.11A). Concurrent with previous results there was a significant reduction (>5 fold) in the frequency and number of $Ly6C^{hi}$ monocytes in WT>WT mice when they were treated with IL-4c ($1.16x10^7$ cells/g ± $5.2x10^6$ vs $1.994x10^6$ cells/g ± $5.42x10^5$)(Fig. 5.11B-C). However, administration of IL4c had no impact on the number of $Ly6C^{hi}$ monocytes in KO>WT mice ($1.33x10^7$ cells/g ± $4.93x10^6$ vs $1.35x10^7$ cells/g ± $2.53x10^6$). Similarly, whereas IL4c treatment led to a significant increase in the proportion and absolute number of hepatic $Ly6C^{lo}$ $CD64^{hi}$ recruited macrophages in WT > WT chimeras ($1.094x10^7$ cells/g ± $3.37x10^6$ vs $2.18x10^7$ cells/g ± $7.67x10^6$), this expansion was absent in KO > WT chimeras ($1.05x10^7$ cells/g ± $2.528x10^6$ vs $1.319x10^7$ cells/g ± $2.43x10^6$)(Fig.

5.11.D-E). Thus, these results demonstrate that IL-4Rα signalling to BM-derived cells is required to produce the IL-4c dependent reduction in Ly6C^{hi} monocytes and increase in Ly6C^{lo} macrophages.

This IL-4Rα-dependent increase in macrophages in IL-4c treated mice at day 3 coincides with the increased macrophage proliferation observed during the timecourse (Fig. 5.4B-C). I therefore hypothesised that this proliferation could contribute, in part, to the observed increase in Ly6C^{lo} CD64^{hi} macrophages in the IL-4c treated mice. I therefore next measured proliferation in the whole body irradiation chimeras, using the MHCII and Ly6C profile to identify Ly6C^{hi} monocytes and recruited Ly6C^{lo} macrophages, and measuring proliferation by Ki67^{+} expression and BrdU^{+} incorporation (Fig. 5.12A-B). This revealed that administration of IL-4c only led to enhanced proliferation of Ly6C^{hi} monocytes and Ly6C^{lo} MHCII^{int} macrophages in the WT>WT mice, while this was abolished by deletion of IL-4Rα in the haematopoietic compartment (Fig. 5.12C). IL-4 driven proliferation within the Ly6C^{hi} monocyte population was similarly dependent on expression of IL-4Rα by BM cells (Fig. 5.12D).

These results would suggest that at least part of the observed expansion of Ly6C^{lo} recruited macrophages is due to IL-4Rα dependent proliferation.

5.4.4 Effect of IL-4Rα deletion in other leukocyte populations with IL-4c treatment

Unlike monocytes and recruited macrophages, a proportion of Kupffer cells and T cells are radio resistant and therefore not fully replaced in whole body irradiation chimeras[90,274] (Fig. 13.5A). Notably, the size of this radio-resistant fraction was similar between recipients of WT and KO BM. As with Ly6C^{lo} CD64^{hi} macrophages, the IL-4c related increase in putative cDC2 cells was dependent on IL-4R signalling on haematopoietic cells. However, the total increase in number of cDC2 cells remained small in comparison to the changes in the tissue monocyte/macrophage populations (Fig. 5.13B). Interestingly, administration of IL-4c in the context of haematopoietic IL-4Rα deficiency resulted in expansion of neutrophils in the liver (Fig. 5.13C). In contrast, the increase in eosinophils observed with IL-4c treatment did not absolutely require haematopoietic IL-4Rα signalling because there is no significant difference between WT>WT and KO>WT mice (Fig. 5.13D). Although the level of eosinophils in KO>WT recipients treated with vehicle control was also seemingly increased making it difficult to say with certainty that exogenous IL-4c drives eosinophilia solely via signalling to non-haematopoietic cells (Fig. 5.13D). Interestingly the reduction in B cells in response to IL-4c observed in Chapter 3 and in the timecourse did seem to be dependent on IL-4Rα signalling to the haematopoietic compartment because it was only observed in the WT>WT mice and not KO>WT mice (Fig. 5.13E).

5.4.5 Reduction in circulating Ly6C^{hi} monocytes is dependent on BM IL-4Rα signalling

Given that I had previously observed that IL-4c induced a reduction in the proportion of circulating monocytes, the setting of whole body radiation chimeras provided the opportunity to assess whether this change was due to direct IL-4R signalling on haematopoietic cells. Indeed, there was only a significant reduction in the proportion of Ly6C^{hi} and Ly6C^{lo} monocytes in blood when IL-4c was administered to recipients of WT BM (Fig. 5.14A-B). Of note, IL-4c administration to KO > WT mice resulted in Ly6C^{hi} monocytes forming a significantly higher proportion of circulating leukocytes than mice treated with vehicle (Fig. 5.14A).

There were no significant effects in proportion observed in any of the other circulating populations despite the elevation in neutrophils observed in the tissues. Lymphocytes were not subdivided on the basis of MHCII expression due to restrictions placed on the staining panel in order to accommodate CD45.1 and CD45.2 staining (Fig. 5.14C-E). Because absolute numbers of blood leukocytes were not obtained from this experiment, I have shown the various populations as parts of a whole to demonstrate that monocytopenia is only observed in the response to CCl_4 + IL-4c when the haematopoietic compartment can signal through IL4R (WT > WT chimeras) (Fig. 5.14F). In this group there does appear to be an increase in lymphocytes but this is not a significant change (Fig. 5.14E).

5.5 Tissue-protected IL-4R$\alpha^{-/-}$ chimeras

The results outlined above established that IL-4Rα signalling within the haematopoietic compartment was indispensable for the observed effects of IL-4c on the monocyte/macrophage compartment during acute liver injury. However, it remained unclear whether this was due to cell intrinsic IL-4Rα signalling by monocytes and macrophages or if it was related to signalling to other BM-derived cells driving a subsequent downstream effect on monocytes and macrophages. Therefore, I next generated tissue protected BM chimeras to allow direct comparison of the response of IL-4Rα-sufficient and IL-4Rα-deficient BM-derived cells in the same environment. The hind limbs of CD45.1^{+}/.2^{+} mice were irradiated with a lead shield protecting the abdomen, torso and head (Fig. 5.15A). Mice were reconstituted with either WT or IL-4R$\alpha^{-/-}$ (CD45.2^{+}) BM as before and left for 8 weeks to allow maximal engraftment. The degree of engraftment was assessed by pre-screening prior to injury. Lethal irradiation was only administered to the hind limbs, and as such chimerism in these mice was partial, with 15-40% of Ly6C^{hi} monocytes deriving from donor BM (Fig. 5.15B-C). The results presented are from two separate experiments and it is notable that the baseline chimerism of circulating leukocytes was variable and differed markedly between experiments, although this is found routinely by other members of the Jenkins group. Moreover, in both these experiments the baseline chimerism was marginally higher in the KO>WT mice and this achieved statistical significance in the second experiment (Fig. 5.15C). This suggests that IL-4R signalling could exert a modest regenerative selective pressure in the BM during haematopoiesis/reconstitution. The gating of liver monocytes/macrophages in these experiments is presented in Fig. 5.15D. As with the blood it was possible to identify the host and donor cells in the recruited hepatic monocyte/macrophage populations based on their CD45.1 and CD45.2 expression (Fig. 5.15D).

5.5.1 Reduction in Ly6C^{hi} monocytes in blood is dependent on intrinsic IL-4Rα signalling

In the blood of WT>WT tissue-protected chimeric mice, there was an increase in the proportion of Ly6C^{hi} monocytes between day 0 and day 3 in response to CCl_4 administration (vehicle treated group; 3.2% ± 0.3 vs 7.1% ± 2.0 $p<0.0001$). Conversely and consistent with my previous experiments, IL-4c treatment led to a significant monocytopenia (Ly6C^{hi} monocytes from 4.4% ± 1.6 to 0.9% ± 0.5 in CCl_4 versus CCl_4+IL4c respectively; $p<0.0001$) (Fig. 5.16A). Notably there also appeared to be a slight reduction in the proportion of Ly6C^{hi} monocytes in the olive oil treated group (4.0% ± 1.3 vs 2.6% ± 0.9, $p=0.04$). That the chimerism in circulating Ly6C^{hi} monocytes was unaffected by genotype between day 0 and day 3 in in mice receiving either olive oil or CCl_4 + veh, demonstrated that endogenous IL-4 does not play a significant role in regulating circulating monocyte numbers during these treatments (Fig. 5.16B). However, IL-4c administration (on day 1) in the context of CCl_4-induced injury resulted in a significant increase in the chimerism of circulating Ly6C^{hi} monocytes between day 0 to day 3 exclusively in the recipients of KO BM. Thus, when the chimerism of circulating Ly6C^{hi} monocytes at day 3 was normalised to that at day 0, only recipients of KO BM treated with IL4c showed elevated chimerism (159.2%±39.0) whereas all other groups sat at ~100% (Fig. 5.16C). These data demonstrate that exogenous IL-4 acts directly on Ly6C^{hi} monocytes or their precursors to reduce their frequency in the blood.

5.5.2 Intrinsic IL-4Rα signalling is necessary for loss of Ly6C^{hi} monocytes and increase in Ly6C^{lo} macrophages

Owing to baseline chimerism varying between mice (Fig5.15C) it is routine to normalise tissue monocytes/macrophages to that of blood monocytes in the same animal[91]. Given that IL-4c treatment affected blood chimerism between day 0 and day 3 in KO>WT mice (Fig. 5.16B) I have presented the results from tissue monocytes and macrophages normalised to both day 0 and day 3 blood Ly6C^{hi} monocytes (Fig. 5.17A-D).

When day 3 hepatic Ly6C^{hi} monocyte tissue chimerism was normalised to day 0 chimerism of blood Ly6C^{hi} monocytes, the result suggested there was an accumulation of KO Ly6C^{hi} monocytes in recipients of KO BM when treated with IL-4c (Fig. 5.17A). However, when hepatic Ly6C^{hi} monocyte chimerism on day 3 was normalised to Ly6C^{hi} chimerism in blood at the same timepoint there was no difference in chimerism in KO>WT mice treated with IL-4c (fig, 5.17B). Suggesting loss of Ly6C^{hi} monocytes in the liver merely reflects a process that is also occurring in the blood. Performing the same analysis with Ly6C^{lo} macrophages I observed that only when normalised to the day 3 blood was there any significant change in the normalised chimerism of the recruited Ly6C^{lo} macrophages and that in this setting there was a lower chimerism in the KO>WT mice treated with IL-4c (Fig. 5.17C-D).

The other leukocyte population where I recognised an effect of intrinsic IL-4Rα signalling was in the neutrophils. Here, I saw an increase in chimerism when KO>WT mice were treated with IL-4c (Fig. 5.17E). However, unlike with Ly6C^{hi} monocytes, I did not detect an effect of IL-4c on neutrophil numbers on day 3 in previous experiments. Indeed, only in IL-4c treated KO>WT mice was there an effect on neutrophil number which was related to an increase in the number of KO donor cells (Fig. 5.17F). This suggested that exogenous IL-4 was somehow limiting neutrophil numbers. In a collaborative project with Professor Sarah Walmsley's group we have shown that IL-4Rα-dependent signalling directly inhibits neutrophil survival in the hypoxic lung and a similar mechanism could be behind the reduced number of donor WT neutrophils in acute liver injury (manuscript in press).

Given these complexities, I decided to use a further approach that didn't rely on normalisation to blood Ly6C^{hi} monocytes to analyse the populations where I observed a change, i.e. the IL-4c treated populations (Fig. 5.16A-D). To perform this analysis, I divided the Tim4^{lo} CD11b^{hi} population into host-derived (CD45.1^{+}/.2^{+}) and donor-derived (CD45.2^{+}) cells and assessed the role of intrinsic IL-4Rα signalling in determining the composition of this compartment (Fig. 5.18A). This analysis demonstrated that while donor cells in the WT>WT tissue protected chimeras phenocopied their host-derived counterparts, the composition of the donor cells in the IL4R KO > WT mice differed markedly from their host equivalents. Specifically, the reduction in Ly6C^{hi} monocytes induced by IL4c was absent amongst KO-derived donor cells but present amongst cells derived from WT BM (Fig. 5.18B). Similarly, the concomitant increase in Ly6C^{lo} macrophages observed with IL-4c treatment was only observed in WT-derived cells (Fig. 5.18C). This result confirmed that intrinsic IL-4Rα signalling was indispensable for the observed monocyte/macrophage phenotype in IL-4c treatment.

The tissue protected chimeras also provided the opportunity to verify that the IL-4Rα-dependent proliferation of recruited monocytes/macrophages previously observed was due to intrinsic IL-4Rα signalling. Indeed, when proliferation was compared between host and donor cells there was a significant reduction in proliferation in the donor population in response to CCl_4 + IL-4c only in the KO>WT mice. This was in both the Ly6C^{hi} monocyte and Ly6C^{lo} macrophage populations suggesting that proliferation of both populations in response to IL-4c is dependent on intrinsic IL-4Rα signalling to these cells (Fig. 5.18D-E).

5.5.3 Technical issues with BM chimeric experiments

3 samples were excluded from all live analyses because of issues with the acquisition of events at flow cytometry. 1 sample blocked the flow cytometer and data was therefore lost and 2 samples had <500 live, CD31^{-}, CD45.2^{+} events obtained. It could be that these cells were lost at some point during

the staining process as the number of events acquired from all fixed samples was sufficient. Notably, because the liver samples were excluded from the analysis I have also excluded the paired blood samples from the live analyses. It is important to note that inclusion of these samples in the blood analyses does not alter the results.

5.6 Discussion

In this chapter I have established that the loss of Ly6C^{hi} monocytes occurs early following IL-4c administration and this appears to be a systemic effect, as it occurs in blood as well as liver. Furthermore, I have demonstrated that this loss of Ly6C^{hi} monocytes is dependent on direct IL-4Rα signalling,

5.6.1 Timecourse

The timecourse experiment revealed a lot about the dynamics of monocytes and macrophages, however the heterogeneity in injury between experiments made comparison of injury at each timepoint not possible. It was particularly at the early timepoints that there was a significant difference in ALT between RL048 and RL071 with the former being more reflective of what I had previously observed. Interestingly when one looks at previous publications using acute doses of CCl_4 they report varying levels of ALT at 24 and varying patterns in ALT dynamics. Goh et al. presented data more akin to RL048 with a high ALT at 24 hours that reduces dramatically by 48 hours post CCl_4, however in different experiments in their manuscript they present a wide range of mean ALT values at 24 hours[33]. In contrast, Karlmark published data more in keeping with RL071 whereby ALT levels were persistently elevated at 24 and 48 hours and then reduced by 72 hours[22]. It is therefore difficult to ascertain which experiment is more reflective of previously published data. Both experiments of my timecourse were performed in the same animal unit but there was a gap of 7 months between experiments which could lead to divergence in microbiota and impact my results because it has been shown, particularly in chronic liver injury, that gut microbiota can impact on hepatic response to injury[275,276]. Notably all mice were injected with CCl_4 sequentially and used in the order they were injected meaning that the time from injection to harvest was the same at each timepoint. Furthermore, mice were all sourced from the same in-house breeding stock and were age and sex matched. Owing to the logistics of such a large experiment it was not possible to use mice from different cages at each timepoint and I cannot therefore exclude cage to cage variability as a cause for the differences seen, however, mice from the same litters were spread across timepoints thus reducing variability to a certain extent. For the above reasons it was not possible to pool the results or make any inferences on the effect of IL-4c on indices of injury or regeneration during the timecourse. While it would have been advantageous to repeat this experiment a third time, this was not possible due to time constraints.

Although there were issues with the analysis of indices of injury, the leukocyte dynamics were replicable between experiments and revealed that IL-4c has a significant and early effect in reducing the proportion of Ly6C^{hi} monocytes in IL-4c treated mice, could this mean that the leukocyte dynamics are not related to the serological markers of injury? Data from APAP induced liver injury would suggest that this reduction in Ly6C^{hi} monocytes could contribute to an early reduction in the inflammatory burden in the liver since Ly6C^{hi} monocytes in this context have a pro-inflammatory gene profile[21]. Furthermore, Mossanen et al. and Holt et al. have demonstrated that Ly6C^{hi} monocytes contribute to the hepatotoxicity in APAP in a CCR2-dependent manner[23,145]. The loss of monocytes could also be responsible for other effects observed in the liver, such as the increased presence of neutrophils in mice receiving IL-4c. Indeed, Ly6C^{hi} monocytes are thought to regulate and limit neutrophilia in APAP-induced injury, as well as other inflammatory pathologies, such as *Toxoplasma gondii* infection[277]. Therefore, it is plausible that the early reduction in Ly6C^{hi} monocytes results in an increase in neutrophils[21] in acute liver injury.

While expansion of the Ly6C^{lo} macrophages in response to exogenous IL-4 was a significant feature of previous day 3 analyses, the increase in these cells did not reach statistical significance in my timecourse. Nevertheless, the kinetics of this expansion was altered by IL-4c, with maximal numbers detected at day 3 in recipients of IL-4c and day 4 in their control counterparts. This change in the proportion of Ly6C^{lo} macrophages suggests that IL-4c is promoting a pro-reparative milieu in the liver by increasing the number of what are considered to be pro-reparative Ly6C^{lo} macrophages[21,23,145]. This could be through promoting the direct conversion of Ly6C^{hi} monocytes into Ly6C^{lo} macrophages, which would fit with the current ideas of how these cells are related. However, my timecourse analyses revealed that the monocyte/macrophage kinetics do not support this. Specifically, the early reduction in Ly6C^{hi} monocytes in IL-4c treated mice was not paralleled by an immediate increase in Ly6C^{lo} macrophages, suggesting that these phenomena might not be related.

5.6.2 LysM Cre; IL-4R$\alpha^{fl/-}$

To test the hypothesis that the observed enhanced repair was due to IL-4 signalling to the monocytes and macrophages the myeloid specific LysM Cre; IL-4R$\alpha^{fl/-}$ mouse line would seem to be the most appropriate tool. However, it had already been demonstrated that in response to sterile peritoneal inflammation and *Schistosomiasis* it was inefficient at deleting the IL-4Rα in recruited cells at a gene level[34]. Here I have demonstrated that in response to CCl_4 induced inflammation the deletion of the IL-4Rα at a protein level in the LysM Cre; IL-4R$\alpha^{fl/-}$ mouse line is also inefficient. This could be because during emergency haematopoesis that occurs during inflammation the level of LysM expression in monocytes is insufficient to induce Cre expression. One technical issue encountered was the difficulty in identifying the IL-4Rα^{+} population because IL-4Rα expression is notoriously difficult to identify[121]. This is in part due to the gene dose effect in this model because Cre^{-} cells have only one allele of the IL-4Rα because the mice are bred as IL-4R$\alpha^{fl/-}$.

5.6.3 Characterisation of IL-4Rα$^{-/-}$ > WT BM Chimeric Mice

Given the inefficiency of IL-4Rα deletion in LysM Cre; IL-4Rα$^{fl/-}$ mice, I decided to use whole body tissue irradiation chimeras to establish whether the reduction in Ly6C^{hi} monocytes and increase in Ly6C^{lo} macrophages was dependent on IL-4R signalling in the haematopoietic lineage. Furthermore, by using whole body irradiation and abrogating IL-4R signaling to all BM cells in KO>WT mice, I sought to ascertain whether IL4 responsiveness by haematopoietic cells was required for the improved indices of repair and regeneration observed with IL-4c treatment. The use of whole body tissue irradiation BM chimeras did not allow the selective deletion of the IL-4Rα in circulating monocytes as it affected all BM cells and also resulted in deletion of the IL-4Rα in Kupffer cells due to the radiosensitive nature of a subset of these cells[278]. Looking at indices of injury in this model suggested that signaling to the haematopoietic compartment was dispensable for the reduction of serum markers of injury as IL-4c administration didn't alter ALT or AST significantly when comparing KO>WT versus WT>WT mice. Furthermore when IL-4c and veh treatment were compared in KO>WT mice I observed a significant reduction in both ALT and AST with IL-4c administration suggesting that this was due to signaling to non-BM derived cells. This result is intriguing because although the changes in the monocyte macrophage compartment are dependent on IL-4Ra signaling (discussed below) these changes don't appear to affect indices of injury. This would be in keeping with the work of Goh et al. that suggested that IL-4Ra signaling to hepatocyte was important during injury[33]. Interestingly when comparing IL-4c and veh treatment in WT>WT mice there was no statistically significant reduction in ALT and AST as previously observed which could suggest that the chimeric experimental model is having an effect on the observed phenotype and may therefore also affect the results seen in KO>WT mice. There could be multiple factors accounting for the altered indices of hepatic injury; firstly, these mice have undergone lethal irradiation of their liver which has been shown to induce increased ALT, AST and fibrosis up to 10 weeks following irradiation with 6Gy[279]. The irradiation could therefore affect any phenotype previously observed, furthermore the mice used in this experiment are older than those used in WT experiments (16 weeks-old vs 8 weeks-old) and it has been shown that the effect of acute CCl_4 varies dependent on the age of the mice. Collins et al. demonstrated that with an acute dose of CCl_4 administered by gavage there was a higher peak ALT in 18 month-old mice compared to 6 week-old mice, and they also showed quicker resolution in ALT in 9 month old mice compared to 6 week-old mice[280]. Thus, age could be a factor in the different responses seen in my experiments, although I did not test this experimentally. Notwithstanding the results regarding indices of injury there did appear to be a trend to lower levels of hepatocyte proliferation in IL-4c treated KO>WT mice when compared to WT>WT mice, suggesting signaling within BM-derived cells could be enhancing liver regeneration which has not previously been demonstrated.

Assessment of the necrotic area proved technically difficult but there was no apparent difference in the area of healthy parenchyma. The main difficulty with any analysis was the heterogeneity of the cellular infiltrate in the necrotic area between all four treatments meaning that to differentiate between them was not possible using a computer algorithm. Histopathological assessment of PAS stained sections was also performed by a pathologist blinded to the samples and the results suggested that there was no enhanced repair in the IL-4c treated mice (data not shown).The intriguing result was that visually at least there was an infiltrate in both the WT>WT and KO>WT mice following IL-4c administration which wasn't present in vehicle-treated mice. Hence, it could be that the cells within the necrotic area are in fact neutrophils in the IL-4c treated KO>WT mice because there was a significant increase in their number observed by flow cytometry. In collaboration with Prof. Sarah Walmsley (Centre for Inflammation Research, University of Edinburgh) we have shown that IL-4 abrogates the prolonged neutrophil survival normally induced by hypoxia both *in vitro* and *in vivo* in liver and lung (manuscript in press). This could be important because the IL-4Rα$^{-/-}$ neutrophils may persist at the site of injury and promote repair. While contrary to the classical view of neutrophils, recent work has described how neutrophils can participate in tissue repair by dismantling damaged blood vessels and orchestrating neoangiogenesis, at least in a setting of thermal injury[281]. Regrettably, there is no validated staining protocol for neutrophils on paraffin embedded sections in liver and I did not obtain fresh frozen samples during these experiments making further interrogation of the cells in the necrotic area difficult.

5.6.4 Effect of IL-4Rα on monocyte/macrophage dynamics

It was intriguing to see that in the tissue IL-4c induced proliferation of the Ly6C^{hi} monocytes. It has been previously shown that monocyte precursors in BM are in cell cycle, whereas only a very small fraction of mature monocytes show signs of proliferation under normal physiological conditions[74,86]. To the best of my knowledge, it has not been previously reported that these cells proliferate in tissue in response to IL-4c stimulation[121]. I also demonstrated using whole body irradiation chimeras that this proliferation was dependent on IL-4R signalling to these cells. Notably, these proliferating cells were evenly distributed in the Ly6C^{hi} monocyte population and did not represent a subset of cells that had acquired characteristics of recruited macrophages but not yet downregulated Ly6C, suggesting they were bona fide proliferating monocytes. All previous work investigating the proliferative effect of IL-4c in tissues has focused on mature macrophages and not monocytes[121,123,206]. Importantly, this behaviour was not seen in Ly6C^{hi} monocytes in blood (data not shown) suggesting that while phenotypically identical, monocytes in tissue have different responsiveness to growth factors etc. Indeed, newly arrived monocytes in other tissues, such as the gut mucosa and dermis have been shown to be transcriptionally distinct from their phenotypic counterparts in blood[97,282]. Moreover, it could reflect that for monocytes to proliferate they must receive a co-factor along with IL-4, which could be absent from the circulation.

What is more intriguing is that whilst these cells are proliferating there is also a reduction in their number in tissue, which is dependent on intrinsic IL-4Rα signalling. It could be that in addition to proliferating, these cells are also converting into Ly6C^{lo} macrophages more quickly. This would fit with my results as I demonstrated an IL-4Rα dependent increase in Ly6C^{lo} macrophages. Indeed it is thought IL-4Rα dependent recruitment of Ly6C^{hi} monocytes and conversion into Ly6C^{lo} macrophages is important for the repair process in Schistosomiasis[204]. Furthermore, a large body of research has reported on the importance of IL-4Rα signaling in the conversion of Ly6C^{lo} macrophages from a type 1 to a type 2 immune phenotype, but the question of whether IL-4 causes conversion of Ly6C^{hi} monocytes to Ly6C^{lo} macrophages has not been adequately addressed[30,185,208]. For instance, although it been suggested that IL-4c promotes this process in the context of thioglycolate-induced peritonitis[203], it was not formally shown that IL-4c specifically drove enhanced conversion of Ly6C^{hi} monocytes to Ly6C^{lo} macrophages. Given this body of evidence I was interested in whether IL-4c was enhancing conversion of Ly6C^{hi} monocytes into Ly6C^{lo} macrophages. If this were the case, one would expect to see that the IL-4c induced reduction in Ly6C^{hi} monocytes coincided with a concomitant increase in Ly6C^{lo} macrophages. However, I observed that there was an early loss of Ly6C^{hi} monocytes in the IL-4c group that occurred on day 2, whereas Ly6C^{lo} macrophage expansion was most prominent on day 3 and this was associated with elevated levels of proliferation. In conjunction, these results suggest that IL-4c may be having effects other than enhancing conversion of Ly6C^{hi} monocytes into Ly6C^{lo} macrophages. Indeed as with the work of others, IL-4c induced proliferation in Ly6C^{lo} macrophages that was dependent on intrinsic IL-4Rα signaling[121,203,206]. It therefore remains possible that IL-4c is having an independent and not yet appreciated effect on Ly6C^{hi}

monocytes to reduce their number in tissue and, at the same time, increasing the number of Ly6C^{lo} macrophages through proliferation.

The suggestion that IL-4c may be having direct effects on Ly6C^{hi} monocytes or their precursors in the BM was reinforced by the results from the blood where it caused a reduction in the proportion of circulating Ly6C^{hi} monocytes before they entered the tissue. Furthermore, the tissue protected chimeras enabled me to identify that this reduction was dependent on intrinsic IL-4Rα signaling on Ly6C^{hi} monocytes before they enter the liver. By normalizing the chimerism of day 3 tissue Ly6C^{hi} monocytes to day 3 blood Ly6C^{hi} monocytes revealed equivalent reduction in chimerism of both blood and tissue Ly6C^{hi} monocytes at day 3. Thus, this suggests that IL-4Rα signaling on monocytes was not affecting monocyte recruitment to the injured liver in IL-4c treatment. I can come to this conclusion because Ly6C^{hi} monocytes in tissue are directly recruited from the blood during injury[21] and if IL-4c treatment had any cell-intrinsic effect on recruitment to the tissue, Ly6C^{hi} monocyte chimerism in KO>WT mice it should differ from that in blood, however the normalized chimerism was not significantly different to other groups.

In the following chapters I will attempt to address at what point of monocyte development and/or differentiation that IL-4 affects in context of acute liver injury and the potential mechanisms involved.

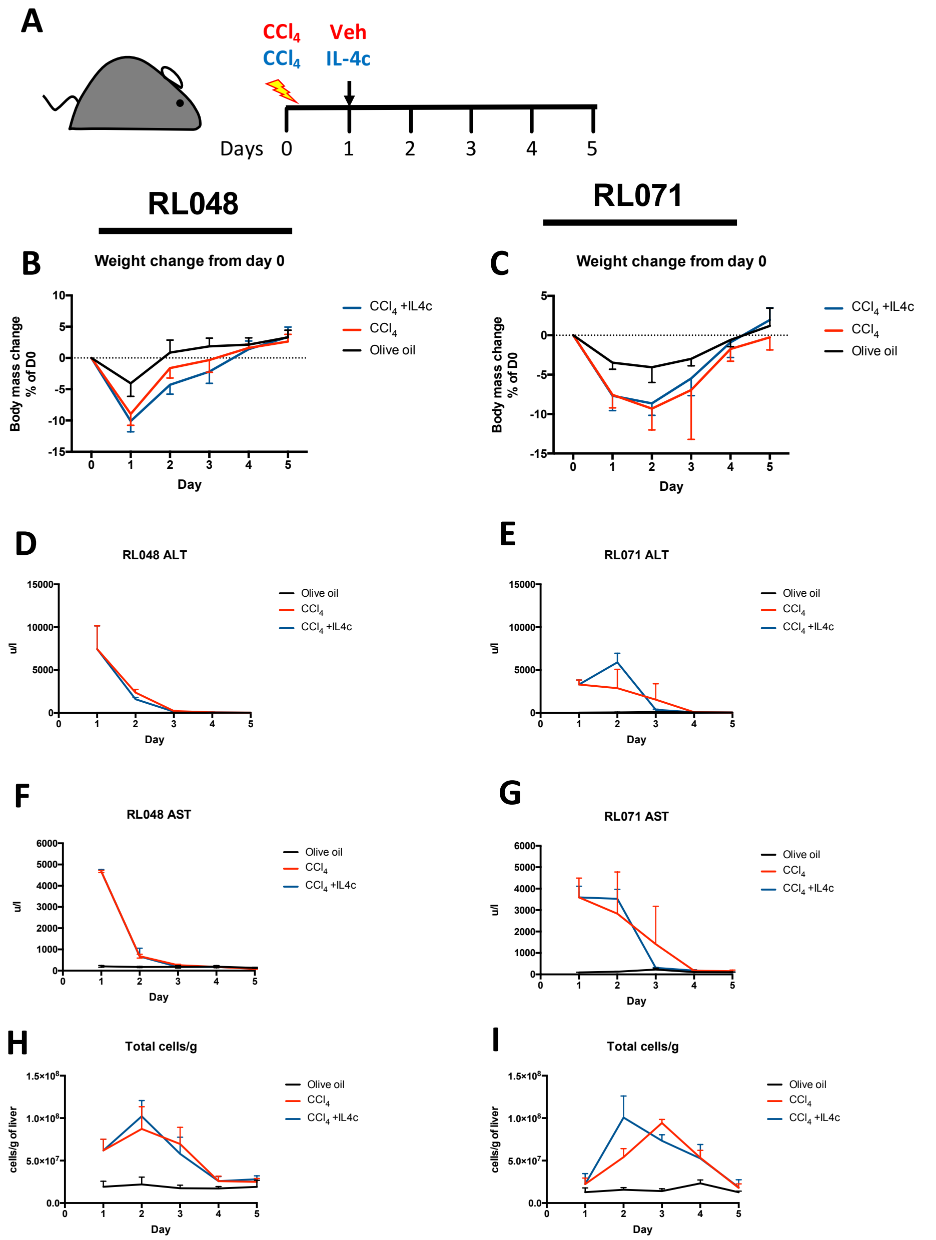

Figure 5-1 Phenotypic analysis of timecourse.

(A) Schematic of experimental model mice. Mice were injected i.p. with 1mg BrdU 2 hrs before necropsy. (B-C) Weight change from baseline in RL048 (B) and RL071 (C). (D-G) Levels of ALT (D-E) and AST (F-G) present in serum of mice at days 1-5 after being administered olive oil, CCl_4 or CCl_4 +IL4-c on day 0 from experiments RL048 and RL071. (H-I) Total numbers of liver leukocytes obtained from mice at days 1-5 after being administered olive oil, CCl_4 or CCl_4 +IL4-c on day 0 from experiments RL048 and RL071. N=3 at each timepoint apart from day 3 RL071 CCl_4 + IL-4c where one sample was excluded. Mean ± SD (one-way ANOVA).

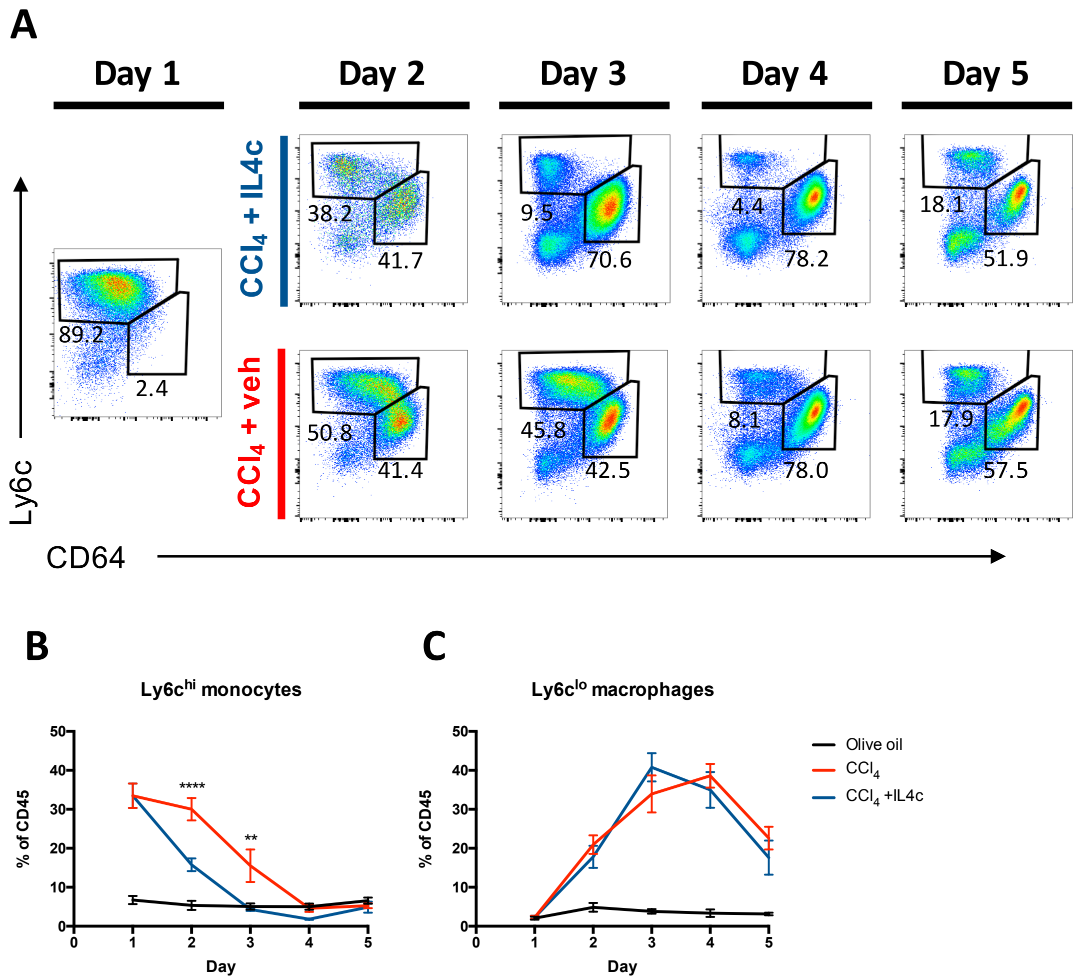

Figure 5-2 Recruited monocyte/macrophage dynamics over time.

(A) Representative Ly6C and CD64 expression by live (7AAD$^-$) CD31$^-$ CD45$^+$ Lin$^-$ Tim4^{lo} CD11b^{hi} single liver cells from mice treated with CCl_4 + veh or CCl_4 + IL-4c at d0. (B-C) Recruited hepatic Ly6C^{hi} CD64^{lo} monocytes and Ly6C^{lo} CD64^{hi} macrophages as a proportion of CD45$^+$ cells at each timepoint. N=5-6 mice/group pooled from 2 independent experiments, mean ± SD (CCl_4 + veh and CCl_4 + IL-4c compared using multiple *t* tests with Holm-Sidak correction).

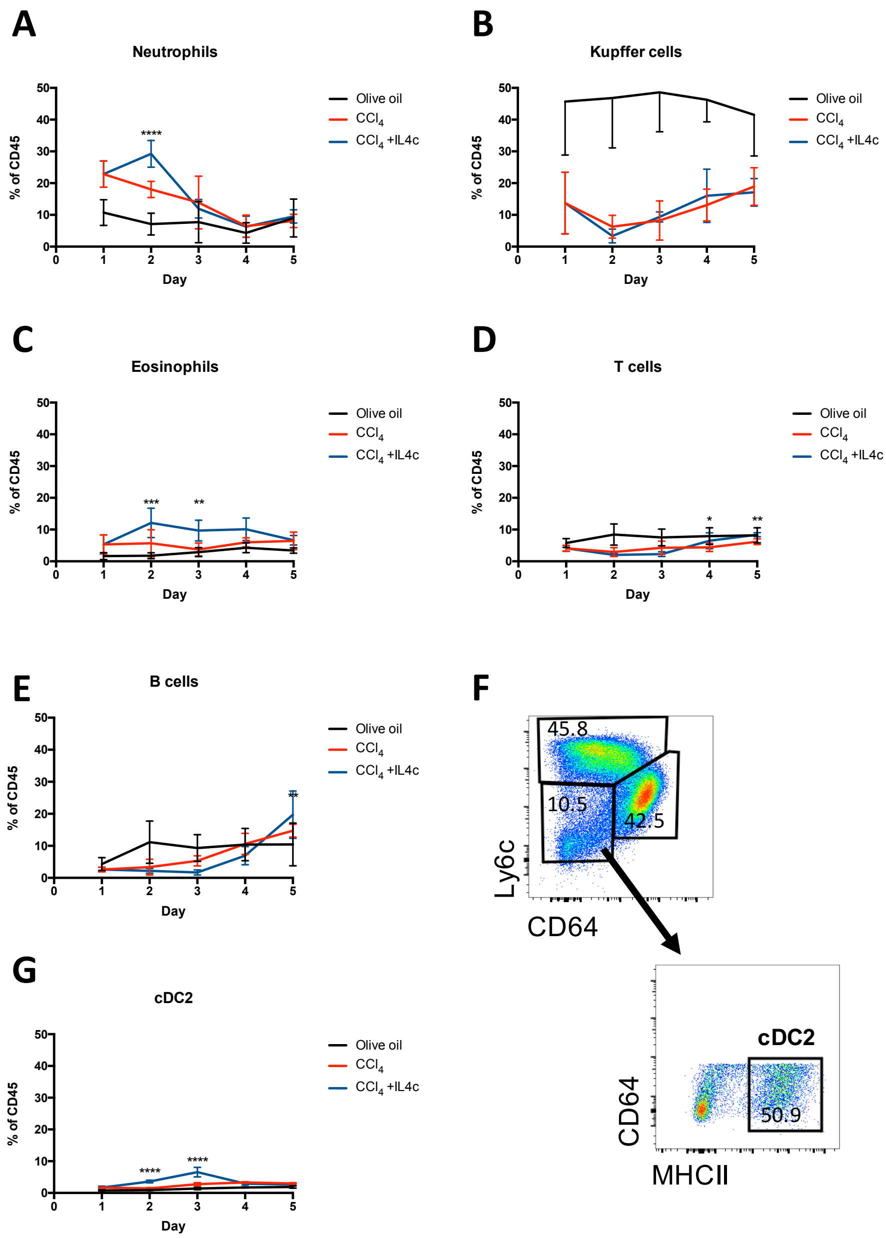

Figure 5-3 Hepatic leukocyte dynamics over time.

(A-E) Frequency of liver neutrophils (A), Kupffer cells (Tim4^{hi} CD11b^{lo}; B), eosinophils (C), T cells (D) and B cells (E) of CD45^{+} cells from mice at days 1-5 after being administered olive oil, CC_{l4} or CCl_4 +IL4-c on day 0. (F) Representative expression of Ly6C and CD64 by Live (7AAD^{-}) single CD31^{-}CD45^{+}Lin^{-} Tim4^{-}CD11b^{hi} liver cells (left) and expression of MHCII by Ly6C^{-}CD64^{-} cells (right) from a mouse given CCl_4+vehicle 3 days earlier. (G) Frequency of liver cDC2 of CD45^{+} cells from mice at days 1-5. N=5-6 mice/group pooled from 2 independent experiments, mean ± SD (CCl_4 + veh and CCl_4 + IL-4c compared using Students *t* tests with Holm-Sidak correction).

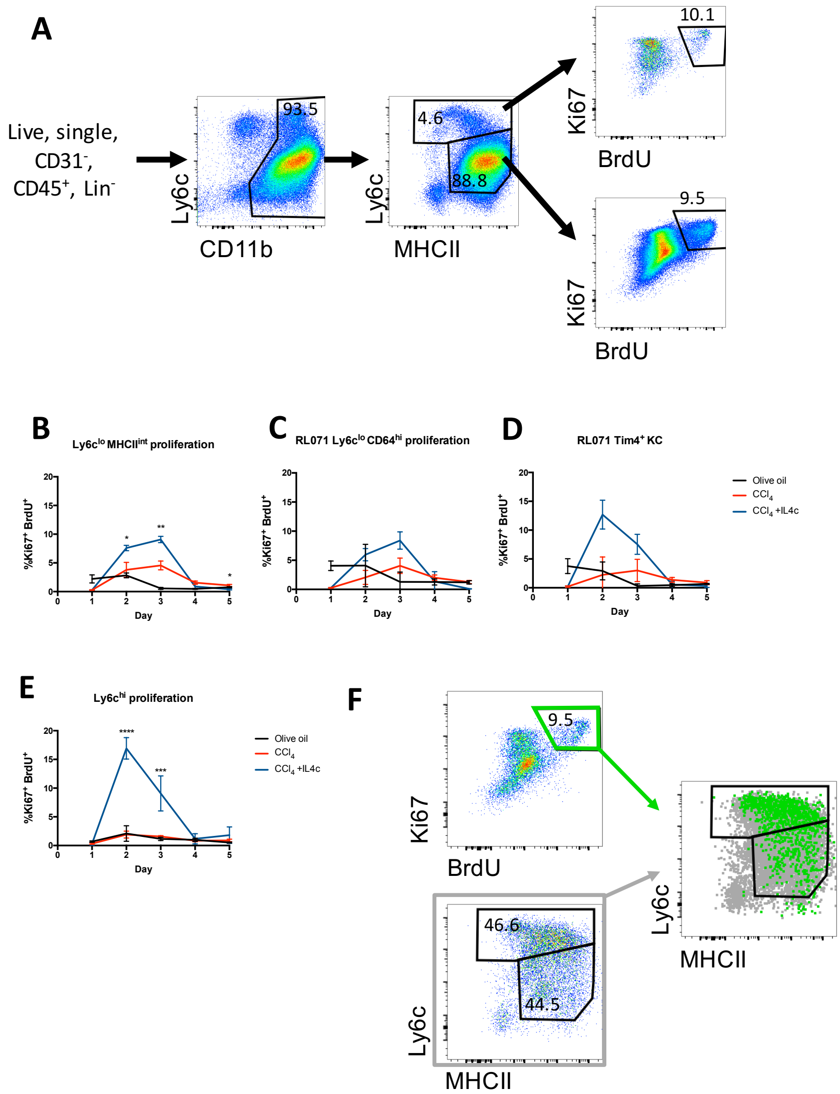

Figure 5-4 Proliferation in recruited monocytes/macrophages over time.

(A) Gating used in fixed samples to identify CD11b+ cells from Live, single, CD31−, CD45+, Lin− cells. Monocytes identified as the Ly6Chi population. KC and recruited macrophages are identified as Ly6Clo MHCIIint cells. Within both these populations proliferating cells are identified as Ki67+ BrdU+. (B) pooled proliferation of KC and recruited macrophages. (C) Ly6Clo CD64hi recruited macrophage proliferation (Live, single, CD31−, CD45+, Lin-, Tim4lo, CD11bhi) from RL071. (D) Tim4+ KC proliferation (Live, single, CD31−, CD45+, Lin-, Tim4hi, CD11lo) from RL071. (E) Recruited Ly6Chi monocyte proliferation. N=5-6 mice/group pooled from 2 independent experiments in (B) & (E). N=2-3 in (C) & (D), mean ± SD (CCl4 + veh and CCl4 + IL-4c compared using multiple T tests with Holm-Sidak correction). (F) Back gating of all proliferating CD11bhi cells onto CD11bhi population as identified in (A).

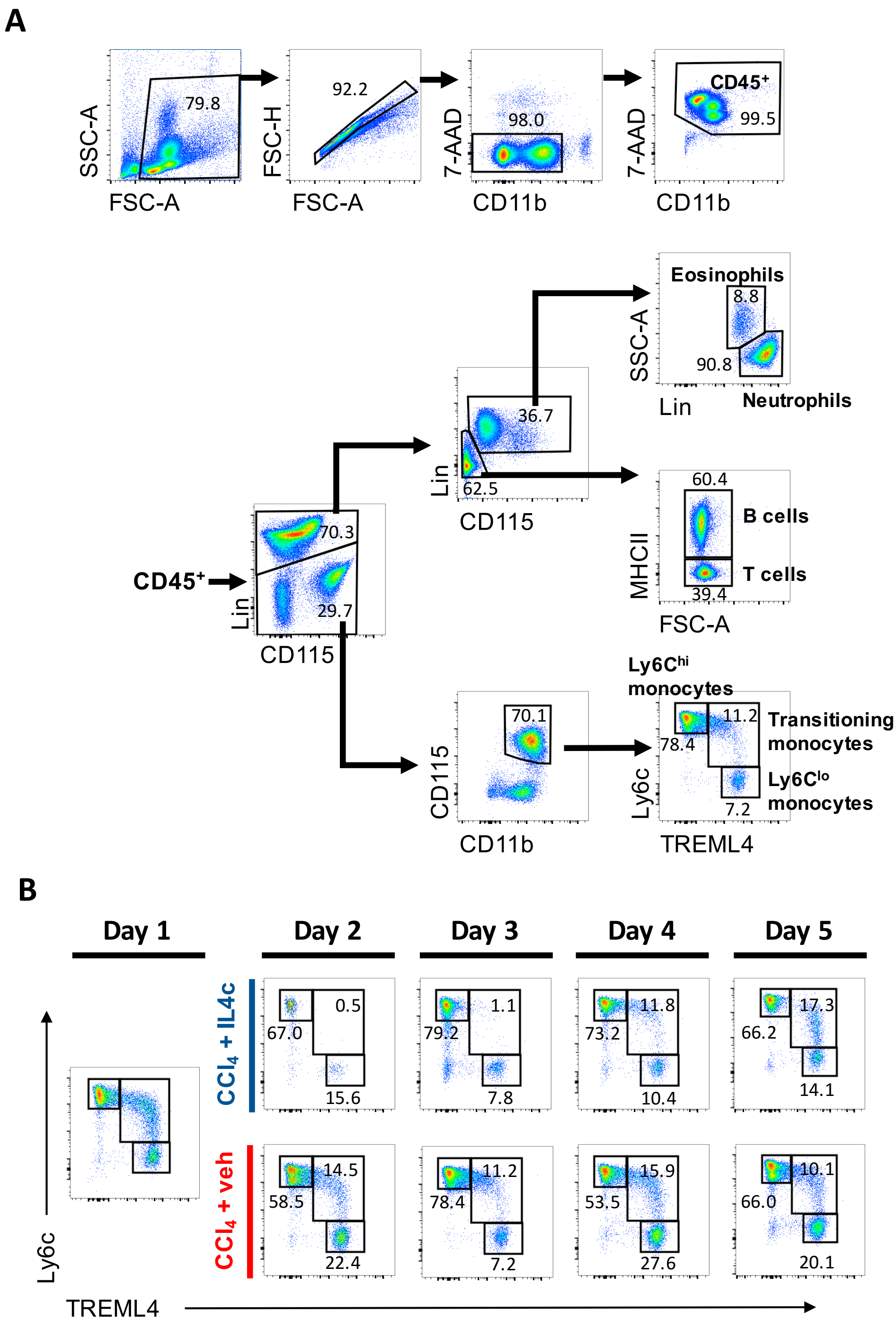

Figure 5-5 Monocytes in blood over time.

(A) Identification of leukocyte populations in blood from a CCl_4 + veh mouse. Lineage gate comprises CD3, CD19, Ly6G and Siglec F. (B) Representative Ly6C and TREML4 expression by single, Live (7AAD), $CD45^+$, Lin^-, $CD11b^{hi}$, $CD115^{hi}$ blood monocytes from CCl_4 + veh and CCl_4 + IL-4c groups at each timepoint.

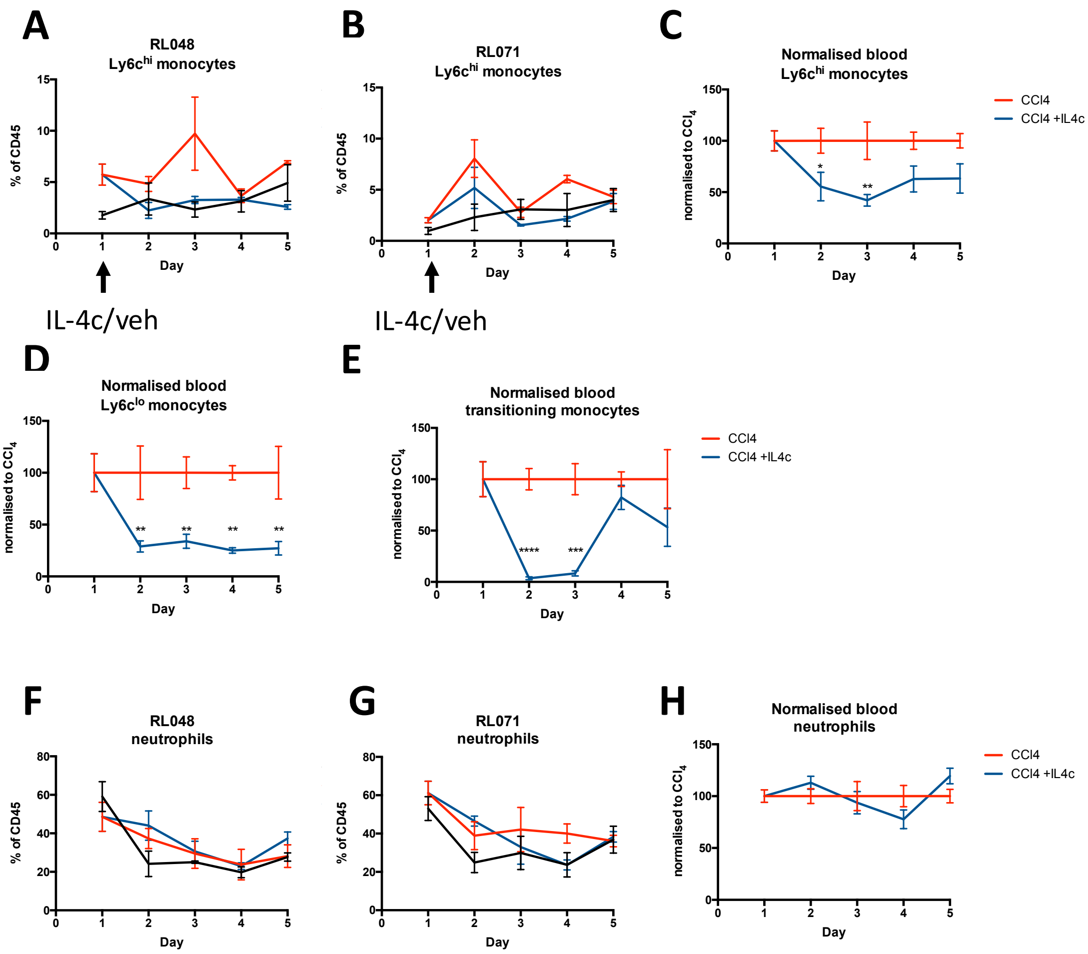

Figure 5-6 Blood monocyte and neutrophil dynamics over time.

IL-4c or veh administered on day 1 (A-B) Proportion of Ly6C^{hi} monocytes in blood over time in RL048 and RL071. (C-D) Pooled proportion of Ly6C^{hi}, Ly6C^{lo} and transitioning blood monocytes normalised to CCl_4 + veh group. Each sample was normalised to the mean proportion of CD45 cells in the CCl_4 + veh group on that day. (F-G) Proportion of neutrophils in blood over time in RL048 and RL071. (H) Pooled proportion of neutrophils normalised to CCl_4 + veh group. Each sample was normalised to the mean proportion of CD45 cells in the CCl_4 + veh group on that day. N=3 mice/group in RL048, n=2-3 mice/group in RL071 and n=5-6 mice/group in pooled samples; mean ± SD (CCl4 + veh and CCl4 + IL-4c compared using multiple T tests with Holm-Sidak correction).

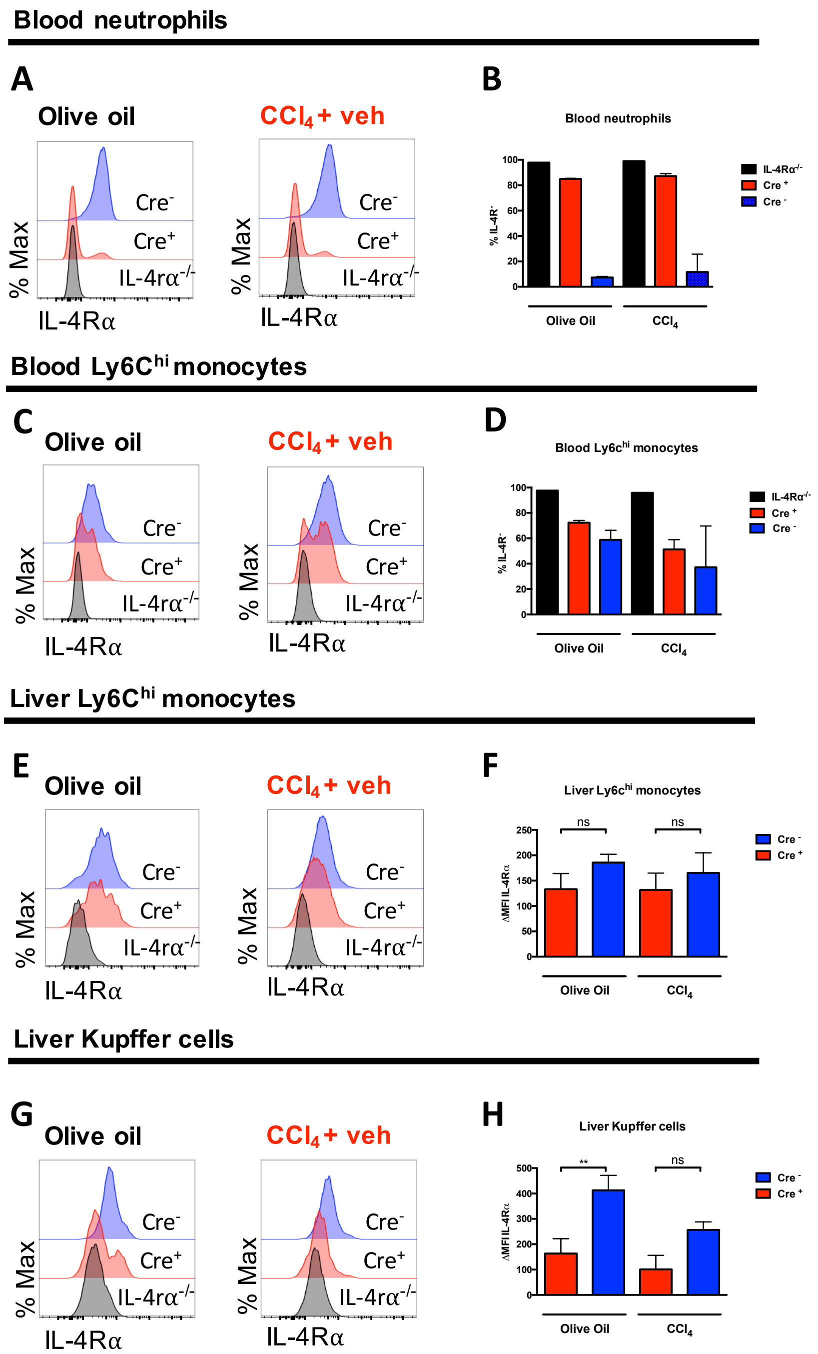

Figure 5-7 Assessment of LysM Cre; IL-4Rα$^{fl/-}$ mice in CCl4 injury.

(A,C,E,G) Representative histograms of IL-4Rα expression in outlined cells from olive oil and CCl_4 + veh treated mice. (B & D) Proportion of IL-4R^{-} blood cells by treatment group. (F & H) Comparison of delta MFI of blood neutrophils calculated using IL-4Rα$^{-/-}$ for each treatment group. N=3 mice/group in Cre^{+} and CRE^{-}, n=1 in IL-4Rα$^{-/-}$ controls; mean ± SD (one-way ANOVA).

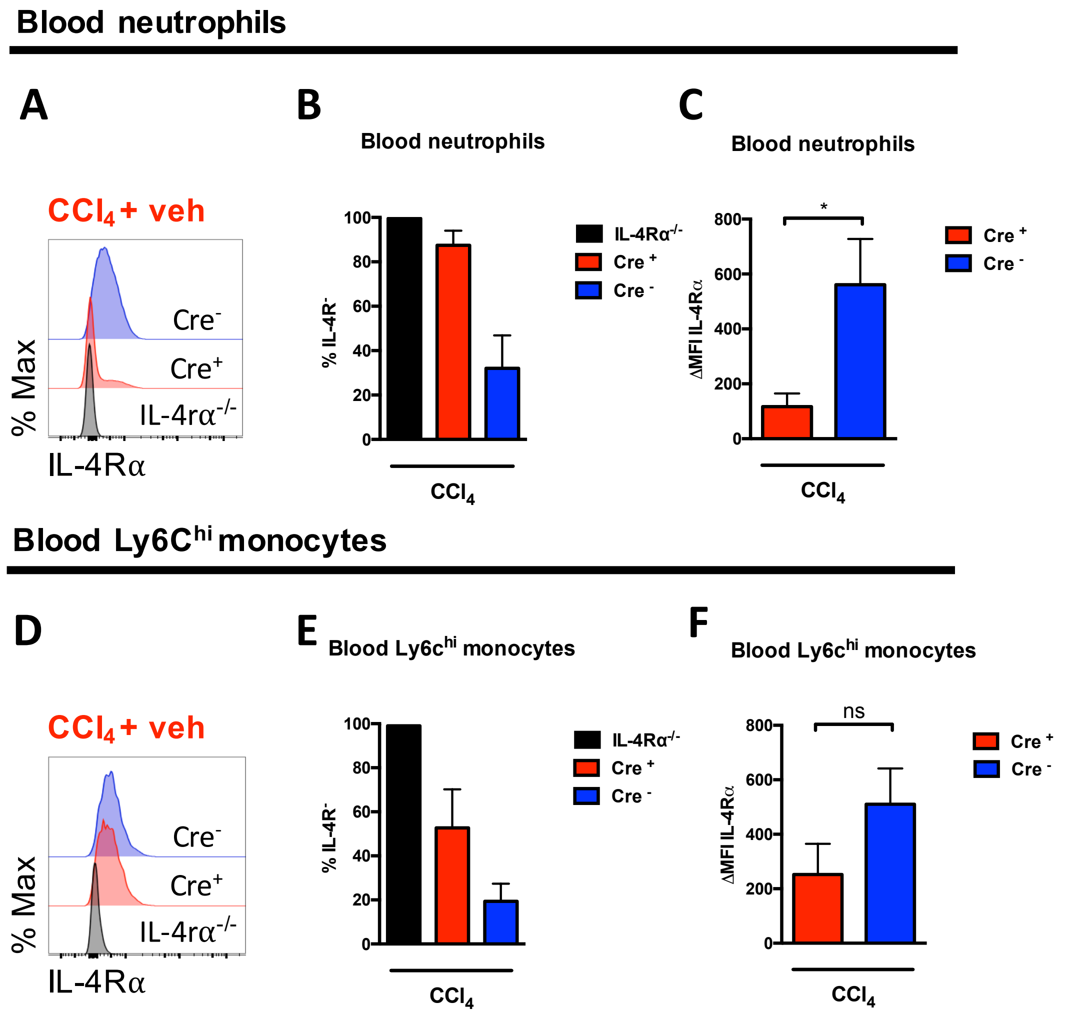

Figure 5-8 Analysis of relevant monocytes and macrophages in LysM Cre; IL-4Rα$^{fl/–}$ mice following CCl_4 injury alone.

(A&D) Representative histograms of IL-4Rα expression in blood neutrophils and Ly6C^{hi} monocytes from CCl_4 treated mice. (B & E) Proportion of IL-4R^{-} blood neutrophils and Ly6C^{hi} monocytes (C & F) Delta MFI of blood neutrophils and Ly6C^{hi} monocytes calculated using IL-4Rα$^{-/-}$. (C-D) N=3 mice/group in Cre^{+} and CRE^{-}, N=1 in IL-4Rα$^{-/-}$ controls; mean ± SD (unpaired T test).

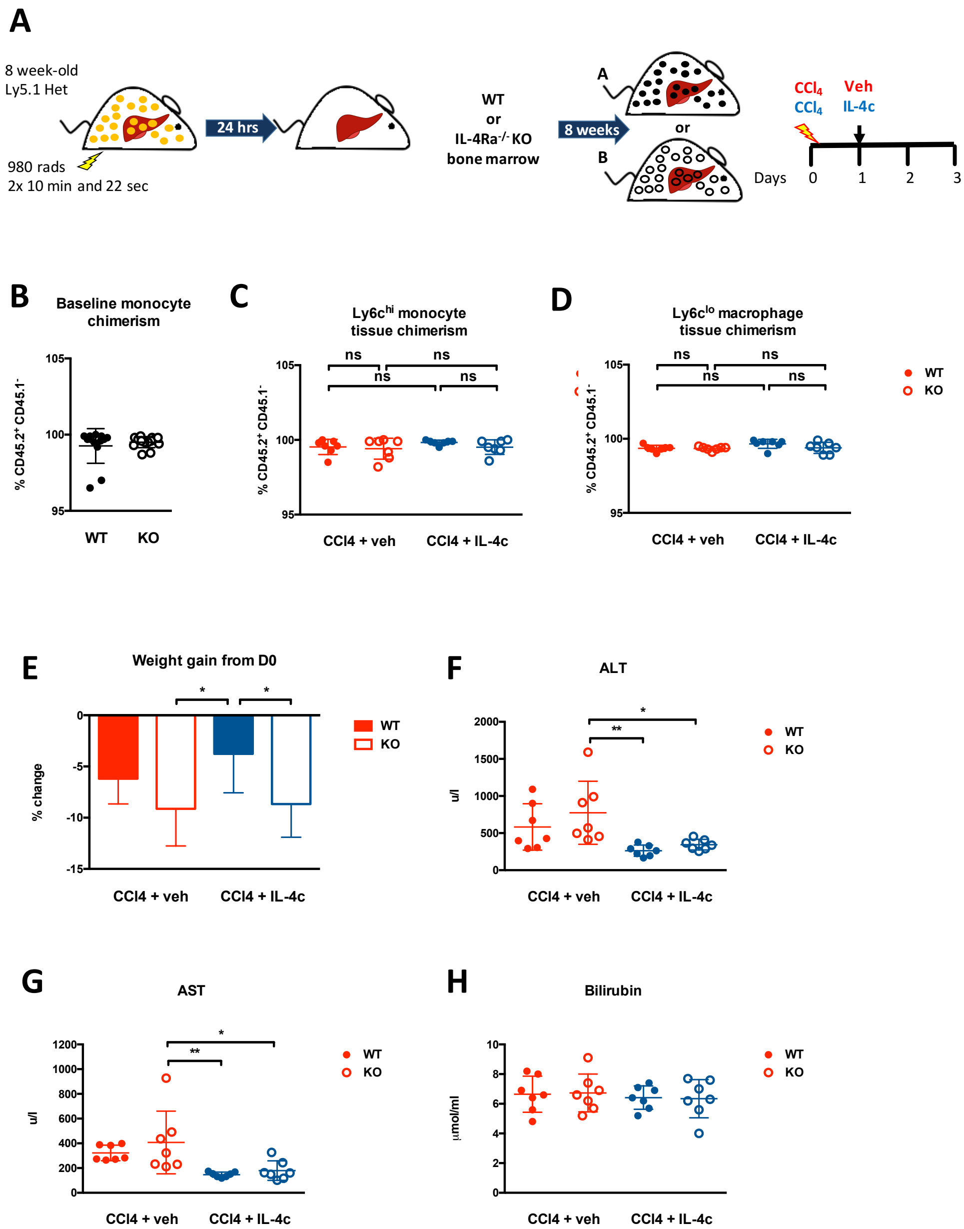

Figure 5-9 Phenotypic assessment of whole body irradiation chimeras.

(A) Schematic representation of whole body irradiation chimeras. Ly5.1 mice were irradiated with a total of 980 rads and reconstituted 24 hours later with either wild-type (WT) CD45.2 or knock-out (KO) IL-4Rα$^{-/-}$ bone marrow via tail vein injection. (B) Baseline Ly6C^{hi} monocyte chimerism in blood on day 0. (C-D) Chimerism of recruited Ly6C^{hi} CD64^{lo} monocytes and Ly6C^{lo} CD64^{hi} macrophages in liver on day 3. (E) Weight change from baseline in WT and KO recipient mice treated with CCl_4 + veh (red) or CCl_4 + IL-4c (blue). (F-H) Serum markers of liver injury (ALT, AST and bilirubin) in the same groups. N=7 mice/group, pooled from 2 independent experiments; mean ± SD (one-way ANOVA).

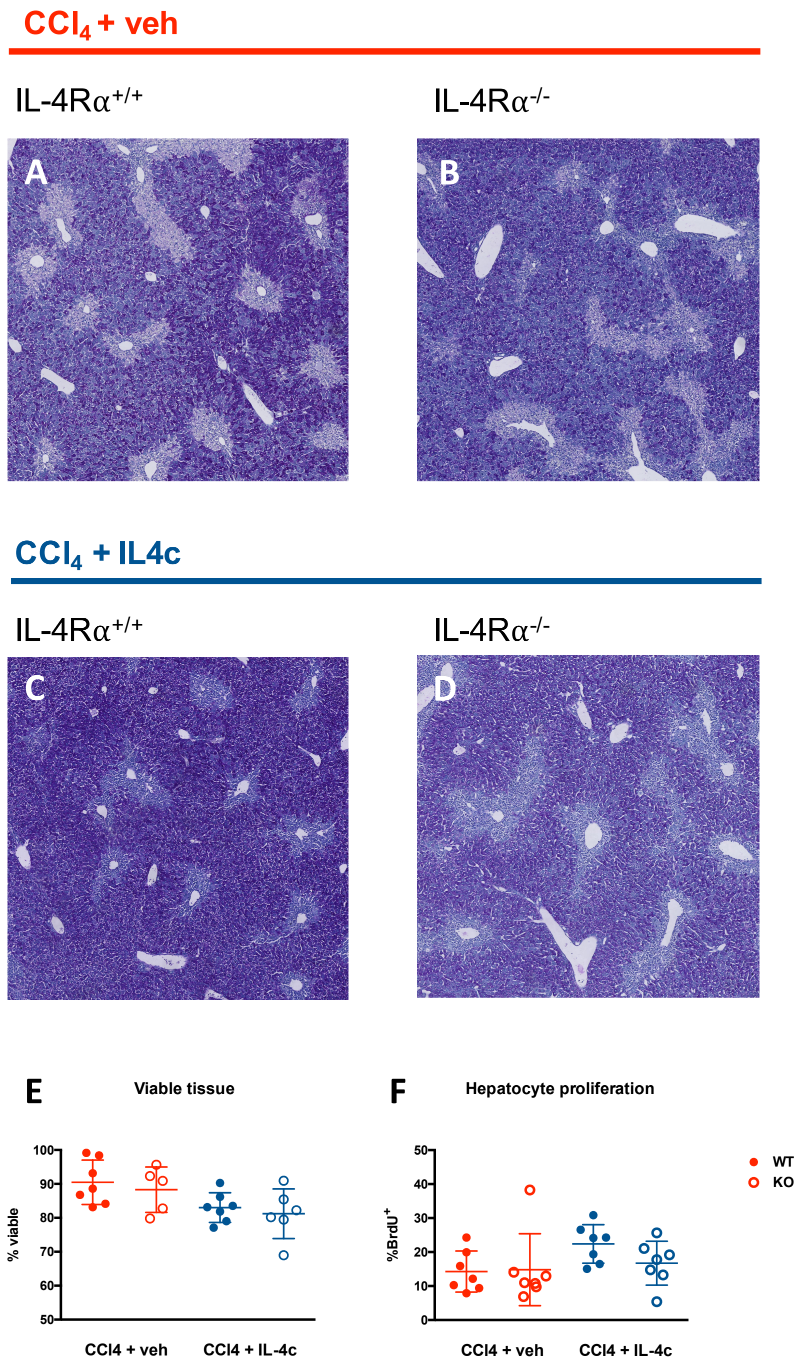

Figure 5-10 Necrotic cell area and proliferation in chimeric mice.

(A-D) 5x representative images from PAS stained sections from the various treatment groups. (E) quantification of necrotic area including cellular infiltrate. (F) Hepatocyte proliferation as quantified by proportion of BrdU^{+} hepatocytes.

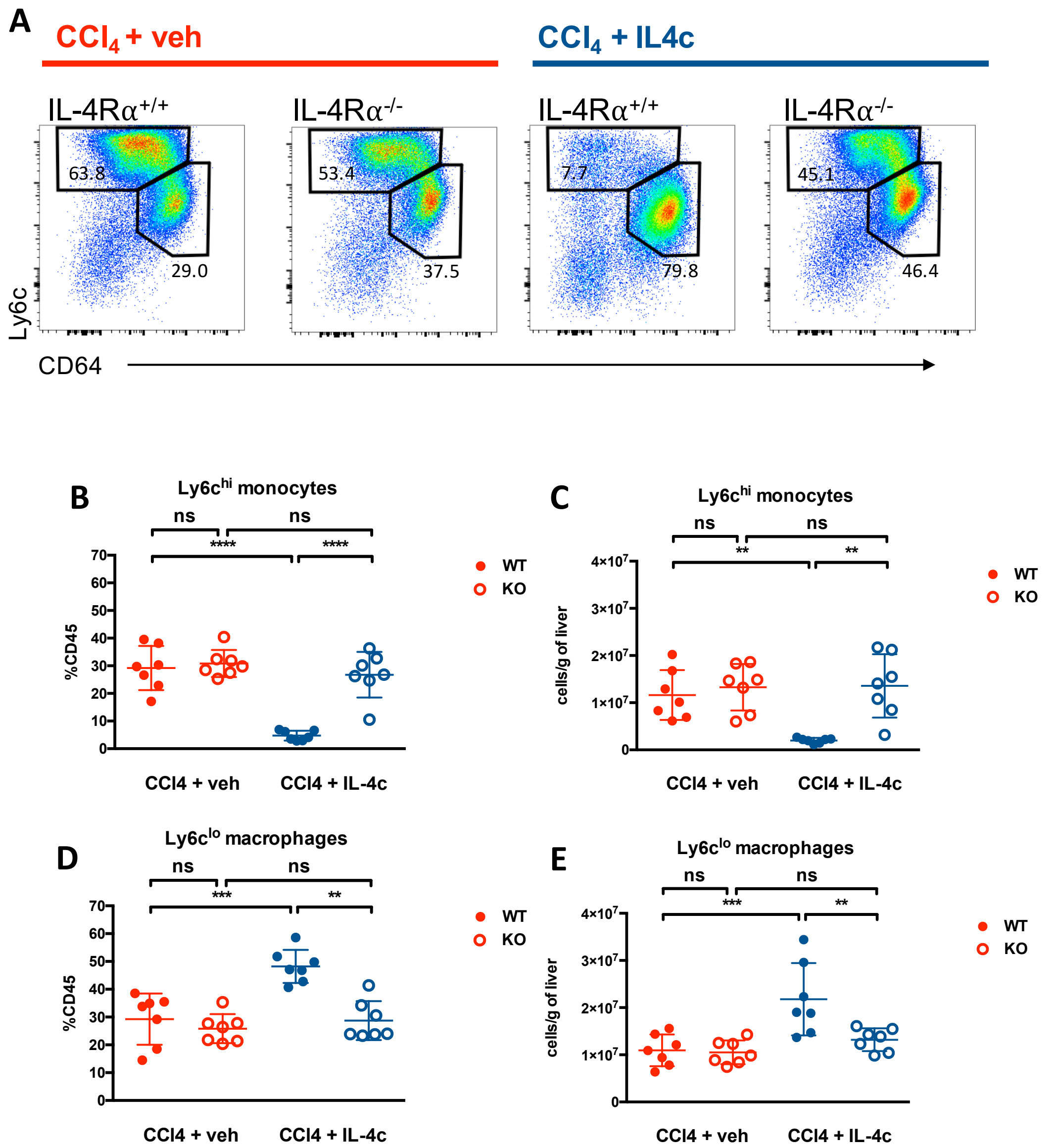

Figure 5-11 Recruited monocyte/macrophage dynamics in chimeric mice.

(A) Representative expression of Ly6C and CD64 by recruited Live (7AAD), single, $CD31^-$, $CD45^+$, Lin^-, $F4/80^{lo}$, $CD11b^{hi}$ cells from WT and KO recipients in CCl_4 + veh and CCl_4 + IL-4c groups. (B-C) Proportion of $CD45^+$ cells and number of cells/g of liver for recruited $Ly6C^{hi}$ $CD64^{lo}$ monocytes. (D-E) Proportion of $CD45^+$ cells and number of cells/g of liver for recruited $Ly6C^{lo}$ $CD64^{hi}$ macrophages. N=7 mice/group, pooled from 2 independent experiments; mean ± SD (one-way ANOVA).

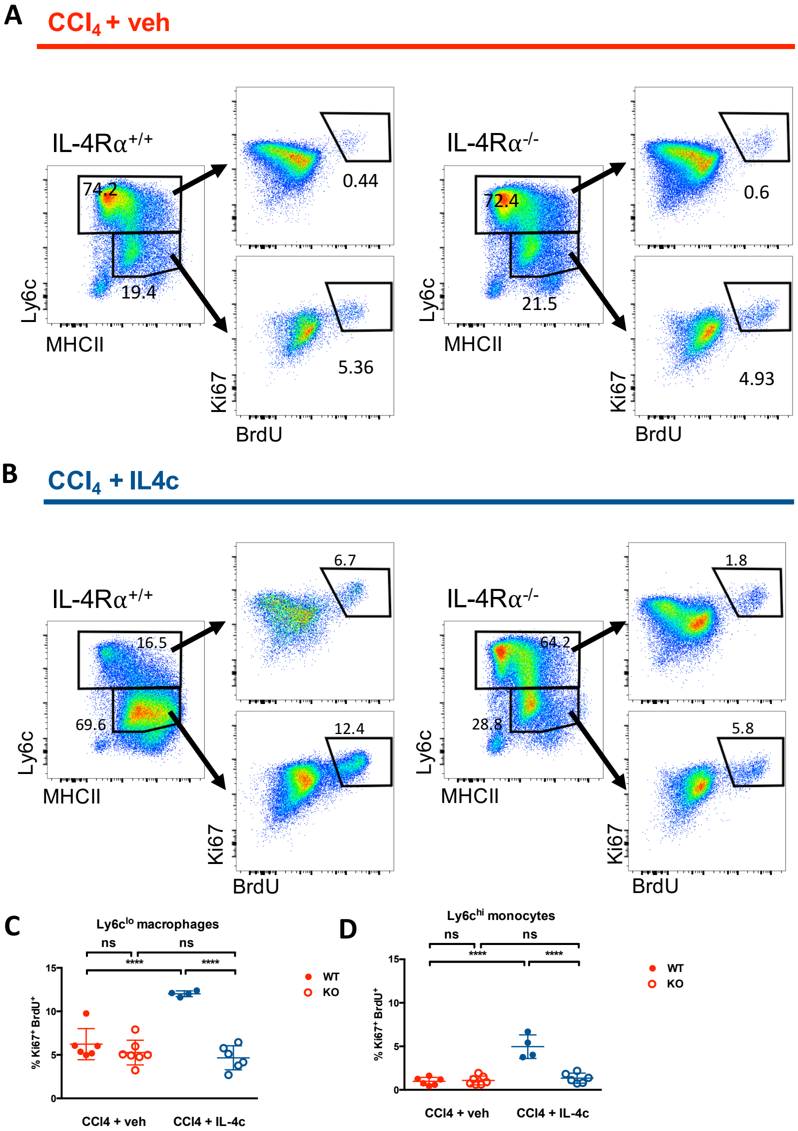

Figure 5-12 Recruited monocyte/macrophage proliferation in chimeric mice.

(A) Representative plots of Live (FVD), single, CD31⁻, CD45⁺, Lin⁻, F4/80^{lo}, CD11b^{hi} cells from both WT and KO recipients treated with CCl_4 + veh. Ly6C^{hi} monocyte and Ly6C^{lo} MHCII^{int} macrophage proliferation identified by Ki67 and BrdU staining. (B) The same plots as (A) but for CCl4 + IL-4c treated mice. (C) Proportion of proliferating Ly6C^{lo} MHCII^{int} macrophages. (D) Proportion of proliferating Ly6C^{hi} monocytes. N=4-7 mice/group, pooled from 2 independent experiments; mean ± SD (one-way ANOVA). 4 mice excluded from proliferation analysis due to a technical issue as no BrdU incorporation could be detected in any leukocyte or non-leukocyte compartment.

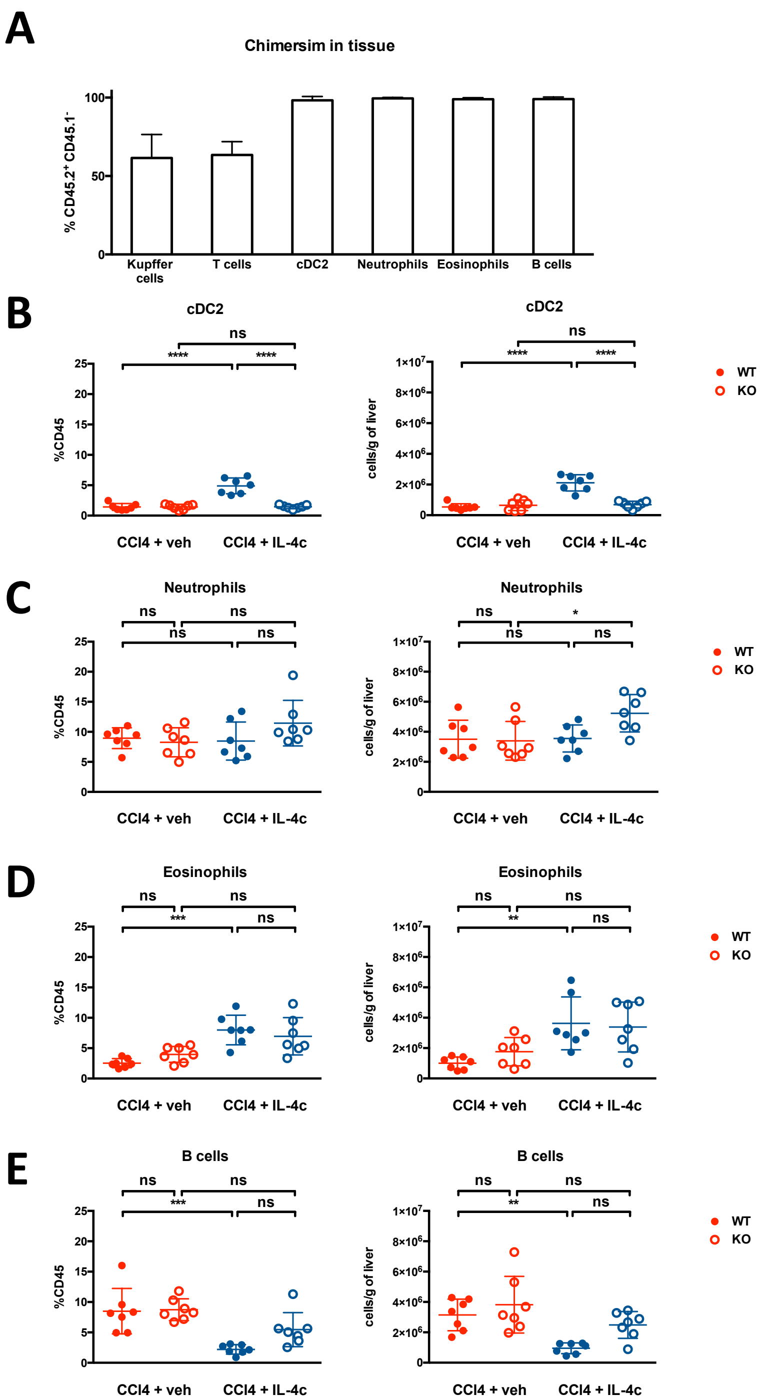

Figure 5-13 Changes in other fully chimeric leukocyte populations.

(A) Liver tissue chimerism of leukocyte populations, Kupffer cells defined as F4/80^{hi} CD11b^{lo}, all treatments pooled together. (B-E) Comparison of proportion of CD45 cells and total cell number/g of liver for populations that are completely chimeric in liver tissue. N=7 mice/group; mean ± SD (one-way ANOVA).

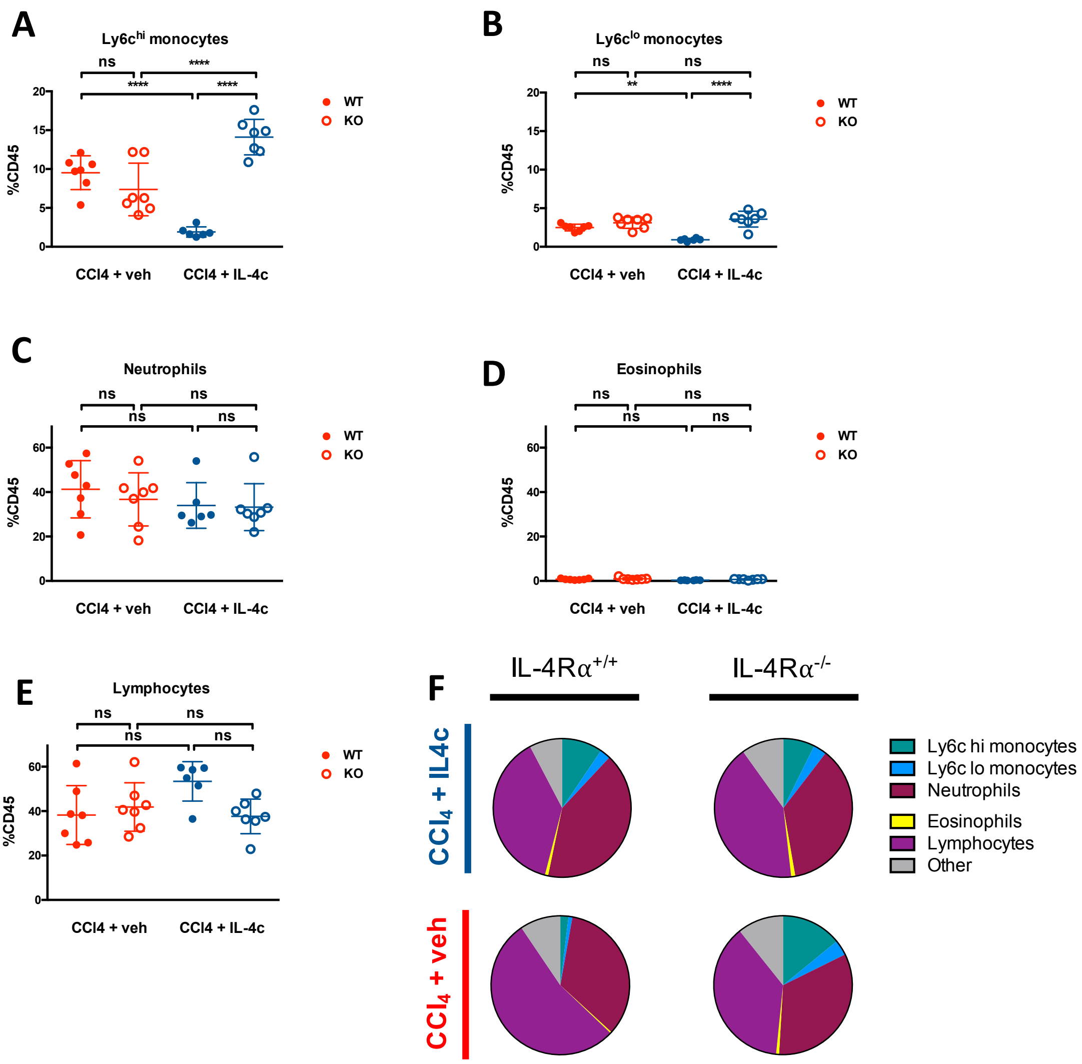

Figure 5-14 Changes in leukocytes in blood in chimeric mice.

(A-E) Comparison of proportion of $CD45^+$ blood leukocytes between treatment and recipient BM groups. Monocytes defined using Ly6C and FSC-A as TREML not used. (F) Parts of a whole for all leukocytes in blood depending on treatment and donor BM. N=7 mice/group; mean ± SD (one-way ANOVA).

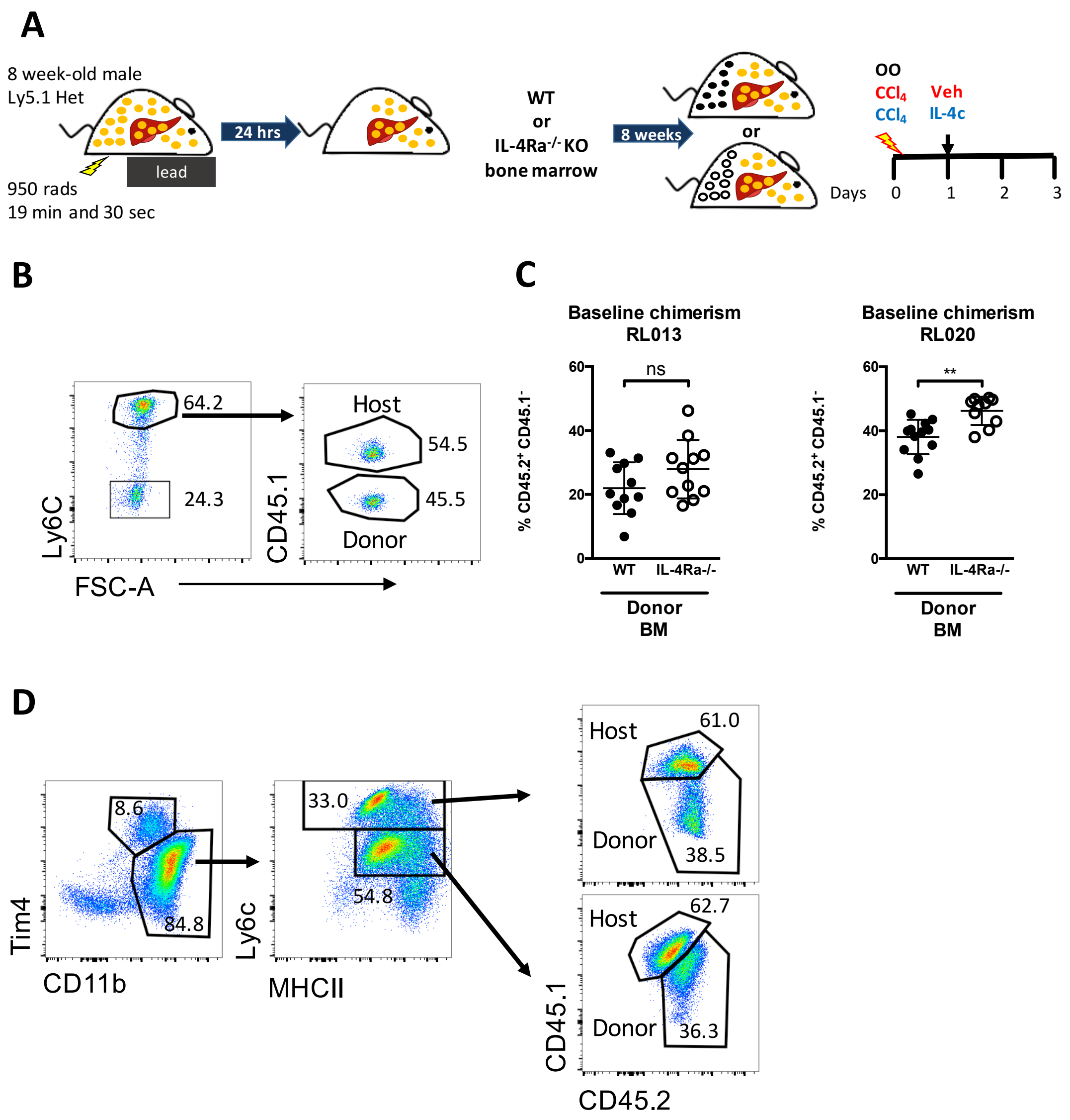

Figure 5-15 Tissue protected irradiation chimeras.

(A) Schematic representation of tissue protected irradiation chimeras. (B) Identification of donor and host cells in blood: Live (Aqua), single, CD45.2$^+$, Lin$^-$, Ly6C^{hi} monocytes from KO>WT mouse in RL020. (C) Baseline chimerism in circulating Ly6C^{hi} monocytes in RL013 and RL020. (D) Identification of host and donor cells in recruited cell population (Live (Aqua), single, CD31$^-$, CD45.2$^+$, Lin$^-$, Tim4^{lo}, CD11b^{hi}). Host (CD45.1$^+$ CD45.2$^+$) and donor (CD45.1$^-$ CD45.2$^+$) cells can be identified in recruited Ly6c^{hi} monocytes and Ly6c^{lo} MHCII^{int} macrophages by expression of CD45.1 and CD45.2. N=10-12 mice/group; mean ± SD (unpaired t test).

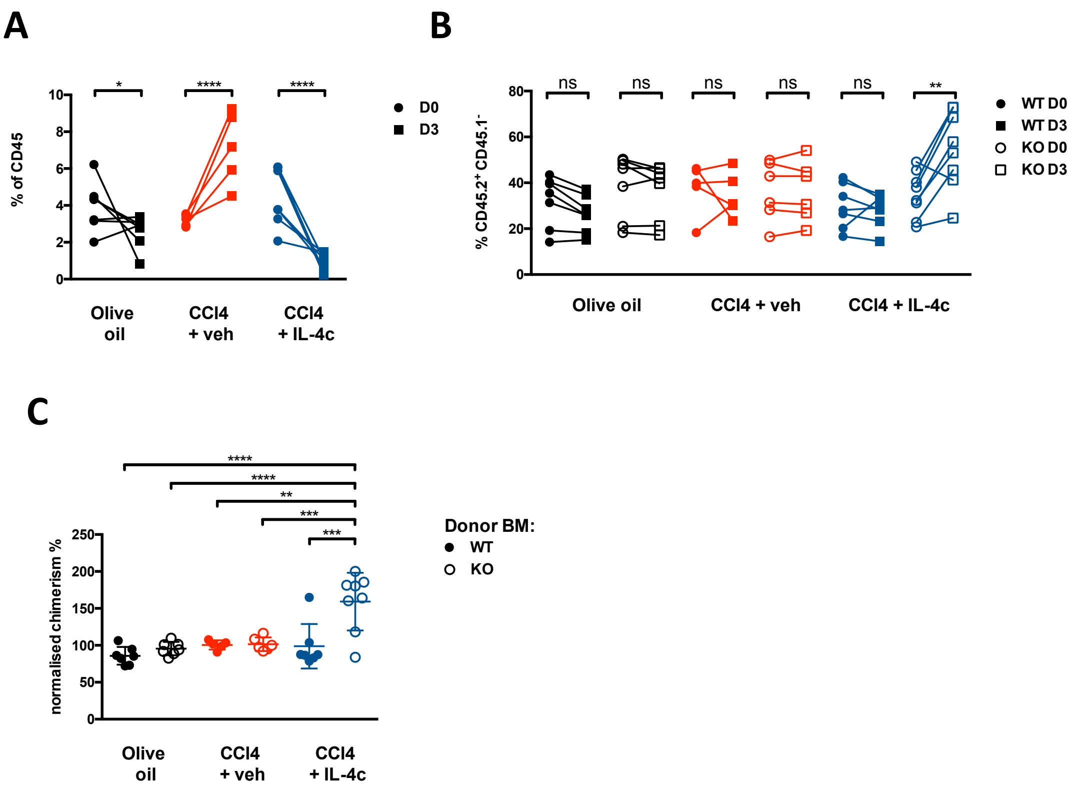

Figure 5-16 Blood Ly6C^{hi} monocytes in tissue protected irradiation chimeras.

(A) The proportion of Ly6C^{hi} monocytes of total CD45^{+} cells in blood of BM chimeric mice treated with olive oil, CCl_4+veh and CCl_4+IL4c at day 0 (before treatment) and day 3. N=5-7 mice/group, pooled from 2 independent experiments (multiple *t* tests with Holm-Sidak correction). (B) Non-host chimerism of blood Ly6C^{hi} monocytes at day 0 and day 3 in each group. (C) Non-host chimerism of blood Ly6C^{hi} monocytes from day 3 normalised to chimerism day 0. N=5-8 mice/group pooled from 2 independent experiments; mean ± SD (multiple *t* tests with Holm-Sidak correction for (A, B), one-way ANOVA for (C).

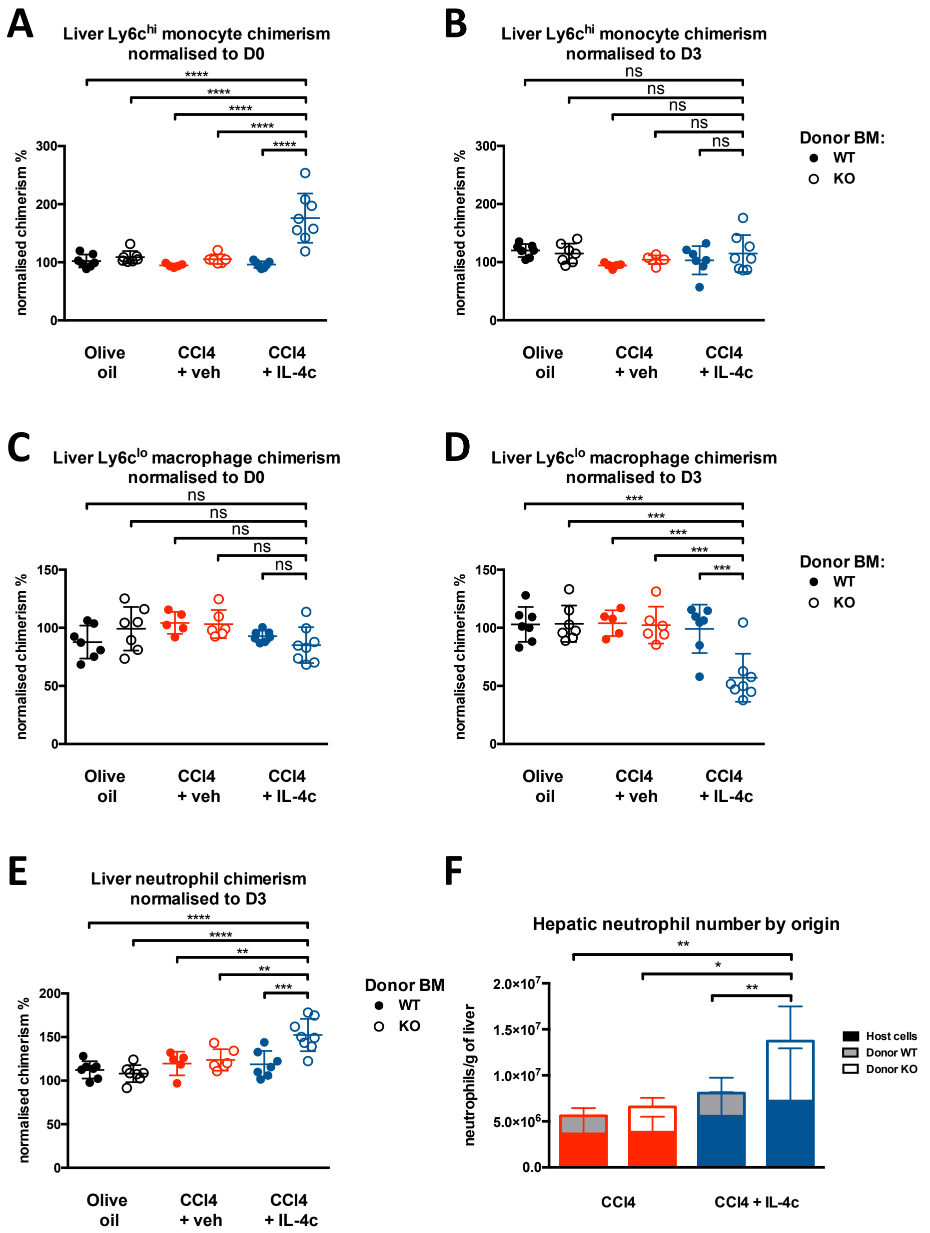

Figure 5-17 Recruited monocyte/macrophage chimerism in tissue protected irradiation chimeras.

(A-B) Chimerism of liver Ly6C^{hi} monocytes normalised to the chimerism of blood Ly6C^{hi} at day 0 (A) or day 3 (B). (C-D) Chimerism of liver Ly6C^{lo} MHCII^{int} macrophage normalised to the chimerism of blood Ly6C^{hi} at day 0 (C) or day 3 (D). (E) Chimerism of liver neutrophils normalised to the chimerism of blood neutrophil at day 3. N=5-8 mice/group pooled from 2 independent experiments, mean ± SD (one-way ANOVA). (F) Number of neutrophils/g by origin. N=5-8 mice/group pooled from 2 independent experiments, mean ± SD (one-way ANOVA of donor cells, no significant differences between host cells).

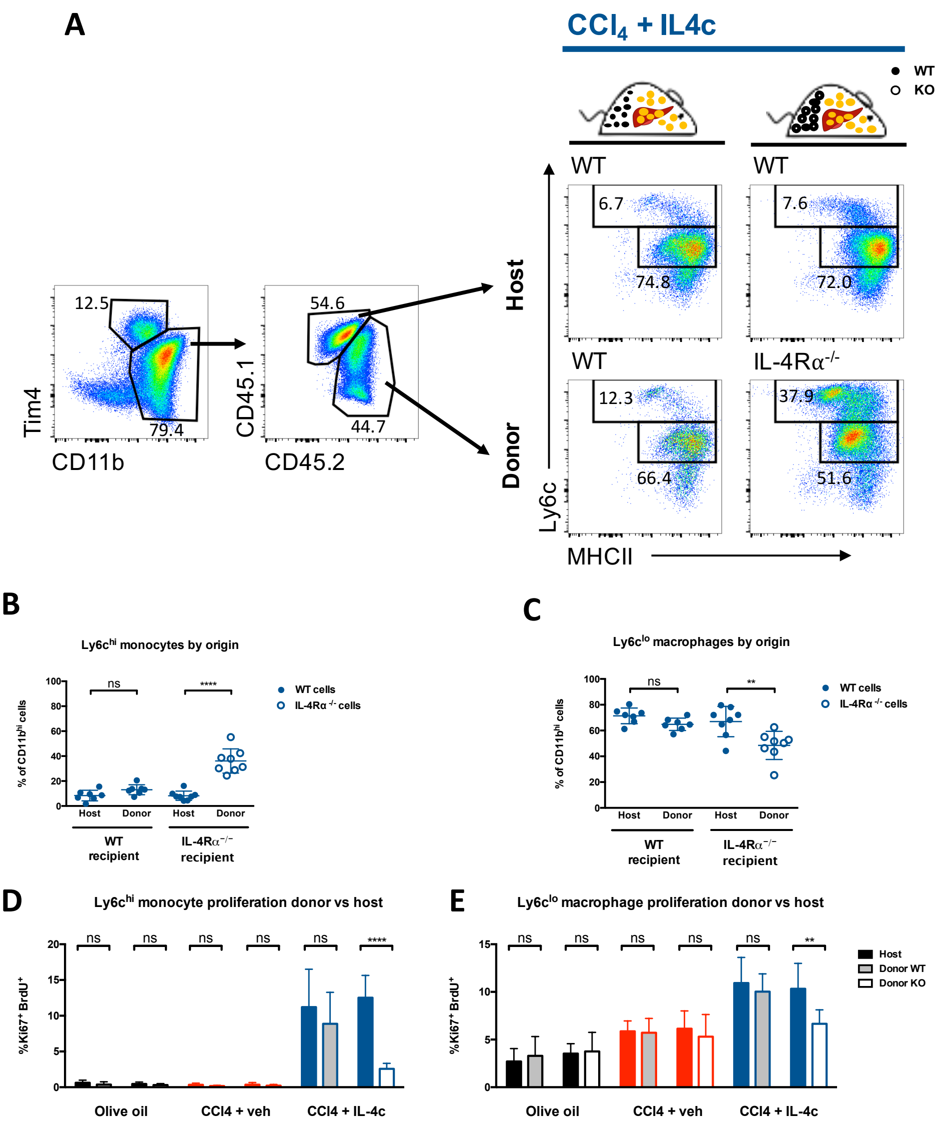

Figure 5-18 Recruited monocyte/macrophage dynamics in tissue protected irradiation chimeras.

(A) Left hand: identification of host and donor populations in recruited Live (Aqua), single, CD31-, CD45.2+, Lin–, Tim4lo, CD11bhi cells. Representative Ly6C and MHCII expression in host and donor recruited cells in CCl_4 + IL-4c mice. (B) Comparison in CCl_4 + IL-4c mice of proportion of recruited (CD11bhi) cells in (A) that are Ly6Chi monocytes depending on IL-4Rα phenotype. (C) The same analysis as (B) but for Ly6lo MHCIIint macrophages. N=7-8 mice/group from 2 independent experiments; mean ± SD (one-way ANOVA). (D-E) Recruited hepatic Ly6Chi monocyte and Ly6clo MHCIIint macrophage proliferation. N=6-8 mice/group from 2 independent experiments; mean ± SD (multiple T tests with Holm-Sidak correction).

Chapter 6 The effect of IL-4 on monocyte viability

6.1 Introduction

The results in Chapter 5 outlined that cell intrinsic IL-4Rα signalling was indispensable for the reduction in Ly6C^{hi} monocytes and increase in Ly6C^{lo} macrophages observed in response to IL-4c. I also saw that the reduction in Ly6C^{hi} monocytes was not limited to those in the injured liver but that there was also an IL-4Rα-dependent reduction in circulating Ly6C^{hi} monocytes. IL-4c has been used extensively to mimic the context of type 2 immunity and drive ‘alternative’ activation of tissue resident macrophages and examine differences between these and recruited macrophages[203,208]. However, none of these studies have focussed on the role of IL-4c in influencing the biology of Ly6C^{hi} monocytes. Furthermore, whether Ly6C^{hi} monocytes are affected in the context of type 2 infection, in which IL-4 is highly abundant, remains unclear. For instance, whereas minimal changes in Ly6C^{hi} monocyte numbers are reported during *L. sigmodontis* infection [123,204], *S. mansoni* induces a potent monocytosis at 7 weeks post infection in C57Bl/6 mice[123]. Thus, it was therefore not evident from the literature what mechanism underpinned the reduction in Ly6C^{hi} monocytes that I had observed in IL-4 treated mice.

In this chapter I initially aimed to establish what is driving the IL-4Rα dependent reduction in Ly6C^{hi} monocytes and whether this could be driven by increased conversion of Ly6C^{hi} monocytes to Ly6C^{lo} macrophages. During my timecourse the reduction in the proportion of Ly6C^{hi} monocytes 24 hrs after IL-4c administration didn’t coincide with a concomitant increase in Ly6C^{lo} macrophages, suggesting that there may be other effects of IL-4c on Ly6C^{hi} monocytes in addition to any effect on conversion. Furthermore, results from BM chimera experiments suggested that the cell intrinsic effects of IL-4c could be related to effects on circulating Ly6C^{hi} monocytes before they enter the tissue or even before they leave the BM. For that reason, I wanted to examine the global effects of IL-4c were on monocytes in both injury and repair, including any effect on BM egress.

6.2 Exogenous IL-4 does not enhance Ly6C^{hi} monocyte differentiation into Ly6C^{lo} macrophages

Previous work has shown that circulating Ly6C^{hi} monocytes give rise to recruited Ly6C^{lo} macrophages in the context of APAP and chronic CCl_4 induced liver injury[21,115]. I therefore set out to establish whether there was a precursor-product relationship between recruited Ly6C^{hi} monocytes and Ly6C^{lo} macrophages in the CCl_4 model of acute liver injury and if so, whether this was enhanced by IL-4. To test this hypothesis, I performed monocyte adoptive transfer experiments to track the fate of monocytes during acute liver injury with or without exogenous IL-4. Ly6C^{hi} monocytes were isolated from bone marrow of *Csf1r*-EGFP transgenic mice (herein referred to as MacGreen)[283] using FACS and then adoptively transferred i.v. into CCl_4 injured mice at the same 24hr timepoint that they received either vehicle or IL-4c (Fig. 6.1A). Ly6C^{hi} monocytes were isolated from bone marrow as single, Live (DAPI$^{–}$), CD45^{+}, Lin (CD3, CD19, Siglec F, Ly6G)$^{–}$, CD117 (c-kit)$^{–}$, CD11b^{hi} cells expressing high levels of GFP (Fig. 6.1B)[283,284]. This allowed sorting of monocytes without using an antibody against the CSF1R whilst simultaneously allowing fate mapping in recipient mice that also didn't rely on antibody staining. 2 days after transfer, liver leukocytes were analysed by flow cytometry and the presence of GFP^{+} cells amongst CD11b^{hi} cells was assessed. identified as: single, Live (7AAD), CD31^{-}, CD45^{+}, Lin (CD3, CD19, Siglec F, Ly6G)$^{–}$, CD11b^{hi}. A clear population of GFP^{+} cells could be identified and importantly, essentially all donor cells adopted a Ly6C^{lo}CD64^{+}CD11b^{hi} Tim4$^{–}$ phenotype by this time (Fig. 6.1C, D) consistent with recruited macrophages. Importantly, similar proportions of transferred Ly6C^{hi} monocytes had converted into Ly6C^{lo} CD64^{hi} macrophages in the CCl_4 + veh and CCl_4 + IL-4c groups, 95.0% ± 3.2 and 97.24% ± 1.9 respectively (Fig. 6.2A-B). Notably, by this time, no donor GFP^{+} cells were detected within blood or spleen (Fig. 6.2C). Of note, 1 mouse was excluded from analysis due to a documented problematic IV injection and a failure to find any GFP^{+} cells at necropsy. Although this experiment worked technically, it was clear that the 48 hour timepoint it was too late to identify an effect of IL-4 on conversion to Ly6C^{lo} macrophages. Therefore I next examined the fate of monocytes 24 hours after transfer. While this was performed as a single experiment with two recipient mice per group, there was no obvious difference in monocyte differentiation at this earlier timepoint, with the vast majority of cells in both groups retaining expression of Ly6C and only expressing low levels of CD64 (Fig. 6.2E). Thus, taken together, these results suggested that IL-4 was not promoting enhanced conversion of Ly6C^{hi} monocytes to Ly6C^{lo} macrophages.

6.3 Effect of IL-4c on monocytes and macrophages in other tissues

Given that IL-4c did not appear to cause accelerated conversion of Ly6C^{hi} monocytes by day 2 post-injury, the reduction in frequency of Ly6C^{hi} monocytes at this time most likely reflected a genuine loss of these cells. Thus, I next sought to establish whether this loss was specific to the liver or if it was a more global phenomenon, and if this occurred in the absence of liver injury[121,206]. The spleen is known to act as a reservoir of Ly6C monocytes that can be mobilized following tissue injury [119]. Hence, I examined the abundance of monocytes in the blood and liver, as well as the spleen from mice given CCl4 ± IL-4c. Furthermore, because CCl_4 is known to cause toxic effects in rat and mice kidneys[285–287], I also examined the effect of IL-4c therapy on monocyte/macrophage dynamics in this site, thereby modelling another inflammatory milieu. Mice were injured with CCl_4 as before and treated with either IL-4c or veh 24 hours later, and compared with olive oil control mice ± IL-4c (Fig. 6.3A). All mice were then culled on day 3 following CCl_4 injury and leukocytes isolated from liver, blood, spleen and kidneys as outlined in the methods section.

6.3.1 Identification of monocytes and macrophages in spleen and kidney

Gating strategies were developed for both splenic and kidney monocyte/macrophage populations based on the gene expression profiles published by the ImmGen Consortium[94].

Isolated leukocytes from spleens were analysed by flow cytometry. Red pulp macrophages were identified as single, live (7AAD$^{–}$), CD45^{+}, Lin (CD3, CD19, Ly6G and Siglec F)$^{–}$, and F4/80^{hi} CD11b^{lo} cells (Fig 6.3B). Amongst F4/80^{lo} CD11b^{hi} cells, cDC were excluded on the basis of high CD11c and MHCII co-expression and Ly6C^{hi} monocytes identified amongst the remaining CD11c$^{–/lo}$ cells (Fig. 6.3B).

Identification by flow cytometry of renal monocytes and macrophages in leukocyte isolates involved the following strategy: removal of debris and subsequent identification of single, live (7AAD$^{–}$), CD45^{+}, Lin (CD3, CD19, Ly6G and Siglec F)$^{–}$ cells. Myeloid cells were then selected on the basis of CD11b, accounting for the CD11b^{int} profile of tissue resident renal macrophages, and then Ly6C and CD64 expression to positively identify the monocyte/macrophage lineage. Resident macrophages were then identified as F4/80^{hi} while F4/80^{lo} cells encompassed recruited Ly6C^{hi} monocytes and Ly6C^{lo} MHCII^{+} macrophages (Fig. 6.3C).

6.3.2 Exogenous IL-4 causes a tissue-wide reduction in Ly6C^{hi} monocytes independent of injury

Analysis of the various tissues following CCl_4 injury revealed that IL-4c induced a significant reduction in frequency of Ly6C^{hi} monocytes in all tissues (Fig. 6.4B). There was also a significant reduction in frequency of Ly6C^{hi} monocytes in the blood and spleen of control (olive oil) mice receiving IL-4c (Fig. 6.4C), although no change was observed in the frequency of Ly6C^{hi} monocytes in the kidneys and livers of these mice. Indeed, analysis of cell numbers in the liver revealed no significant change in the monocyte number in uninjured mice upon treatment with IL-4c (Fig. 6.5A). CCl_4 + veh resulted in a significant increase in Ly6C^{hi} monocytes, however addition of IL-4c resulted in a two-fold reduction in the mean number of hepatic Ly6C^{hi} monocytes and abrogation of the increase in Ly6C^{hi} monocytes observed in CCl4 + veh mice (Fig. 6.5A). There was also a two-fold reduction in the mean number of Ly6C^{hi} monocytes in blood with IL-4c treatment in injured mice but none of the observed changes were statistically significant (Fig. 6.5B). As in the liver, there was a significant increase in the number of splenic Ly6C^{hi} monocytes upon injury but in contrast to the liver IL-4c caused a significant reduction in the number of splenic Ly6C^{hi} monocytes in both injured and uninjured mice when compared to vehicle treated mice (Fig. 6.5C). Finally, only in injured mice did IL-4c have a significant effect on the number of renal Ly6C^{hi} monocytes (Fig. 6.5D).

In summary IL-4c caused a global reduction in proportion of Ly6C^{hi} monocytes in liver, blood, spleen and kidney (Fig. 6.4B&C). Furthermore, in tissues IL-4c treatment abrogated any observed increase in the number of Ly6C^{hi} monocytes caused by CCl_4 injury (Fig. 6.5A,C-D).

6.4 Effect of IL-4c on recruited and resident macrophages in different tissues

Owing to the previously observed effects of IL-4c promoting expansion of hepatic resident and recruited macrophages, I wanted to also examine the effect of IL-4c on these populations both in the injured liver and in other tissues. In the liver IL-4c resulted in an increase in number of KC in both injured and uninjured mice (Fig. 6.6A). However, in the spleen and kidney IL-4c only had a significant effect on red pulp macrophages in uninjured mice and not any other groups (Fig. 6.6B&C). Ly6C^{lo} macrophages in the liver increased in number in injured mice treated with IL-4c, although this did not reach significance as in previous chapters (Fig. 6.6D). There was no effect of IL-4c on splenic Ly6C^{lo} monocytes or recruited kidney Ly6C^{lo} macrophages (Fig. 6.6E&F).

6.5 The effect of IL-4c on egress of leukocytes from bone marrow

From these results, it was evident that IL-4c has systemic effects on Ly6C^{hi} monocytes in both injured and control mice. I therefore hypothesised that IL-4c could be altering monocyte biology at the level of the BM, for instance by altering the rate of Ly6C^{hi} monocyte egress. To test this hypothesis, I used a short-term BrdU pulse-chase method to measure monocyte release into the circulation (Fig. 6.7A)[86,117]. Mice were administered BrdU 12 hours prior to being sacrificed on day 3 of the CCl_4 model. Because circulating monocytes do not proliferate to any great extent in steady state, BrdU positive monocytes in circulation represent cells that have arisen from proliferating transitional premonocytes in the bone marrow that have entered circulation within the 12 preceding hours[78]. At necropsy blood was taken via cardiac puncture whereupon leukocyte populations were identified as previously described (Fig. 5.5) and the proportion of BrdU$^+$ cells determined in all populations.

6.5.1 No reduction in output of circulating Ly6C^{hi} monocytes with IL-4c treatment

Analysis of Ly6C^{hi} monocytes in blood revealed a baseline output of 26.5% ± 8.6 for Ly6C^{hi} monocytes in control (olive oil + veh) mice (Fig. 6.7B-C), which is similar to that reported for steady state previously [86,90]. This was significantly increased in CCl_4 + veh mice (53.9% ± 9.7) suggesting injury drives increased monocyte production. Importantly, administration of IL-4c had no impact on this elevated level of monocyte output (56.3% ± 9.1) (Fig. 6.7C), despite an expected reduction in frequency/numbers of Ly6C^{hi} monocytes. Notably, IL-4c administration in the absence of inflammation (olive oil + IL-4c) appeared to significantly increase monocyte output from BM (60.7% ± 10.9) (Fig. 6.7C). This effect of IL-4c in control mice appeared to be almost exclusive to Ly6C^{hi} monocytes, as no differences were detected in Ly6C^{lo} monocytes, neutrophils and B cells, although there were small but significant increases in the proportion of BrdU$^+$ T cells and eosinophils in control mice given IL-4c (Fig. 6.7C-H). Hence, the equivalent degree of BrdU incorporation in monocytes from injured mice treated with or without IL-4c would suggest that the global reduction in monocytes that accompanies IL-4 treatment does not occur due to decreased output from the bone marrow.

6.6 Exogenous IL-4 increased death of Ly6C^{hi} monocytes *in vivo*

I next hypothesised that IL-4c was influencing monocyte viability. To test this hypothesis, I decided to harvest 24 hours after administration of IL-4c because we saw that there was already a significant reduction in monocytes in both tissue and blood at this timepoint (Fig. 5.2 & 5.6). Furthermore, to determine whether IL-4c affect BM output at this earlier timepoint, I performed a 12 hours BrdU pulse chase assay as before (Fig. 6.8A). As a control, I also included *Il4ra*$^{-/-}$ mice to show definitively that the effects of treatment with IL-4c were due to IL-4Rα signalling. At the end-point blood, liver and spleen were all analysed.

6.6.1 IL-4c causes a significant reduction in monocytes across all tissues within 24hrs

As previously observed at the 48hrs timepoint in section 6.3.2, there was a significant reduction in proportion of Ly6C^{hi} monocytes in blood 24hrs after treatment with IL-4c (Fig. 6.8B) but this loss was abrogated when IL-4c was administered to IL-4R$\alpha^{-/-}$ mice (Fig. 6.8B). Consistent with the experiments in section 6.4.1, IL-4c had no effect on the output of Ly6C^{hi} monocytes from the bone marrow at this 24hr time point, with no difference in the proportion of BrdU$^+$ monocytes amongst groups (Fig. 6.8C). The degree of BrdU labelling at 24hr reflected my previous results at 48hrs, with 52.3% ± 6.6, 51.5% ± 4.1 and 49.3% ± 5.8 of Ly6C^{hi} monocytes being BrdU$^+$ in the CCl_4 + veh, CCl_4 + IL-4c and IL-4R$\alpha^{-/-}$ CCl_4 + IL-4c groups respectively. Furthermore, as observed at 48hrs post IL-4c treatment, there was a significant reduction in number of splenic and hepatic Ly6C^{hi} monocytes 24hrs following IL-4c treatment, a reduction that was abrogated in IL-4R$\alpha^{-/-}$ mice (Fig. 6.8D-E).

It should be noted that the results from the BrdU pulse-chase experiment are from a single experiment due to a failure to detect any BrdU incorporation in the repeat experiment. Although the exact reason for these issues is unclear, it was likely due to a problem with the stock of BrdU used or the DNase step because it was a universal problem in all samples. Furthermore, one sample in the CCl_4 + veh group in the initial experiment didn't have any positive $BrdU^+$ cells in any populations and was therefore excluded from the analysis as it was assumed that there had been an issue with the injection of BrdU.

6.6.2 IL-4c decreases viability of circulating $Ly6C^{hi}$ monocytes as measured by 7AAD

To assess monocyte viability, I first assessed the proportion staining positive for 7-AAD, a fluorescent dye that intercalates into DNA of cells with reduced membrane integrity. It was evident by looking at 7AAD staining in circulating $Ly6C^{hi}$ monocytes that IL-4c treatment was leading to increased levels of apoptotic/dead monocytes (Fig. 6.9A-B), which was abolished in IL-4R$\alpha^{-/-}$ mice (Fig. 6.9C). Similar results were obtained from blood $Ly6C^{hi}$ monocytes from my timecourse analysis (Fig. 6.9D). When the proportion of $7AAD^+$ cells was analysed in the spleen it was apparent that although both experiments showed a significant increase in $7AAD^+$ $Ly6C^{hi}$ monocytes with IL-4c treatment, the degree of change caused by IL-4c was different between experiments (Fig. 6.9E-F). Notably however, there was no significant difference in proportion of $7AAD^+$ $Ly6C^{hi}$ monocytes in the liver (Fig. 6.9G).

6.6.3 IL-4c treatment induces an increase in circulating apoptotic $Ly6C^{hi}$ monocytes

To qualify the decreased viability observed, I also assessed expression of phosphatidylserine using the annexin V reagent. Using an FMO to set the annexin V^+ gate, I found there was a significant increase in the proportion of annexin V^+ circulating $Ly6C^{hi}$ monocytes in the IL-4c treated group that was not observed in IL4Rα deficient mice (Fig. 6.10A&B). Interestingly, the increased level of 7-AAD^+ cells amongst splenic $Ly6C^{hi}$ monocytes treated with IL-4c was not paralleled by increased proportions of annexin V$^+$ cells. In one experiment there was a very high proportion of annexin V$^+$ cells in all groups which makes this result interesting in itself as it could suggest that there is something that has affected the viability of all the cells. This meant that the data from the two experiments could not be pooled and have therefore been presented side by side (Fig. 6.10C-D). In agreement with 7AAD uptake, there was no significant effect of IL-4c on the proportion of annexin V$^+$ hepatic Ly6C^{hi} monocytes (Fig. 6.10E).

Notably the disparity observed in the 7AAD staining in splenic Ly6C^{hi} monocytes between experiments was also reflected by a significant difference in annexin V staining. This suggested that the difference in staining reflected genuine differences in cell viability between experiments rather than technical differences in staining between experiments (Fig. 6.9D and 6.10C). A possible explanation could be that a technical error in the processing resulted in increased death in all groups in RL052 splenic Ly6C^{hi} monocytes.

Using annexin V in combination with 7AAD enabled the subdivision of annexin V$^+$ cells into early apoptotic and late necrotic populations in the blood (Fig. 6.11A). This analysis in blood demonstrated that there was an increase in the proportion of both early apoptotic and late apoptotic/necrotic Ly6C^{hi} monocytes with IL-4c treatment (Fig. 6.11B-C).

6.7 Assessing Ly6C^{hi} monocyte viability in vitro

To interrogate the decreased viability observed *in vivo*, I developed an assay to assess monocyte viability in vitro. To do this, Ly6C^{hi} monocytes were FACS purified (gating in Fig. 6.12A) from the BM and cultured overnight in the presence of recombinant CSF1 or different concentrations of recombinant IL-4. Ly6C^{hi} monocytes were isolated as in Fig. 6.12A and cultured for 16 hours in low adherence plates with a variety of treatments as outlined. The following day cells were analysed by flow cytometry with Ly6C^{hi} monocytes being identified as single, CD45^{+} and Ly6C^{hi} (Fig. 6.12B).

6.7.1 Ly6C^{hi} monocyte viability is reduced by rIL-4 in a dose dependent manner

I first performed a pilot experiment, pooling cells from multiple mice to allow for technical replicates within each treatment. This showed that the viability of monocytes cultured in media alone was only 60.0% ± 5.2, which could be significantly improved (95.3% ± 1.4) by the addition of murine recombinant colony stimulating factor 1 (rCSF-1; 50ng/ml). Notably, addition of IL-4, regardless of concentration, significantly reduced viability compared with both the rCSF-1 and non-supplemented media groups (Fig. 6.12C).

Given the intriguing result from the pilot experiment, I sought to establish if the decreased viability was dose dependent and I therefore titrated the dose of IL-4 further, from 20ng/ml to 0.02ng/ml. As before, I observed a significant reduction in viability with 20ng/ml and 2ng/ml concentrations of rIL-4 but this was lost when a dose of 0.02ng/ml was used (Fig. 6.13A-B). As baseline viability in media alone cultures was variable between two repeat experiments (Fig. 6.13C), the viability in treatment groups was normalised to the baseline group of media alone (Fig. 6.13D) thereby allowing the data to be pooled. This pooled analysis revealed that decreased viability returns to baseline with decreasing rIL-4 concentration but even 0.2 ng/ml appears to have a significant effect on monocyte viability (Fig. 6.13D).

To ensure the decreased viability was due to the actions of IL-4 specifically, I performed an experiment combining rIL-4 with a neutralising anti-IL-4 antibody (11B11). Importantly, the decreased viability observed with the 2ng/ml dose of rIL-4 was reversed by the addition of 11B11 into the culture, demonstrating that the increased levels of cell death were due to the direct effect of IL-4 (Fig. 6.13E).

6.7.2 IL-4-induced reduction in viability is abrogated by addition of CSF-1

Mirroring the dependence of most tissue macrophages on CSF1 in vivo, it is common to use rCSF-1, or a source of CSF-1 such as L929 media[288,289], to generate BM-derived macrophages (BMDM). Indeed, I observed in my pilot experiment that addition of rCSF-1 significantly increased monocyte viability (Fig. 6.12C). Thus, I next asked if rCSF-1 could rescue the decreased viability observed in rIL-4 treated monocytes. Co-culture of monocytes with 2ng/ml rIL-4 and 50ng/ml of rCSF-1 resulted in an improvement in viability from 26.4% ± 11.0 with IL-4 alone to 79.3% ± 6.3, but also a significant increase in viability compared to cells cultured in media alone 54.1% ± 18.0 (Fig. 6.14A). As before, because of variability between experiments, I have also presented normalised viability where the viability in each condition has been normalised to the media alone baseline viability. This analysis also demonstrates that the reduced viability is rescued by exogenous CSF-1 (Fig. 6.14B). Using a reducing concentration of rCSF-1, it was apparent that viability of monocytes decreased with concentration of rCSF-1 and that with a dose of 3.125ng/ml of rCSF-1 addition of rIL-4 decreased viability significantly compared to rCSF-1 alone 62.6% ± 0.7 vs 69.5% ± 1.8 respectively (Fig. 6.14C). Thus, although this experiment was only performed once due to time limitations, monocytes appeared to become more sensitive to IL-4-induced death under CSF-1 limited conditions.

6.7.3 rIL-13 has a similar effect to rIL-4

Because IL-13 also signals through the type 2 IL-4R, I assessed whether IL-13 had similar effects on monocyte viability to IL-4. Notably, addition of IL-13 (20ng/ml and 2ng/ml) caused a significant reduction in viability compared to media alone and the effect was comparable to that caused by addition of IL-4(2ng/ml). Thus, while only performed once, this experiment suggests a likely equivalent potential for both IL-4 and IL-13 to control of monocyte viability (Fig. 6.14D).

6.7.4 IL-4c has no effect on viability in cultured macrophages

It is well established that IL-4 causes 'alternative' activation, proliferation and accumulation of tissue resident macrophages [121,174]. However, given my findings showing a role for IL-4 in reduced monocyte viability, I wanted to assess whether this also occurred in mature macrophages and if this was a phenomenon that had been overlooked previously. I decided to use peritoneal macrophages for this purpose as they are easy to obtain and their extraction requires little manipulation (e.g. no enzymatic digestion). Peritoneal macrophages were sorted by FACS as single, live (DAPI), $CD45^{+}$, Lin^{-}, $CD102^{+}$ (Fig. 6.15A). After 16 hours in culture viability was analysed the following day by flow cytometry (Fig. 6.15B). Strikingly and in contrast to $Ly6C^{hi}$ monocytes, viability of macrophages was unaffected by addition of IL-4, with no significant difference between any of the groups (Fig. 6.15C).

6.8 Nanostring analysis of circulating $Ly6C^{hi}$ monocytes

To gain further insight into the effects of IL-4 on monocytes, I decided to analyse what, if any, changes were happening at the gene level. Because the reduction in frequency of circulating monocytes happens at least by 24 hours following IL-4c treatment (Fig. 6.8B), I sorted blood $Ly6C^{hi}$ monocytes from olive oil, CCl4 + veh and CCl4 +IL-4c treated mice at this timepoint (Fig. 6.16A). Monocytes were sorted and then analysed using the Nanostring Mouse Myeloid V2 assay profiling 754 genes. Due to time constraints in my project, I have not been able to validate any of the observed gene differences but have focused more on the overall pattern observed.

6.8.1 No significant change in olive oil compared to CCl_4 + veh

Upon analysis, there were no genes in the comparison of olive oil and CCl_4 + veh that reached significance (adj p-value < 0.05) and demonstrated a Log2 fold-change of at least ±1.5 (Fig. 6.16B). This means that the changes observed are of doubtful biological significance and for this reason no further analysis was performed on these samples. Interestingly, this was despite the clear increase in turnover of monocytes upon injury revealed by the 12 hr BrdU pulse chase experiment (Fig. 6.7C).

6.8.2 IL-4c causes marked changes in gene expression of Ly6C^{hi} blood monocytes

There was a significant down regulation of genes with IL-4c treatment. Of the 317 genes with enough reads of sufficient quality to be included in the analysis, 202 genes had a Log2 fold-change of at least ± 1.5 and a p-value of <0.01. Of these genes with a p-value of <0.01, 190 were significantly downregulated when comparing expression in CCl_4 + IL-4c vs a baseline of CCl_4 + veh (Fig. 6.16C). Of the genes with a Log2 fold-change of at least ± 1.5, I have presented the 50 most significantly changed genes in the bar chart (Fig. 6.16D) and they are also annotated in the volcano plot (Fig. 6.16C). It is notable that there are multiple genes associated with cell adhesion and migration that are downregulated and of the most significantly downregulated genes, the one with largest change is *Nr4a1* (Log2 fold change of -5.18)(Fig. 6.16D). Although not one of the 50 most significantly altered genes, *Cx3cr1* showed a large change in expression, with a Log2 fold change of -7.38 and an adjusted p-value of 0.00036. Interestingly, high expression of *Cx3cr1* and *Nr4a1* are features of Ly6C^{lo} monocytes and given one fate of Ly6C^{hi} monocytes is to differentiate into Ly6C^{lo} monocytes, these data suggest that IL-4 could change the fate of monocytes in blood. The most upregulated gene was *Ccl24,* also known as eosinophil chemotactic protein 2. Notably, within the 50 most significantly altered genes the only other genes that were upregulated were *Cdc20*, *Kif20a* and *280104Rik* which are all involved in cell cycling. Unfortunately, the Nanostring platform did not include specific genes that are solely associated with cell cycling, such as *Mki67*.

Thus, as well as affecting the turnover dynamics of monocytes, exogenous IL-4 results in marked changes in the transcriptional profile of these cells.

6.9 Conclusion

During this chapter I have outlined that the loss of Ly6C^{hi} monocytes observed in the liver following IL-4c administration to CCl_4 injured mice is not solely limited to the liver but is also observed in blood, spleen and kidneys. Furthermore, I have found that IL-4c administration both in vivo and in vitro specifically affects the viability of Ly6C^{hi} monocytes which may contribute to the loss of Ly6C^{hi} monocytes. I have also attempted to identify the gene expression profiles that underpin these changes.

6.9.1 Adoptive transfer

In the first section of this chapter, I showed that Ly6C^{hi} blood monocytes are recruited to the liver following CCl_4-induced acute injury where they convert into Ly6C^{lo} CD64^{hi} macrophages. These findings are in keeping with previous work that utilised adoptive transfer of cells to demonstrate the monocyte/macrophage dynamics during APAP-induced acute liver injury and chronic liver injury with CCl_4[21,115]. Importantly, my work demonstrates that administration of exogenous IL-4 does not alter this conversion. My initial experiments assessed the fate of monocytes 48hrs after transfer and because they had all converted to Ly6C^{lo} macrophages, this timepoint was deemed too late to detect any accelerated conversion induced by IL-4c therapy. Indeed, Ramachandran et al. have shown that adoptively transferred Ly6C^{hi} monocytes convert into Ly6C^{lo} cells with 20 hours of transfer, albeit in the chronic CCl_4 model of liver injury[115]. However, I performed additional analysis at an earlier timepoint (24hrs) and detected no difference in the fate of monocytes in the presence of exogenous IL-4 but I can't exclude that this could occur between the 24 and 48 hour timepoint. Unfortunately, I was unable to repeat this latter experiment in the time available due, in part, to difficulty in obtaining MacGreen donor mice. Having established the system, a repeat experiment could include more end points (e.g. 24, 36 and 48 hrs), to ensure any effect of IL-4c was not being missed. The kinetics of Ly6C^{hi} monocyte differentiation that I observed was slower than that seen in the

APAP model, wherein $Ly6C^{hi}$ monocytes started to differentiate within 24hrs by losing Ly6C and gaining F4/80 expression, and full differentiation was evident 48hrs after APAP, although some $Ly6C^{hi}$ monocytes remained[21]. This may reflect the nature of the model, with APAP damage occurring within 12hours and recovery by 72hours[41]. Alternatively, monocyte differentiation may be distinct based on the context of the environment into which they arrive.

Although I did not manage to definitively demonstrate the effect of IL-4c on conversion, subsequent results suggested that IL-4c was having effects on monocytes in blood unrelated to the inflammatory milieu of the CCl_4 injured liver. I therefore decided to concentrate on dissecting this global process rather than the conversion hypothesis which was limited to the liver.

6.9.2 IL-4c causes a systemic reduction in $Ly6C^{hi}$ monocytes

There was a significant reduction in the proportion of circulating $Ly6C^{hi}$ monocytes with IL-4c treatment not only following injury with CCl_4 but also in uninjured mice. This implied that IL-4c was having a significant effect on monocytes in homeostasis and that an inflammatory environment is not a pre-requisite for the observed reduction in $Ly6C^{hi}$ monocytes. Indeed, analysis of the spleen, which acts as a reservoir of $Ly6C^{hi}$ monocytes when emergency haematopoiesis is overwhelmed[119], revealed a similar significant reduction in $Ly6C^{hi}$ monocytes with IL-4c treatment in both injured and uninjured mice. This was also reflected by a significant reduction in numbers of $Ly6C^{hi}$ monocytes in the spleen which was not seen in the blood. However, this probably reflects that counting method used for blood was not optimal which led to variable cell numbers. Interestingly, in the absence of injury, IL-4c had no significant effect on the proportion or number of $Ly6C^{hi}$ monocytes identified in kidney or liver. This could reflect the fact that, unlike the spleen, these tissues are not reservoirs of $Ly6C^{hi}$ monocytes. Instead, monocytes are recruited during inflammation where they become the dominant mononuclear phagocytes in these tissues[21,130,290,291]. For this reason, the increased number of Ly6C^{hi} monocytes observed in the kidney upon CCl_4 injury would be expected given that it has been demonstrated to cause renal inflammation, although the leukocyte populations have not been previously quantified [285–287]. It would therefore appear to be the case that IL-4c only causes reduction in Ly6C^{hi} monocytes in the liver and kidney following injury with hepatic and nephro-toxins. However, when examining numbers of cells this reduction with IL-4c treatment was only statistically significant in the kidney. In the liver, there was a non-significant reduction in the number of Ly6C^{hi} monocytes which contrasted results from previous experiments where IL-4c caused a significant reduction in Ly6C^{hi} monocytes on day 3 when compared to vehicle controls (Fig. 3.9C and 5.11C). I suspect that the result was not significant because one mouse had a high total liver cell count and it is reassuring that when looking at percent of CD45% cells there was a highly significant ($p<0.001$) reduction in Ly6C^{hi} monocytes.

The expansion of resident macrophages in uninjured liver and spleen in response to IL-4c treatment is consistent with previous work examining macrophage IL4 responsiveness[121,292]. Notably, there was no appreciable change in the number of resident macrophages in the kidney, although the underlying reasons for this remain unclear. Although speculative, it is plausible that tissue resident macrophages in the kidney fail to express IL-4R to the same level as their counterparts in other tissues. Alternatively, anatomical positioning in the kidney may restrict some macrophages exposure to IL-4c and it is therefore foreseeable that IL-4c may not have the same effect as it does in the spleen and liver[293].

6.9.3 No effect of IL-4c on egress of Ly6C^{hi} monocytes from bone marrow

It was evident from the above results that the reduction in monocytes caused by IL-4c was not limited to the liver or to the setting of inflammation. This implication that IL-4c was having a global effect lead me to address whether it was reducing BM egress of Ly6C^{hi} monocytes because it has been suggested that in neutrophils IL-4 actually inhibits migration of neutrophils from the BM to tissues[294]. My short-term BrdU pulse-chase experiments supported published work demonstrating BM output of Ly6C^{hi} monocytes was approximately 26% over 12hours[117]. Furthermore, Ly6C^{hi} monocyte labelling of ~60% appears to be the maximal labelling achievable during inflammation[86,117]. In my model this is the level achieved in both CCl_4 injured groups, but also in the olive oil + IL-4c group, suggesting that IL-4c is not restricting BM egress of monocytes and if anything, promotes monocyte output. To the best of my knowledge, this is the first demonstration that exogenous IL-4 can alter monocyte dynamics at the level of the BM.

Because I did not perform analysis on BM, it remains unclear as to what point in monocyte development/differentiation that IL-4c is having an effect. I cannot therefore rule out that it may have an effect on the incorporation of BrdU by monocytes in the BM. An effect on the BM would seem unlikely, however, because the proportion of BrdU^{+} Ly6C^{hi} monocytes was the same between CCl_4 + veh and CCl_4 + IL-4c groups and if IL-4c were affecting BrdU incorporation in the BM it would also need to simultaneously affect egress from the BM. The absence of neutrophil BrdU labelling in all groups was initially confusing as I would have expected to see some labelling in CCl_4 + veh mice given the neutrophilia associated with CCl_4 injury. However, this may reflect the fact that BrdU labels immature neutrophils which have to mature before appearing in blood; a process estimated to take 48-72 hours. Thus, mature neutrophils would not be labelled in a 12 hour BrdU pulse chase system[295].

In conclusion, it would seem likely that the reduction in circulating Ly6C^{hi} monocytes in response to IL-4c is not a reflection of reduced output from the BM. Although, it is important to note that to show this definitively a time course assessing BrdU labelling of Ly6C^{hi} monocytes in BM and circulation in both IL-4c and veh treated mice would be needed. Sadly, I did not have time to perform this experiment during my PhD.

6.9.4 IL-4c decreases viability of circulating Ly6C^{hi} monocytes

That monocyte output was unaltered by IL-4c raised the question, what is the underlying cause of monocytopenia in IL-4c-treated mice? The two remaining options were that IL-4c was causing sequestration of monocytes in another as yet unidentified tissue or that it was affecting their viability. While I cannot rule out the former explanation, my ex vivo analysis of markers of viability strongly suggests IL-4 does drive substantive apoptosis of monocytes in vivo. Owing to the significant reduction in hepatic and circulating Ly6C^{hi} monocytes observed on day 2 and the large reduction in splenic Ly6C^{hi} monocytes on day 3, I assessed apoptosis within these different populations on day 2 as it seemed likely this would potentially yield the greatest proportion of dying cells.

Having established that Ly6C^{hi} monocytes dynamics following IL-4c treatment were the same on day 2 as day 3 in blood, liver and spleen I could then attempt to establish whether IL-4c was influencing Ly6C^{hi} monocyte viability. 7-AAD binds to DNA and therefore enables the identification of dead and dying cells where it can cross the disrupted cell membrane[296]. Annexin V allows the identification of apoptotic cells because it binds to phosphatidyl serine exposed on the surface when apoptotic cells flip their cell membrane, however it also enters cells with disrupted membranes and so stains necrotic and late apoptotic cells too[297,298]. Combined analysis of 7AAD and Annexin V staining patterns in the blood revealed that there was a distinct population of early apoptotic cells in addition to the late apoptotic/necrotic cells that was significantly greater in frequency when injured mice were treated with IL-4, demonstrating a novel finding that IL-4 drives apoptosis of circulating monocytes in vivo at least following acute liver injury.

Notably in the liver there were no significant effects of IL-4c on either 7-AAD or annexin V positivity, suggesting there may be protective factors that could prevent monocyte death present in the liver (discussed below).

6.9.5 IL-4c decreases viability of Ly6C^{hi} monocytes in vitro

I initially developed an in vitro culture system for Ly6C^{hi} monocytes to assess the effect of IL-4c on their phenotype. There is a paucity of literature on in vitro culture systems for monocytes, primarily because they are used as a means to make macrophages rather than interrogate the biology of monocytes[150,255,288]. Not including any monocyte/macrophage survival factors in the culture was intentional to preserve the monocyte phenotype, as was the decision to culture cells in low adherence plates since it has been long suggested that adherence to plastic can alter their activation state[299]. It has previously been shown that rCSF-1 is important for survival of monocytes in culture because if it is removed early (on day 4) from cultures of BMDMs there is decreased viability observed[300]. Furthermore, Louis et al. demonstrated that CSF-1 is required for the in vitro survival of blood Ly6C^{hi} monocytes[82] it is therefore not surprising that I observed a reduction in viability in monocytes cultured in media alone. It has been previously reported in the early nineties that IL-4 can affect monocyte viability of human peripheral blood mononuclear cells (PBMCs) in vitro[220,301]. In contrast to my data, these studies suggested that IL-4 only affected viability of PBMCs activated in vitro by inflammatory stimuli (IL-1, TNF-α and LPS). However, Mangan et al. analysed death in vitro at a 48 hrs timepoint when they found that in unstimulated cells viability was already as low as 10%[220]. This makes it difficult to ascertain whether IL-4 decreases viability at this late timepoint when there are already very few viable cells; indeed, when they looked earlier IL-4 appeared to decrease viability when given to unstimulated cells and those stimulated with IL-1 but had no effect on LPS treated cells. Given that the half-life of Ly6C^{hi} monocytes during homeostasis is 20hrs[86] and I have demonstrated that there is increased BM output of Ly6C^{hi} monocytes during injury, it will be important to examine viability at the earlier timepoint that I have done here.

It is also important to consider that following injury there was a significant reduction in the proportion of Ly6C^{hi} monocytes in all tissues analysed (Fig. 6.4) and not just blood and spleen. This could reflect that monocytes elicited by an inflammatory stimulus may be intrinsically more susceptible to death, a theory proposed by Mangan et al.[220]. An intrinsic susceptibility to death could result in increased output of Ly6C^{hi} monocytes from the BM in an attempt to replace the 'unfit' circulating cells (Fig. 6.7). Further insight might be provided by transcriptomic analysis of these cells and this is discussed later.

Mangan et al. did also demonstrate that the viability of PBMCs cultured with CSF-1 was the same following 48 hours of culture whether they were cultured with or without IL-4[220]. My results concurred with this and I found that the addition of CSF-1 largely overcame the effect of IL-4, hence, high concentrations of CSF-1 appear to be able to inhibit IL-4-induced apoptosis of both mouse and human monocytes in vitro. These results emphasise the beneficial effect of CSF-1 which acts as a survival signal for macrophages[302] and in my and Mangan et al.'s work it appears to promote survival in monocytes. Increased tissue concentrations of CSF-1 could explain why the viability of liver Ly6C^{hi} monocytes was unaffected IL-4c. Indeed, it has previously been demonstrated that in the liver tissue there is an increase in CSF-1 mRNA expression which peaks at 24hrs following APAP induced injury[21] and it is also known that following APAP injury in humans the levels of circulating CSF-1 in serum increase[16]. To add further weight to my hypothesis, it would be worth quantifying serum and tissue levels of CSF-1 over time.

6.9.6 Significant reduction in gene expression in IL-4c treated monocytes

It was notable that there was no difference in gene expression between olive oil and CCl_4 + veh treated mice. This is surprising because during other inflammatory stimuli, such as *Toxoplasma gondii* infection, monopoiesis is affected giving rise to phenotypically- and transcriptionally-distinct monocytes[277]. Furthermore, using single-cell RNAseq it has recently been proposed that different infective stimuli can alter the Ly6C^{hi} monocyte progenitor to be either granulocyte-monocyte progenitors (GMPs) or monocyte-dendritic cell progenitors (MDPs) which confers a different genetic signature on the Ly6C^{hi} monocytes[303]. Finally, during bleomycin-induced sterile damage, Satoh et al. demonstrated the appearance of distinct pro-fibrotic monocytes which they termed segregated-nucleus-containing atypical monocytes (SatM)[304]. Given the above results and the fact that CCl_4 injury appears to induce increased turnover of Ly6C^{hi} monocytes, it is surprising that the Nanostring analysis failed to identify any differences in the genetic profile of the circulating Ly6C^{hi} monocytes. This could be related to the limited pool of genes that are examined by the Nanostring platform and more powerful RNAseq analysis could potentially identify differences.

The major finding from my Nanostring analysis of monocyte gene expression was that IL-4 appeared to largely result in down-regulation of gene expression when compared with that of control cells from uninjured or injured mice. While this could reflect the restricted 770 genes measured in the Nanostring, it closely parallels the effect of IL-4 on gene expression in inflammatory monocyte-derived macrophages recruited into the peritoneal cavity, as determined by microarray[203]. Specifically, Gundra et al. found that in thioglycolate elicited monocyte-derived macrophages from mice treated with IL-4, there was a down regulation of 1,249 genes compared to upregulation of only 368 genes[203]. Hence, further unbiased transcriptomic analysis of the effect of IL-4 on blood monocytes may reveal if these cells largely respond to IL-4 by downregulation rather than up-regulation of gene expression. How IL-4 promotes apoptosis remains unclear. Notably, I did not identify obvious changes in expression of genes that could be responsible for the enhanced apoptosis, for example expression of antiapoptotic genes such as BCL2 appeared to remain unaffected. Amongst the most differentially expressed genes were *Nr4a1* and *Cx3cr1,* both of which have been proposed as a critical regulators of Ly6C^{lo} monocytes[65–67,136,305]. Specifically, it is thought that NR4A1 and CX3CR1 play a role in promoting monocyte survival, with mice deficient for *Nr4a1* or *Cx3cr1* having significantly fewer circulating Ly6C^{lo} monocytes. However, according to the Immgen database, *Nr4a1* and *Cx3cr1* is upregulated by Ly6C^{hi} monocytes in blood compared with their counterparts in BM. Thus, it is plausible that NR4A1 and CX3CR1 play a similar role in promoting survival in Ly6C^{hi} monocytes. Indeed, *Nr4a1*$^{-/-}$ cells appear to have a competitive disadvantage over their WT counterparts in generating Ly6C^{hi} (and Ly6C^{lo}) monocytes in the setting of mixed radiation BM chimeras[65]. Therefore, IL-4R signalling in monocytes may cause downregulation of NR4A1 and prevent monocyte endurance. Interestingly, loss of *Nr4a1* leads to DNA damage in monocytes and if I had had more time, this would have been an important feature to check in IL-4 treated monocytes.

Interestingly, the most significantly upregulated gene was CCL24 which was also observed by gundra et al. in resident and monocyte derived macrophages from mice treated with IL-4c[203]. It is also important for eosinophil recruitment[306] and could therefore underlie the increased eosinophil numbers seen in the injured liver following delivery of IL-4c (Fig. 3.10A). This data gives an idea of the global gene changes resulting from exposure to IL-4 and reveals down regulation of certain genes associated with monocyte survival. However, it doesn't provide the depth of analysis required to ascertain what pathways underlie the mechanism of increased apoptosis that was observed in Ly6C^{hi} monocytes (Fig. 6.11). More in-depth analysis using RNAseq could potentially provide further insight into the underlying mechanisms of the increased Ly6Chi monocyte death. Given the findings of separate subsets of Ly6C^{hi} monocytes during inflammation demonstrated by others[277,303,304] it may be that single-cell RNAseq would be a more powerful tool to elucidate the pathways involved.

6.9.7 Summary

In this chapter I have demonstrated that following IL-4c administration there is a global reduction in Ly6C^{hi} monocytes which appears to be dependent on the death of Ly6C^{hi} monocytes and not an alteration in their output from the BM. Going forward I wanted to assess whether this finding could be applied to other models of inflammation that are characterised by a Ly6C^{hi} monocytosis.

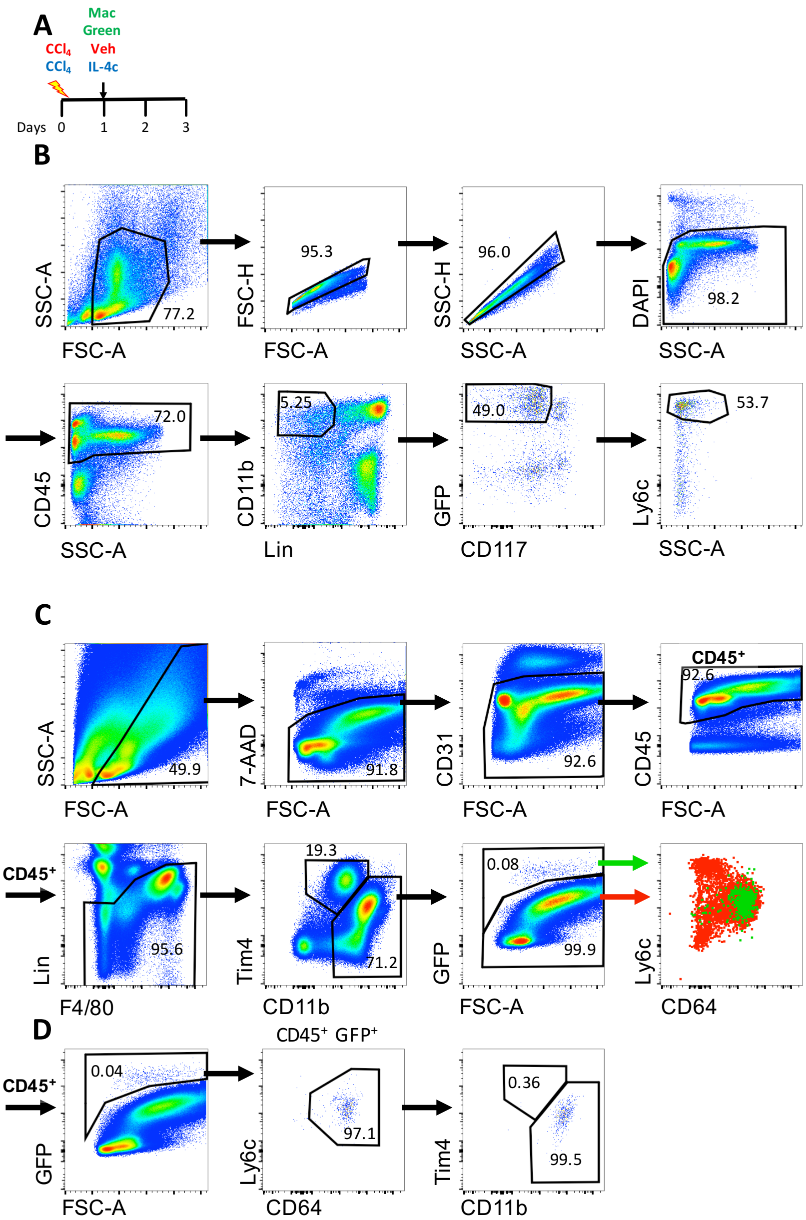

Figure 6-1 Monocyte adoptive transfer.

(A) Schematic of adoptive transfer model. GFP+ Ly6C^{hi} monocytes were sorted by FACS as in (B) and injected via tail vein on the same day as IL-4c or veh treatment. (B) BM was sorted by FACS identifying single, Live (DAPI), CD45+, CD11b+, Lin (NK1.1, CD19, CD3, Ly6G, Siglec F)$^{-}$, CD117 (c-kit)+, GFP+, Ly6c+. (C) On day 3 following harvest recruited hepatic mononuclear phagocytes are identified as live (7AAD), CD31^{-}, CD45+, Lin^{-}, Tim4^{lo}, CD11b^{hi}. GFP positive and negative cells are identified within this CD11b^{hi} population. (D) Gating strategy used to identify proportion of Ly6C^{lo} CD64+ macrophages within live (7AAD), Lin^{-}, CD45+ GFP+ cells.

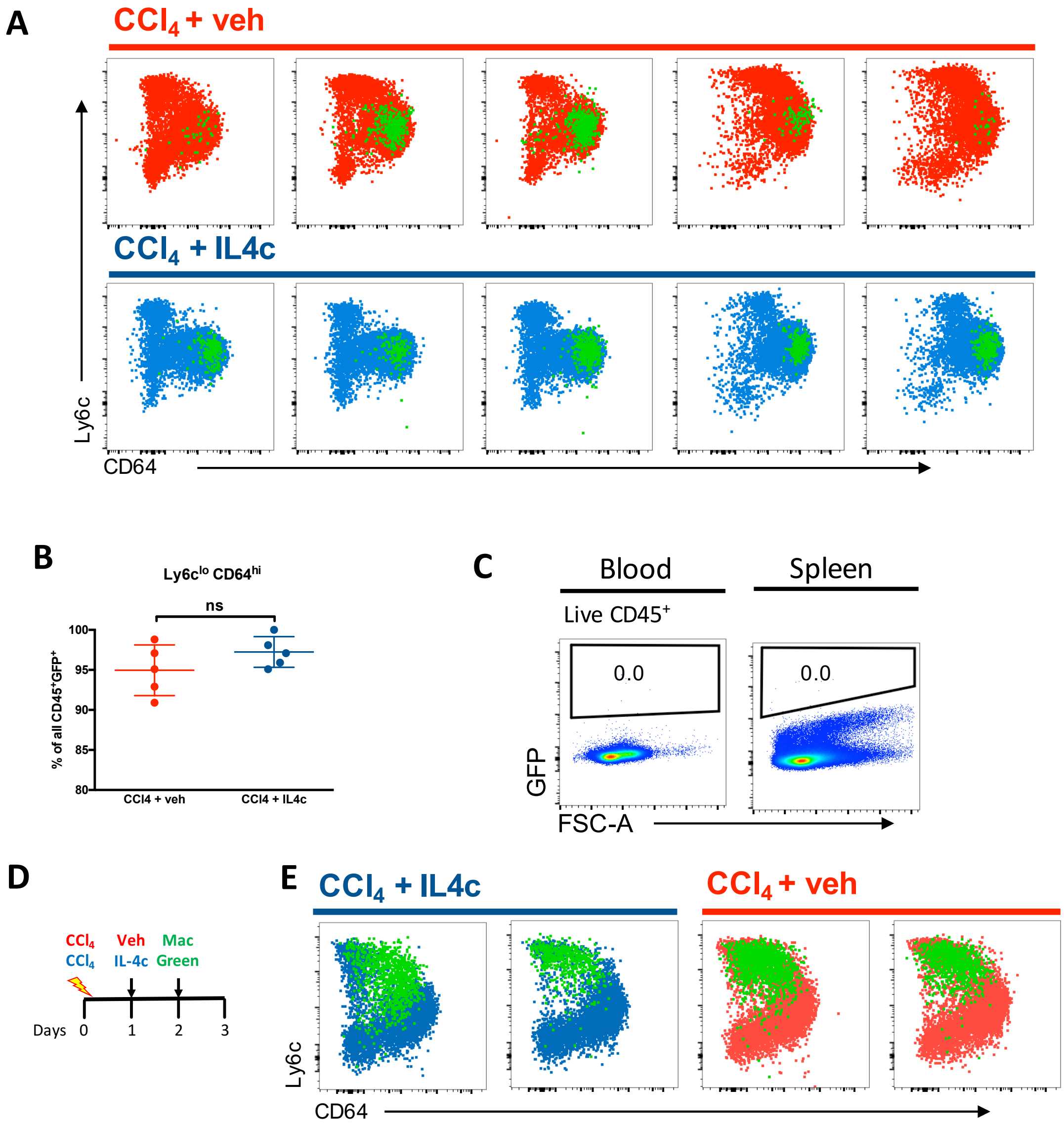

Figure 6-2 Maturation of GFP+ monocytes.

(A) Ly6C and CD64 expression by live (7AAD$^-$), CD31$^-$, CD45$^+$, Lin$^-$, Tim4^{lo}, CD11b^{hi} liver cells from recipients of CCl_4 + veh (red) or CCl_4 + IL-4c (blue) with donor monocyte-derived cells overlaid (green). (B) Proportion of adoptively transferred cells that have adopted the Ly6C^{lo} CD64^{hi} phenotype. N=6 mice/group, pooled from 2 independent experiments (unpaired *t* test). (C) Representative plots of GFP$^+$ cells in blood and spleen. (D) Schematic of adoptive transfer of GFP$^+$ Ly6C^{hi} monocytes administered 24 hrs after veh and IL-4c treatment and harvested 24 hrs later. (E) Ly6C and CD64 expression by live (7AAD$^-$), CD31$^-$, CD45$^+$, Lin$^-$, Tim4^{lo}, CD11b^{hi} liver cells from recipients of CCl_4 + veh (red) or CCl_4 + IL-4c (blue) with donor monocyte-derived cells overlaid (green). N=2 from 1 experiment.

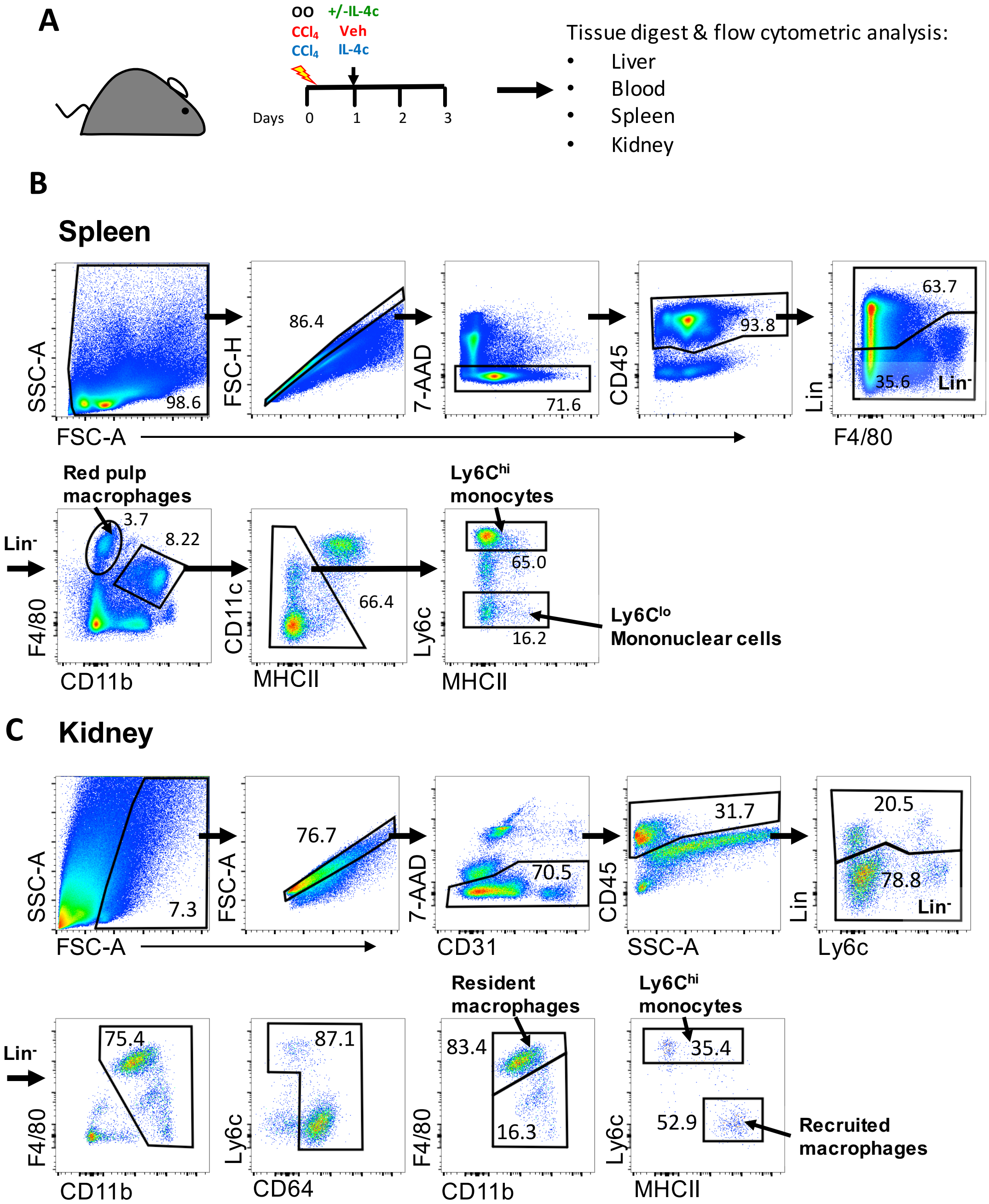

Figure 6-3 IL-4c treatment in multiple tissues.

(A) Schematic of experimental model mice, blood, liver, spleen and kindeys were harvested on day 3. (B-C) Representative plots of gating strategy used to identify monocytes and macrophages in spleen and kidney. Lineage gate in both panels comprised: CD3, CD19, Ly6G and Siglec-F.

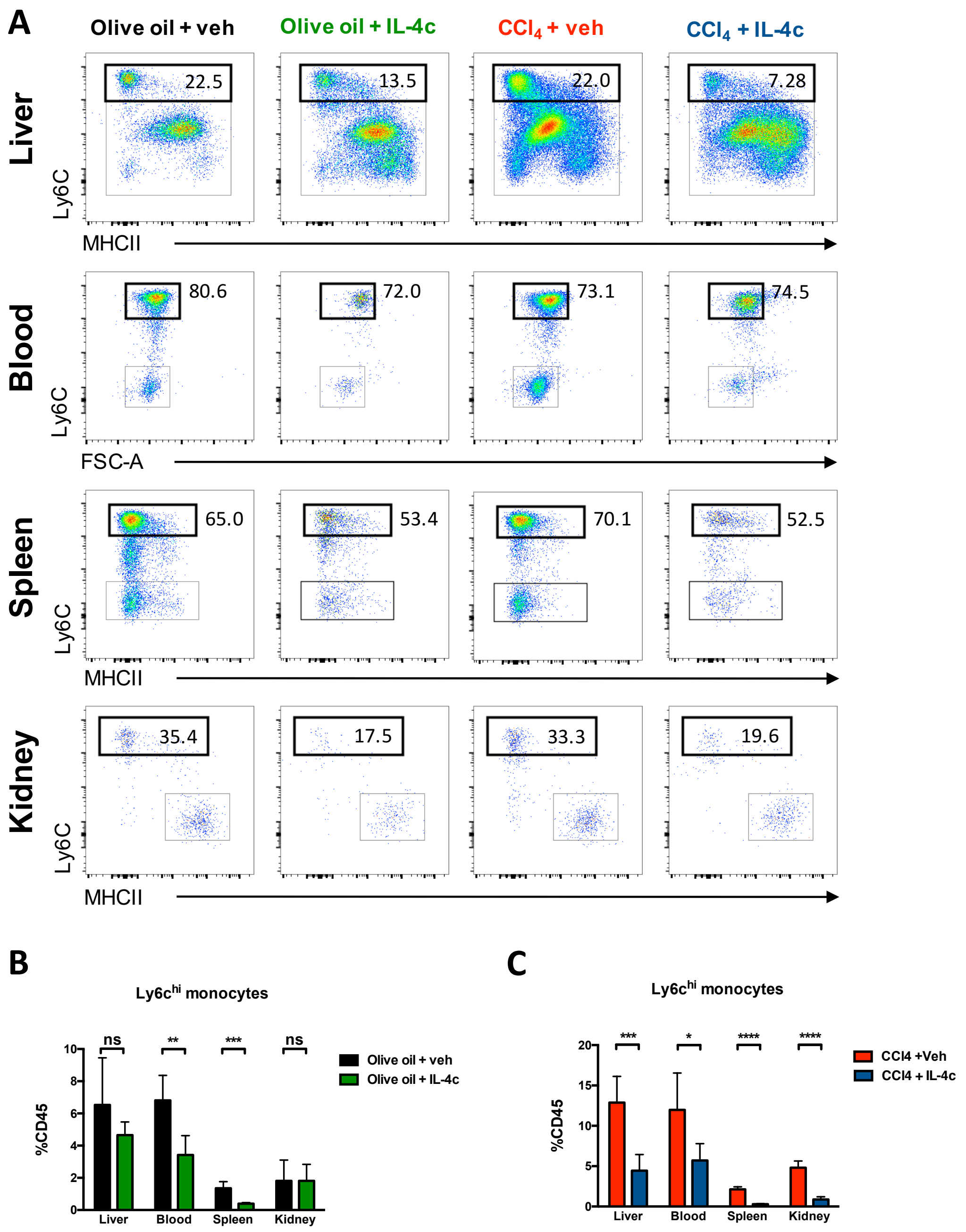

Figure 6-4 Effect of IL-4c on monocyte populations.

(A) Representative expression of Ly6C and MHCII by Lin⁻ CD11b^{hi} cells from liver, blood, spleen and kidney of mice administered olive oil or CCl4 ± IL-4c. (B) Frequency of Ly6C^{hi} monocytes of total CD45^{+} cells in each tissue in mice administered either olive oil + veh or olive oil + IL-4c. N=6 mice/group (multiple *t* tests with Holm-Sidak correction). (C) Frequency of Ly6C^{hi} monocytes of total CD45^{+} cells in each tissue in mice administered either CCl_4 + veh or CCl_4+ IL-4c. N=6 mice/group (multiple *t* tests with Holm-Sidak correction).

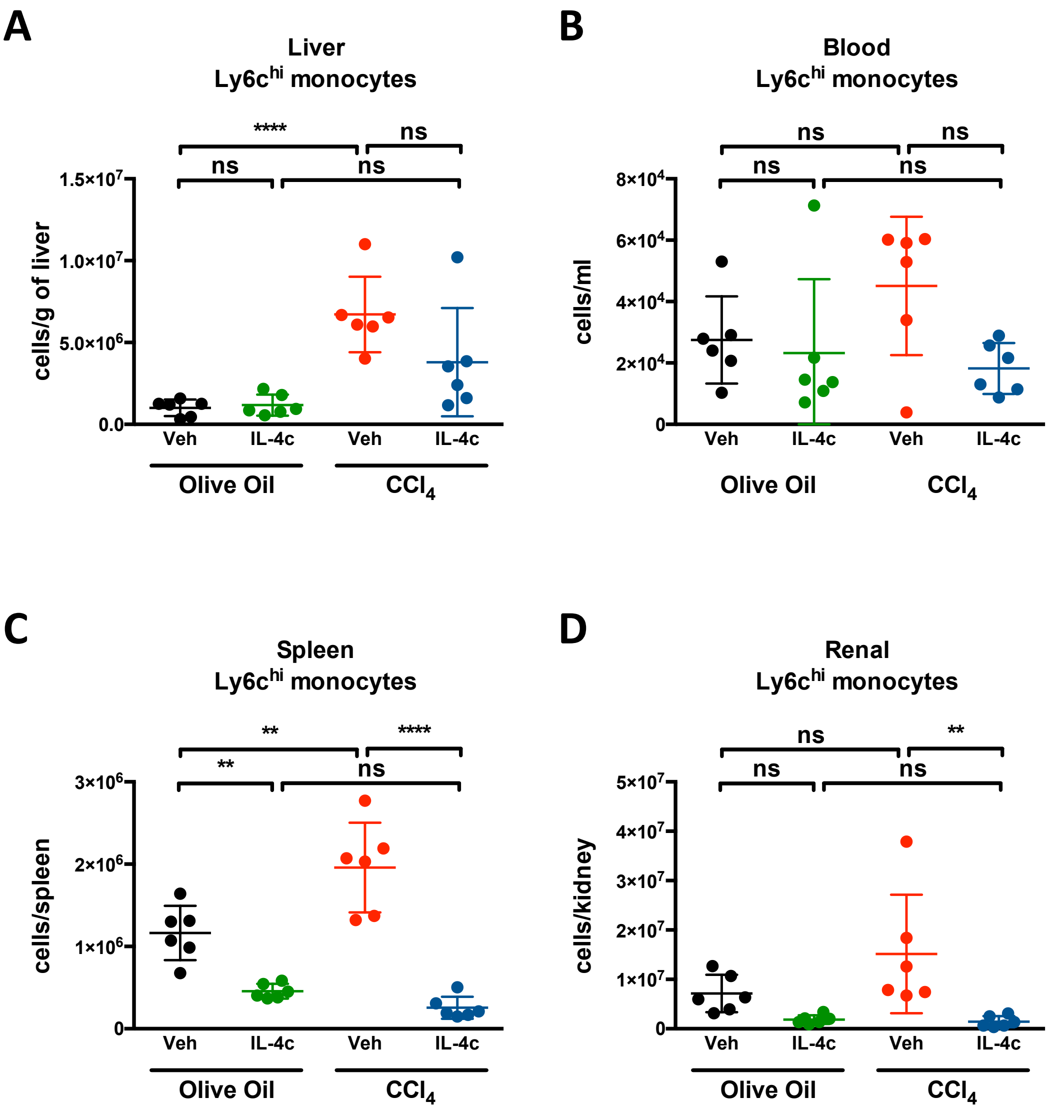

Figure 6-5 Effect of IL-4c on monocyte numbers.

(A-D) Number of Ly6C^{hi} monocytes in liver, blood, spleen and kidney of mice administered olive oil or CCl4 ± IL-4c. N=6 mice/group, pooled from 2 experiments, mean ± SD (one-way ANOVA).

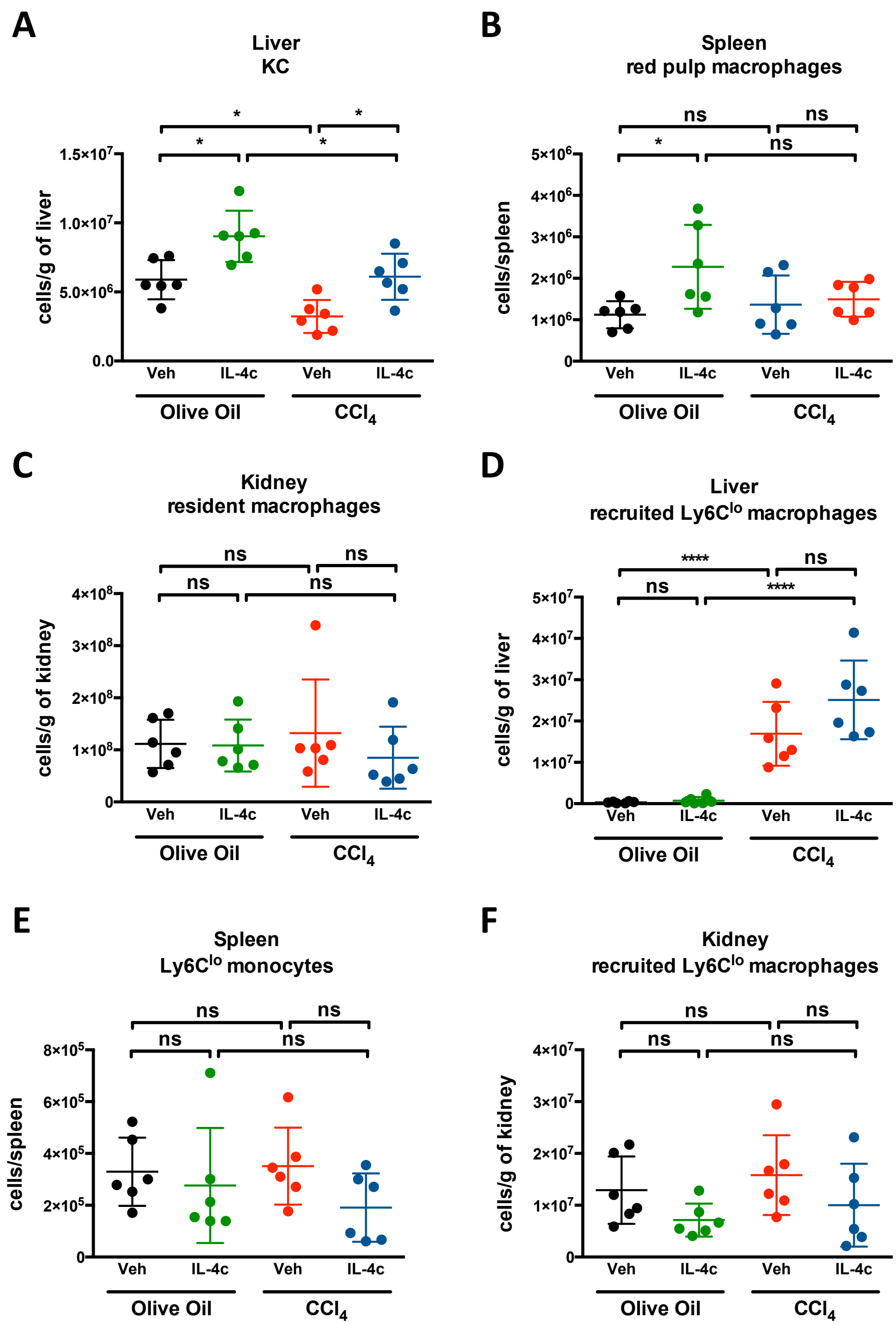

Figure 6-6 Number of macrophages in tissues.

(A-F) Number of resident and recruited macrophages per tissue. N=6 mice/group, pooled from 2 experiments, mean ± SD (one-way ANOVA).

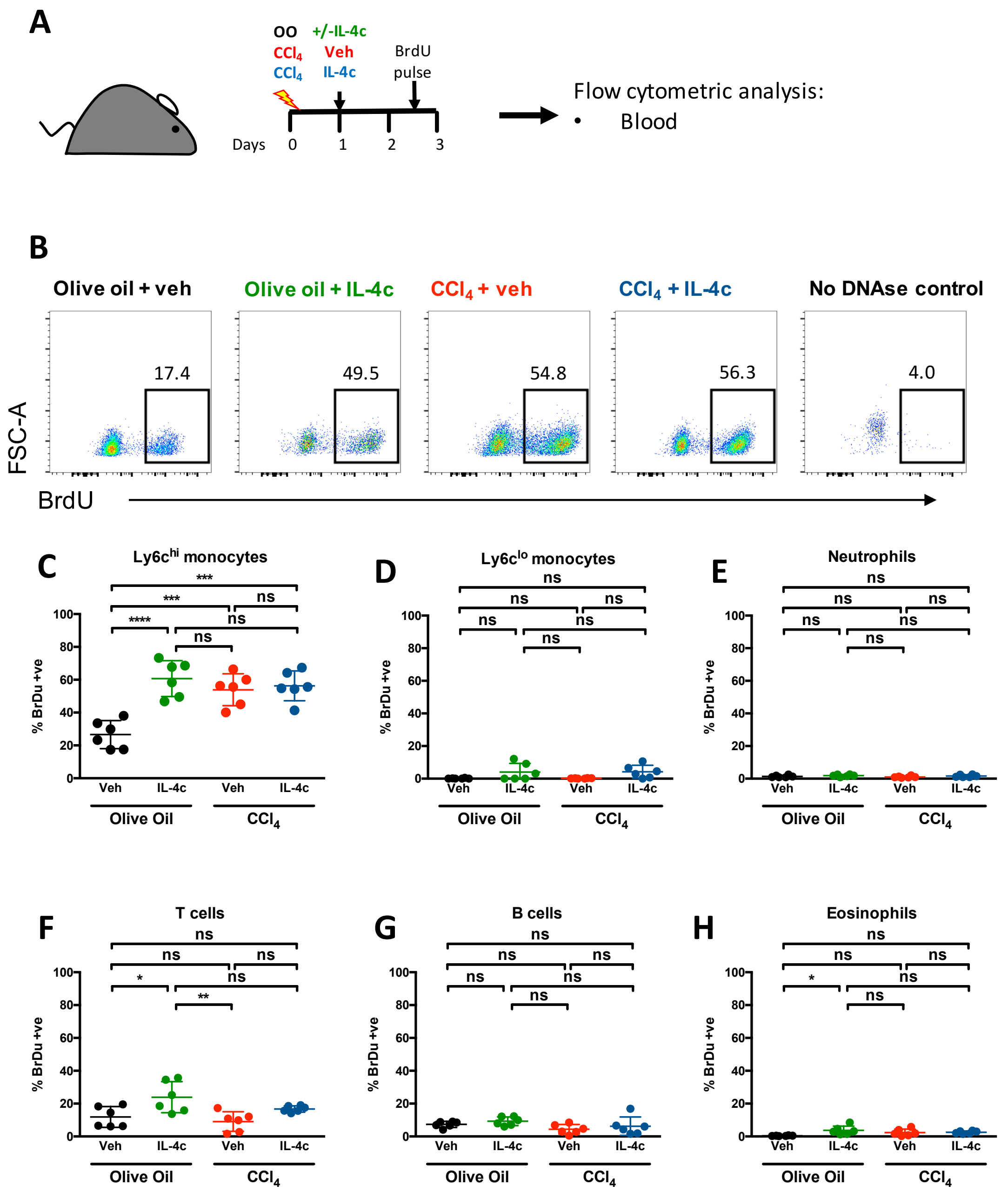

Figure 6-7 Proportion of BrdU+ cells in blood.

(A) Schematic of experimental model all mice were given either olive oil or CCl_4 + veh or IL-4c 24 hours later. All mice were pulsed with 1mg BrdU i.p 12 hours prior to necropsy on day 3. (B) Representative plots of BrdU and FSC-A expression in Live (7AAD), $CD45^+$, Lin (CD3, CD19, Ly6G and Siglec F)$^-$, $CD11b^+$, $CD115^+$, $Ly6C^{hi}$ monocytes. (C-H) Proportion of $BrdU^+$ cells for identified leukocyte populations. N=6 mice/group, pooled from 2 experiments, mean ± SD (one-way ANOVA).

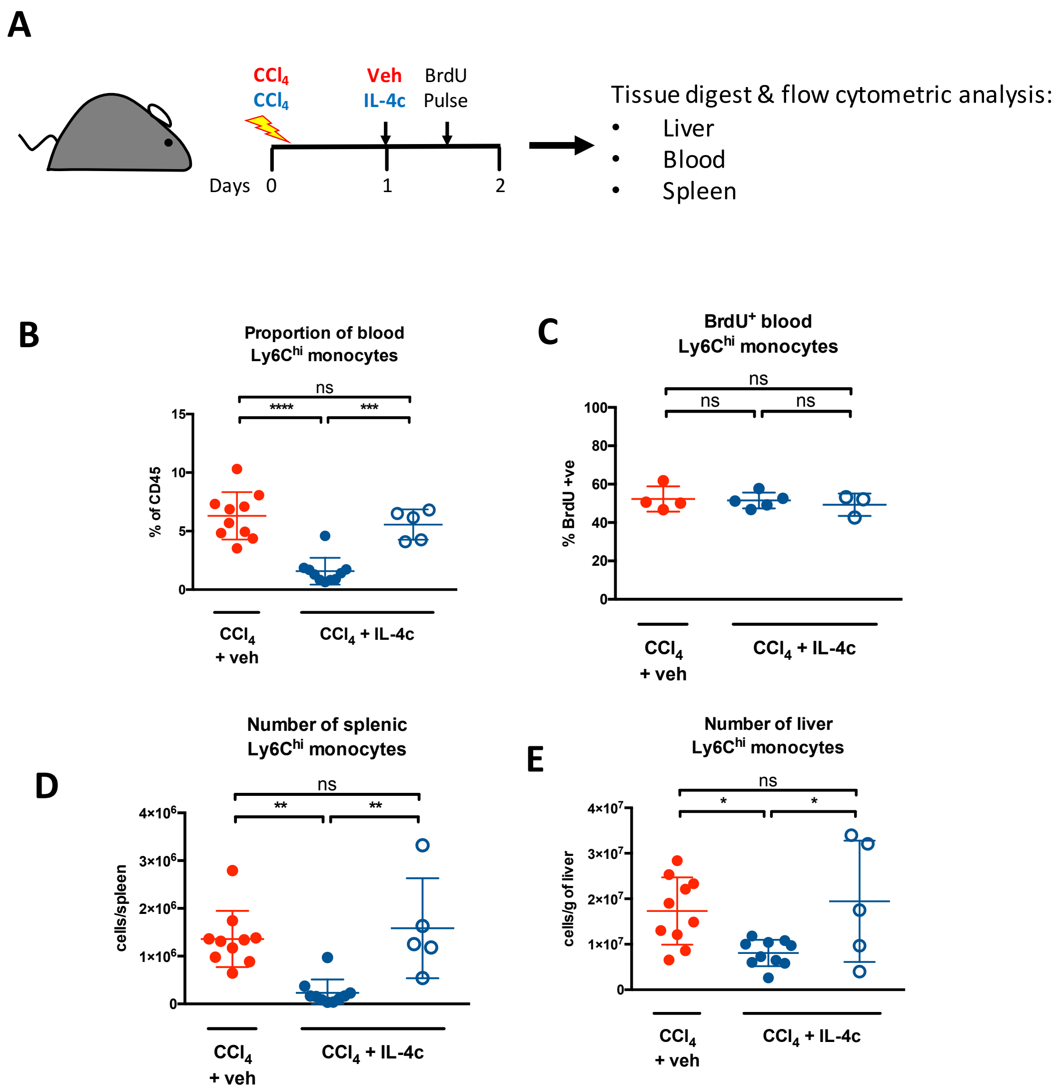

Figure 6-8 Ly6Chi monocyte dynamics in blood, spleen and liver 24 hrs after IL-4c.

(A) Schematic of experimental model all mice were given CCl_4 and then veh or IL-4c 24 hours later. A control population of 5 IL-4Ra$^{-/-}$ mice were given CCl_4 + IL-4c. All mice were pulsed with 1mg BrdU i.p 12 hours prior to necropsy on day 2. (B) Proportion of Ly6C^{hi} monocytes in blood. N=10 mice/group, N=5 mice group for control, pooled from 2 experiments, mean ± SD (one-way ANOVA). (C) Proportion of BrdU^{+} Ly6C^{hi} monocytes N=3-5 mice/group mean ± SD (one-way ANOVA). (D-E) Number of Ly6C^{hi} monocytes in spleen and liver. N=10 mice/group, N=5 mice group for control, pooled from 2 experiments, mean ± SD (one-way ANOVA).

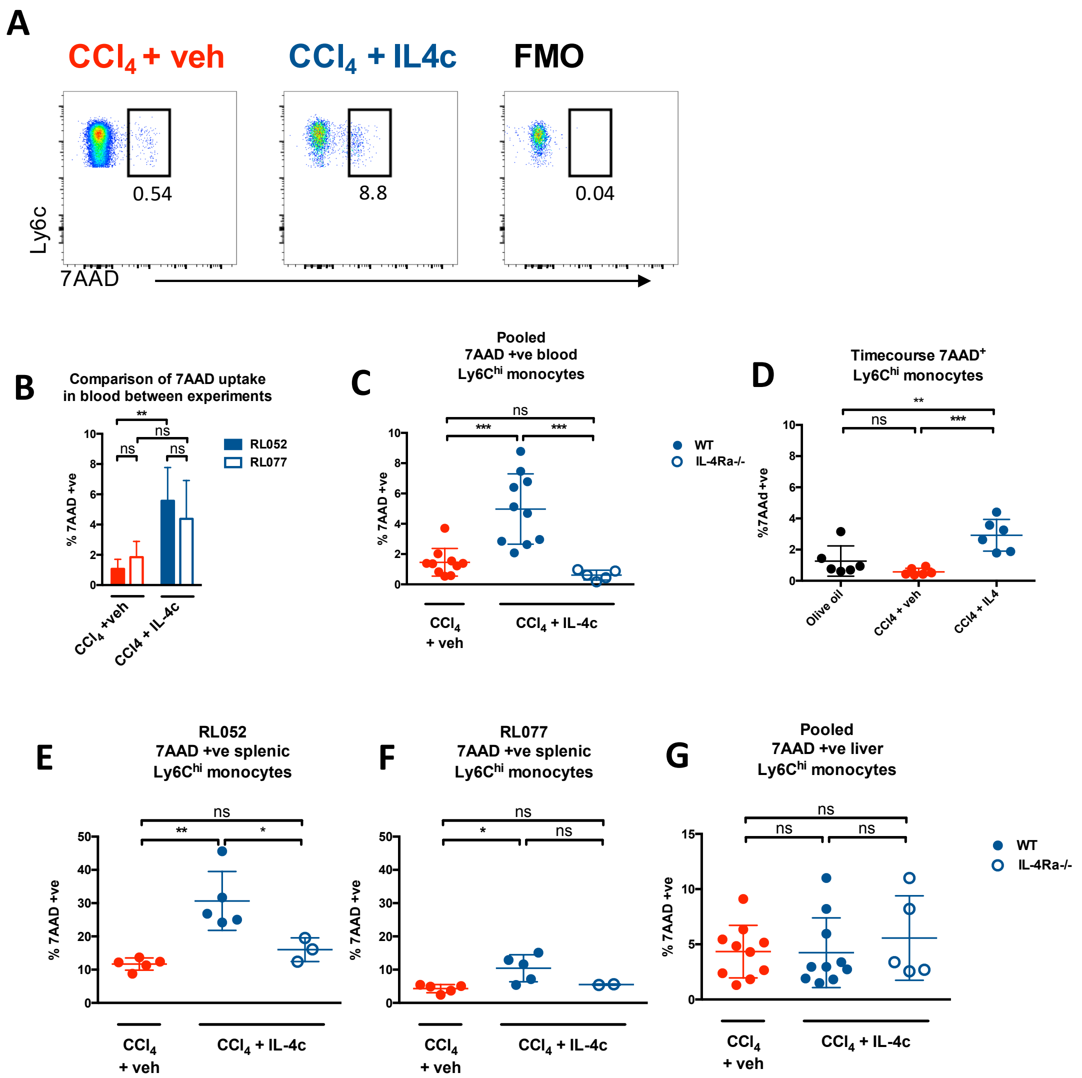

Figure 6-9 Assessment of monocyte viability in response to IL-4.

(A) Representative expression of Ly6C and 7AAD staining by Live (7AAD), CD45$^+$, Lin (CD3, CD19, Ly6G and Siglec F)$^-$, CD11b$^+$, CD115$^+$, Ly6C^{hi} monocytes. (B) Comparison of proportion of 7AAD$^+$ Ly6C^{hi} monocytes in blood from separate experiments. (N=5). (C) Proportion of 7AAD$^+$ Ly6C^{hi} monocytes in blood. (N=10 and 5 for control). (D) Comparison of proportion of 7AAD$^+$ Ly6C^{hi} monocytes in blood from separate experiments. (N=6). (E-F) Comparison of proportion of 7AAD$^+$ Ly6C^{hi} monocytes in spleen from RL052 and RL077 respectively (N=5 and 2-3 for control). (G) Proportion of 7AAD$^+$ Ly6C^{hi} monocytes in liver pooled data from 2 experiments (N=10 and 5 for control). Mean ± SD (one-way ANOVA).

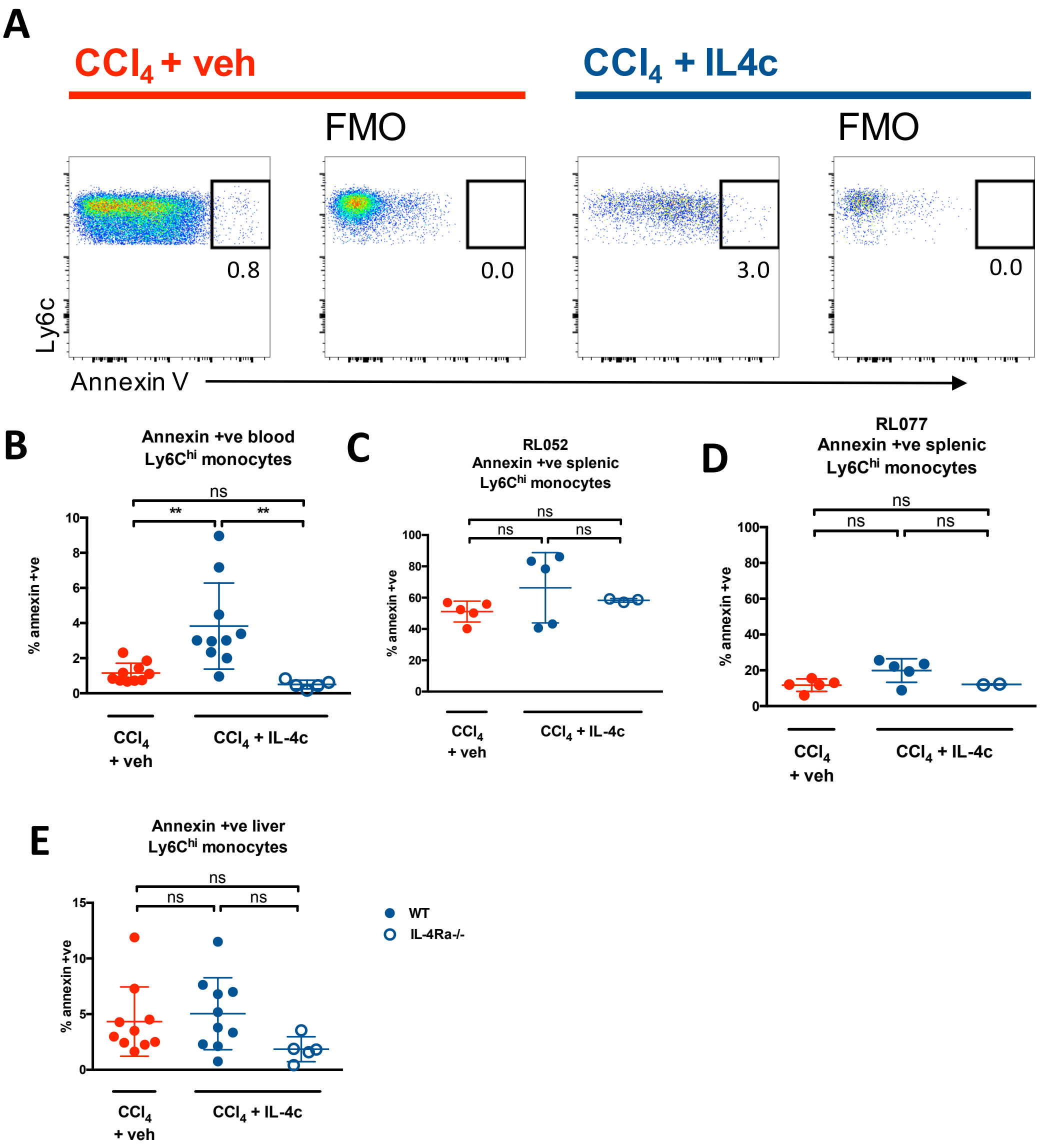

Figure 6-10 Proportion of Annexin V+ of monocytes and macrophages in tissues.

(A) Representative plots of Ly6C and Annexin V. expression in Live (7AAD), CD45$^+$, Lin (CD3, CD19, Ly6G and Siglec F)$^-$, CD11b$^+$, CD115$^+$, Ly6C^{hi} monocytes. (B) Proportion of Annexin V$^+$ Ly6C^{hi} monocytes in blood (N=10 and 5 for control). (C-D) Comparison of proportion of Annexin V$^+$ Ly6C^{hi} monocytes in spleen from RL052 and RL077 respectively (N=5 and 2-3 for control). (E) Proportion of Annexin V$^+$ Ly6C^{hi} monocytes in liver (N=10 and 5 for control) pooled data from 2 experiments (N=10 and 5 for control). Mean ± SD (one-way ANOVA).

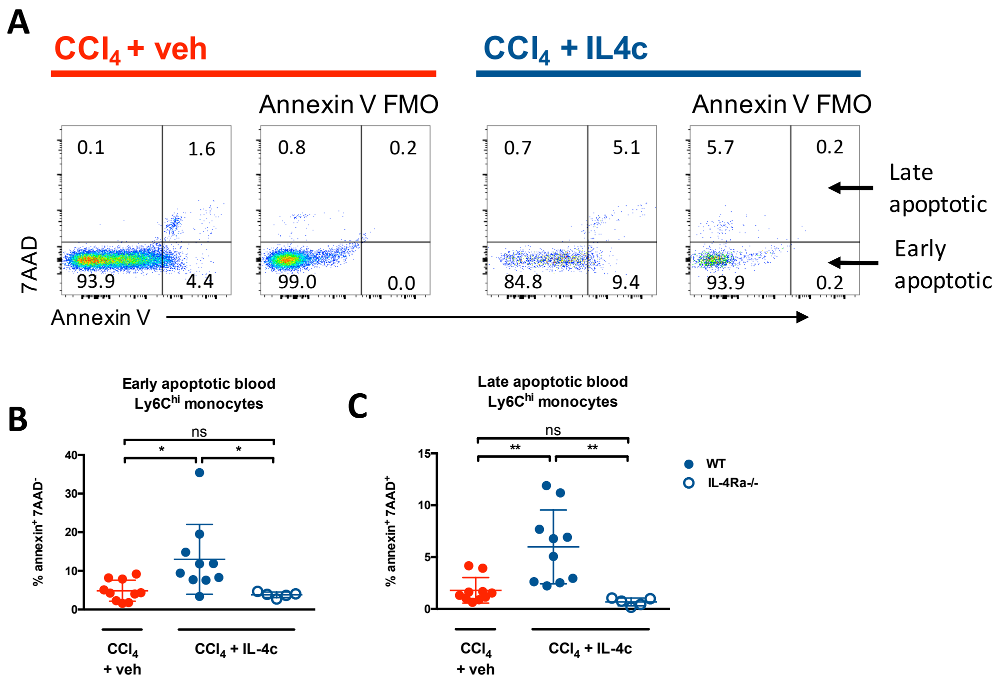

Figure 6-11 Late and early apoptotic Ly6Chi monocytes.

(A) Representative plots of 7AAD and Annexin V. expression in Live (7AAD), CD45$^+$, Lin (CD3, CD19, Ly6G and Siglec F)$^-$, CD11b$^+$, CD115$^+$, Ly6C^{hi} monocytes. (B) Proportion of early apoptotic blood Ly6C^{hi} monocytes. (C) Proportion of early apoptotic blood Ly6C^{hi} monocytes. N=10 and 5 for control, pooled from 2 experiments, mean ± SD (one-way ANOVA).

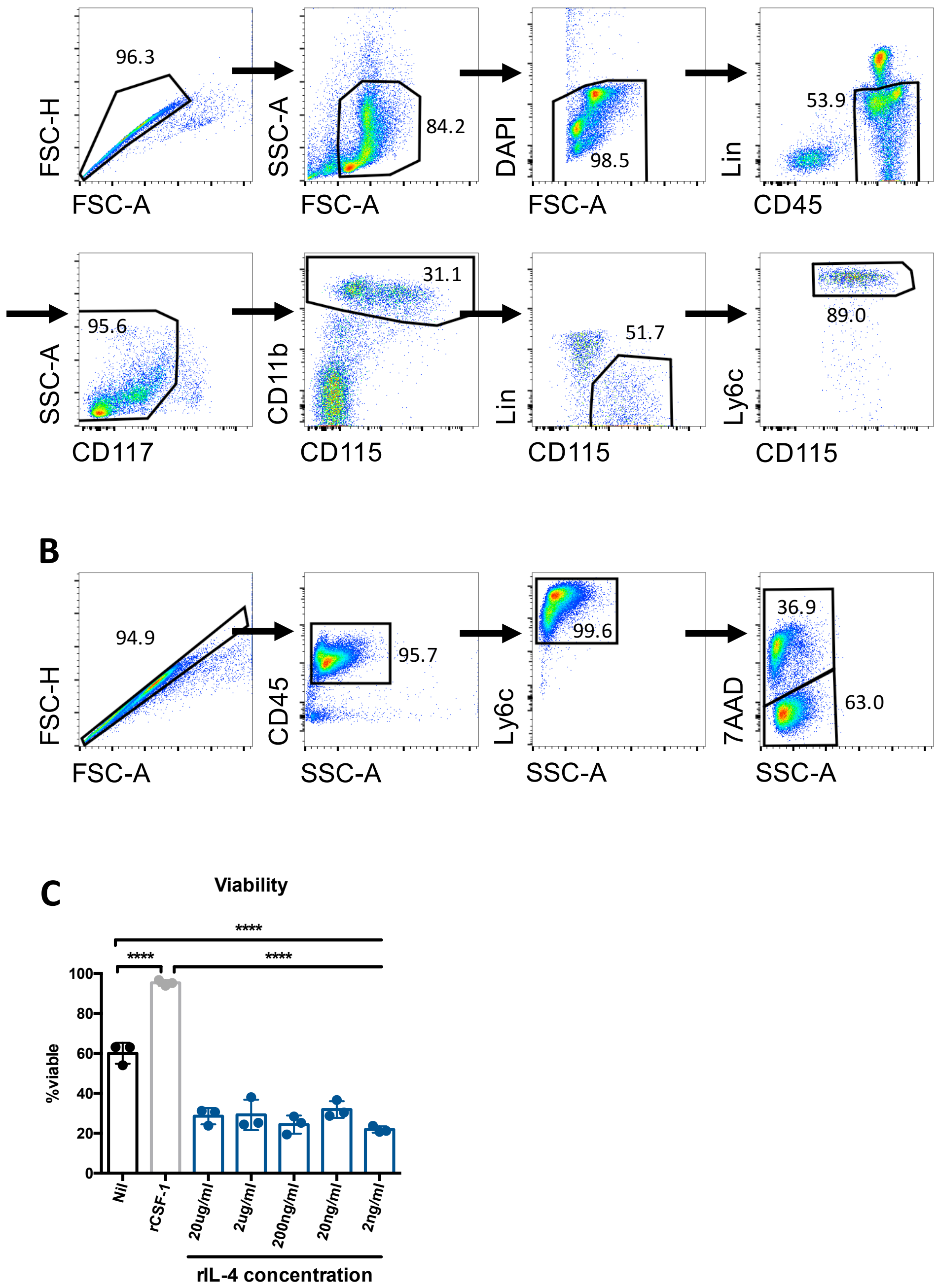

Figure 6-12 In vitro culture of monocytes.

(A) Gating strategy to sort Ly6^{hi} monocytes from bone marrow. (B) Gating strategy to identify live and dead Ly6C^{hi} monocytes following in vitro culture. (C) Proportion of viable monocytes according to culture conditions. N=3 technical replicates per group, 3 donor mice, mean ± SD (one-way ANOVA).

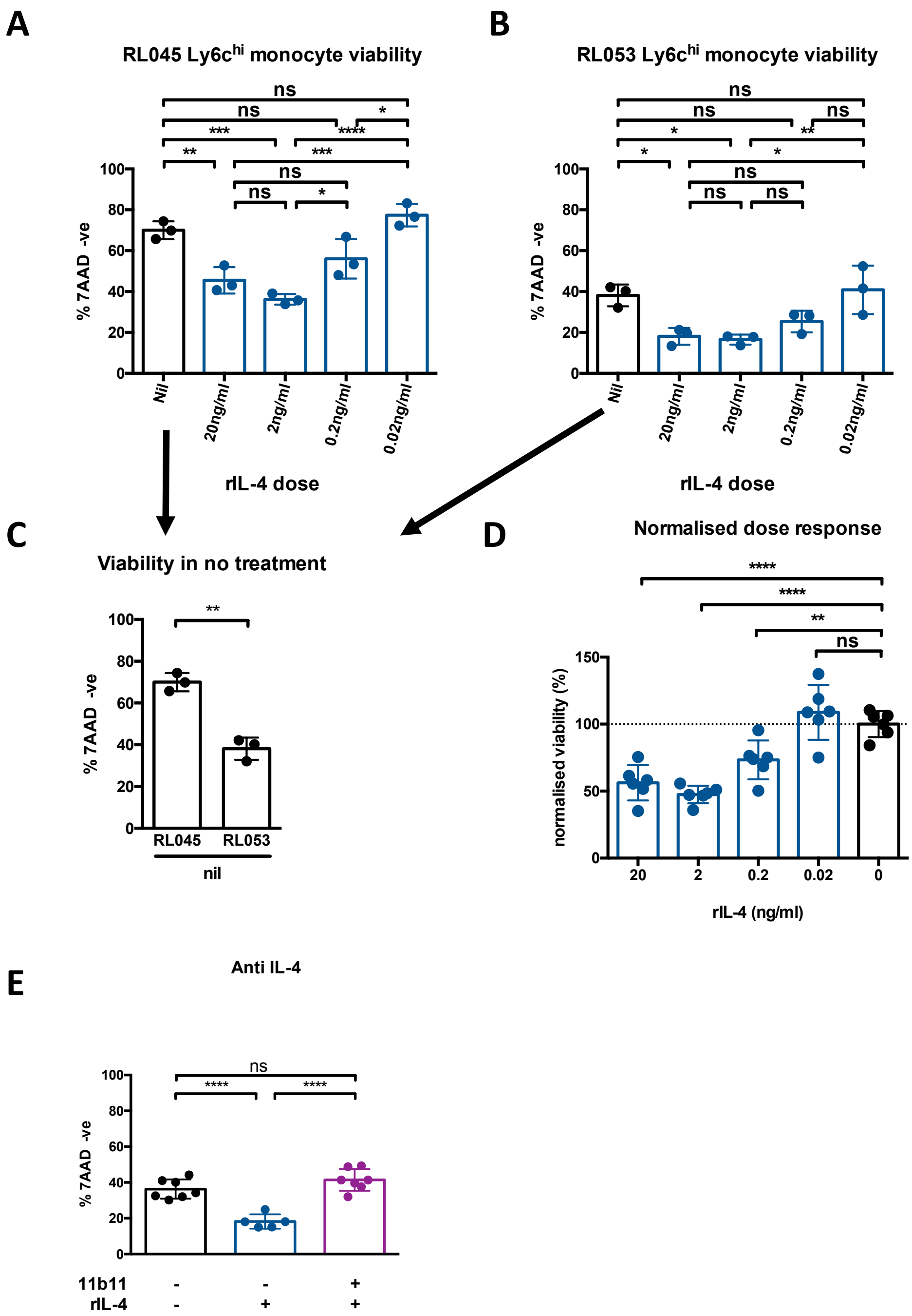

Figure 6-13 Dose effect of rIL-4 in vitro.

(A-B) Proportion of viable Ly6C^{hi} monocytes. N=3 biological replicates/group. (C) Comparison of viability in untreated monocytes from RL045 and RL053. (D) Ly6C^{hi} monocyte viability normalised to no treatment group. N=6 biological replicates/group pooled from 2 experiments. (E) Ly6C^{hi} monocyte viability following treatment with 11b11 (1mg/ml). N=5-7 biological replicates pooled from 2 experiments, mean ± SD (one-way ANOVA).

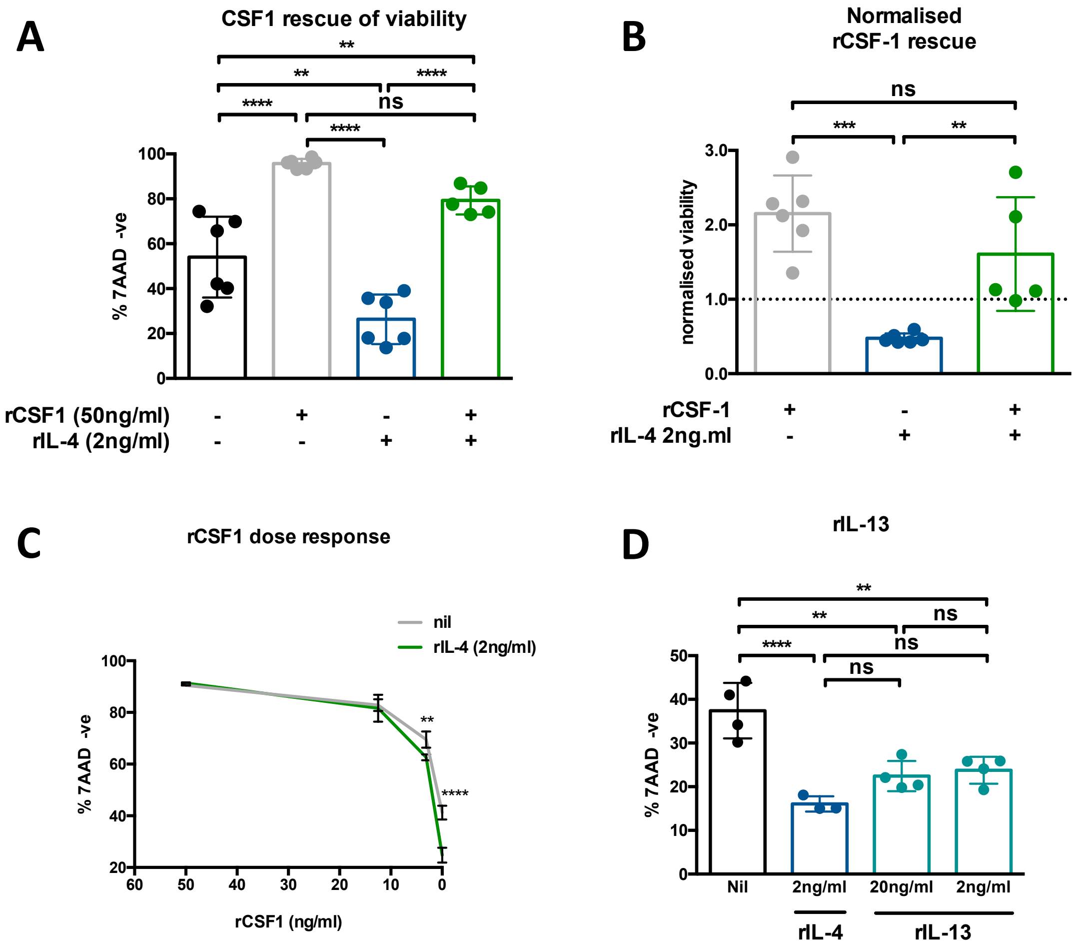

Figure 6-14 Effect of CSF-1 on viability in vitro.

(A) Proportion of viable Ly6C^{hi} monocytes. N=5-6 biological replicates/group. (B) Ly6C^{hi} monocyte viability normalised to no treatment group. N=5-6 biological replicates/group pooled from 2 experiments. (C) Dose titration of rCSF-1 in Ly6C^{hi} monocytes cultured with media or media + rIL-4. N=3 biological replicates/group, mean ± SD (multiple *t* tests with Holm-Sidak correction). (D) Proportion of viable Ly6C^{hi} monocytes cultured with rIL-13 or rIL-4. N=3-4 biological replicates/group. Unless otherwise stated mean ± SD (one-way ANOVA).

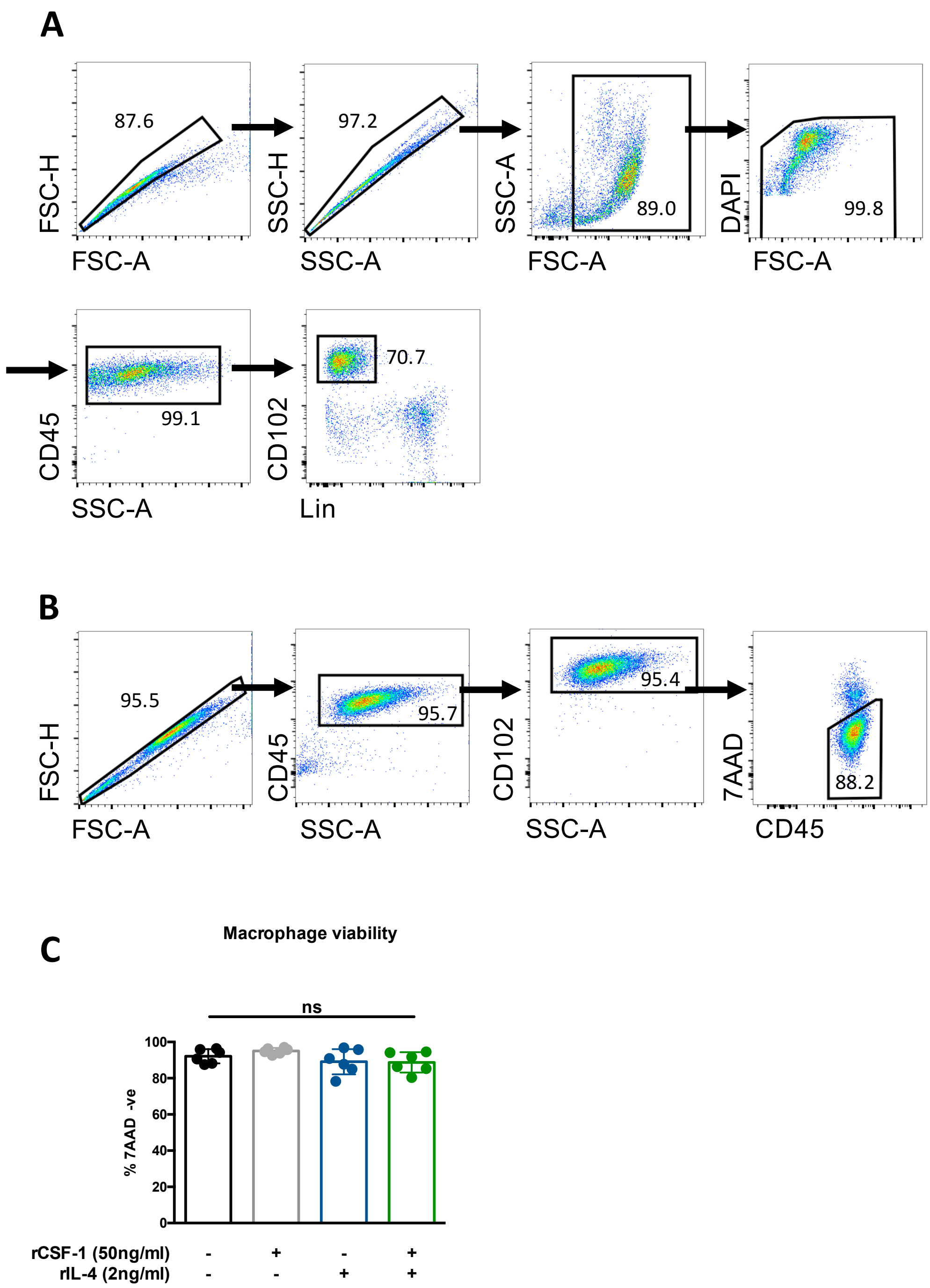

Figure 6-15 Peritoneal macrophages in vitro.

(A) Gating strategy to sort CD102⁺ macrophages from bone peritoneal washes. (B) Gating strategy to identify live and dead CD102⁺ macrophages following in vitro culture (D) Proportion of viable CD102⁺ macrophages following overnight culture with combinations of rIL-4 and rCSF-1. N=6 biological replicates/group pooled from 2 experiments, mean ± SD (one-way ANOVA).

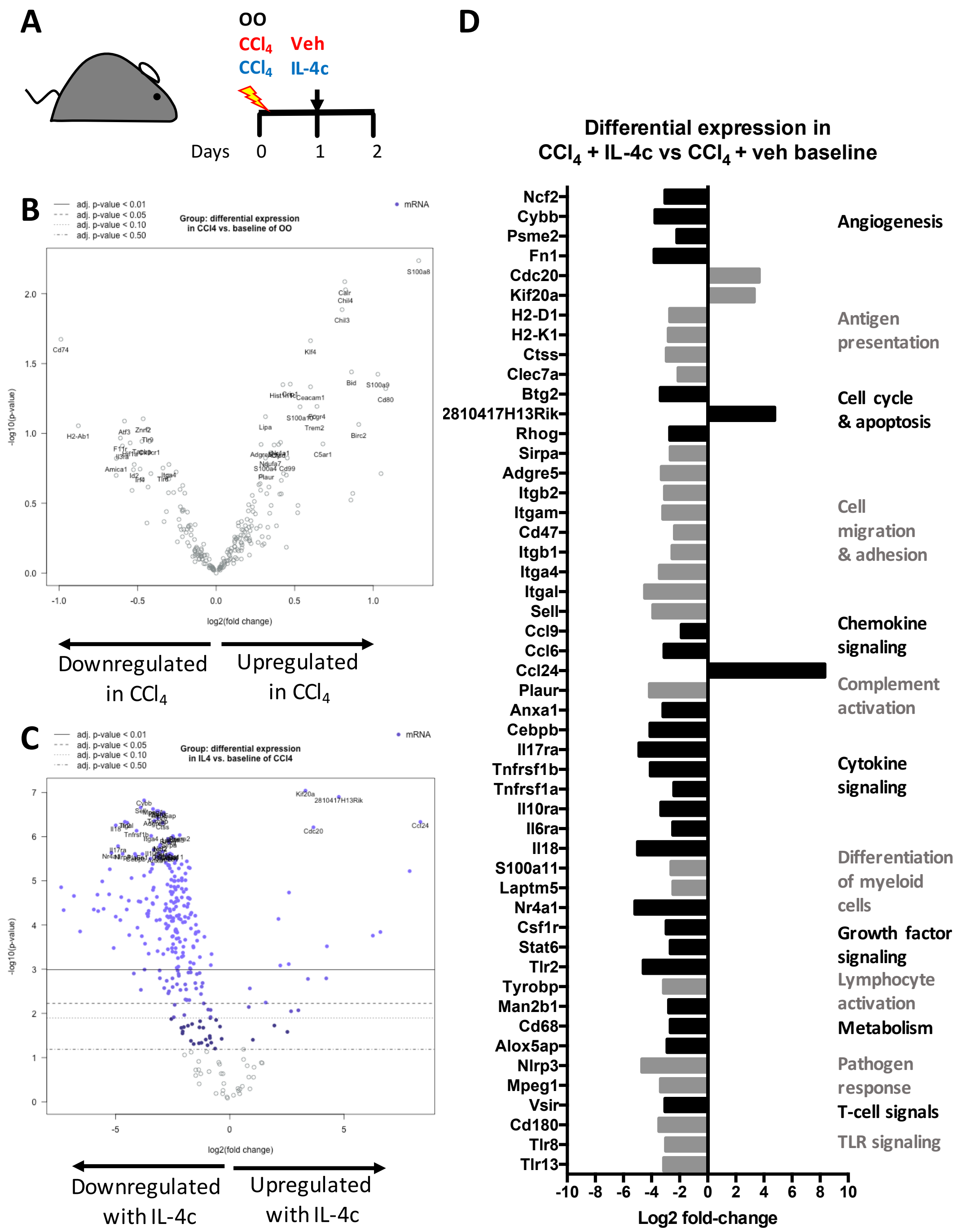

Figure 6-16 Nanostring on circulating Ly6Chi monocytes.

(A) Schematic of experimental plan mice either received olive oil; CCl_4 + veh or CCl_4 + IL-4c. (B) Volcano plot of olive oil vs a baseline of CCl_4 + veh. (C) Volcano plot of CCl_4 + IL-4c vs a baseline of CCl_4 + veh. (D) Log2 fold-change of 50 most significantly differentiated genes in CCl_4 + IL-4c vs a baseline of CCl_4 all P<0.01.

Chapter 7 Therapeutic IL-4c in APAP and DSS colitis

7.1 Introduction

I observed in earlier chapters that therapeutic IL-4c treatment improved indices of acute liver injury secondary to CCl_4-induced hepatocyte necrosis. I have also demonstrated in this injury setting that coincident with accelerated repair, therapeutic IL-4c causes a significant reduction in recruited Ly6C^{hi} monocytes and an increase in recruited Ly6^{lo} macrophages. Due to a lack of reliable genetic tools to comprehensively determine a causative effect between IL-4R signalling to monocytes and monocyte-derived macrophages and the observed acceleration in repair, I chose instead to focus the final months of my PhD research on the novel role for IL-4 in driving monocyte death. Therefore, I chose to establish whether this effect of IL-4c could be replicated in other models of inflammation characterised by Ly6C^{hi} monocytosis. Similar to acute CCl_4 injury, acetaminophen (APAP) causes zone 3 necrosis around the central vein and regeneration is dependent on recruitment of monocytes[42,45,307]. As a brief reminder, pro-inflammatory Ly6C^{hi} monocytes are recruited following APAP injury within the first 12 hours and contribute to the injury, but are also required for tissue repair by converting into Ly6C^{lo} macrophages which are characterised by high expression of pro-reparative genes [21,23]. The importance of the initial recruitment of Ly6C^{hi} monocytes is emphasised by the impaired healing observed when their recruitment was inhibited using *Ccr2*$^{-/-}$ mice or the anti-CCR2 monocyte depleting antibody (MC21)[21,145]. I therefore hypothesised that therapeutic IL-4c administration in APAP injured mice would be beneficial by reducing the number of pro-inflammatory Ly6C^{hi} monocytes while promoting expansion of pro-reparative Ly6C^{lo} macrophages. Given the pan-tissue nature of the phenotype observed with IL-4c treatment, I also decided to examine a model of monocytic inflammation in another tissue. Dextran sodium sulphate (DSS) induced colitis is one of the commonest models of human inflammatory bowel disease (IBD). DSS is administered in the drinking water which leads to disruption of the epithelial barrier and subsequent exposure of the lamina propria to luminal microbiota that in turn drives a submucosal inflammatory response and intestinal ulceration[308]. The resulting illness develops over the course of a week with mice reaching a humane endpoint at between day 6 and 8[253,309,310]. The humane endpoints are defined by a clinical score which is calculated on a daily basis by quantifying: weight loss; stool consistency; blood loss and general appearance[253]. This daily score enables longitudinal assessment of disease severity and therefore offers the potential to assess in real-time the effect of IL-4c over the disease course. Importantly, DSS colitis is characterised by an increase in CCR2 dependent Ly6C^{hi} monocytes in the colonic lamina propria during inflammation[116,117]. Furthermore, it has been shown that depleting monocytes using the MC21 antibody results in an amelioration in DSS colitis, as measured by a reduced endoscopic colitis score, less weight loss and a reduction in colonic pro-inflamatory cytokines (e.g. IL-6, IL1β and IFNγ)[116]. I therefore hypothesised that reducing Ly6C^{hi} monocytes using IL-4c would also be beneficial.

Hence in this chapter I will use two disease models in which monocytes are considered to potentiate pathology but which manifest in distinct tissue sites to determine whether therapeutic IL-4 can coincidentally knock down monocytosis and lead to reduced disease severity.

7.2 Early IL-4c treatment in APAP

Zigmond et al. had previously observed in APAP that the hepatic Ly6C^{hi} monocytosis peaks at 24hrs post injury and returns to basal levels by 72hrs by which time Ly6C^{hi} monocytes have converted to Ly6C^{lo} macrophages[21]. This is significantly earlier than I observed in the acute CCl_4 injury model where the Ly6C^{hi} monocytosis persisted until at least 72 hours post-injury (Fig. 5.2)[21]. Given the earlier apparent conversion and/or loss of monocytes during APAP I decided in my pilot experiment to administer IL-4c at 12 hours after administration of APAP rather than at 24hrs as done in the CCl_4 model, and harvest mice 12 hours later (Fig. 7.1A).

7.2.1 Early IL-4c administration is detrimental in APAP

12 hours following treatment with IL-4c or veh it was evident by observation of the animals that the IL-4c group were sicker than the veh treated group, with decreased movement and piloerection exhibited by all IL-4c treated mice compared with only one veh treated mouse. However, there was no difference in weight loss between treatment groups at the endpoint (Fig. 7.1B) and due to the small sample size, it was also not possible to say with any confidence whether there was a definitive effect of IL-4c on serological markers of liver injury such as ALT, AST, bilirubin and albumin (Fig. 7.1C-F). Due to technical reasons, I was unable to obtain blood from one of the mice in the IL-4c treated group.

7.2.2 Trend to reduced Ly6C^{hi} monocytes with IL-4c

There was a trend to a reduction in the proportion of Ly6C^{hi} monocytes in the livers of mice given APAP + IL-4c compared to APAP + veh treatment (20.2% ± 5.5 vs 36.6% ± 17.4), however this was not evident when corrected for numbers and may reflect changes in other CD45^{+} populations (Fig. 7.2A-B). There was no apparent change in proportion of recruited Ly6C^{lo} MHCII^{int} macrophages between veh and IL-4c treated groups (Figs. 7.2C-D), which remained conspicuously absent in all groups. There was however a reduction in Kupffer cells with APAP treatment when compared to PBS controls but there was no difference between IL-4c and veh treated mice (Fig. 7.2E-F). I did observe a trend to an increase in both proportion and number of neutrophils in the APAP + IL-4c group when compared to APAP and saline (Fig 7.2G-H). Zigmond et al. suggested that persistent neutrophilia that arises in the absence of monocytes is detrimental in liver injury[21] and I therefore sought to determine if there was any correlation between the high neutrophil counts found during flow cytometric analysis and the elevated hepatic serum enzymes. Indeed, there was a significant correlation between enzyme level (ALT and AST) and neutrophil number, with a pearson correlation of 0.88 and 0.89 for ALT and AST respectively (Fig. 7.2I-J). Notably, the mouse from the

APAP + veh group with the highest ALT and AST demonstrated decreased movement at the time of necropsy and had elevated numbers of neutrophils when compared to the other mice in this group (Fig. 7.2H). This pilot experiment suggested that IL-4c treatment might have an effect on neutrophils which may be of interest given the known role of Ly6C^{hi} monocytes in regulating neutrophil number[21]. The lack of obvious improvement in animal health and indeed, potential decline as determined by clinical signs, meant that, in consultation with the named veterinary surgeon, I deemed it not appropriate to repeat this experiment from a 3R perspective.

7.3 IL-4c treatment 24 hours after APAP

Due to the potential detrimental effect of IL-4 treatment when delivered 12hrs post APAP injury and the working hypothesis that this might primarily be due to increased numbers of neutrophils, I hypothesised that IL-4c administration at 24hrs post injury may be beneficial as Zigmond et al. showed that neutrophil numbers had plateaued by this point[21]. I therefore performed a second pilot experiment where IL-4c was administered 24 hours following APAP and harvest mice 48 hours later (Fig. 7.3A).

7.3.1 Phenotypic analysis following IL-4c administration

As before, IL-4c treatment had no effect on mouse weight (Fig. 7.3B). There was a trend to lower ALT (Fig. 7.3C) and a significant reduction in AST (Fig. 7.3D) in mice treated with IL-4c compared to veh, 114.0 u/l ± 42.0 vs 249.7 u/l ± 142.8 and 109.2 u/l ± 28.5 vs 234.3 ± 93.2, respectively. There was no significant difference in bilirubin or albumin between treatment groups (Fig. 7.3E-F). Furthermore, there was no evidence of decreased mobility or piloerection in any of the mice as was seen with administration of IL-4c at 12hrs.

7.3.2 Effect of IL-4c treatment on leukocyte populations

Analysis by flow cytometry revealed a possible trend to a reduction in number of Ly6C^{hi} monocytes following IL-4c treatment compared to veh (1.4×10^6

cells/g ± $8.8x10^5$ vs $4.4x10^6$ cells/g ± $1.9x10^6$) (Fig. 7.4A-B). However, unlike in CCl_4 injury, this was not reflected by a concomitant increase in $Ly6C^{lo}$ $CD64^{hi}$ macrophages and there was in fact a significant reduction in proportion of $Ly6C^{lo}$ macrophages with IL-4c treatment, although this wasn't reflected by a reduction in numbers (Fig. 7.4C-D). As with CCl_4 there was a significant reduction in proportion of Kupffer cells in all groups that received APAP when compared to veh, although this did not translate to a significant difference in numbers (Fig. 7.4E-F). In contrast to early administration of IL-4c in APAP, there was no effect of IL-4c administration on neutrophil numbers (Fig. 7.4G-H). Similar to my observations in the CCl_4 model, there was a significant increase in proliferation in hepatic $Ly6C^{hi}$ monocytes but there was no effect on $Ly6C^{lo}$ macrophage proliferation, which was unexpected (Fig. 7.4I-J). In the blood, as with IL-4c treatment in CCl_4 injury there was a reduction in the proportion of $Ly6C^{hi}$ monocytes (Fig. 7.4K).

Hence, as with CCl_4-mediated injury, delivery of IL-4c at 24hrs post APAP led to reduced indices of injury and loss of $Ly6C^{hi}$ monocytes from the blood. However, in contrast to CCL_4-mediated injury and the promising pilot data generated following delivery of IL-4 at 12hrs post APAP injury, the numbers and frequencies of monocytes in the liver remained largely unaffected following delivery of IL-4 at 24hrs post APAP. Furthermore, the potential increase in hepatic neutrophils seen with IL-4 delivery at 12hrs post APAP was not observed following delivery of IL-4 at 24hrs post APAP.

7.3.3 Technical issues

One of the wild type control mice has been excluded from analyses because it had an ALT of 1340 u/l, a level normally observed in mice experiencing liver injury and it also had a significantly elevated proportion of hepatic $Ly6C^{hi}$ monocytes on analysis suggesting that for some reason this mouse had an acute liver injury. Furthermore, one of the mice in the APAP + veh group had a white lesion in the left lobe of liver at necropsy and I therefore analysed the caudate lobe of this mouse liver too. Analysis of the results showed that in the left lobe there was a significant inflammatory infiltrate associated with the lesion I have therefore presented the results from the caudate lobe as these were in keeping with the results from the other APAP + veh mice. Finally, one of the blood samples from a mouse in the uninjured group was significantly haemolysed rendering the interpretation of bilirubin invalid.

7.4 DSS colitis model

As outlined above, I wanted to establish if IL-4c administration following initiation of DSS colitis could be beneficial. It was therefore necessary to establish the dynamics of 2% DSS colitis in our animal unit because the rate of onset of colitis is highly dependent on the gut microbiota[311]. In a pilot experiment, I administered 2% DSS to wild type mice for 6 days (Fig. 7.5A). As has been reported in the literature, there was an initial weight gain in the DSS treated group compared to the H_2O control group[312,313] (Fig. 7.5B). This weight gain persisted until day 6 when there was a significant reduction in weight compared to the H_2O group, this was also reflected by a significant increase in the disease activity index (DAI) at this point (Fig. 7.5C).

7.4.1 Analysis of monocytes and macrophages in DSS colitis

To interrogate the effects of IL-4c on the monocyte/macrophage populations, I performed flow cytometric analysis of enzymatically digested colon, as per published protocols [314]. Monocytes and macrophages were identified as previously described as single, live (7-AAD), $CD45^+$, Lin (CD3, CD19, Ly6C and NK1.1)$^-$, Siglec F^-, $CD11b^{hi}$, $Ly6C^{hi}$ and $CD64^{hi}$ (Fig. 7.5D)[117]. Within this population it was possible to identify newly arrived $Ly6C^{hi}$ $MHCII^{lo}$ monocytes (P1), transitioning $Ly6C^{hi}$ $MHCII^{hi}$ (P2) and $Ly6C^{lo}$ $MHCII^{hi}$ colonic macrophages (P3)[90]. As described previously[116,117], there was a significant increase on day 6 in the proportion of P1 and P2 monocytes in the colons of mice that received DSS, that was paralleled by a significant reduction in proportion of resident macrophages (P3) (Fig. 7.6A-B). When corrected for number of cells/colon there was a trend for an increase in P1 monocytes in DSS-treated mice ($3.3x10^5$ cells/colon ± $2.2x10^5$ vs $1.7x10^4$ cells/colon vs

$4.0x10^3$) accompanied by a significant increase in the P2 population ($3.5x10^5$ cells/colon ± $1.4x10^5$ vs $2.0x10^4$ cells/colon vs $5.1x10^3$) and a trend towards reduced numbers of the P3 macrophages in the DSS group ($2.9x10^5$ cells/colon ± $1.7x10^5$ vs $4.6x10^5$ cells/colon vs $7.8x10^4$) (Fig. 7.6C). As expected from the work of others, the development of DSS colitis also resulted in a significant increase in the proportion of circulating Ly6C^{hi} monocytes (Fig. 7.6D)[116,117].

7.5 IL-4c treatment during DSS colitis

Having established in the pilot experiment that there was the expected Ly6C^{hi} monocytosis present in the colons of mice given DSS, I next needed to establish at what timepoint to administer IL-4c to modulate the inflammatory response. Unpublished work by Dr. Calum Bain had shown that there is a Ly6C^{hi} monocytosis in the colon on day 3 prior to the development of any clinical signs of colitis, suggesting this could be an ideal time to intervene with IL-4c. To ensure there was a Ly6C^{hi} monocytosis in my hands with this model, I first performed analysis of colons at day 3 of DSS delivery. Analysis of colons revealed there to be a limited but significant increase in the proportion of P1 monocytes at this timepoint but no change in P2 or P3 populations, offering a potential target for IL-4c treatment (Fig. 7.7A).

7.5.1 Inconsistent outcomes in IL-4c treatment in DSS

Given these results, I decided to administer IL-4c on day 3 and again on day 5 and day 7 to account for the half-life of IL-4c (~48 hours)[32] (Fig. 7.7B). The experiment involved 3 cages of mice that received DSS. One cage (cage 3, n=4) was harvested on day 3 to provide an indication of the leukocyte populations at the time when IL-4c was administered. Cage 1 (n=7) and cage 2 (n=5) had 3 mice in each cage that received IL-4c and the rest received veh control, these 2 cages were harvested on day 8. At necropsy on day 8, 3 age matched wild type mice were sourced from the same breeding colony to be used as controls for the colon lengths and subsequent flow cytometry. Notably one mouse in the DSS + veh group in cage 2 had to be culled on day

6 because of significant weight loss. Another DSS + veh mouse in cage 1 demonstrated piloerection and decreased movement on the day of necropsy and was found to have a hydronephrotic kidney secondary to ureteric obstruction and was therefore excluded from analysis. When mice from the two cages were analysed together there was no apparent difference in weight loss, DAI or colon length between treatment groups (Fig. 7.7C-E). However, it appeared that, when analysed separately, there was a slight difference in the kinetics of weight loss between cages 1 and 2, with weight loss in cage 1 starting in the veh group on day 6 that by day 7 and 8 was significantly greater than in the IL-4c treatment group (Fig. 7.7F.i). Contrasting this, it appeared that the weight loss in cage 2 may have commenced earlier and by day 8 all mice had reached the humane end-point of 20% weight loss, unlike cage 1 where no mice reached the threshold of 20% weight loss (Fig. 7.7F.ii). Furthermore, when I analysed the DAI, IL-4c treatment significantly improved the scores of mice in cage 1 while in cage 2 the trend was the opposite with higher scores in the IL-4c treated mice (Fig. 7.7G). DSS-induced colitis is characterised by colon shortening and so I analysed the colon length in each group. While IL-4c treatment reduced colon shortening in mice from cage 1, this was not the case in cage 2 (Fig. 7.7H).

To circumvent the difficulties of cage to cage variability, I performed a further set of experiments where 10 mice from the same cage were given 2% DSS colitis and either IL-4c or veh every 48 hours from day 3 onwards (Fig. 7.8A). Although I initially planned the necropsy on day 8, in the first of these experiments this had to be brought forward to day 7 due to most mice reaching the humane endpoints. Therefore, in the second experiment I chose day 7 as the end point to make these experiments comparable. In experiment 1 the weight loss in the IL-4c treated group paralleled that of the veh treated group until day 7 (Fig. 7.8B). However, in the IL-4c treatment group one mouse was culled on the afternoon of day 5 due to significant weight loss and 2 were culled on the morning of day 7 because they were exhibiting clinical signs consistent with reaching a humane endpoint and were therefore culled prior to being weighed. This had the effect of skewing the results because once the sick mice were removed from the analysis the weight loss in the IL-4c group seemed to be less significant on day 7 (fig. 7.8B). In experiment 2 the weight loss was, if anything, greater in the IL-4c treated group following the commencement of IL-4c treatment on day 3 (Fig. 7.8C). Of note in experiment 2, one mouse from each group was culled due to significant weight loss on day 5. In experiment 1 there was no difference in DAI scores with mice starting to exhibit clinical scores of more than 2 by day 6 (Fig. 7.8D). In experiment 2, mice were starting to exhibit DAI scores of more than 2 by day 6 with a significantly worse score in the IL-4c treated mice by day 7 (Fig. 7.8E). The trajectory of the DAI scores and weight loss appeared less precipitous in experiment 2.

In the above experiments only in one cage did administration of IL-4c starting on day 3 appear to have a beneficial effect and this coincided with later onset of symptoms in all mice as indicated by the DAI score. Indeed in the larger experiment IL-4c had no beneficial effect on weight loss and DAI score with it proving to significantly worsen the DAI in one cage.

7.5.2 Effect of IL-4c administration from day 3 on colonic monocytes in DSS colitis

The administration of IL-4c meant that the protocol to isolate lamina propria leukocytes had to be adjusted, as cell viability with the standard protocol was very poor. I shall address this further in the discussion section. Furthermore, because the end-point was brought forward due to welfare reasons in the second set of experiments, I was unable to perform flow cytometry on the colon samples due to unavailability of flow cytometers and a lack of assistance to harvest a large number of colons and perform the specialised leukocyte isolation protocol.

IL-4c treatment caused a significant reduction in the proportion of P1 monocytes causing a reduction to baseline levels (Fig. 7.9A). Notably the reduction in P1 monocytes was not just reflective of an IL-4c mediated increase in MHCII expression because there was no accompanying increase in P2 and P3 populations, which are defined by MHCII expression (Fig. 7.9B-C). Furthermore, when colonic monocytes and macrophages were defined by Ly6C and CD64 expression, the same pattern of a significant reduction in the proportion of Ly6C^{hi} monocytes was evident (Fig. 7.9D). As with acute liver injury, there was a significant reduction in proportion of circulating Ly6C^{hi} TremL4^{-} monocytes with IL-4c treatment compared to veh (Fig. 7.9E). Furthermore, there was also a reduction in transitioning Ly6C^{hi} TremL4^{+} monocytes with IL-4c treatment compared to all groups (Fig. 7.9F).

7.5.3 Administration of IL-4 from day 2 is detrimental in DSS colitis

The only time when IL-4c appeared to show any potential benefit was when mice demonstrated colitic signs as defined by an elevated DAI at a later time point (Fig. 7.7G). I hypothesised that administration of IL-4c earlier on day 2 of DSS rather than day 3 may be beneficial to all mice because it has been shown that delivery of the anti-CCR2 antibody (MC21) from day 2 ameliorates DSS-induced [116].

I therefore performed two identical experiments where 10 mice from the same cage were given 2% DSS and either IL-4c or veh every 48 hours from day 2 onwards with harvest on day 7 (Fig. 7.10A). One mouse in the DSS + IL-4c group was culled on day 6 in experiment 1 as it had reached the humane endpoint of >20% weight loss. Once again, the baseline kinetics were different between experiments with weight loss below baseline occurring in the veh treated group on day 6 in experiment 1 but on day 7 in experiment 2 (Fig. 7.10B-C). In contrast to results obtained when IL-4c was delivered on day 3, there was significantly greater weight loss in the IL-4c treated group compared to the veh treated group in both experiments when

IL-4c treatment was started at day 2 (Fig. 7.10B-C). This increased weight loss in the IL-4c treatment group was also reflected in the DAI score which was significantly higher in IL-4c treated mice from day 5 onwards in experiment 1 and day 7 in experiment 2 (Fig. 7.10D-E). The detrimental effect of IL-4c was further emphasised when I analysed the colon lengths at day 7 which trended towards being shorter in the IL-4c group when compared to the veh group in both experiment 1 (5.9cm ± 1.1 vs 6.5cm ± 0.9) and experiment 2 (5.8cm ± 0.8 vs 7.0cm ± 0.9) (Fig. 7.10F-G). When the colon lengths were pooled, it revealed a significant shortening in the colons in the IL-4c treated group when compared to the veh group (Fig. 7.10H).

7.5.4 Administration of IL-4c from day 2 has an inconsistent effect on colonic monocytes and macrophages

Analysis of leukocytes on day 7 revealed that in both experiments there was an increase in the proportion of P1 monocytes in DSS treated mice given veh treatment compared to naïve controls, although this only reached significance in the first experiment (Fig. 7.11A-B). Furthermore, there was a significant reduction in P1 monocytes with IL-4c treatment in experiment 1, although it must be noted there were only two viable samples in the IL-4c treatment group (Fig. 7.11A), whereas there was no effect of IL-4c treatment on the frequency of colonic monocytes in experiment 2 (Fig. 7.11B). Analysis of the P2 transitioning monocytes showed that in experiment 1 there was no effect of IL-4c and in experiment 2 the proportion of P2 monocytes in the IL-4c treated group was significantly increased over veh controls (Fig. 7.11C-D). There were also no differences in either experiments in the proportion of P3 macrophages, including when compared to wild type mice (Fig. 7.11E-F).

7.6 Discussion

In this chapter I attempted to establish whether the effect of IL-4c on monocytes could be replicated in 2 different models of hepatic and colonic inflammation characterised by monocytic infiltration of the affected organ.

7.6.1 IL-4c in APAP

The pilot study in which I administered IL-4c early (12hrs) post APAP-driven injury produced a promising trend towards a reduction in the proportion of Ly6C^{hi} monocytes in the liver but this was not actually reflected in a reduction in their number. Furthermore, IL-4c administration at this timepoint made mice sick and I observed a linear correlation between neutrophil number and serological markers of injury (ALT and AST). Could this increase in neutrophils result in a more detrimental outcome for these mice? The exact roll of neutrophils following DILI is complex and controversial but it is thought that the initial recruitment of neutrophils to the liver during the necroinflammatory phase is an essential part of the inflammatory response where they are involved in the clearance of debris. However because they also produce toxic nitric oxide (NO) and ROS, it is important that their behaviour is regulated and that they are removed when they are no longer required so that they do not cause excess liver damage [19,281,315–317]. It has been proposed by the Graubardt et al. that following APAP induced injury Ly6C^{hi} monocytes and Ly6C^{lo} macrophages regulate this neutrophil activation, apoptosis and clearance [21,52]. They proposed that during the necroinflammation phase of injury Ly6C^{hi} monocytes activate ROS production in neutrophils and positively mediate the phagocytosis of necrotic debris; however, later on during the repair phase they promote apoptosis of neutrophils and macrophages remove these dead cells.[52]. Could it be that an effect of IL-4c on Ly6C^{hi} monocytes is altering neutrophil dynamics in my model? Interestingly, IL-4c failed to induce neutrophil accumulation when given at 24hrs but also failed to give rise to elevated clinical signs and appeared to be beneficial by measurements of liver enzymes in serum.

Could IL-4c be having a direct effect on neutrophils? In non-sterile injury, Woytschak et al. have suggested that neutrophil influx and migration during bacterial skin infection is actually inhibited by administration of IL-4, which they propose antagonises granulocyte stimulating factor (G-CSF)[294].

Specifically, Woytschak et al found that the reduction in neutrophils in skin wounds resulted in greater susceptibility to infection. Another model of a mild hepatitis involves the administration of α–Galcer which is an agonist of iNKT cells that causes a rapid production of Th2 (IL-4) and subsequently Th1 (IFNγ) cytokines and a mild hepatitis[318]. In this model, it is suggested that iNKT cells rapidly produce IL-4 which promotes neutrophil accumulation resulting in hepatitis. They concluded that the hepatic accumulation of neutrophils was dependent on IL-4Rα/STAT6 signalling because they identified less neutrophils in tissue sections at 16 and 72 hours post α–Galcer administration in IL-4$^{-/-}$ and IL-4R$\alpha^{-/-}$ mice. Concurrent with this observed reduction in neutrophils they also observed a reduction in ALT, AST and necrotic cell area in both IL-4$^{-/-}$ and IL-4R$\alpha^{-/-}$ mice. Interestingly this result contrasts what was observed by Goh et al. and Ryan et al. where indices of injury were worse in IL-4R$\alpha^{-/-}$ mice following acute CCl_4 and APAP respectively[33,173]. Furthermore, both the Woytschak and Wang data contrasts my results in whole body BM chimeric mice (Fig. 5.13C) and tissue protected chimeric mice (Fig. 5.17E), which suggest that exogenous IL-4c limits neutrophil numbers. Work performed in collaboration with Professor Sarah Walmsley's group would suggest that this is due to IL-4Rα-dependent signalling directly inhibiting hypoxic neutrophil survival (manuscript in press).

Hence, while IL-4R signalling to neutrophils may directly limit their survival/accumulation, this could be context and time dependent due to the effect of monocyte-dependent mechanisms that normally act to counter-regulate neutrophil recruitment[21,52]. Therefore in my model there could be a cell intrinsic inhibitory effect of IL-4c administration counterbalanced by a promotion of neutrophil survival through IL-4-driven monocyte death. Interestingly in my CCl_4 timecourse experiment there was an increase in proportion of neutrophils on day 2 with IL-4c treatment but I did not observe the same detrimental effect on the mice as I observed with the increase in neutrophils in APAP. It could be that at this timepoint in CCl_4 injury increased neutrophils are not detrimental and therefore an increase in proportion does not have a negative effect, indeed they may well be beneficial at this timepoint as they have been shown to have an important role in the clearance of necrotic debris following sterile liver injury[52,281]. Furthermore the increase in Ly6C^{lo} macrophages the following day during the repair phase in CCl_4 enhance clearance of the dead neutrophils as Graubardt et al. propose is important in APAP [52].

Using the working hypothesis that a too early reduction in monocytes was detrimental to mice during APAP, I performed one further pilot experiment to administer the IL-4c treatment 24 hours after APAP. This regime did not result in elevated clinical signs and indeed, like in IL-4c treatment following CCL4 injury, it led to a significant reduction in AST. Furthermore IL-4c treatment resulted in a significant reduction in the proportion of circulating Ly6C^{hi} monocytes. However, no significant difference in the numbers or frequencies of recruited hepatic Ly6C^{hi} monocytes was detected. Due to the lack of significance in either the 12hr or 24hr regime pilot experiments, it remains impossible to say if IL-4 may have an effect on monocyte numbers in the APAP model. The lack of a strong effect when IL-4 was given at 24hrs and mice harvested at 72hrs may be related to the more rapid resolution of Ly6C^{hi} monocytosis during APAP injury. Zigmond et al. found that by 72 hours following APAP administration the proportion of Ly6C^{hi} monocytes had returned to baseline suggesting that to observe a difference in proportion of Ly6C^{hi} monocytes in my model it might be necessary to harvest mice a day earlier[21]. In order to take this work forward it would be necessary to perform a timecourse to determine if there is any significant effect of IL-4c administration on Ly6C^{hi} monocyte dynamics in APAP. Performing a timecourse would also enable further assessment of the effect of IL-4c on indices of repair and regeneration because administration at 24hrs post injury showed a non-significant reduction in ALT and a significant reduction in AST (Fig. 7.3). Notably Mossanen et al. showed that administration of an oral

CCR2/CCR5 inhibitor (Cenicriviroc) at 1-2hrs post APAP resulted in reduced liver injury but did not appear to have an effect on the subsequent repair process[23]. Their data would suggest that attempting to reduce Ly6C^{hi} monocytes at 12 hours, as I have done, is too late since the injurious effect of Ly6Chi monocytes has already occurred.

Another intriguing result from this series of APAP experiments was that there was no increase in proportion of macrophages following IL-4c treatment as had been observed with CCl_4 injury. In fact, at the 72hr timepoint there was a trend for a reduction in their proportion when compared to the veh treated group. In keeping with their lack of expansion, there was also no increase in proliferation of these Ly6C^{lo} CD64^{hi} macrophages with IL-4c treatment in APAP (Fig. 7.4J), which again contrasted what I had found in the CCl_4 model (Fig. 5.4). The reason for not seeing significant proliferation in Ly6C^{lo} macrophages in APAP could be related to the timing of the response to injury. Alternatively, the nature of the insult may limit other factors, such as CSF1 which might act in concert with IL-4 to promote proliferation. As outlined above, a timecourse experiment examining proliferation and levels of e.g. CSF1 would be necessary in order to address these alternatives.

Due to the time constraints of my PhD, the lack of a strong effect of IL-4c on hepatic monocytosis, and because it became apparent that the difference in monocyte/macrophage dynamics between the CCl_4 and APAP model would have necessitated another timecourse, I chose to focus on the DSS model of colitis model rather than repeating the pilot APAP experiments. Furthermore, while the APAP model did appear to be promising in that there was a significant reduction in AST and a trend to a reduction in ALT at the day 3 timepoint, the issue remained that I was unable to assess the effect of IL-4c treatment on functional outcomes. One possible way of assessing functional outcomes would be to determine survival with humane end points. In this experiment the administration of a higher dose of APAP would result in a significant proportion of mice reaching predefined humane endpoints[41] whereupon I could assess whether IL-4c treatment was protective. However, having discussed this with colleagues who had performed similar experiments they had found that any intervention was required around the time of APAP administration because most of the deaths occurred within the first 24 hours. Given that I thought early IL-4c administration was detrimental this did not seem to be a viable experimental model. In contrast, the DSS model of colitis did offer a model of Ly6C^{hi} monocytosis where the duration of the model enabled longitudinal assessment of disease severity using DAI and body weight[116,253].

7.6.2 IL-4c in DSS-induced colitis

Having validated that there was a significant colonic Ly6C^{hi} monocytosis in 2% DSS colitis at both day 3 and 6, I decided to administer IL-4c every second day from day 3 onwards. However, these experiments were hampered by the large degree of cage to cage variability in disease susceptibility. This has been reported previously and is attributed to differences in the commensal microbiota. Consistent with this, germ free mice develop less histological damage to colonic mucosa when administered DSS [319]. More recently it has been shown that in NMRI mice microbiota is required for development of normal DSS colitis but the absence of microbiota impairs intestinal barrier function[320]. Li et. al set out to establish the effects of different microbiota by analysing the effect of the 2.5% chronic DSS colitis model on 3 separate groups of age and sex matched specific pathogen free C57Bl/6 mice purchased from the same supplier at different times and subsequently housed in the same animal facility[310]. Even in mice from the same supplier and housed in the same facility they demonstrated significant differences in DAI, weight loss and colon length between groups and found that these differences were dependent on initial gut microbiota. Potential difference in microbiota could explain the differences in response to DSS particularly because I was unable to obtain mice from the same mother for all experiments. Given the number of mice needed, it was not feasible to co-house all mice in an attempt to reduce microbiota variability. Furthermore, co-housing and mixing of bedding was limited by my use of male mice, which become aggressive in these conditions [312,321]. To mitigate against the variable onset of colitic symptoms, I decided to start IL-4c administration a day earlier to ensure that the IL-4c was present at the start of the monocytosis, Interestingly when IL-4c was administered on day 2 the colitis, as assessed by weight loss, DAI score and colon length, was worse in the IL-4c treatment groups irrespective of whether cages developed onset of colitic symptoms on day 5 (first experiment) or day 6 (second experiment). This could be explained by previously published work suggesting that administration from day 0 of exogenous IL-33 in the 3.5% acute DSS colitis model results in exacerbation of colitis in an IL-4 dependent manner[322]. Others have also shown that constitutive absence of IL-4 in IL-4$^{-/-}$ mice results in less severe colitis[323]. This result would suggest that IL-4 administration at the start of colitis would likely be detrimental. Given that in experiment 1 I observed a reduction in proportion of Ly6C^{hi} monocytes with IL-4c, why did I not replicate the results of Zigmond et al. and demonstrate improvement in colitic signs? Firstly, using MC21, Zigmond et al. demonstrated complete inhibition of Ly6C^{hi} monocytes, while treatment with IL-4c only caused partial knock-down. Secondly, the MC21 antibody is specific for CCR2-bearing cells, which largely relates to monocytes in blood, whereas IL-4c will affect any cell that expresses the IL-4Rα, including T and B cells that Stevceva et al. proposed could be deleterious in DSS colitis when activated by IL-4[323]. Finally, IL-4 appears to have differing effects on circulating and tissue-resident monocyte/macrophages, which is unlikely to be the case with CCR2 blockade due to the lack of CCR2 by mature intestinal macrophages[90,117]. One technical issue common to all the DSS experiments was that administration of IL-4c had a detrimental effect on the yield of live cells. For this reason I have not presented cell numbers because the cell counts obtained in the IL-4c treated colons are artificially low due to the death of cells during the digestion process. It is known that type 2 immune cytokines increase mucus production in the gut[154] and this increased mucus is thought to be important for protection against helminth infection by impeding their ability to interact with the host and to thrive and survive[324]. It is therefore plausible that during the leukocyte isolation process the exposure of the mucus and its contents could impact on leukocyte survival as it is designed to be a harsh environment for helminths to which leukocytes are not normally exposed due to the epithelial barrier. To mitigate against this, I adapted the digestion protocol to use a more gentle enzyme cocktail comprising Liberase TL and DNAse rather than a combination of collagenase V, collagenase D, dispase and DNAse as previously published[314]. This was guided by work that had been done Dr. Jones in Professor MacDonald's group at the University of Manchester where they found that the liberase digestion protocol lead to improved leukocyte viability in the Th2 setting (personal communication). Although the gentler digestion process resulted in better cellular yields from IL-4c treated mice, there were still samples that had to be excluded due to very high levels of cell death. One further approach would have been to perform analysis of sections of colon, however there is not a reliable antibody to identify monocytes in tissue sections and it would therefore require repeating the experiments using reporter strains that can identify cells of a monocyte origin such as a *Csf1r*-EGFP [283] or a *Cx3cr1*$^{+/gfp}$ reporter line [62].

7.6.3 Summary

IL-4c administration in DSS colitis, like in APAP, could potentially be beneficial with the appropriate timing. The advantage of DSS colitis was the duration of the model enabled longitudinal assessment of DAI, however the variability meant that it was difficult to accurately time the administration of the IL-4c. With further experiments using tools to homogenise the microbiota between mice (cross-fostering, antibiotics and even fecal gavage)[321] it may be possible to establish a beneficial effect with IL-4c treatment. In this setting it would be necessary to recharacterize the dynamics of disease activity and also perform a timecourse to characterise the monocyte response. I would hope that by doing this I would be able to establish the ideal time to administer IL-4c to cause a beneficial reduction in Ly6C^{hi} monocytes similar to that seen with MC21 administration. I would expect that early administration of IL-4c would be best i.e. day 2 or 3 post starting DSS, indeed as I saw above IL-4c administration starting on day 3 appeared to beneficial in 1 cage. It would be also interesting to assess the effect on colonic macrophages as Smith et al. previously demonstrated that in BALB/c mice *S. mansoni* infection conferred protection against DSS colitis that was dependent on infiltrating colonic macrophages[325].

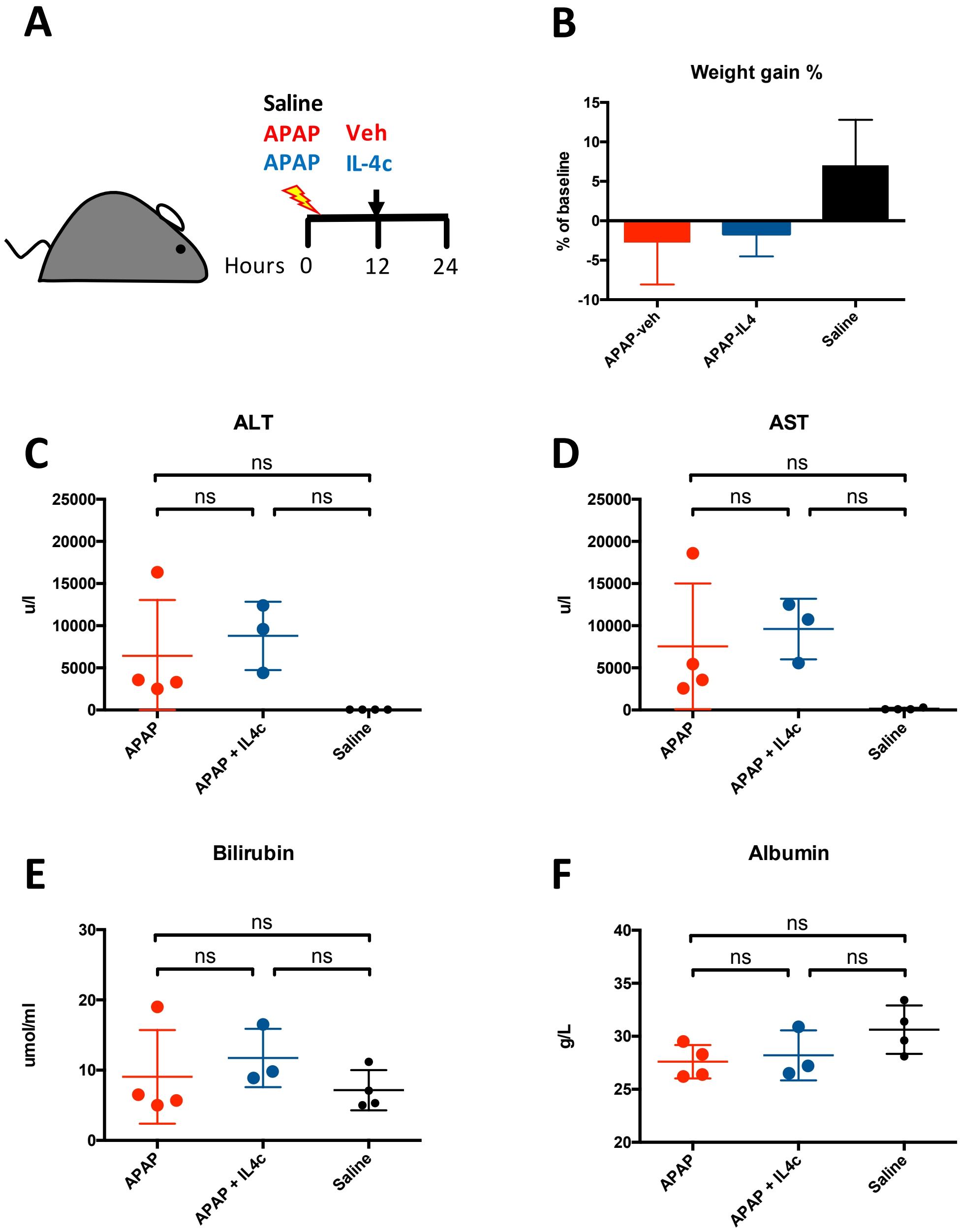

Figure 7-1 Phenotypic assessment of APAP overdose with early IL-4c .

(A) Schematic of injury model APAP was administered I.P. and then IL-4c or veh 12 hours later. (B) Weight change from baseline. (C-F) Serum markers of liver injury. N=3-4 mice/group, mean ± SD (one-way ANOVA).

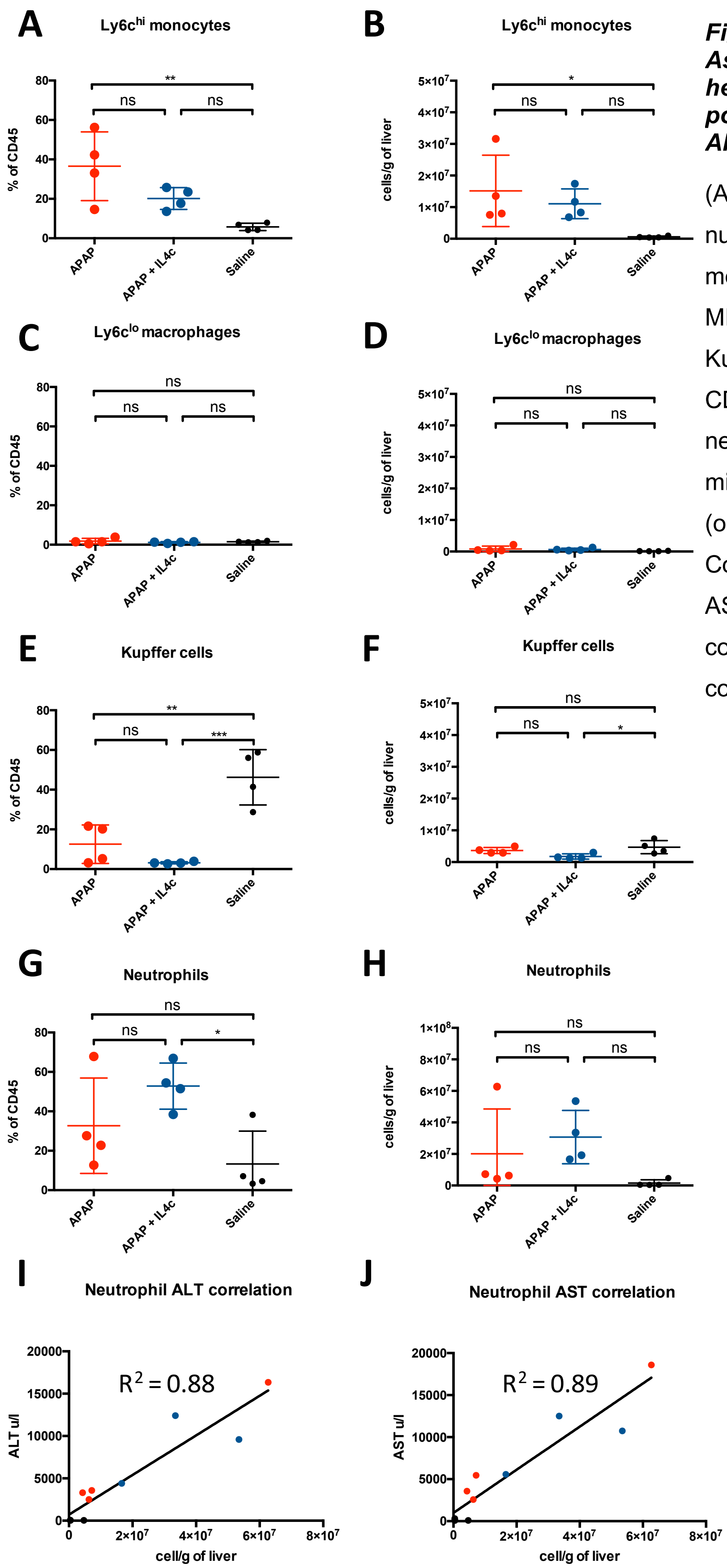

Figure 7-2 Assessment of hepatic leukocyte populations post APAP + early IL-4c.

(A-H) Proportion and number of Ly6C^{hi} moncytes, Ly6C^{lo} MHCII^{int} macrophages, Kupffer cells (F4/80^{hi} CD11b^{lo}) and neutrophils. N=4 mice/group, mean ± SD (one-way ANOVA). (I-J) Correlation of ALT and AST to neutrophil count. N=12 (Pearson correlation).

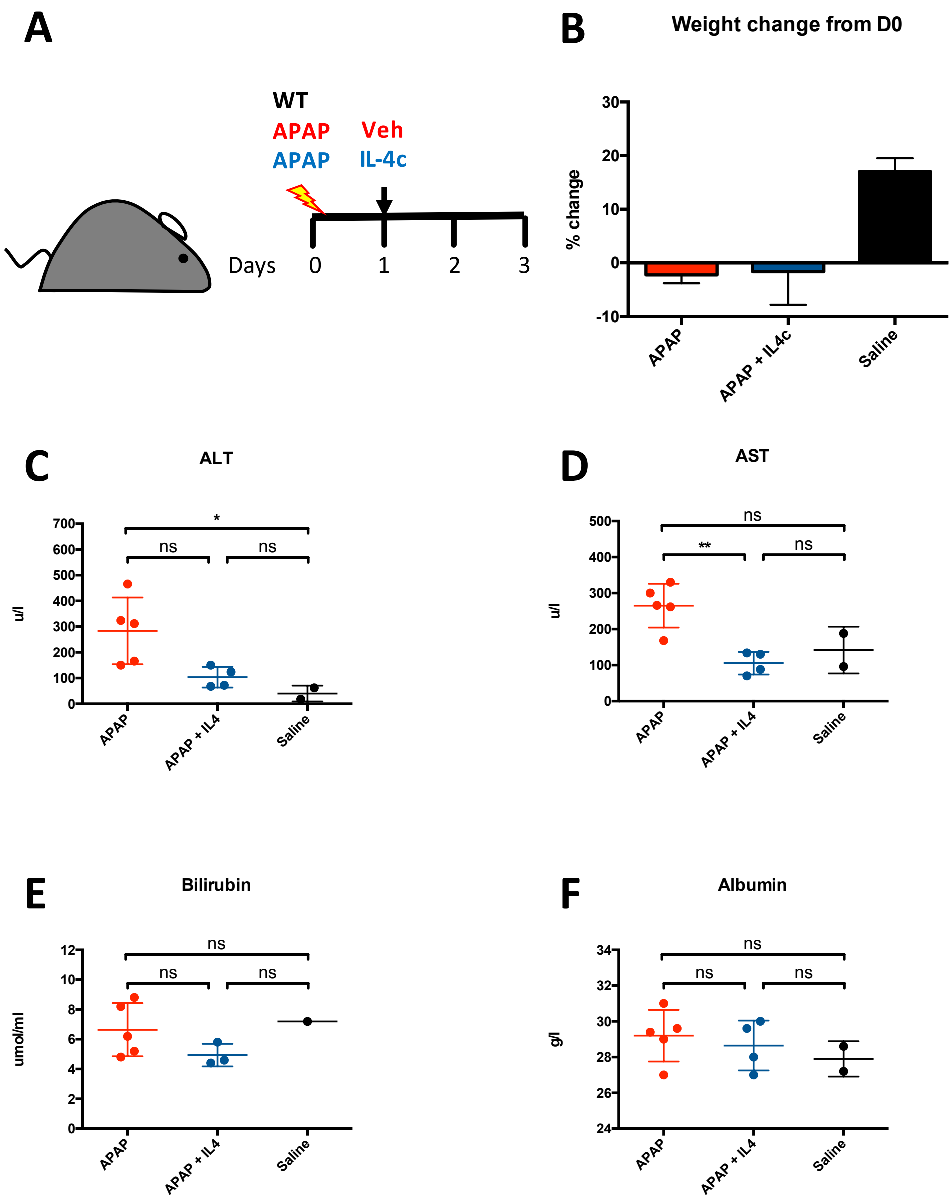

Figure 7-3 Phenotypic assessment of APAP overdose with late IL-4c.

(A) Schematic of injury model APAP was administered I.P. and then IL-4c or veh 24 hours later. (B) Weight change from baseline. (C-F) Serum markers of liver injury. N=4-6 and 1-2 for WT control, mean ± SD (one-way ANOVA).

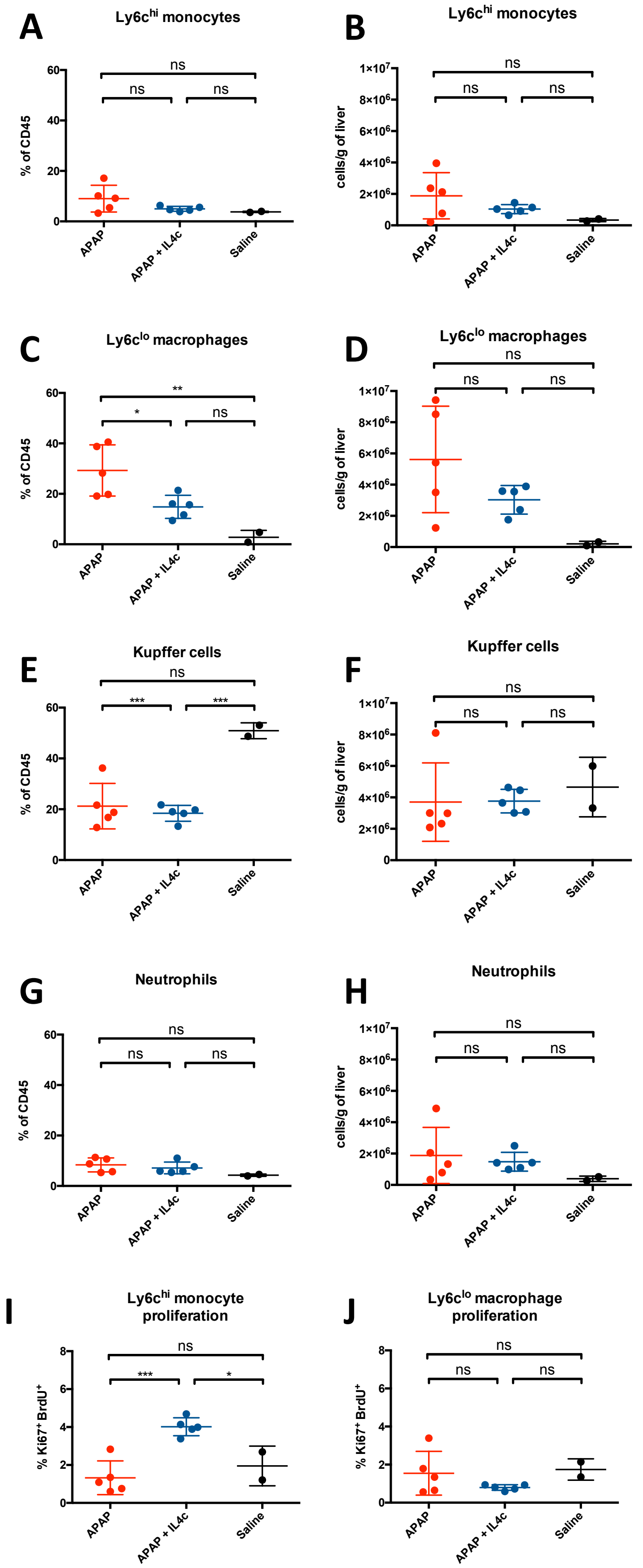

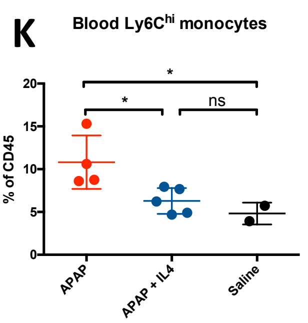

Figure 7-4 Assessment of leukocyte populations post APAP + late IL-4c.

(A-H) Proportion and number of hepatic Ly6C^{hi} monocytes, Ly6C^{lo} CD64^{hi} macrophages, Kupffer cells (Tim4^{hi} CD11b^{lo}) and neutrophils. (I-J) Proportion of proliferating (Ki67^{+} BrdU^{+}) hepatic Ly6C^{hi} monocytes and Ly6C^{lo} macrophages. (K) Proportion of blood Ly6C^{hi} monocytes. N=5 + 2 WT control mice/group. Mean ± SD (one-way ANOVA).

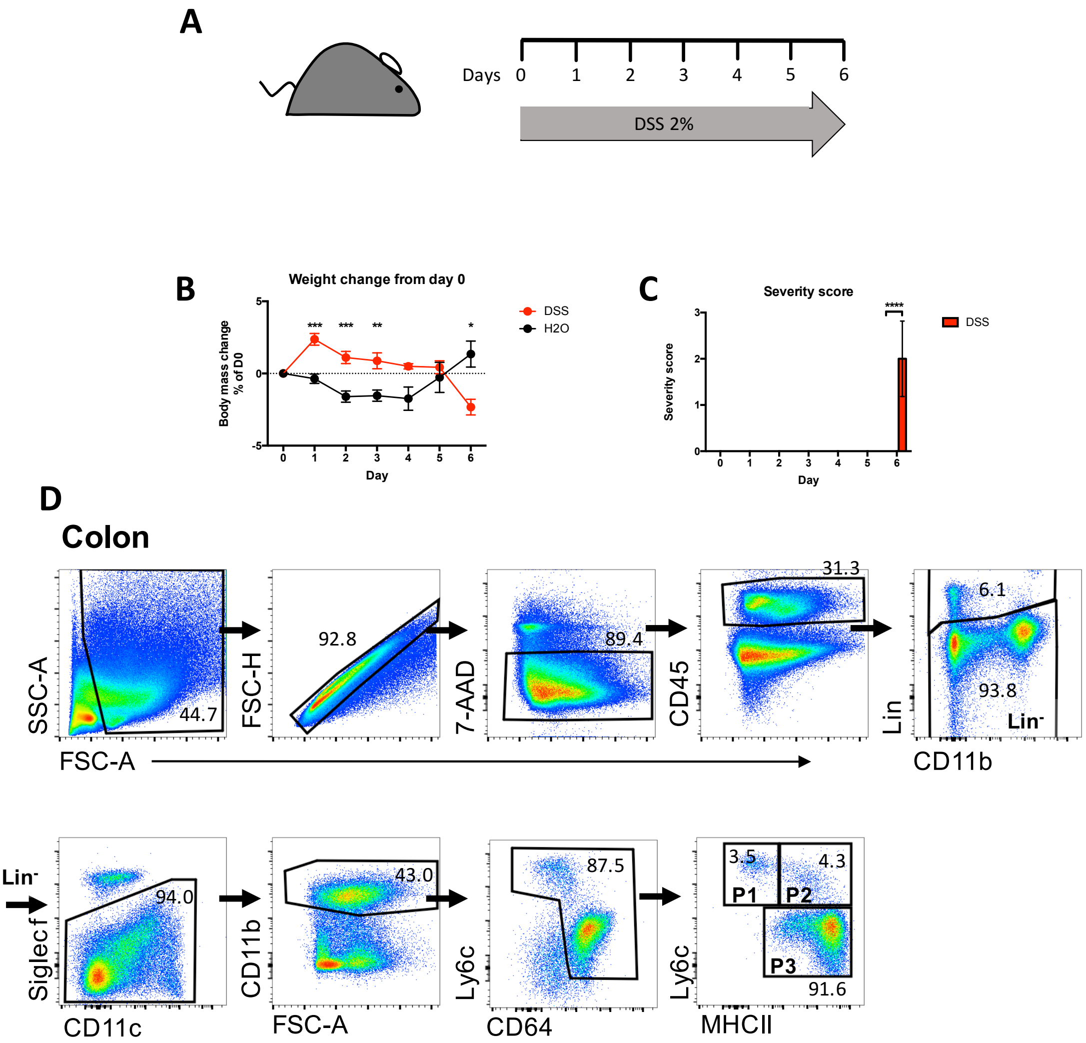

Figure 7-5 DSS colitis model.

(A) Schematic of model: mice were given 2% DSS in their drinking water or water alone for 3 or 6 days and then harvested. (B) Weight change from day 0. (C) Severity score. N=8 mice/group but 4 per group harvested on day 3, mean ± SEM (DSS and water compared using multiple *t* tests with Holm-Sidak correction). (D) Gating strategy employed to identify colonic monocyte and macrophage populations, Lineage gate: CD3, CD19, Ly6G and NK1.1.

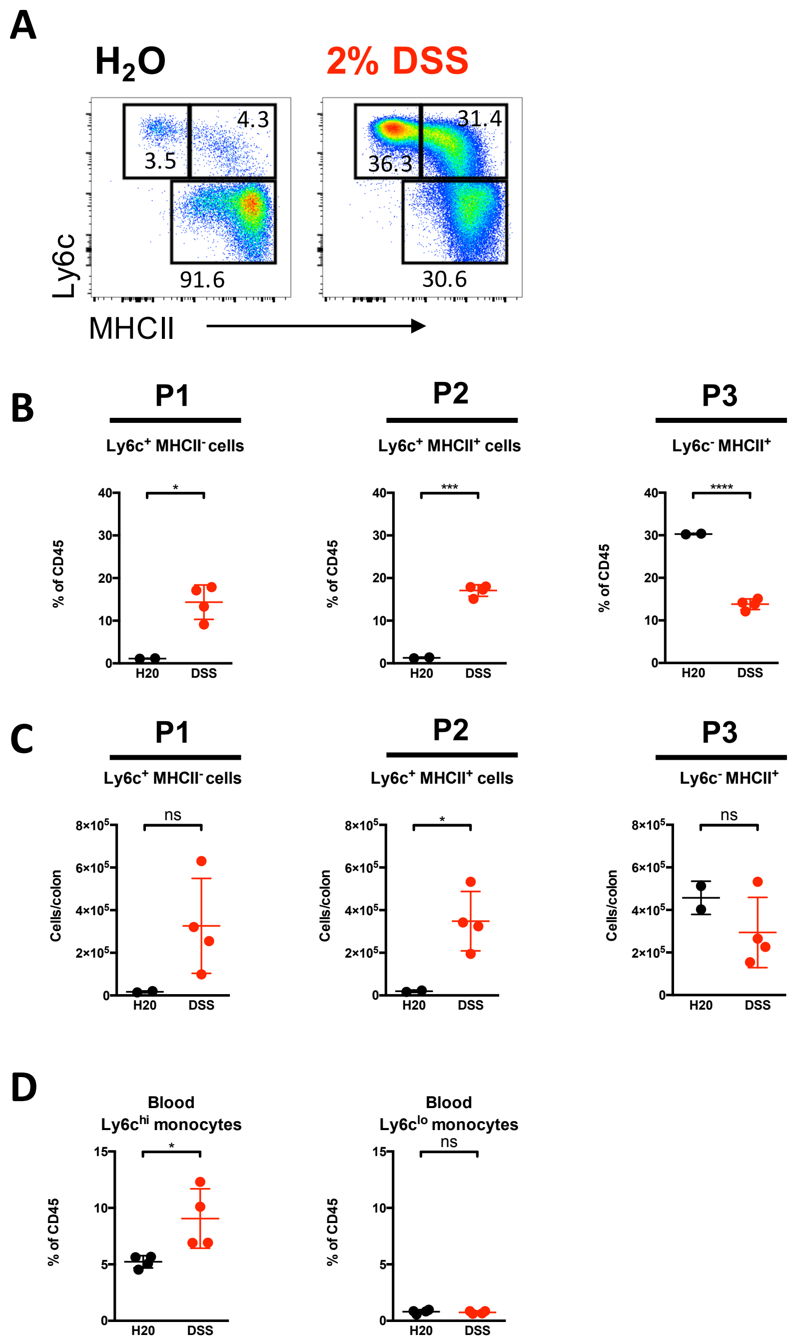

Figure 7-6 Characterisation of the monocyte/macrophage compartment in DSS-induced colitis.

(A) Representative plots of Live (7AAD), CD45$^+$, Lin$^-$, Siglec f$^-$, CD11b^{hi} monocytes and macrophages. (B) Proportion of P1, P2 and P3 mononuclear phagocytes. (C) Number/colon of P1, P2 and P3 mononuclear phagocytes. N= 2-4 mice/group, mean ± SD (unpaired *t* test). (D) Proportion of Blood Ly6Chi monocytes. N= 4 mice/group, mean ± SD (unpaired *t* test).

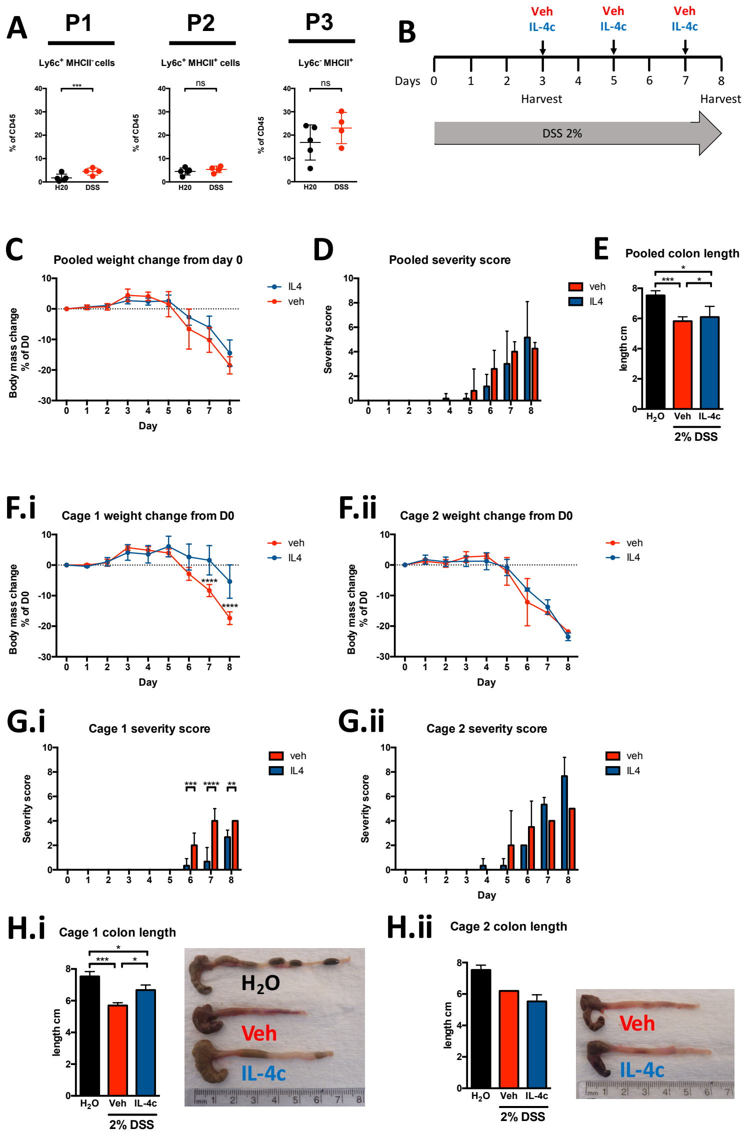

Figure 7-7 Determining the effects of IL-4c on disease progression of DSS-induced colitis.

(A) Proportion of P1, P2 and P3 mononuclear phagocytes on day 3 following start of DSS model. (B) Schematic of model: mice were given 2%DSS in their drinking water and given IL-4c 0.2mg/g IL-4c or veh control every 48 hours from day 3 onwards. (C & F) Weight loss from day 0 pooled and individual cages mean ± SD (multiple *t* tests with Holm-Sidak correction). (D & G) Disease activity index pooled and individual cages mean mean ± SD (multiple *t* tests with Holm-Sidak correction). (E & H) Colon length by pooled and individual cages with representative pictures with naïve H_2O controls. Mean ± SD (one-way ANOVA). Cage 1 n=3 mice/group, cage 2 n=3 for IL-4c and 2 for veh until day 6.

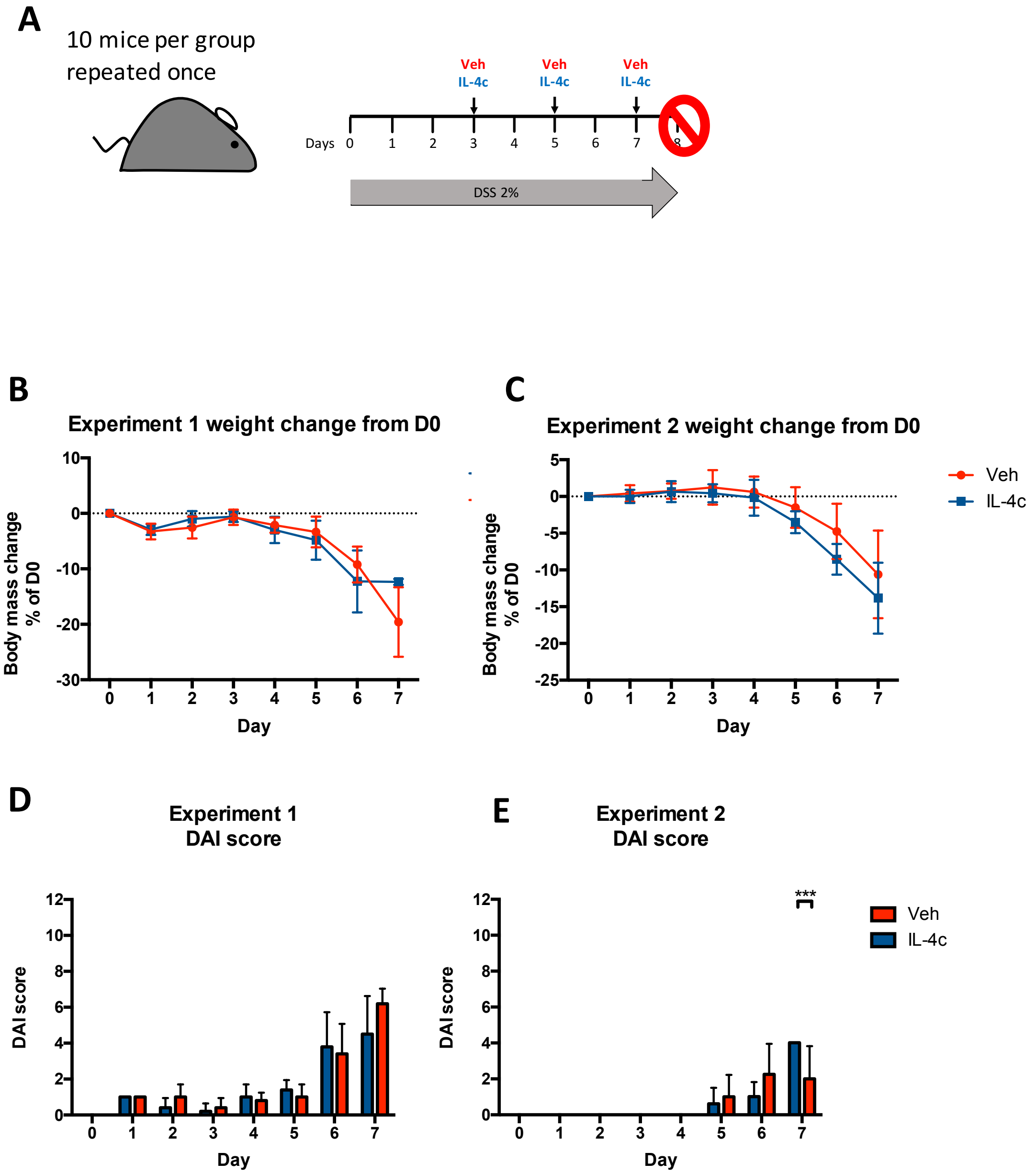

Figure 7-8 Determining the effects of IL-4c on disease progression of DSS-induced colitis.

(A) Schematic of model: 10 mice/experiment were given 2%DSS in their drinking water and given IL-4c 0.2mg/g IL-4c or veh control every 48 hours from day 3 onwards. (B-C) Weight loss from day 0 in both experiments. Mean ± SD. (D-E) Disease activity index by cage. Mean ± SD. (multiple *t* tests with Holm-Sidak correction). N=5 mice/group. Experiment 1: 3 IL-4c mice culled on day 6-7; Experiment 2: 1 IL-4c and 1 veh mouse culled on day 5.

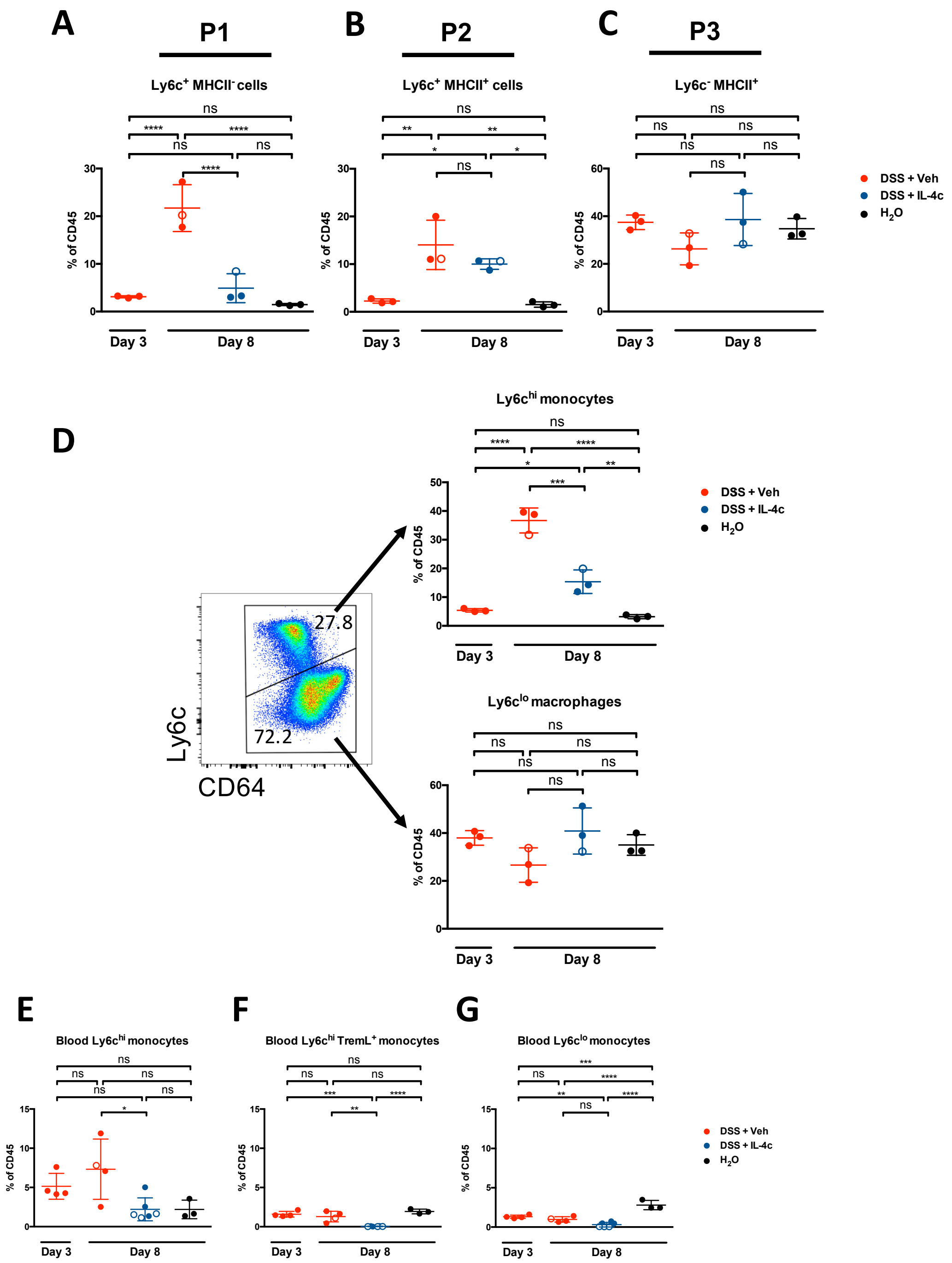

Figure 7-9 Mononuclear phagocytes following IL-4c during DSS.

(A-C) Proportion of P1, P2 and P3 mononuclear phagocytes following start of DSS model. Empty circle signifies cage 2. N=3 mice/group. (D) Proportion of Ly6C^{hi} CD64^{lo} monocytes and Ly6C^{lo} CD64^{hi} macrophages. N=3 mice/group. (E-G) Proportion of monocytes in blood. Empty circle signifies cage 2. N=3-6 mice/group. Mean ± SD (one-way ANOVA).

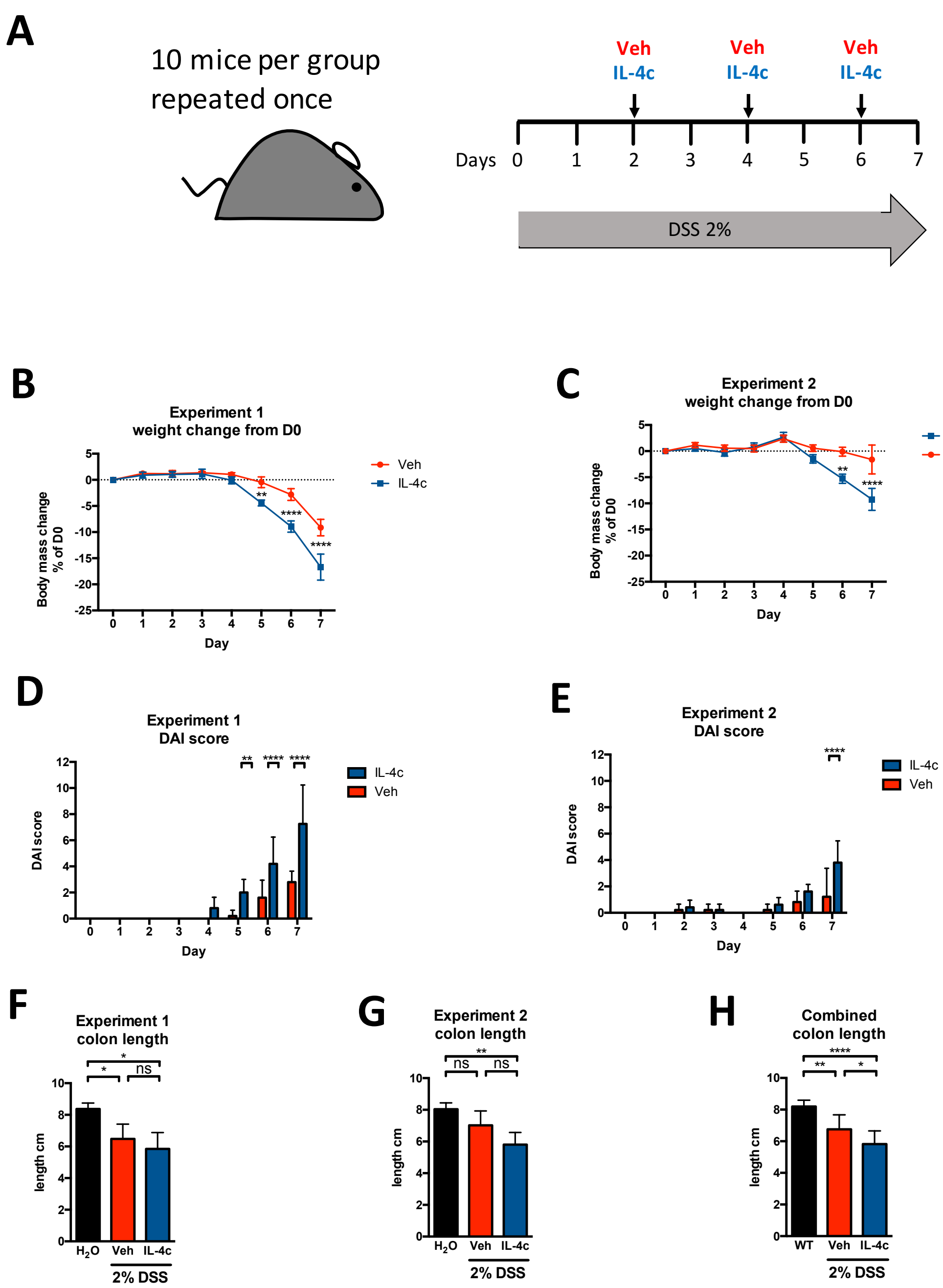

Figure 7-10 Administration of IL-4 from day 2 is detrimental in DSS colitis.

(A) Schematic of model: 10 mice/experiment were given 2%DSS in their drinking water and given IL-4c 0.2mg/g IL-4c or veh control every 48 hours from day 2 onwards. (B-C) Weight loss from day 0 in both experiments. Mean ± SEM. (D-E) Disease activity index by cage. Mean ± SD. (multiple *t* tests with Holm-Sidak correction). (F-G) Colon length by cage and combined. Mean ± SD (one-way ANOVA). N=5 mice/group. Experiment 1: 1 IL-4c mouse culled on day 6.

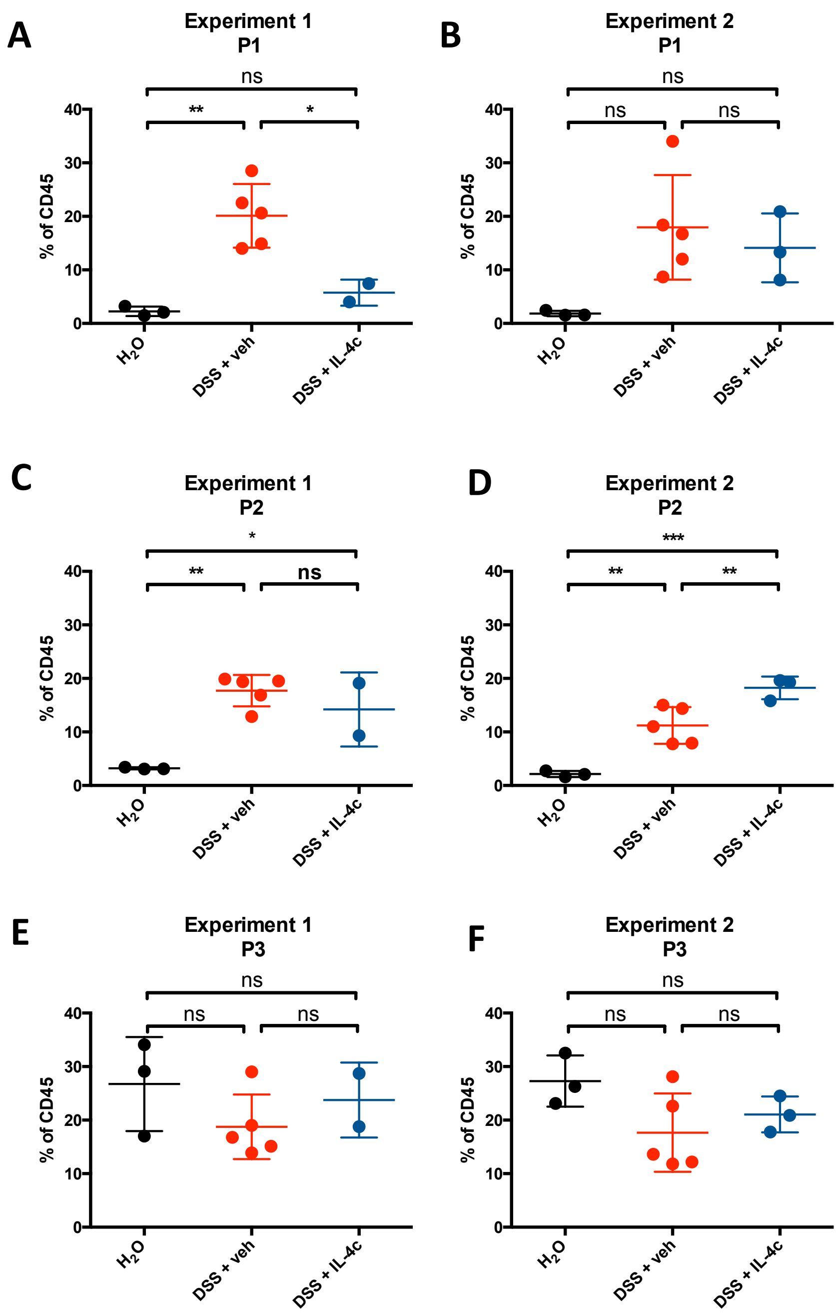

Figure 7-11 Analysis of monocyte/macrophage populations in DSS colitis ± IL-4c starting on day 2.

(A-F) Proportion of P1, P2 and P3 mononuclear phagocytes by experiment. N= 2-5 mice/group, mean ± SD (one-way ANOVA).

Chapter 8 Discussion

8.1 IL-4c as a therapeutic

As emphasised in the introduction there is a significant burden of acute drug-induced liver injury with more than 50% of all incidences of acute liver failure in the USA and UK attributable to this cause[1]. Acute liver failure has significant mortality, and in its most severe form, the only treatment is liver transplantation which necessitates lifelong immunosuppression, increasing the risk of opportunistic infections and individuals developing lymphoproliferative disease[326]. Furthermore, liver transplantation in the setting of acute liver failure is associated with a 21% 1 year mortality[1]. Thus, there is an urgent need to develop therapies that can avoid the use of the limited resource of liver transplantation. I have built on the work of Goh et al. and demonstrated that IL-4c administration following acute DILI with CCl_4 results in an improvement in measures of hepatic injury and regeneration[33]. I observed that IL-4c administration 24hrs following CCl_4 mediated injury resulted in a reduction of the markers of hepatic injury: ALT, AST and necrotic cell area 48hrs later. Furthermore, this regimen of IL-4c administration also resulted in an increase in hepatic regeneration as measured by hepatocyte proliferation.

The results from my series of exploratory experiments designed to determine whether IL-4 has a similar therapeutic potential in the clinically relevant APAP model of DILI and a model of colitis were less clear. APAP overdose is the most common cause of acute DILI in the UK and US and although CCl_4 replicates the zonal necrosis of APAP overdose, the underlying mechanisms of injury differ as do the leukocyte dynamics and dynamics of injury and regeneration[18,21,22,145,327]. Unfortunately, I was unable to establish whether there was a therapeutic benefit to IL-4c administration in APAP, possibly due to the seemingly faster dynamics of injury and leukocyte recruitment when compared with CCl_4. There did certainly appear to be a time dependent effect of IL-4c administration in both APAP and DSS colitis; earlier administration was detrimental in APAP and the timing of administration in relation to onset of colitis in the DSS model appeared to have an effect on severity scoring as there were animals that appeared to demonstrate a less severe phenotype with IL-4c treatment. The effect of timing may be related to the changes in monocyte/macrophage dynamics, as recent work using transcriptomic analysis of human monocytes has suggested that IL-4 has a time dependent effect on mononuclear phagocyte differentiation in vitro, even in the absence of an inflammatory stimulus[217]. Furthermore, altering the balance of other leukocytes either directly or indirectly will have an effect on the repair process. Indeed in the liver following APAP it has been shown that Ly6C^{hi} monocytes have a direct effect on reducing neutrophil number and reducing their immune function[52]. In the DSS model I did not identify any definitive effect on the analysed leukocyte populations that corelated with poor outcomes. Nevertheless, IL-4c had a consistent effect of reducing Ly6C^{hi} monocytes in the colitis model. Although throughout my project I have focused primarily on the effect of IL-4c on myeloid cells it could be that effects on parenchymal or stromal populations may alter outcome as these are important in liver injury and DSS colitis[45,328]. Due to time and resource constraints I was unable to assess this using BM chimeric mice. Nonetheless, approaches that specifically target the monocyte/macrophage lineage could be beneficial therapeutically. For instance, could it be possible to use diabodies as outlined in RA in the introduction to target IL-4c to specifically target the monocytes and macrophages to mitigate any negative off target effects?[246].

Although it is inconclusive as to whether IL-4c administration is of benefit in these other models of sterile inflammation, the one result that was consistently replicated across all models of injury was the reduction in the proportion of circulating Ly6C^{hi} monocytes. I will therefore now focus my discussion on interpreting both the in vitro and in vivo data pertaining to the effects of IL-4c on the monocyte/macrophage populations.

8.2 Effect of IL-4c on recruited monocytes and macrophages

The reduction in Ly6C^{hi} monocytes resulting from treatment of CCL_4-injured mice with IL-4c was associated with an increase in recruited Ly6C^{lo} macrophages. Owing to the previously documented pro-reparative effects of recruited Ly6C^{lo} macrophages in APAP and the reported pro-inflammatory function of Ly6C^{hi} monocytes[21,23], I had hypothesised that a reduction in Ly6C^{hi} monocytes and an increase in Ly6C^{lo} macrophages in conjunction with the direct pro-regenerative effects of IL-4 on hepatocytes demonstrated by Goh et al. would enhance the repair process in acute CCl_4 injury. To abrogate IL-4Rα signalling to monocytes and their progeny I attempted to use the LysM Cre; IL-4R$\alpha^{fl/-}$ line. I established, however, that the LysM Cre; IL-4R$\alpha^{fl/-}$ line led to deletion of IL-4Rα in only a very limited proportion of monocytes during CCl_4 induced inflammation and was not going to be useful to dissect whether the enhanced repair observed with IL-4c treatment was due to the changes elicited in the monocyte/macrophage compartment. Hence, although whole body irradiation is an imperfect tool, I used it to attempt to establish if IL-4 signalling to the haematopoietic was important in the observed phenotype. As discussed in Chapter 5, because there are caveats to this model (e.g. age of the mice and the potential effects of ionising irradiation on response to injury), the fact that there was no significant effect on serological markers of injury does not rule out a role for haematopoietic cells in the beneficial effect of IL-4c. One encouraging result was the trend to reduced hepatocyte proliferation in mice where IL-4R deficiency was restricted to the haematopoietic compartment (i.e. KO > WT mice). Importantly because BM chimeras results in the loss of IL-4Rα on not only monocytes and macrophages but also other leukocyte populations, changes in these other populations might antagonise and mask the potential beneficial effects of IL-4c administration on monocytes/macrophages. For example, recent work from a collaboration with the Walmsley group suggests

IL-4 signalling may limit the enhancement of neutrophil survival that occurs in hypoxic environments (in press).

Ideally, I would use a monocyte specific Cre to target these cells in order to overcome the above problems, however this unfortunately has not yet been developed. There is encouraging work from the group of Florent Ginhoux who presented work at Keystone Myeloid 2018 pertaining to a monocyte marker Ms4a3 that is reported to be exclusively expressed on cMOPs, the progenitor of monocytes. Thus, when mice in whom Cre is driven by *Ms4a3* are crossed with *Rosa26*-TdTomato reporter mice, monocytes are very efficiently labeled, although notably so are neutrophils and eosinophils. It may be therefore that a monocyte specific Cre driver is on the horizon which would help in establishing the role of monocytes in the observed phenotype.

8.2.1 Effect of IL-4c on Ly6C^{hi} monocytes

The CCl_4 injury model provided a platform to study the effect of exogenous IL-4 signaling to mononuclear phagocytes during sterile inflammation. As would have been predicted by previous work, the expansion of Ly6C^{lo} macrophages was IL-4Rα dependent and involved IL-4Rα dependent proliferation[121,206]. Importantly, this expansion did not appear to result from increased conversion of Ly6C^{hi} monocytes but, as outlined in Chapter 6, I did not get the opportunity to show this definitively. The expansion of Ly6C^{lo} macrophages was not observed in all experiments, whereas reduction in Ly6C^{hi} monocytes was a constant feature in recipients of IL-4c. Strikingly, the reduction in Ly6C^{hi} monocytes was not only found in the liver but also the blood, spleen and kidneys of CCl_4 injured mice and even in the blood and spleen of uninjured mice. IL-4c appeared to induce Ly6C^{hi} monocyte apoptosis in circulating cells, and not affect their egress from the BM. Notably IL-4c had no effect on Ly6C^{hi} monocyte viability in the liver but did reduce the viability of BM derived Ly6C^{hi} monocytes in vitro.

This in vitro work suggests that other signals such as CSF-1 can rescue the decreased viability observed so it is possible that tissue related signals such as growth factors could promote the survival of Ly6C^{hi} monocytes once they enter the tissue. To establish if CSF-1 is an important survival signal in tissues a future direction could be to assay CSF-1 levels in both tissue and blood during injury to determine if there is a difference in concentrations. Another approach would be to deliver CSF1-Fc in combination with IL-4c to determine if this protects against IL-4 induced death. An alternative mechanism underlying the protection of monocytes from death could be that once these Ly6C^{hi} monocytes enter the tissue they may have already begun to differentiate from their blood counterparts sufficiently that their response to IL-4 changes away from a pro-apoptotic response to a pro-proliferative one more in keeping with macrophages. Indeed, monocytes in the colonic mucosa and dermis have been shown to be transcriptionally-distinct from their phenotypically identical counterparts in blood[98,282]. Thus, it is entirely plausible that liver monocytes are at a different stage of differentiation. However, as far as I am aware, a comparison of hepatic and circulating Ly6C^{hi} monocytes has not been performed but is clearly warranted. This could be done by comparing blood and tissue monocyte expression of other monocyte specific markers like CCR2 and CD14[60] or by comparing their transcriptome. In addition to directly comparing tissue and blood monocytes at a population level, the application of single cell RNA sequencing (scRNAseq) could allow dissection of the differentiation trajectory of monocytes in different contexts. This is an experiment that I am planning to perform in the near future.

Another surprising finding was the IL-4Rα dependent proliferation of liver Ly6C^{hi} monocytes in response to IL-4c in CCl_4 and APAP injured mice. Monocytes are known to exit cell cycle before exiting the BM and while IL-4 is known to trigger proliferation in tissue resident macrophages[206], proliferation of monocytes in the setting of type 2 immunity has not been described previously. As described in the Introduction, CXCR4^{hi} premonocytes in the bone marrow proliferate under normal physiological conditions. Upon downregulation of CXCR4, which is thought to act as an "anchoring signal" through interacting with CXCL12, they are able to egress which is paralleled by an exit from cell cycle[78]. In their work, Chong et al. also demonstrated that CXCR4 signal was also important in the margination of Ly6C^{hi} monocytes in the lung during inflammation[78]. Could this "anchoring signal" be important to allow monocytes to proliferate and once monocytes are anchored in the tissue they can proliferate and therefore respond to the strong signal to proliferate from IL-4c. A future experiment looking at CXCR4 expression in both blood and tissue monocytes would be interesting to assess whether this is one potential mechanism in the observed phenotype.

These differential responses of monocytes to IL-4 depending on their environment would be in keeping with the recent work by Borsugi et al. and Minutti et al. who have both proposed that the environment affects the acquisition of an alternatively activated phenotype in macrophages[210,329]. Indeed, Minutti et al. demonstrated in the liver co-factors are required to generate the stereotypical proliferation and RELMα expression in macrophages following IL-4c administration. In the liver the co-factor was identified as C1q, but whether C1q has distinct effects on monocytes is unknown. To determine if a co-factor is responsible for protecting liver monocytes, a future experiment could examine the response of FACS-purified Ly6C^{hi} monocytes from injured liver to IL-4c exposure in vitro where co-factors would be absent.

To the best of my knowledge, the apoptosis of circulating Ly6C^{hi} monocytes or their proliferation in response to IL-4 has not been reported before. My proposed model for IL-4c in acute CCl_4 injury is outlined below (Fig. 8.1).

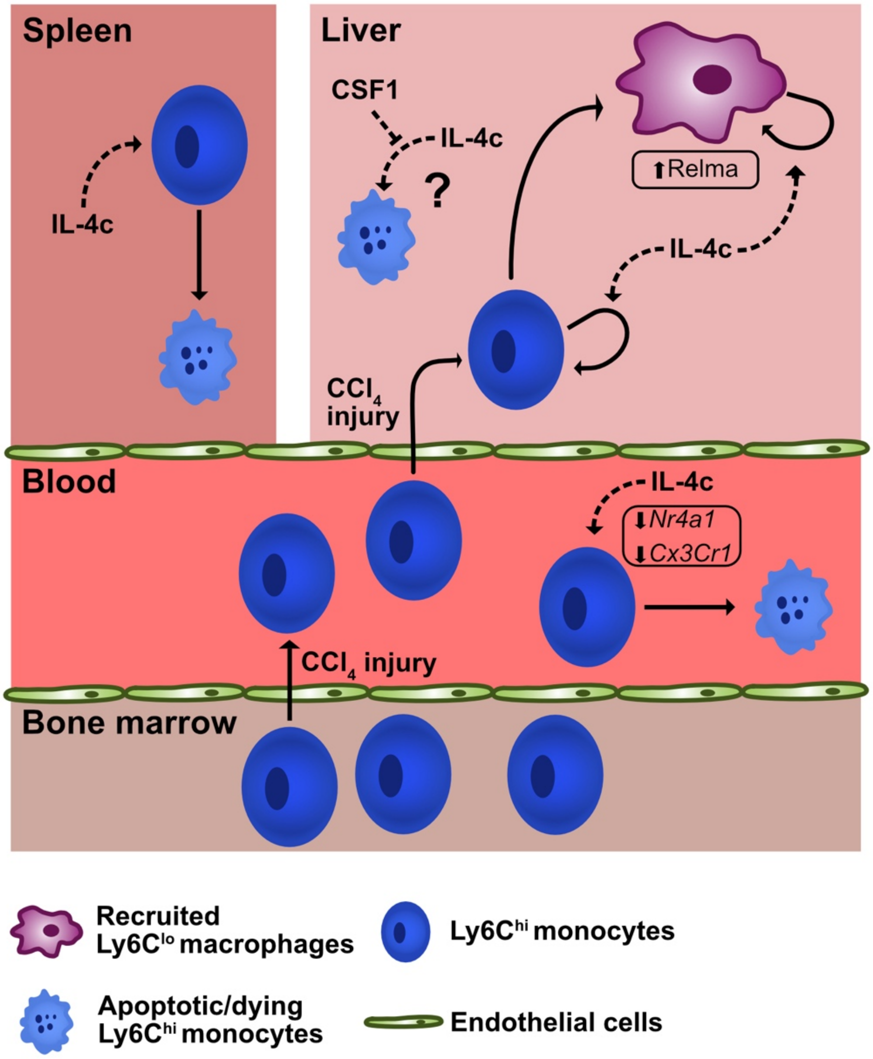

Figure 8-1 Model of the effect of IL-4c on monocytes and macrophages during acute liver injury with CCl4.

CCl_4 injury results in recruitment of Ly6C^{hi} monocytes from the bone marrow into the circulation and these cells are subsequently recruited to the injured liver where they convert into Ly6C^{lo} macrophages. IL-4c causes apoptosis of circulating Ly6C^{hi} monocytes and death of Ly6C^{hi} monocytes in the splenic reservoir resulting in a reduction of Ly6C^{hi} monocytes. In the liver IL-4c causes proliferation and alternative activation of recruited Ly6C^{lo} macrophages causing an increase in their number. In vitro CSF1 inhibits IL-4 driven Ly6C^{hi} monocyte death and this could be a protective mechanism for Ly6C^{hi} monocytes upon entering the liver. Concurrent with the death of circulating Ly6C^{hi} monocytes IL-4c also promotes their proliferation without causing an increase in their number in the liver.

8.3 Future directions

The finding that IL-4c was inducing apoptosis of Ly6C^{hi} monocytes echoed and extended in vitro work with human PBMCs from 1992[220] by demonstrating a direct effect of IL-4c on monocyte viability in vivo. The fact that a similar effect has been shown in human PBMCs is also relevant as it increases the possibility that the therapeutic effects observed in murine models could be translatable to humans. To take things forward it is important to try to elucidate the mechanisms underlying the decreased viability of Ly6C^{hi} monocytes.

8.3.1 Transcriptomic analysis

As an initial step in this process that was feasible within the time and financial constraints of my PhD, I first examined gene expression in circulating Ly6C^{hi} monocytes using the Nanostring platform. I used this platform because of the small amount of input material required (5000 cells) and the low yield of circulating monocytes in the IL-4c treated mice.

Analysis of circulating Ly6C^{hi} monocytes using the Nanostring platform revealed a significant downregulation of 211 genes in CCl_4 + IL-4c treated mice when compared to CCl_4 + veh mice. This was even more interesting because the CCl4 + veh vs olive oil comparison revealed no significant changes in transcriptome. Linking the results of the Nanostring analysis to potential mechanisms underlying the observed increased monocyte death with IL-4c the downregulation of *Nr4a1* and *Cx3cr1* were potentially interesting. The former has been demonstrated to be important for Ly6C^{hi} monocyte survival[65,67,330] and the latter has been proposed to be important in Ly6C^{lo} monocyte survival as CX3CR1 signaling promotes the expression of the anti-apoptotic protein Bcl2[331]. This could be important because although Ly6C^{hi} monocytes do not express high levels of CX3CR1 they are universally positive for this chemokine receptor[62].

To complement the Nanostring data I have also performed scRNAseq using the 10x genomics platform on hepatic mononuclear phagocytes. This approach also allowed for more in-depth sequencing of monocytes than was achievable with Nanostring, although I only sequenced tissue monocytes and not circulating monocytes due to the cost of the assay. With regards to the monocytes, scRNAseq also provided the opportunity to address the relationship between tissue Ly6C^{hi} monocytes and recruited Ly6C^{lo} macrophages. Pseudotime analysis will allow the identification of potential relationships between cell clusters, making it possible to reconstruct the developmental progression of cells. This could potentially identify whether IL-4c affects the transition from Ly6C^{hi} monocyte to Ly6C^{lo} macrophage as this remains an outstanding question from my project[332,333]. As alluded to above the scRNAseq was only performed on hepatic mononuclear cells and it would have been useful to have blood Ly6C^{hi} monocytes in order to answer the questions outlined earlier as to whether once monocytes were recruited into tissue they are partially differentiated and can therefore behave differently in response to IL-4c (i.e. with regards to proliferation and survival). I hope that the scRNAseq analysis will at least help to answer some of the outstanding questions from my project.

8.3.2 Pathophysiological relevance

Given that this project has evolved from one looking at the therapeutic effect of exogenous IL-4c to one examining the effect of IL-4 on monocytes, an important outstanding question is whether there is a pathophysiological setting where IL-4 causes a measurable decrease in viability of Ly6C^{hi} monocytes. In an attempt to address this, we made contact with Prof K. Else at the University of Manchester whose group are studying the effect of IL-4 signalling to macrophages during infection with the intestinal nematode *Trichuris muris.* They have been using CX3CR1cre:IL4R$\alpha^{fl/fl}$ mice infected with *T. muris*, however they have not found a reliable change in frequency of monocytes in these mice upon infection compared with controls at multiple timepoints: 3hrs, day 3, 7, 10, 14 and 18) (personal communication). Furthermore, retrospective analysis of 50:50 chimeras using IL-4R$\alpha^{+/+}$ and IL-4R$\alpha^{-/-}$ BM generated by Jenkins et al. revealed no measurable effect of loss of IL-4Rα on blood monocytes during infection with *L. sigmodontis* (data not shown)[121]. However, in both these settings there is a lack of a strong systemic Th2 response accompanied by detectable circulating IL-4 in serum at the timepoints that have been analysed[121,334]. Another interesting model to study would be schistosomiasis. As I described in the introduction, acute schistosomiasis is characterized by an initial Th1 dominated response dominated by production of proinflammatory cytokines such as TNF-α, IL-1, IL-6 and Th1 cell cytokines like IFNγ in the first 3-5 weeks of infection when the host is exposed to migrating immature parasites[164,335]. Then at 6 weeks, antigens released by eggs upon sexual maturation of infecting worms results in a DC dependent activation of a Th2 response[164,336]. It was at this 6 week point that Nascimento et al. demonstrated a significant increase in circulating monocytes which increases further in week 7 post infection. This is surprising because they propose that this coincides with the Th2 response, however, in other models of infection and inflammation in the liver[21,22,31], colon [116,117], heart[118–120] and peritoneum[86,121] monocytosis is normally associated with a Th1 response. Circulating levels of IL-4 are difficult to measure and Nascimento et al. have not included these in their publication but a recent publication by Wang et al. demonstrated that circulating IL-4 levels increase at week 4 and remain at a constant level until week 9 when they begin to decline[337]. Although it is difficult to extrapolate between work performed by different groups, these results would certainly suggest that the increase in Ly6C^{hi} monocytes occurs after the increase in circulating IL-4 levels[204,337]. Interestingly a paper from 1988 demonstrated that CSF-1 levels in the serum of infected animals starts to increase at 6 weeks post infection, also corresponding with the time at which an increase in Ly6C^{hi} monocytes was observed by Nascimento but 2 weeks after Wang observed an increase in circulating IL-4[204,338]. Could IL-4 be suppressing Ly6C^{hi} monocyte numbers until CSF-1 is produced to allow their survival and recruitment to the site of infection? To answer this question it would be interesting to perform a timecourse in *S. mansoni* infected mice looking at the monocyte response in correlation with changes in circulating and tissue cytokines, with a particular focus on IL-4 and CSF-1.

8.4 Why does IL-4 cause monocyte apoptosis?

It had previously been demonstrated that IL-4 promotes the expansion of macrophage numbers through local proliferation and not enhanced recruitment of Ly6C^{hi} monocytes. Furthermore, Ly6C^{hi} monocytes that are recruited during Th2 immunity through IL-4Rα independent mechanisms arrive in a non-inflammatory environment where they are converted into an alternatively activated macrophage[121]. Jenkins et al. suggested that these two effects ultimately result in a non-inflammatory environment to contain worm infection and repair tissue independent of macrophage source. My data adds to this by showing that in addition to not promoting recruitment of Ly6C^{hi} monocytes IL-4 actually inhibits their recruitment by reducing circulating numbers through apoptosis.

This novel role for IL-4 could reflect a further mechanism by which Th2 immunity can control the inflammatory milieu. It may be important to control the origin of macrophages in the Th2 inflammatory milieu because recent data has demonstrated that alternatively activated macrophages derived from monocytes and tissue macrophages are phenotypically and functionally distinct[203]. It is possible that inhibition of Ly6C^{hi} monocyte recruitment through a reduction in their number enables the establishment of the pro-reparative milieu in response to helminth infection. Indeed, Vannella et al. proposed that tissue resident macrophages are important for controlling the magnitude of the granulomatous response following *S. mansoni* infection and the recruited macrophages are responsible for the suppression of fibrosis in chronic infection. This would provide a rationale for IL-4 inhibiting monocyte recruitment as it would allow the early control of the granulomatous response by resident macrophages and then when CSF-1 begins to be produced this enhances survival of Ly6C^{hi} monocytes allowing their recruitment and maturation into macrophages that suppress the fibrosis[338].

8.5 Summary

Owing to a lack of specific tools to identify a role for IL-4c in modulating mononuclear cell responses to acute liver injury the focus of my project evolved from primarily focusing on the potential therapeutic impact of IL-4c following acute CCl_4 liver injury to one investigating the effect of IL-4c on Ly6C^{lo} macrophages and Ly6C^{hi} monocytes following an inflammatory insult. The results remain equally important because they identify the potential for IL-4c to reduce the number of potentially deleterious Ly6C^{hi} monocytes while promoting the expansion Ly6C^{lo} pro-reparative macrophages. This is important because alternatives (e.g. MC21 and Cenicriviroc) simply inhibit Ly6C^{hi} monocyte recruitment without the beneficial effect of enhancing Ly6C^{lo} macrophage numbers whereas I have shown clearly that IL-4c both reduces Ly6C^{hi} monocytes and expands Ly6C^{lo} macrophages[21,23,116]. By following up on the interesting results generated during the project, I think I have identified an exciting novel role for IL-4 in regulating the mononuclear phagocyte compartment and I am excited to follow up the work from my PhD and further attempt to dissect the pathways involved.

References

1. Bernal, W. & Wendon, J. Acute Liver Failure. *N. Engl. J. Med.* **369**, 2525–2534 (2013).

2. Trey, C. & Davidson, C. The management of fulminant hepatic failure. *Prog Liver Dis* **3**, 282–298 (1970).

3. O'Grady, J. G. ., Schalm, S. W. & Williams, R. Acute liver failure : redefining the syndromes. *Lancet* **342**, 273–275 (1993).

4. Takahashi, H. & Zeniya, M. Hepatitis E. *Liver Immunol. Princ. Pract.* 243–252 (2014). doi:10.1007/978-3-319-02096-9_17

5. Wasley, A., Fiore, A. & Bell, B. P. Hepatitis A in the era of vaccination. *Epidemiol. Rev.* **28**, 101–111 (2006).

6. Lee, H. C. Acute liver failure related to hepatitis B virus. *Hepatol. Res.* **38**, 9–13 (2008).

7. Lee, W. M. Drug-induced acute liver failure. *Clin. Liver Dis.* **17**, 575–586 (2013).

8. Wendon, J. *et al.* EASL Clinical Practical Guidelines on the management of acute (fulminant) liver failure. *J. Hepatol.* **66**, 1047–1081 (2017).

9. Brok, J., Buckley, N. & Gluud, C. Interventions for paracetamol (acetaminophen) overdose (Review). *Cochrane Libr.* (2009). doi:10.1002/14651858.CD003328.pub2.www.cochranelibrary.com

10. Keays, R. *et al.* Intravenous acetylcysteine in paracetamol induced fulminant hepatic failure: a prospective controlled trial. *Bmj* **303**, 1026–1029 (1991).

11. Jepsen, P., Schmidt, L. E., Larsen, F. S. & Vilstrup, H. Long-term prognosis for transplant-free survivors of paracetamol-induced acute liver failure. *Aliment. Pharmacol. Ther.* **32**, 894–900 (2010).

12. Bernal, W. *et al.* Lessons from look-back in acute liver failure? A single centre experience of 3300 patients. *J. Hepatol.* **59**, 74–80 (2013).

13. Lee, W. M., Squires, R. H., Nyberg, S. L., Doo, E. & Hoofnagle, J. H. Acute liver

failure: Summary of a workshop. *Hepatology* **47**, 1401–1415 (2008).

14. Burra, P. *et al.* EASL Clinical Practice Guidelines: Liver transplantation. *J. Hepatol.* **64**, 433–485 (2016).

15. Moore, J. K. *et al.* Patients with the worst outcomes after paracetamol (acetaminophen)-induced liver failure have an early monocytopenia. *Aliment. Pharmacol. Ther.* 443–454 (2016). doi:10.1111/apt.13878

16. Stutchfield, B. M. *et al.* CSF1 Restores Innate Immunity After Liver Injury in Mice and Serum Levels Indicate Outcomes of Patients With Acute Liver Failure. *Gastroenterology* **149**, 1896-1909.e14 (2015).

17. Weber, L. W. D., Boll, M. & Stampfl, A. Hepatotoxicity and mechanism of action of haloalkanes: carbon tetrachloride as a toxicological model. *Crit. Rev. Toxicol.* **33**, 105–136 (2003).

18. Taniguchi, M., Takeuchi, T., Nakatsuka, R., Watanabe, T. & Sato, K. Molecular process in acute liver injury and regeneration induced by carbon tetrachloride. *Life Sci.* **75**, 1539–1549 (2004).

19. Markose, D., Kirkland, P., Ramachandran, P. & Henderson, N. C. Immune cell regulation of liver regeneration and repair. *J. Immunol. Regen. Med.* **2**, 1–10 (2018).

20. Hoehme, S. *et al. Prediction and validation of cell alignment along microvessels as order principle to restore tissue architecture in liver regeneration*. *Proceedings of the National Academy of Sciences* **107**, (2010).

21. Zigmond, E. *et al.* Infiltrating Monocyte-Derived Macrophages and Resident Kupffer Cells Display Different Ontogeny and Functions in Acute Liver Injury. *J. Immunol.* **193**, 344–353 (2014).

22. Karlmark, K. R. *et al.* Hepatic recruitment of the inflammatory Gr1+ monocyte subset upon liver injury promotes hepatic fibrosis. *Hepatology* **50**, 261–274 (2009).

23. Mossanen, J. C. *et al.* Chemokine (C-C motif) receptor 2-positive monocytes aggravate the early phase of acetaminophen-induced acute liver injury. *Hepatology* **64**, 1667–1682 (2016).

24. Ju, C. & Tacke, F. Hepatic macrophages in homeostasis and liver diseases: from pathogenesis to novel therapeutic strategies. *Cell. Mol. Immunol.* **13**, 1–12 (2016).

25. Chen, F. *et al.* An essential role for TH2-type responses in limiting acute tissue damage during experimental helminth infection. *Nat. Med.* **18**, 260–266 (2012).

26. Gause, W. C., Wynn, T. a & Allen, J. E. Type 2 immunity and wound healing: evolutionary refinement of adaptive immunity by helminths. *Nat. Rev. Immunol.* **13**, 607–14 (2013).

27. Karp, C. L. & Murray, P. J. Non-canonical alternatives: What a macrophage is 4. *J. Exp. Med.* **209**, 427–431 (2012).

28. Herbert, D. R. *et al.* Alternative macrophage activation is essential for survival during schistosomiasis and downmodulates T helper 1 responses and immunopathology. *Immunity* **20**, 623–635 (2004).

29. Seno, H. *et al.* Efficient colonic mucosal wound repair requires Trem2 signaling. *Proc. Natl. Acad. Sci. U. S. A.* **106**, 256–261 (2009).

30. Knipper, J. a *et al.* Interleukin-4 Receptor a Signaling in Myeloid Cells Controls Collagen Fibril Assembly in Skin Repair Article Interleukin-4 Receptor a Signaling in Myeloid Cells Controls Collagen Fibril Assembly in Skin Repair. *Immunity* **43**, 803–816 (2015).

31. Blériot, C. *et al.* Liver-Resident Macrophage Necroptosis Orchestrates Type1Microbicidal InflammationandType-2-Mediated Tissue Repair during Bacterial Infection. *Immunity* **42**, 1–14 (2015).

32. Finkelman, F. D. *et al.* Anti-cytokine antibodies as carrier proteins. Prolongation of in vivo effects of exogenous cytokines by injection of cytokine-anti-cytokine antibody complexes. *J. Immunol.* **151**, 1235–1244 (1993).

33. Goh, Y. P. S. *et al.* Eosinophils secrete IL-4 to facilitate liver regeneration. *Proc. Natl. Acad. Sci. U. S. A.* **110**, 9914–9 (2013).

34. Vannella, K. M. *et al.* Incomplete deletion of IL-4Rα by LysM(Cre) reveals distinct subsets of M2 macrophages controlling inflammation and fibrosis in chronic schistosomiasis. *PLoS Pathog.* **10**, e1004372 (2014).

35. Poisson, J. *et al.* Liver sinusoidal endothelial cells: Physiology and role in liver diseases. *J. Hepatol.* **66**, 212–227 (2017).

36. Sorensen, K. K. *et al.* The scavenger endothelial cell: a new player in homeostasis

and immunity. *AJP Regul. Integr. Comp. Physiol.* **303**, R1217–R1230 (2012).

37. Terpstra, V. & Berkel, T. J. C. Van. Scavenger receptors on liver Kupffer cells mediate the in vivo uptake of oxidatively damaged red blood cells in mice Scavenger receptors on liver Kupffer cells mediate the in vivo uptake of oxidatively damaged red blood cells in mice. *Hematology* **95**, 2157–2163 (2010).

38. Heymann, F. *et al.* Liver Inflammation Abrogates Immunological Tolerance Induced by Kupffer Cells. *Hepatology* **62**, 279–291 (2015).

39. Theurl, I. *et al.* On-demand erythrocyte disposal and iron recycling requires transient macrophages in the liver. *Nat. Med.* (2016). doi:10.1038/nm.4146

40. Balmer, M. L. *et al.* The liver may act as a firewall mediating mutualism between the host and its gut commensal microbiota. *Sci. Transl. Med.* **6**, 237ra66 (2014).

41. Bhushan, B. *et al.* Pro-regenerative signaling after acetaminophen-induced acute liver injury in mice identified using a novel incremental dose model. *Am. J. Pathol.* **184**, 3013–3025 (2014).

42. Yuan, L. & Kaplowitz, N. Mechanisms of Drug Induced Liver Injury. *Clin. Liver Dis.* **17**, 507–508 (2013).

43. Kietzmann, T. Metabolic zonation of the liver: The oxygen gradient revisited. *Redox Biol.* **11**, 622–630 (2017).

44. Giboney, P. T. Mildly Elevated Liver Transaminase Levels in the Asymptomatic Patient. *Am. Fam. Physician* **71**, 1105–1110 (2005).

45. Forbes, S. J. & Newsome, P. N. Liver regeneration — mechanisms and models to clinical application. *Nat. Rev. Gastroenterol. Hepatol.* (2016). doi:10.1038/nrgastro.2016.97

46. Higgins, G. & Anderson, R. Experimental pathology of the liver. *Arch. Pathol.* **12**, 186 (1931).

47. Michalopoulos, G. K. & Defrances, M. C. Liver Regeneration. **276**, (1997).

48. Emre, S. & Umman, V. Split liver transplantation: An overview. *Transplant. Proc.* **43**, 884–887 (2011).

49. Bird, T. G. *et al.* TGFβ inhibition restores a regenerative response in acute liver injury by suppressing paracrine senescence. *Sci. Transl. Med.* **10**, 1–15 (2018).

50. Scott, C. L., Zheng, F., Baetselier, P. De & Martens, L. Bone marrow derived monocytes give rise to self-renewing and fully differentiated Kupffer cells. *Nat. Commun.* 1–10 (2016). doi:10.1038/ncomms10321

51. Huebener, P. *et al.* The HMGB1 / RAGE axis triggers neutrophil- mediated injury amplification following necrosis Find the latest version : The HMGB1 / RAGE axis triggers neutrophil-mediated injury amplification following necrosis. *JCI* **125**, 539–550 (2015).

52. Graubardt, N. *et al.* Ly6Chimonocytes and their macrophage descendants regulate neutrophil function and clearance in acetaminophen-induced liver injury. *Front. Immunol.* **8**, 1–17 (2017).

53. van Furth, R. *et al.* [Mononuclear phagocytic system: new classification of macrophages, monocytes and of their cell line]. *Bull. World Health Organ.* **47**, 651–8 (1972).

54. Yona, S. & Gordon, S. From the reticuloendothelial to mononuclear phagocyte system - The unaccounted years. *Front. Immunol.* **6**, 1–7 (2015).

55. Metchnikoff, E. pathologisehe Anatomic und Physiologic. *Arch. fur Pathol. Anat. und Physiol. und fur Klin. Med.* (1875).

56. Guilliams, M. *et al.* Dendritic cells, monocytes and macrophages: a unified nomenclature based on ontogeny. *Nat. Rev. Immunol.* **14**, 571–578 (2014).

57. Passlick, B., Flieger, D. & Ziegler-Heitbrock, H. Identification and characterization of a novel monocyte subpopulation in human peripheral blood. *Blood* **74**, 2527–2534 (1989).

58. Ziegler-heitbrock, L. *et al.* Nomenclature of monocytes and dendritic cells in blood Nomenclature of monocytes and dendritic cells in blood. *Blood* **116**, 5–7 (2010).

59. Wong, K. L. *et al.* Gene expression profiling reveals the defining features of the classical, intermediate, and nonclassical human monocyte subsets. *Blood* **118**, e16–e31 (2011).

60. Ingersoll, M. *et al.* Comparison of gene expression profiles between human and

mouse monocyte subsets. *Blood* **115**, 10–20 (2010).

61. Fong, a M. *et al.* Fractalkine and CX3CR1 mediate a novel mechanism of leukocyte capture, firm adhesion, and activation under physiologic flow. *J. Exp. Med.* **188**, 1413–1419 (1998).

62. Geissmann, F., Jung, S. & Littman, D. R. Blood monocytes consist of two principal subsets with distinct migratory properties. *Immunity* **19**, 71–82 (2003).

63. Briseño, C. G. *et al.* Distinct Transcriptional Programs Control Cross-Priming in Classical and Monocyte-Derived Dendritic Cells. *Cell Rep.* **15**, 2462–2474 (2016).

64. Mildner, A. *et al.* Genomic Characterization of Murine Monocytes Reveals C/EBPβ Transcription Factor Dependence of Ly6C− Cells. *Immunity* **46**, 849–862 (2017).

65. Hanna, R. N. *et al.* The transcription factor NR4A1 (Nur77) controls bone marrow differentiation and the survival of Ly6C- monocytes. *Nat. Immunol.* **12**, 778–785 (2011).

66. Thomas, G. D. *et al.* Deleting an Nr4a1 Super-Enhancer Subdomain Ablates Ly6Clow Monocytes while Preserving Macrophage Gene Function. *Immunity* **45**, 975–987 (2016).

67. Carlin, L. M. *et al.* Nr4a1-dependent Ly6Clow monocytes monitor endothelial cells and orchestrate their disposal. *Cell* **153**, 362–375 (2013).

68. Paul, F. *et al.* Transcriptional Heterogeneity and Lineage Commitment in Myeloid Progenitors. *Cell* **163**, 1663–1677 (2015).

69. Pietras, E. M. *et al.* Functionally Distinct Subsets of Lineage-Biased Multipotent Progenitors Control Blood Production in Normal and Regenerative Conditions. *Cell Stem Cell* **17**, 35–46 (2015).

70. Kondo, M. *et al.* Identification of clonogenic common lymphoid progenitors in mouse bone marrow. *Cell* **91**, 661–72 (1997).

71. Fogg, D. *et al.* A Clonogenic Bone Marrow Progenitor Specific for Macrophages and Dendritic Cells. *Science (80-.).* **311**, 83–88 (2006).

72. Varol, C. *et al.* Monocytes give rise to mucosal, but not splenic, conventional dendritic cells. *J. Exp. Med.* **204**, 171–180 (2007).

73. Ginhoux, F. & Jung, S. Monocytes and macrophages : developmental pathways and tissue homeostasis. *Nat. Publ. Gr.* **14**, 392–404 (2014).

74. Hettinger, J. *et al.* Origin of monocytes and macrophages in a committed progenitor. *Nat. Immunol.* **14**, 821–830 (2013).

75. Velten, L. *et al.* Human haematopoietic stem cell lineage commitment is a continuous process. *Nat. Cell Biol.* **19**, 271–281 (2017).

76. Giladi, A. *et al.* Single-cell characterization of haematopoietic progenitors and their trajectories in homeostasis and perturbed haematopoiesis. *Nat. Cell Biol.* **20**, (2018).

77. Rodriguez-Fraticelli, A. E. *et al.* Clonal analysis of lineage fate in native haematopoiesis. *Nature* **553**, 212–216 (2018).

78. Chong, S. Z. *et al.* CXCR4 identifies transitional bone marrow premonocytes that replenish the mature monocyte pool for peripheral responses. *J. Exp. Med.* **213**, 2293–2314 (2016).

79. Ogawa, M. *et al.* Expression and Function of c-kit in Hemopoietic Progenitor Cells. *J. Exp. Med.* **174**, 63–71 (1991).

80. Dai, X.-M. *et al.* Targeted disruption of the mouse CSF-1 receptor gene results in osteopetrosis, mononuclear phagocyte deficiency, increased primititive progenitor cell frequencies and reproductive defects. *Blood* **99**, 111–120 (2002).

81. Mossadegh-Keller, N. *et al.* M-CSF instructs myeloid lineage fate in single haematopoietic stem cells. *Nature* **497**, 239–243 (2013).

82. Louis, C. *et al.* Specific Contributions of CSF-1 and GM-CSF to the Dynamics of the Mononuclear Phagocyte System. *J. Immunol.* **195**, 134–144 (2015).

83. Dekoter, R. P., Walsh, J. C. & Singh, H. PU . 1 regulates both cytokine-dependent proliferation and differentiation of granulocyte / macrophage progenitors. *EMBO J.* **17**, 4456–4468 (1998).

84. Schulz, C. *et al.* A Lineage of Myeloid Cells independent of Myb and Hematopoietic Stem Cells. *Science (80-.).* **336**, 86–90 (2012).

85. Kueh, H. Y., Champhekhar, A., Nutt, S. L., Elowitz, M. B. & Rothenberg, E. V. Positive feedback between PU.1 and the cell cycle controls myeloid differentiation.

Science (80-.). **341**, 670–673 (2013).

86. Yona, S. *et al.* Fate Mapping Reveals Origins and Dynamics of Monocytes and Tissue Macrophages under Homeostasis. *Immunity* **38**, 79–91 (2013).

87. Kurihara, B. T., Warr, G., Loy, J. & Bravo, R. Mice Lacking the CCR2 Chemokine Receptor. *J Exp Med* **186**, 1757–1762 (1997).

88. Serbina, N. V., Salazar-Mather, T. P., Biron, C. A., Kuziel, W. A. & Pamer, E. G. TNF/iNOS-producing dendritic cells mediate innate immune defense against bacterial infection. *Immunity* **19**, 59–70 (2003).

89. Serbina, N. V & Pamer, E. G. Monocyte emigration from bone marrow during bacterial infection requires signals mediated by chemokine receptor CCR2. *Nat. Immunol.* **7**, 311–317 (2006).

90. Bain, C. C. *et al.* Constant replenishment from circulating monocytes maintains the macrophage pool in the intestine of adult mice. *Nat. Immunol.* **15**, 929–37 (2014).

91. Bain, C. C. *et al.* Long-lived self-renewing bone marrow-derived macrophages displace embryo-derived cells to inhabit adult serous cavities. *Nat. Commun.* **7**, 1–14 (2016).

92. Auffray C *et al.* Monitoring of Blood Vessels and Tissues by a Population of Monocytes with Patrolling Behavior. *Science (80-.).* **317**, 666–671 (2007).

93. Mowat, A. M., Scott, C. L. & Bain, C. C. Barrier-tissue macrophages: functional adaptation to environmental challenges. *Nat. Med.* **23**, 1258–1270 (2017).

94. Gautier, E. L. *et al.* Gene-expression profiles and transcriptional regulatory pathways that underlie the identity and diversity of mouse tissue macrophages. *Nat. Immunol.* **13**, 1118–28 (2012).

95. Ginhoux, F., Schultze, J. L., Murray, P. J., Ochando, J. & Biswas, S. K. New insights into the multidimensional concept of macrophage ontogeny, activation and function. *Nat. Immunol.* **17**, 34–40 (2015).

96. Hashimoto, D. *et al.* Tissue-resident macrophages self-maintain locally throughout adult life with minimal contribution from circulating monocytes. *Immunity* **38**, 792–804 (2013).

97. Tamoutounour, S. *et al.* CD64 distinguishes macrophages from dendritic cells in the gut and reveals the Th1-inducing role of mesenteric lymph node macrophages during colitis. *Eur. J. Immunol.* **42**, 3150–3166 (2012).

98. Tamoutounour, S. *et al.* Origins and functional specialization of macrophages and of conventional and monocyte-derived dendritic cells in mouse skin. *Immunity* **39**, 925–938 (2013).

99. Zigmond, E. & Jung, S. Intestinal macrophages: Well educated exceptions from the rule. *Trends Immunol.* **34**, 162–168 (2013).

100. Mildner, A., Yona, S. & Jung, S. A Close Encounter of the Third Kind. Monocyte-Derived Cells. *Adv. Immunol.* **120**, 69–103 (2013).

101. Guilliams, M. & Scott, C. L. Does niche competition determine the origin of tissue-resident macrophages? *Nat. Rev. Immunol.* **17**, 451–460 (2017).

102. Shaw, T. N. *et al.* Tissue-resident macrophages in the intestine are long lived and defined by Tim-4 and CD4 expression. *J. Exp. Med.* jem.20180019 (2018). doi:10.1084/jem.20180019

103. Guilliams, M. *et al.* Alveolar macrophages develop from fetal monocytes that differentiate into long-lived cells in the first week of life via GM-CSF. *J. Exp. Med.* **210**, 1977–1992 (2013).

104. Sawai, C. M. *et al.* Hematopoietic Stem Cells Are the Major Source of Multilineage Hematopoiesis in Adult Animals. *Immunity* **45**, 597–609 (2016).

105. Gibbings, S. L. *et al.* Transcriptome analysis highlights the conserved difference between embryonic and postnatal-derived alveolar macrophages. *Blood* **126**, 1357–1366 (2015).

106. Lavin, Y. *et al.* Tissue-resident macrophage enhancer landscapes are shaped by the local microenvironment. *Cell* **159**, 1312–1326 (2014).

107. David, B. A. *et al.* Combination of Mass Cytometry and Imaging Analysis Reveals Origin, Location, and Functional Repopulation of Liver Myeloid Cells in Mice. *Gastroenterology* **151**, 1176–1191 (2016).

108. Trapnell, B. C., Whitsett, J. A. & Nakata, K. Pulmonary Alveolar Proteinosis. *N. Engl. J. Med.* **349**, 2527–2539 (2003).

109. van de Laar, L. *et al.* Yolk Sac Macrophages, Fetal Liver, and Adult Monocytes Can Colonize an Empty Niche and Develop into Functional Tissue-Resident Macrophages. *Immunity* **44**, 755–768 (2016).

110. Plantinga, M. *et al.* Conventional and Monocyte-Derived CD11b+ Dendritic Cells Initiate and Maintain T Helper 2 Cell-Mediated Immunity to House Dust Mite Allergen. *Immunity* **38**, 322–335 (2013).

111. Cheong, C. *et al.* Microbial stimulation fully differentiates monocytes to DC-SIGN/CD209 + dendritic cells for immune T cell areas. *Cell* **143**, 416–429 (2010).

112. Langlet, C. *et al.* CD64 Expression Distinguishes Monocyte-Derived and Conventional Dendritic Cells and Reveals Their Distinct Role during Intramuscular Immunization. *J. Immunol.* **188**, 1751–1760 (2012).

113. Cros, J. *et al.* Human CD14 dim Monocytes Patrol and Sense Nucleic Acids and Viruses. *Immunity* **33**, 375–386 (2010).

114. Michaud, J.-P., Bellavance, M.-A., Prefontaine, P. & Rivest, S. Real-Time In Vivo Imaging Reveals the Ability of Monocytes to Clear Vascular Amyloid Beta. *Cell Rep.* **5**, 646–653 (2013).

115. Ramachandran, P. *et al.* PNAS Plus: Differential Ly-6C expression identifies the recruited macrophage phenotype, which orchestrates the regression of murine liver fibrosis. *Proc. Natl. Acad. Sci.* **109**, (2012).

116. Zigmond, E. *et al.* Ly6Chi Monocytes in the Inflamed Colon Give Rise to Proinflammatory Effector Cells and Migratory Antigen-Presenting Cells. *Immunity* **37**, 1076–1090 (2012).

117. Bain, C. C. *et al.* Resident and pro-inflammatory macrophages in the colon represent alternative context-dependent fates of the same Ly6Chi monocyte precursors. *Mucosal Immunol.* **6**, 498–510 (2013).

118. Nahrendorf, M. *et al.* The healing myocardium sequentially mobilizes two monocyte subsets with divergent and complementary functions. *J. Exp. Med.* **204**, 3037–3047 (2007).

119. Swirski, F. K. *et al.* Identification of Splenic Reservoir Monocytes and Their Deployment to Inflammatory Sites. *Science (80-.).* **325**, 612–616 (2009).

120. Epelman, S. *et al.* Article Embryonic and Adult-Derived Resident Cardiac Macrophages Are Maintained through Distinct Mechanisms at Steady State and during Inflammation. *Immunity* **40**, 91–104 (2014).

121. Jenkins, S. J. *et al.* IL-4 directly signals tissue-resident macrophages to proliferate beyond homeostatic levels controlled by CSF-1. *J. Exp. Med.* **210**, 2477–91 (2013).

122. La Flamme, A. C., Patton, E. A., Bauman, B. & Pearce, E. J. IL-4 Plays a Crucial Role in Regulating Oxidative Damage in the Liver During Schistosomiasis. *J. Immunol.* **166**, 1903–1911 (2001).

123. Campbell, S. M. *et al.* Myeloid cell recruitment versus local proliferation differentiates susceptibility from resistance to filarial infection. *Elife* **7**, 1–17 (2018).

124. Noy, R. & Pollard, J. W. Tumor-Associated Macrophages: From Mechanisms to Therapy. *Immunity* **41**, 49–61 (2014).

125. Nicholson, L. B., Raveney, B. J. E. & Munder, M. Monocyte dependent regulation of autoimmune inflammation. *Curr. Mol. Med.* **9**, 23–29 (2009).

126. Neal, L. M. & Knoll, L. J. Toxoplasma gondii Profilin Promotes Recruitment of Ly6C hi CCR2 + Inflammatory Monocytes That Can Confer Resistance to Bacterial Infection. *PLoS Pathog.* **10**, 1–13 (2014).

127. Serbina, N. V, Jia, T., Hohl, T. M. & Pamer, E. G. Monocyte-Mediated Defense Against Microbial Pathogens. *Annu. Rev. Immunol.* **26**, 421–452 (2008).

128. Tsou, C. L. *et al.* Critical roles for CCR2 and MCP-3 in monocyte mobilization from bone marrow and recruitment to inflammatory sites. *J. Clin. Invest.* **117**, 902–909 (2007).

129. Tacke, F. *et al.* Monocyte subsets differentially employ CCR2 , CCR5 , and CX3CR1 to accumulate within atherosclerotic plaques. *JCI* **117**, (2007).

130. Shi, C. & Pamer, E. G. Monocyte Recruitment During Infection and Inflammation. *Nat Rev Immunol* **11**, 762–774 (2011).

131. Shi, C. *et al.* Monocyte Trafficking to Hepatic Sites of Bacterial Infection Is Chemokine Independent and Directed by Focal Intercellular Adhesion Molecule-1 Expression. *J. Immunol. (Baltimore, Md 1950)* **184**, 6266–6274 (2010).

132. Hänninen, A., Maksimow, M., Alam, C., Morgan, D. J. & Jalkanen, S. Ly6C supports preferential homing of central memory CD8+ T cells into lymph nodes. *Eur. J. Immunol.* **41**, 634–644 (2011).

133. Liao, B. F., Ali, J., Greene, T. & Muller, W. A. Molecule (PECAM) Is Sufficient to Block Transendothelial Migration In Vitro and In Vivo. **185**, (1997).

134. Zimmermann, H. W., Trautwein, C. & Tacke, F. Functional role of monocytes and macrophages for the inflammatory response in acute liver injury. *Front. Physiol.* **3**, 1–18 (2012).

135. Selzner, N. *et al.* ICAM-1 triggers liver regeneration through leukocyte recruitment and Kupffer cell-dependent release of TNF-??/IL-6 in mice. *Gastroenterology* **124**, 692–700 (2003).

136. Hilgendorf, I. *et al.* Integrative Physiology Ly-6C high Monocytes Depend on Nr4a1 to Balance Both Inflammatory and Reparative Phases in the Infarcted Myocardium. *Circ. Res.* 1611–1622 (2014). doi:10.1161/CIRCRESAHA.114.303204

137. Grainger, J. R. *et al.* Inflammatory monocytes regulate pathologic responses to commensals during acute gastrointestinal infection. *Nat. Med.* **19**, 713 (2013).

138. Hanna, R. N. *et al.* Patrolling monocytes control tumor metastasis to the lung. *Science (80-.).* **350**, 985–991 (2015).

139. Heymann, F. & Tacke, F. Immunology in the liver — from homeostasis to disease. *Nat. Rev. Gastroenterol. Hepatol.* **4**, 88–110 (2016).

140. Martin-murphy, B. V, Holt, M. P. & Ju, C. The role of damage associated molecular pattern molecules in acetaminophen-induced liver injury in mice. *Toxicol. Lett.* **192**, 387–394 (2010).

141. Dambach, D. M., Watson, L. M., Gray, K. R., Durham, S. K. & Laskin, D. L. Role of CCR2 in Macrophage Migration Into the Liver During Acetaminophen-Induced Hepatotoxicity in the Mouse. 1093–1103 doi:10.1053/jhep.2002.33162

142. Antoniades, C. G. *et al.* Source and Characterization of Hepatic Macrophages in Acetaminophen-Induced Acute Liver Failure in Humans. *Hepatology* **56**, 735–746 (2012).

143. Mosher, B. *et al.* Inhibition of Kupffer cells reduced CXC chemokine production and

liver injury. *J. Surg. Res.* **99**, 201–210 (2001).

144. Triantafyllou, E. *et al.* MerTK expressing hepatic macrophages promote the resolution of inflammation in acute liver failure. *Gut* **67**, 333–347 (2018).

145. Holt, M. P., Cheng, L. & Ju, C. Identification and characterization of infiltrating macrophages in acetaminophen-induced liver injury. *J Leukoc Biol* **84**, 1410–1421 (2008).

146. Leuschner, F. *et al.* Rapid monocyte kinetics in acute myocardial infarction are sustained by extramedullary monocytopoiesis. *J Exp Med* **209**, 123–138 (2012).

147. Rothlin, C. V, Carrera-silva, E. A., Bosurgi, L. & Ghosh, S. TAM Receptor Signaling in Immune Homeostasis. *Annu. Rev. Immunol.* **33**, 355–391 (2015).

148. Gill, U. S. *et al.* Fine needle aspirates comprehensively sample intrahepatic immunity. *Gut* **0**, 1–11 (2018).

149. Forbes, S. J. International ClinicalTrials Registry Platform. Macrophages therapy for liver cirrhosis (MATCH trial). (2016). Available at: https://ukctg.nihr.ac.uk/trials/trial-details/trial-details?trialNumber=ISRCTN10368050.

150. Fraser, A. R. *et al.* Development, functional characterization and validation of methodology for GMP-compliant manufacture of phagocytic macrophages: A novel cellular therapeutic for liver cirrhosis. *Cytotherapy* **19**, 1113–1124 (2017).

151. Moore, J. K. *et al.* Phenotypic and functional characterization of macrophages with therapeutic potential generated from human cirrhotic monocytes in a cohort study. *Cytotherapy* **17**, 1604–1616 (2015).

152. Gieseck, R. L. *et al.* Interleukin-13 Activates Distinct Cellular Pathways Leading to Ductular Reaction, Steatosis, and Fibrosis. *Immunity* 1–14 (2016). doi:10.1016/j.immuni.2016.06.009

153. Chiaramonte, M. G., Donaldson, D. D., Cheever, A. W. & Wynn, T. a. An IL-13 inhibitor blocks the development of hepatic fibrosis during a T-helper type 2-dominated inflammatory response. *J. Clin. Invest.* **104**, 777–785 (1999).

154. Johansson, M. E. V., Sjövall, H. & Hansson, G. C. The gastrointestinal mucus system in health and disease. *Nat. Rev. Gastroenterol. Hepatol.* **10**, 352–361 (2013).

155. Kawakami, K., Taguchi, J., Murata, T. & Puri, R. K. The interleukin-13 receptor ⎵2 chain: an essential component for binding and internalization but not for interleukin-13–induced signal transduction through the STAT6 pathway. *Immunobiology* **97**, 2673–2679 (2011).

156. Wills-Karp, M. & Finkelman, F. D. Untangling the complex web of IL-4- and IL-13-mediated signaling pathways. *Sci. Signal.* **1**, pe55 (2008).

157. Kaplan, M. H., Schindler, U., Smiley, S. T. & Grusby, M. J. Stat6 is required for mediating responses to IL-4 and for the development of Th2 cells. *Immunity* **4**, 313–319 (1996).

158. Donaldson, D. D. *et al.* The murine IL-13 receptor alpha 2: molecular cloning, characterization, and comparison with murine IL-13 receptor alpha 1. *J. Immunol.* **161**, 2317–2324 (1998).

159. Wood, N. *et al.* Enhanced Interleukin (IL)-13 Responses in Mice Lacking IL-13 Receptor α 2. *J. Exp. Med.* **197**, 703–709 (2003).

160. Chiaramonte, M. G. *et al.* Regulation and Function of the Interleukin 13 Receptor α 2 During a T Helper Cell Type 2–dominant Immune Response. *J. Exp. Med.* **197**, 687–701 (2003).

161. Mentink-Kane, M. M. *et al.* IL-13 receptor alpha 2 down-modulates granulomatous inflammation and prolongs host survival in schistosomiasis. *Proc. Natl. Acad. Sci. U. S. A.* **101**, 586–590 (2004).

162. Hershey, G. K. K. IL-13 receptors and signaling pathways : An evolving web. *J Allergy Clin Immunol* **111**, 677–690 (2003).

163. Ramalingam, T. R. *et al.* Unique functions of the type II interleukin 4 receptor identified in mice lacking the interleukin 13 receptor alpha1 chain. *Nat. Immunol.* **9**, 25–33 (2008).

164. Pearce, E. J. & MacDonald, A. S. The immunobiology of schistosomiasis. *Nat. Rev. Immunol.* **2**, 499–511 (2002).

165. Heller, N. M. *et al.* Type I IL-4Rs selectively activate IRS-2 to induce target gene expression in macrophages. *Sci. Signal.* **1**, 1–15 (2008).

166. Brunet, L. R., Finkelman, F. D., Cheever, A. W., Kopf, M. A. & Pearce, E. J. IL-4

protects against TNF-alpha-mediated cachexia and death during acute schistosomiasis. *J. Immunol.* **159**, 777–85 (1997).

167. Fallon, P. G., Richardson, E. J., McKenzie, G. J. & McKenzie, A. N. J. Schistosome Infection of Transgenic Mice Defines Distinct and Contrasting Pathogenic Roles for IL-4 and IL-13: IL-13 Is a Profibrotic Agent. *J. Immunol.* **164**, 2585–2591 (2000).

168. Kaplan, M. H., Whitfield, J. R., Boros, D. L. & Grusby, M. J. Th2 cells are required for the Schistosoma mansoni egg-induced granulomatous response. *J. Immunol.* **160**, 1850–1856 (1998).

169. Marsland, B. J., Kurrer, M., Reissmann, R., Harris, N. L. & Kopf, M. Nippostrongylus brasiliensis infection leads to the development of emphysema associated with the induction of alternatively activated macrophages. *Eur. J. Immunol.* **38**, 479–488 (2008).

170. Sutherland, T. E. *et al.* Ym1 induces RELMα and rescues IL-4Rα deficiency in lung repair during nematode infection. *PLOS Pathog.* **14**, 1–27 (2018).

171. DeAngelis, R. a. *et al.* A Complement-IL-4 Regulatory Circuit Controls Liver Regeneration. *J. Immunol.* **188**, 641–648 (2011).

172. Fausto, N., Campbell, J. S. & Riehle, K. J. Liver regeneration. *Hepatology* **43**, 45–53 (2006).

173. Ryan, P. M. *et al.* Endogenous interleukin-4 regulates glutathione synthesis following acetaminophen-induced liver injury in mice. *Chem. Res. Toxicol.* **25**, 83–93 (2012).

174. Stein, M., Keshav, S., Harris, N. & Gordon, S. Interleukin 4 potently enhances murine macrophage mannose receptor activity: a marker of alternative immunologic macrophage activation. *J. Exp. Med.* **176**, 287–292 (1992).

175. Allen, J. E. & Sutherland, T. E. Host protective roles of type 2 immunity: Parasite killing and tissue repair, flip sides of the same coin. *Semin. Immunol.* **26**, 329–340 (2014).

176. Thomas, G. D. *et al.* The biology of nematode- and IL4R ⎵ -dependent murine macrophage polarization in vivo as defined by RNA-Seq and targeted lipidomics. *Blood* **120**, 93–105 (2012).

177. Loke, P. *et al.* IL-4 dependent alternatively-activated macrophages have a distinctive

in vivo gene expression phenotype. *BMC Immunol.* **3**, 1–11 (2002).

178. Zhu, Z., Zheng, T., Homer, R. J. & Kim, Y. Acidic Mammalian Chitinase in Asthmatic Th2 Inflammation and IL-13 Pathway Activation. **304**, 1678–1683 (2004).

179. Kzhyshkowska, J., Yin, S., Liu, T., Riabov, V. & Mitrofanova, I. Role of chitinase-like proteins in cancer. *Biol Chem* **397**, 231–247 (2016).

180. Ydens, E. *et al.* Acute injury in the peripheral nervous system triggers an alternative macrophage response. *J. Neuroinflammation* 1–17 (2012).

181. Loke, P. *et al.* Alternative Activation Is an Innate Response to Injury That Requires CD4 + T Cells to be Sustained during Chronic Infection. *J Immunol* **179**, 3926–3936 (2007).

182. Lee, C. G. *et al.* Role of breast regression protein 39 (BRP-39)/ chitinase 3-like-1 in Th2 and IL- 13 – induced tissue responses and apoptosis. *J Exp Med* **206**, 1149–1166 (2009).

183. Webb, D. C., Mckenzie, A. N. J. & Foster, P. S. Expression of the Ym2 Lectin-binding Protein Is Dependent on Interleukin (IL) -4 and IL-13 Signal Transduction. *J. Biol. Chem.* **276**, 41969–41976 (2001).

184. Welch, J. S. *et al.* T H 2 Cytokines and Allergic Challenge Induce Ym1 Expression in Macrophages by a STAT6-dependent Mechanism *. *J. Biol. Chem.* **277**, 42821–42829 (2002).

185. Allen, J. E., Sutherland, T. E. & Ru, D. IL-17 and neutrophils : unexpected players in the type 2 immune response. *Curr. Opin. Immunol.* **34**, 99–106 (2015).

186. Sutherland, T. E. *et al.* Chitinase-like proteins promote IL-17-mediated neutrophilia in a tradeoff between nematode killing and host damage. *Nat. Immunol.* 1–10 (2014). doi:10.1038/ni.3023

187. Gordon, S. ALTERNATIVE ACTIVATION OF MACROPHAGES. *Nat. Rev. Immunol.* **3**, 23–35 (2003).

188. Peranzoni, E. *et al.* Role of arginine metabolism in immunity and immunopathology. *Immunobiology* **212**, 795–812 (2008).

189. Hesse, M. *et al.* Differential Regulation of Nitric Oxide Synthase-2 and Arginase-1 by

Type 1/Type 2 Cytokines In Vivo: Granulomatous Pathology Is Shaped by the Pattern of L-Arginine Metabolism. *J. Immunol.* **167**, 6533–6544 (2001).

190. Pesce, J. T. *et al.* Arginase-1 – Expressing Macrophages Suppress Th2 Cytokine – Driven Inflammation and Fibrosis. *PLoS Pathog.* **5**, 1–15 (2009).

191. Barron, L. *et al.* Role of Arginase 1 from Myeloid Cells in Th2-Dominated Lung Inflammation. *PLoS One* **8**, 1–11 (2013).

192. Kasmi, K. C. El *et al.* Toll-like receptor – induced arginase 1 in macrophages thwarts effective immunity against intracellular pathogens. *Nat. Immunol.* **9**, 1399–1406 (2008).

193. Munder, M. *et al.* Th1/Th2-Regulated Expression of Arginase Isoforms in Murine Macrophages and Dendritic Cells. *J Immunol* **163**, 3771–3777 (1999).

194. Modolelp, M., Corraliza, I. M., Link, F. & Eichmannl, K. Reciprocal regulation of the nitric oxide synthase / ai : ginase balance in mouse bone marrow-derived macrophages by TH 1 and TH 2 cytokines. *Eur. J. Immunol.* **25**, 1101–1104 (1995).

195. Corraliza, I. M., Soler, G., Eichmann, K. & Modolell, M. Arginase induction by supressors of nitric oxide synthesis (IL-4, iL-10 and PGE2) in murine bone-marrow-derived macrophages. *Biochem. Biophys. Res. Commun.* **206**, 667–673 (1995).

196. Martin, L. *et al.* Granulocyte-macrophage colony-stimulating factor increases L -arginine transport through the induction of CAT2 in bone marrow-derived macrophages. *Am J Physiol Cell Physiol* **290**, 1364–1372 (2006).

197. Rodriguez, P. C. *et al.* Arginase I in myeloid suppressor cells is induced by COX-2 in lung carcinoma. *J Exp Med* **202**, 931–939 (2005).

198. Gordon, S. & Martinez, F. O. Alternative activation of macrophages: Mechanism and functions. *Immunity* **32**, 593–604 (2010).

199. Nair, M. G. *et al.* Alternatively activated macrophage-derived RELM- a is a negative regulator of type 2 inflammation in the lung. *J Exp Med* **206**, 937–952 (2009).

200. Wynn, T. A. & Vannella, K. M. Macrophages in Tissue Repair, Regeneration, and Fibrosis. *Immunity* **44**, 450–462 (2016).

201. Turnbull, I. R. *et al.* Cutting Edge: TREM-2 Attenuates Macrophage Activation. *J.*

Immunol. **177**, 3520–3524 (2006).

202. Liao, X. *et al.* Krüppel-like factor 4 regulates macrophage polarization. *J. Clin. Invest.* **121**, (2011).

203. Gundra, U. M. *et al.* Alternatively activated macrophages derived from monocytes and tissue macrophages are phenotypically and functionally distinct. *Blood* **123**, 110–123 (2013).

204. Nascimento, M. *et al.* Ly6Chi Monocyte Recruitment Is Responsible for Th2 Associated Host-Protective Macrophage Accumulation in Liver Inflammation due to Schistosomiasis. *PLoS Pathog.* **10**, (2014).

205. Egawa, M. *et al.* Inflammatory Monocytes Recruited to Allergic Skin Acquire an Anti-inflammatory M2 Phenotype via Basophil-Derived Interleukin-4. *Immunity* **38**, 570–580 (2012).

206. Jenkins, S. J. *et al.* Local Macrophage Proliferation, Rather than Recruitment from the Blood, Is a Signature of TH2 Inflammation. *Science (80-.).* (2011).

207. Gundra, U. M. *et al.* Vitamin A mediates conversion of monocyte-derived macrophages into tissue-resident macrophages during alternative activation. *Nat. Immunol.* **18**, 642–653 (2017).

208. Bosurgi, L. *et al.* Macrophage function in tissue repair and remodeling requires IL-4 or IL-13 with apoptotic cells. *Science (80-.).* **1076**, eaai8132 (2017).

209. Poon, I. K. H., Lucas, C. D. & Rossi, A. G. Apoptotic cell clearance : basic biology and therapeutic potential. *Nat. Publ. Gr.* **14**, 166–180 (2014).

210. Minutti, C. M. *et al.* Local amplifiers of IL-4Ra-mediated macrophage activation promote repair in lung and liver. *Science (80-.).* **356**, 1076–1080 (2017).

211. Tenner, A. J. Membrane receptors for soluble defense collagens. *Innate Immun.* 34–41 (1999).

212. Jakubzick, C. *et al.* steady state tissues and transport antigen to lymph nodes. *Immunity* **39**, (2014).

213. Menezes, S. *et al.* The Heterogeneity of Ly6Chi Monocytes Controls Their Differentiation into iNOS+ Macrophages or Monocyte-Derived Dendritic Cells.

Immunity **45**, 1205–1218 (2016).

214. Mcdonald, B. *et al.* Intravascular Danger Signals Guide Neutrophils to Sites of Sterile Inflammation. *Science (80-.).* **330**, 362–366 (2010).

215. Dal-Secco, D. *et al.* A dynamic spectrum of monocytes arising from the in situ reprogramming of CCR2+ monocytes at a site of sterile injury. *J. Exp. Med.* **212**, 447–456 (2015).

216. Patel, A. A. *et al.* The fate and lifespan of human monocyte subsets in steady state and systemic inflammation. *J. Exp. Med.* 1–11 (2017). doi:10.1084/jem.20170355

217. Sander, J. *et al.* Cellular Differentiation of Human Monocytes Is Regulated by Time-Dependent Interleukin-4 Signaling and the Transcriptional Regulator NCOR2. *Immunity* **47**, 1051–1066 (2017).

218. Mottis, A., Mouchiroud, L. & Auwerx, J. Emerging roles of the corepressors NCoR1 and SMRT in homeostasis. *Genes Dev.* **27**, 819–835 (2013).

219. Ikeda, N. *et al.* Emergence of immunoregulatory Ym1 $^{+}$ Ly6C ^{hi} monocytes during recovery phase of tissue injury. *Sci. Immunol.* **3**, eaat0207 (2018).

220. Mangan, D. F., Robertson, B. & Wahl, S. M. IL-4 enhances programmed cell death (apoptosis) in stimulated human monocytes. *J. Immunol. (Baltimore, Md 1950)* **148**, 1812–1816 (1992).

221. Palm, N. W., Rosenstein, R. K. & Medzhitov, R. Allergic host defences. *Nature* **484**, 465–472 (2012).

222. Osborne, L. C. *et al.* Virus-helminth coinfection reveals a microbiota-independent mechanism of immunomodulation. *Science (80-.).* **345**, 578–583 (2014).

223. Potian, J. A. *et al.* Preexisting helminth infection induces inhibition of innate pulmonary anti-tuberculosis defense by engaging the IL-4 receptor pathway. *J. Exp. Med.* **208**, 1863–74 (2011).

224. Gabrilovich, D. I., Ostrand-rosenberg, S. & Bronte, V. Coordinated regulation of myeloid cells by tumours. *Nat. Publ. Gr.* **12**, 253–268 (2012).

225. Gocheva, V. *et al.* IL-4 induces cathepsin protease activity in tumor-associated macrophages to promote cancer growth and invasion. *Genes Dev.* **24**, 241–255

(2010).

226. Rankin, J. A. *et al.* Phenotypic and physiologic characterization of transgenic mice expressing interleukin 4 in the lung: lymphocytic and eosinophilic inflammation without airway hyperreactivity. *Proc. Natl. Acad. Sci. U. S. A.* **93**, 7821–5 (1996).

227. Oh, C. K., Geba, G. P. & Molfino, N. Investigational therapeutics targeting the IL-4/IL-13/STAT-6 pathway for the treatment of asthma. *Eur. Respir. Rev.* **19**, 46–54 (2010).

228. Su, Z. *et al.* Lebrikizumab Treatment in Adults with Asthma. *Methods* **365**, 1088–1098 (2011).

229. Wenzel, S. *et al.* Dupilumab in Persistent Asthma with Elevated Eosinophil Levels. *N. Engl. J. Med.* **368**, 2455–2466 (2013).

230. Beck, L. a *et al.* Dupilumab treatment in adults with moderate-to-severe atopic dermatitis. *N Engl J Med* **371**, 130–139 (2014).

231. Strait, R. T., Morris, S. C., Smiley, K., Urban, J. F. & Finkelman, F. D. IL-4 Exacerbates Anaphylaxis. *J. Immunol.* **170**, 3835–3842 (2003).

232. Morris, S. C. *et al.* IL-4 Induces In Vivo Production of IFN- by NK and NKT Cells. *J. Immunol.* **176**, 5299–5305 (2006).

233. Miossec, P. & van den Berg, W. Cytokine balance in arthritis. *Arthritis Rheum.* **40**, 2105–2115 (1997).

234. Arend, W. P. & Dayer, J. Inhibition of the production and effects of interleukin-1 and tumour necrosis factor a in rheumatoid arthritis. *Arthritis Rheum.* **38**, 151–160 (1995).

235. Perdriger, A. Infliximab in the treatment of rheumatoid arthritis. *Biol. Targets Ther.* 183–191 (2009).

236. Joosten, L. A. B. *et al.* Protection against cartilage and bone destruction by systemic interleukin-4 treatment in established murine type II collagen- induced arthritis. *Arthritis Res.* **1**, 81–91 (1999).

237. Moreno, J. L., Kaczmarek, M., Keegan, A. D. & Tondravi, M. IL-4 suppresses osteoclast development and mature osteoclast function by a STAT6-dependent mechanism: Irreversible inhibition of the differentiation program activated by RANKL. *Blood* **102**, 1078–1086 (2003).

238. Joosten, L. A. *et al.* ROLE OF INTERLEUKIN-4 AND INTERLEUKIN-10 IN MURINE COLLAGEN-INDUCED ARTHRITIS Protective Effect of Interleukin-4 and Interleukin-10 Treatment on Cartilage Destruction. *Arthritis Rheum.* **40**, 249–260 (1997).

239. Fine, J. S. *et al.* Impairment of leukocyte trafficking in a murine pleuritis model by IL-4 and IL-10. *Inflammation* **27**, 161–174 (2003).

240. Ghoreschi, K. *et al.* Interleukin-4 therapy of psoriasis induces Th2 responses and improves human autoimmune disease. *Nat. Med.* **9**, 40–46 (2003).

241. Hahn, M. & Ghoreschi, K. The role of IL-4 in psoriasis. *Expert Rev. Clin. Immunol.* **13**, 171–173 (2017).

242. Onderdijk, A. J. *et al.* IL-4 Downregulates IL-1β and IL-6 and Induces GATA3 in Psoriatic Epidermal Cells: Route of Action of a Th2 Cytokine. *J. Immunol.* **195**, 1744–1752 (2015).

243. Chatterjee, P. *et al.* Cotreatment with interleukin 4 and interleukin 10 modulates immune cells and prevents hypertension in pregnant mice. *Am. J. Hypertens.* **28**, 135–142 (2015).

244. Ramani, T. *et al.* Cytokines : The Good , the Bad , and the Deadly. *Int. J. Toxicol.* **34**, 355–365 (2015).

245. Holliger, P. & Prospero, T. " Diabodies ": Small bivalent and bispecific antibody fragments. *Proc. Natl. Acad. Sci.* **90**, 6444–6448 (1993).

246. Hemmerle, T., Doll, F. & Neri, D. Antibody-based delivery of IL4 to the neovasculature cures mice with arthritis. *Proc. Natl. Acad. Sci.* **111**, 12008–12012 (2014).

247. Fernandes, J. C. Therapeutic application of antibody fragments in autoimmune diseases: current state and prospects. *Drug Discov. Today* **00**, 1–7 (2018).

248. Kawalkowska, J. Z. *et al.* Targeted IL-4 therapy synergizes with dexamethasone to induce a state of tolerance by promoting Treg cells and macrophages in mice with arthritis. *Eur. J. Immunol.* **46**, 1246–1257 (2016).

249. Goodnow, C. C., Sprent, J., Barbara, B. F. & Vinuesa, C. G. Cellular and genetic mechanisms of self tolerance and autoimmunity. *Nature* **435**, 590–597 (2005).

250. Guillot, C. *et al.* Lethal Hepatitis After Gene Transfer of IL-4 in the Liver Is Independent of Immune Responses and Dependent on Apoptosis of Hepatocytes: A Rodent Model of IL-4-Induced Hepatitis. *J. Immunol. (Baltimore, Md 1950)* **166**, 5225–5253 (2010).

251. Bizzaro, D. *et al.* Sex-dependent differences in inflammatory responses during liver regeneration in a murine model of acute liver injury. *Clin. Sci.* **132**, 255–272 (2018).

252. Huang, H.-L. Hepatoprotective effects of baicalein against CCl_4 -induced acute liver injury in mice. *World J. Gastroenterol.* **18**, 6605 (2012).

253. Ho, G. T. *et al.* MDR1 deficiency impairs mitochondrial homeostasis and promotes intestinal inflammation. *Mucosal Immunol.* **11**, 120–130 (2018).

254. Monvoisin, A. *et al.* VE-cadherin-CreERT2 transgenic mouse: A model for inducible recombination in the endothelium. *Dev. Dyn.* **235**, 3413–3422 (2006).

255. Campana, L. *et al.* The STAT3-IL-10-IL-6 Pathway Is a Novel Regulator of Macrophage Efferocytosis and Phenotypic Conversion in Sterile Liver Injury. *J. Immunol.* **200**, 1169–1187 (2017).

256. Pearce, E. J. *et al.* Schistosoma mansoni in IL-4-deficient mice. *Int. Immunol.* **8**, 435–444 (1996).

257. Hawley, C. A. *et al. Csf1r* -mApple Transgene Expression and Ligand Binding In Vivo Reveal Dynamics of CSF1R Expression within the Mononuclear Phagocyte System. *J. Immunol.* ji1701488 (2018). doi:10.4049/jimmunol.1701488

258. Devisscher, L. *et al.* Non-alcoholic steatohepatitis induces transient changes within the liver macrophage pool. *Cell. Immunol.* **322**, 74–83 (2017).

259. Wermeling, F., Anthony, R. M., Brombacher, F. & Ravetch, J. V. Acute inflammation primes myeloid effector cells for anti-inflammatory STAT6 signaling. *Proc. Natl. Acad. Sci. U. S. A.* **110**, 13487–91 (2013).

260. Rosenberg, H. F., Dyer, K. D. & Foster, P. S. Eosinophils: Changing perspectives in health and disease. *Nat. Rev. Immunol.* **13**, 9–22 (2013).

261. Voehringer, D., van Rooijen, N. & Locksley, R. M. Eosinophils develop in distinct stages and are recruited to peripheral sites by alternatively activated macrophages. *J. Leukoc. Biol.* **81**, 1434–1444 (2007).

262. Toor, I. S. *et al.* E Eosinophils have an essential role in cardiac repair following myocardial infarction. *Heart* **103**, A152–A152 (2017).

263. Barnes, P. J. Immunology of asthma and chronic obstructive pulmonary disease. *Nat. Rev. Immunol.* **8**, 183–192 (2008).

264. Thomas, J. a. *et al.* Macrophage therapy for murine liver fibrosis recruits host effector cells improving fibrosis, regeneration, and function. *Hepatology* **53**, 2003–2015 (2011).

265. DeLeve, L. Liver sinusoidal endothelial cells and liver regeneration. *J. Cinical Investig.* **123**, 1861–1866 (2013).

266. Wang, L. *et al.* Liver sinusoidal endothelial cell progenitor cells promote liver regeneration in rats. *J. Cinical Investig.* **122**, 1567–1573 (2012).

267. Wang, Y. *et al.* Ephrin-B2 controls VEGF-induced angiogenesis and lymphangiogenesis. *Nature* **465**, 483–486 (2010).

268. Okabe, Y. & Medzhitov, R. Tissue-specific signals control reversible program of localization and functional polarization of macrophages. *Cell* **157**, 832–844 (2014).

269. Muzumdar, M. D., Tasic, B., Miyamichi, K., Li, L. & Luo, L. A Global Double-Fluorescent Cre Reporter Mouse. *Genesis* **45**, 593–605 (2007).

270. Swirski, F. K. & Nahrendorf, M. Leukocyte Behavior in. *Atherosclerosis* **161**, 161–166 (2013).

271. Murray, P. J. & Wynn, T. a. Protective and pathogenic functions of macrophage subsets. *Nat. Rev. Immunol.* **11**, 723–737 (2011).

272. Clausen, B. E., Burkhardt, C., Reith, W., Renkawitz, R. & Förster, I. Conditional gene targeting in macrophages and granulocytes using LysMcre mice. *Transgenic Res.* **8**, 265–277 (1999).

273. Takeda, K. *et al.* Enhanced Th1 Activity and Development of Chronic Enterocolitis in Mice Devoid of Stat3 in Macrophages and Neutrophils. *Immunity* **10**, 39–49 (1999).

274. Liu, S. *et al.* Effects of radiation on T regulatory cells in normal states and cancer: Mechanisms and clinical implications. *Am. J. Cancer Res.* **5**, 3276–3285 (2015).

275. Mazagova, M. *et al.* Commensal microbiota is hepatoprotective and prevents liver fibrosis in mice. *FASEB J.* **29**, 1043–1055 (2015).

276. Brenner, D. A., Paik, Y.-H. H. & Schnabl, B. Role of Gut Microbiota in Liver Disease. *J. Clin. Gastroenterol.* **49 Suppl 1**, 25–27 (2015).

277. Askenase, M. H. *et al.* Bone-Marrow-Resident NK Cells Prime Monocytes for Regulatory Function during Infection. *Immunity* **42**, 1130–1142 (2015).

278. Klein, I. *et al.* Kupffer cell heterogeneity: Functional properties of bone marrow-derived and sessile hepatic macrophages. *Blood* **110**, 4077–4085 (2007).

279. Kim, J. & Jung, Y. Radiation-induced liver disease: current understanding and future perspectives. *Exp. Mol. Med.* **49**, e359 (2017).

280. Collins, B. H. *et al.* Association of age dependent liver injury and fibrosis with immune cell populations. *Liver Int* **33**, 1175–1186 (2014).

281. Wang, J. *et al.* Visualizing the function and fate of neutrophils in sterile injury and repair. *Science (80-.).* **358**, 111–116 (2017).

282. Schridde, A. *et al.* Tissue-specific differentiation of colonic macrophages requires TGFβ receptor-mediated signaling. *Mucosal Immunol.* **10**, 1387–1399 (2017).

283. Sasmono, R. T. *et al.* A macrophage colony-stimulating factor receptor-green fluorescent protein transgene is expressed throughout the mononuclear phagocyte system of the mouse. *Blood* **101**, 1155–1163 (2003).

284. Francke, A. *et al.* Generation of Mature Murine Monocytes from Heterogeneous Bone Marrow and Description of Their Properties. *J. Histochem. Cytochem.* **59**, 813–825 (2011).

285. Yoshioka, H., Usuda, H., Nonogaki, T. & Onosaka, S. Carbon tetrachloride-induced lethality in mouse is prevented by multiple pretreatment with zinc sulfate. *J. Toxicol. Sci.* **41**, 55–63 (2016).

286. Ozturk, F., Ucar, M., Ozturk, I. C., Vardi, N. & Batcioglu, K. Carbon tetrachloride-induced nephrotoxicity and protective effect of betaine in Sprague-Dawley rats. *Urology* **62**, 353–356 (2003).

287. Makni, M., Chtourou, Y., Garoui, E. M., Boudawara, T. & Fetoui, H. Carbon

tetrachloride-induced nephrotoxicity and DNA damage in rats: Protective role of vanillin. *Hum. Exp. Toxicol.* **31**, 844–852 (2012).

288. Haideri, S. S. *et al.* Injection of embryonic stem cell derived macrophages ameliorates fibrosis in a murine model of liver injury. *npj Regen. Med.* **2**, 14 (2017).

289. Casella, G. *et al.* IL4 induces IL6-producing M2 macrophages associated to inhibition of neuroinflammation in vitro and in vivo. *J. Neuroinflammation* **13**, 1–10 (2016).

290. Jakubzick, C. V., Randolph, G. J. & Henson, P. M. Monocyte differentiation and antigen-presenting functions. *Nat. Rev. Immunol.* **17**, 349–362 (2017).

291. Eis, V. *et al.* Chemokine Receptor CCR1 but Not CCR5 Mediates Leukocyte Recruitment and Subsequent Renal Fibrosis after Unilateral Ureteral Obstruction. *J. Am. Soc. Nephrol.* **15**, 337–347 (2004).

292. Milner, J. D. *et al.* Sustained IL-4 exposure leads to a novel pathway for hemophagocytosis, inflammation, and tissue macrophage accumulation. *Blood* **116**, 2476–2483 (2010).

293. Munro, D. A. D. & Hughes, J. The origins and functions of tissue-resident macrophages in kidney development. *Front. Physiol.* **8**, 1–13 (2017).

294. Woytschak, J. *et al.* Type 2 Interleukin-4 Receptor Signaling in Neutrophils Antagonizes Their Expansion and Migration during Infection and Inflammation. *Immunity* **45**, 172–184 (2016).

295. Evrard, M. *et al.* Developmental Analysis of Bone Marrow Neutrophils Reveals Populations Specialized in Expansion, Trafficking, and Effector Functions. *Immunity* **48**, 364-379.e8 (2018).

296. Schmid, I., Krall, W. J., Uittenbogaart, C. H., Braun, J. & Giorgi, J. V. Dead Cell Discrimination With 7-Amino-Actinomycin D\nin Combination With Dual Color Immunof luorescence\nin Single Laser Flow Cytometry. *Cytometry* **208**, 204–208 (1992).

297. Koopman, G. *et al.* Annexin V for Flow Cytometric Detection of Phosphatidylserine Expression on B Cells Undergoing Apoptosis. *Blood* **3**, 11–12 (1994).

298. Crowley, L. C., Marfell, B. J., Scott, A. P. & Waterhouse, N. J. Quantitation of apoptosis and necrosis by annexin V binding, propidium iodide uptake, and flow

cytometry. *Cold Spring Harb. Protoc.* **2016**, 953–957 (2016).

299. Kelley, J. L., Rozek, M. M., Suenram, C. A. & Schwartz, C. J. Activation of human blood monocytes by adherence to tissue culture plastic surfaces. *Exp. Mol. Pathol.* **46**, 266–278 (1987).

300. Haim, Y. O., Unger, N. D., Souroujon, M. C., Mittelman, M. & Neumann, D. Resistance of LPS-activated bone marrow derived macrophages to apoptosis mediated by dexamethasone. *Sci. Rep.* **4**, (2014).

301. Yamamoto, M. *et al.* Absence of exogenous interleukin-4-induced apoptosis of gingival macrophages may contribute to chronic inflammation in periodontal diseases. *Am. J. Pathol.* **148**, 331–339 (1996).

302. Hume, D. A. & MacDonald, K. P. A. Therapeutic applications of macrophage colony-stimulating factor-1 (CSF-1) and antagonists of CSF-1 receptor (CSF-1R) signaling. *Blood* **119**, 1810–1820 (2012).

303. Yáñez, A. *et al.* Granulocyte-Monocyte Progenitors and Monocyte-Dendritic Cell Progenitors Independently Produce Functionally Distinct Monocytes. *Immunity* **47**, 890-902.e4 (2017).

304. Satoh, T. *et al.* Identification of an atypical monocyte and committed progenitor involved in fibrosis. *Nature* **541**, 96–101 (2017).

305. Jung, S. *et al.* Analysis of Fractalkine Receptor CX3CR1 Function by Targeted Deletion and Green Fluorescent Protein Reporter Gene Insertion. *Mol. Cell. Biol.* **20**, 4106–4114 (2000).

306. Menzies-Gow, A. *et al.* Eotaxin (CCL11) and Eotaxin-2 (CCL24) Induce Recruitment of Eosinophils, Basophils, Neutrophils, and Macrophages As Well As Features of Early- and Late-Phase Allergic Reactions Following Cutaneous Injection in Human Atopic and Nonatopic Volunteers. *J. Immunol.* **169**, 2712–2718 (2002).

307. Lee, W. Drug-induced hepatotoxicity. *N. Engl. J. Med.* **333**, 1118–1127 (2003).

308. Okayasu, I. *et al.* A novel method in the induction of reliable experimental acute and chronic ulcerative colitis in mice. *Gastroenterology* **98**, 694–702 (1990).

309. Hernandez-Gea, V., Toffanin, S., Friedman, S. L. & Llovet, J. M. Role of the microenvironment in the pathogenesis and treatment of hepatocellular carcinoma.

Gastroenterology **144**, 512–27 (2013).

310. Li, M., Wu, Y., Hu, Y., Zhao, L. & Zhang, C. Initial gut microbiota structure affects sensitivity to DSS-induced colitis in a mouse model. *Sci. China Life Sci.* **61**, 1–8 (2017).

311. Nguyen, T. L. A., Vieira-Silva, S., Liston, A. & Raes, J. How informative is the mouse for human gut microbiota research? *Dis. Model. Mech.* **8**, 1–16 (2015).

312. Chassaing, B., Aitken, J. D., Malleshappa, M. & Vijay-Kumar, M. Dextran Sulfate Sodium (DSS)-Induced Colitis in Mice. *Curr Potoc Immunol* **104**, 1199–1216 (2014).

313. Ginzel, M. *et al.* Dextran sodium sulfate (DSS) induces necrotizing enterocolitis-like lesions in neonatal mice. *PLoS One* **12**, 1–17 (2017).

314. Bain, C. C. & Mowat, A. M. CD200 receptor and macrophage function in the intestine. *Immunobiology* **217**, 643–651 (2012).

315. Jaeschke, H., Williams, C. D., Ramachandran, A. & Bajt, M. L. Acetaminophen hepatotoxicity and repair: The role of sterile inflammation and innate immunity. *Liver Int.* **32**, 8–20 (2012).

316. Ishida, Y. *et al.* Opposite roles of neutrophils and macrophages in the pathogenesis of acetaminophen-induced acute liver injury. *Eur. J. Immunol.* **36**, 1028–1038 (2006).

317. Marques, P. E. *et al.* Chemokines and mitochondrial products activate neutrophils to amplify organ injury during mouse acute liver failure. *Hepatology* **56**, 1971–1982 (2012).

318. Wang, H., Feng, D., Park, O., Yin, S. & Gao, B. Invariant NKT cell activation induces neutrophil accumulation and hepatitis: Opposite regulation by IL-4 and IFN-γ. *Hepatology* **58**, 1474–1485 (2013).

319. Hudcovic, T., Štěpánková, R., Cebra, J. & Tlaskalová-Hogenová, H. The Role of Microflora in the Development of Intestinal Inflammation: Acute and Chronic Colitis Induced by Dextran Sulfate in Germ-Free and Conventionally Reared Immunocompetent and Immunodeficient Mice. *Folia Microbiol. (Praha).* **46**, 565–572 (2001).

320. Hernandez-Chirlaque, C. *et al.* Germ-free and antibiotic-treated mice are highly susceptible to epithelial injury in DSS colitis. *J. Crohn's Colitis* **10**, 1324–1335 (2016).

321. Laukens, D., Brinkman, B. M., Raes, J., De Vos, M. & Vandenabeele, P. Heterogeneity of the gut microbiome in mice: Guidelines for optimizing experimental design. *FEMS Microbiol. Rev.* **40**, 117–132 (2015).

322. Pushparaj, P. N. *et al.* Interleukin-33 exacerbates acute colitis via interleukin-4 in mice. *Immunology* **140**, 70–77 (2013).

323. Stevceva, L., Pavli, P., Husband, A., Ramsay, A. & Doe, W. F. Dextran sulphate sodium-induced colitis is ameliorated in interleukin 4 deficient mice. *Genes Immun.* **2**, 309–316 (2001).

324. Sharpe, C., Thornton, D. J. & Grencis, R. K. A sticky end for gastrointestinal helminths; the role of the mucus barrier. *Parasite Immunol.* **40**, 1–10 (2018).

325. Smith, P. *et al.* Infection with a helminth parasite prevents experimental colitis via a macrophage-mediated mechanism. *J. Immunol.* **178**, 4557–4566 (2007).

326. Penn, I. Posttransplantation De Novo Tumors in liver Allograft Recipients. *Hepatology* **2**, 52–59 (1996).

327. Mcgill, M. R. *et al.* The mechanism underlying acetaminophen- induced hepatotoxicity in humans and mice involves mitochondrial damage and nuclear DNA fragmentation. *J. Clin. Invest.* **122**, 1574–83 (2012).

328. Hidalgo-Garcia, L., Galvez, J., Rodriguez-Cabezas, M. E. & Anderson, P. O. Can a conversation between mesenchymal stromal cells and macrophages solve the crisis in the inflamed intestine? *Front. Pharmacol.* **9**, 1–12 (2018).

329. Bosurgi, L. *et al.* Macrophage function in tissue repair and remodeling requires IL-4 or IL-13 with apoptotic cells. *Science* **356**, 1072–1076 (2017).

330. Hanna, R. N. *et al.* NR4A1 (Nur77) Deletion Polarizes Macrophages Toward an Inflammatory Phenotype and Increases Atherosclerosis Phenotype and Increases Atherosclerosis. *Cell. Biol.* **1**, (2011).

331. Landsman, L. *et al.* CX 3 CR1 is required for monocyte homeostasis and atherogenesis by promoting cell survival. *Blood* **113**, 963–973 (2009).

332. Macaulay, I. C. *et al.* Single-Cell RNA-Sequencing Reveals a Continuous Spectrum of Differentiation in Hematopoietic Cells. *Cell Rep.* **14**, 1–12 (2016).

333. Haghverdi, L., Büttner, M., Wolf, F. A., Buettner, F. & Theis, F. J. Diffusion pseudotime robustly reconstructs lineage branching. *Nat. Methods* **13**, 845–848 (2016).

334. Taylor, M. D., Betts, C. J. & Else, K. J. Peripheral cytokine responses to Trichuris muris reflect those occurring locally at the site of infection. *Infect. Immun.* **68**, 1815–1819 (2000).

335. Jesus, A. R. De *et al.* Clinical and Immunologic Evaluation of 31 Patients with Acute Schistosomiasis mansoni. *J. Infect. Dis.* **185**, 98–105 (2018).

336. Macdonald, A. S. *et al.* CD8 − Dendritic Cell Activation Status Plays an Integral Role in Influencing Th2 Response Development. *J. Immunol. (Baltimore, Md 1950)* **167**, 1982–1988 (2001).

337. Wang, Y. *et al.* Up-regulation of Interleukin-21 Contributes to Liver Pathology of Schistosomiasis by Driving GC Immune Responses and Activating HSCs in Mice. *Sci. Rep.* **7**, 1–11 (2017).

338. Clark, C. R., Chen, B. D. M. & Boros, D. L. Macrophage progenitor cell and colony-stimulating factor production during granulomatous Schistosmiasis mansoni in mice. *Infect. Immun.* **56**, 2680–2685 (1988).

339. Guilliams, M., Mildner, A. & Yona, S. Developmental and Functional Heterogeneity of Monocytes. *Immunity* **49**, 595–613 (2018).